

PETROLOGY OF AN ECLOGITE- AND PYRIGARNITE-BEARING POLYMETAMORPHIC
ROCK COMPLEX AT CABO ORTEGAL, NW SPAIN

BY

D. E. VOGEL

SUMMARY

At Cabo Ortegal, paragneisses are found in association with amphibolites, metagabbros, amphibolized eclogites, amphibolized (plagio)pyrigarnites, and serpentized ultrabasic rocks. On the basis of petrographical and chemical evidence, their geological history was reconstructed as follows:

Precambrian sedimentation of graywackes, was rapidly succeeded by intrusion of gabbroic sills and stocks and by emplacement of ultrabasic rocks.

During an orogeny of supposed Precambrian age, the rocks in the area were subjected to mesozonal metamorphism in the upper part of the sequence and to catazonal metamorphism in the lower parts. Mesozonally-metamorphosed gneisses formed staurolite-almandine subfacies associations; their gabbroic inclusions were transformed into amphibolites. Catazonally-metamorphosed gneisses became partially anatexitic, and kyanite-almandine associations with or without biotite were formed in the unmelted portions (restite). Gabbro sills were altered into foliated eclogites (\pm *a*-zoisite \pm kyanite \pm carinthine) in the eastern part of the area and into non-foliated (plagio)pyrigarnite (high-pressure granulite) in its central and western parts. The ultrabasites were transformed into garnet peridotites. Evidence of isoclinal folding has been found in the eclogites and, less conspicuously, in the ultrabasic rocks.

Renewed local intrusion of gabbro was followed by catazonal retrograde metamorphism (hornblende-clinopyroxene-almandine subfacies grade) in zones affected by pegmatoid injection or by penetrative deformation. Retrograde alterations could only be demonstrated for the mafic rocks from the appearance of greenish-brown hornblende or the formation of a new foliation. The newly-intruded gabbros were partly metamorphosed and acquired a *flaser* texture.

After the Precambrian orogeny, gabbroic and granitic rocks once again intruded locally; the age of their intrusion is placed at $500 \pm$ m.y. by analogy with similar intrusions in southern Galicia. These rocks were altered into schistose amphibolite and orthogneiss during the Hercynian orogeny; the metamorphic rocks were remetamorphosed and (re)folded under amphibolite facies conditions (kyanite-almandine-muscovite subfacies grade over the whole of the investigated area). In the paragneisses an assemblage of biotite + muscovite \pm garnet \pm kyanite was formed, while quartz and plagioclase recrystallized. Two consecutive phases of deformation caused isoclinal folds, followed in most cases by open folding. In the eclogites and in the (plagio)pyrigarnites, the association blue-green hornblende + plagioclase + epidote \pm garnet was formed secondarily after the catazonal associations. The eclogites were boudinaged; internal folding did not take place, and amphibolization was confined to the rims of boudins and pegmatoid injections as well as to narrow zones of penetrative deformation. More intensive tectonization (internal isoclinal folding, overprinted by open folds) caused the (plagio)pyrigarnites to be more extensively retrograded during the Hercynian orogeny. They were altered for the most part into laminated (garnet) amphibolites. The metagabbros were likewise altered into laminated (garnet) amphibolites, with textures ranging from mylonitic to gabbroic. In the ultrabasic rocks, garnet peridotites were replaced by amphibole or chlorite peridotites. Isoclinal as well as open folds were formed. During the Hercynian orogeny, the stratigraphic sequence was overturned in the eastern as well as in the western part of the area (formation of a "mushroom-shaped" dome); and in the western part a zone of overthrust with isoclinally-folded blastomylonites, boudinaged ultrabasites, and microfolded amphibolites was formed.

Post-Hercynian activities consisted mainly of ubiquitous hydrothermal action accompanied by local greenschist-facies retrogradations in most of the rocks and by extensive serpentinization in the ultrabasites. Normal faulting, resulting in mainly vertical block-movements, accompanied locally by brecciation or mylonitization, and small-scale emplacement of tonalitic and gabbroic dykes, also took place after the Hercynian orogenesis.

CONTENTS

Introduction	123	I. The Concepenido Complex	128
A. Geographical information	123	A. Eclogites	128
B. Geological setting	124	1. Occurrence	128
C. Outline of the geology of Cabo Ortegal	124	2. Nomenclature	129
1. Review of previous studies at Cabo Ortegal	124	3. Varieties of eclogite	129
2. Rock-types represented on the geological map	124	4. Amphibolization	130
3. Dating of major geological events	126	5. Symplectitization	132
4. The framework of this study	126	6. Mineralogy	132
5. Acknowledgements	127	7. Retrograde eclogite	134

a. Hornblende eclogite	135	4. Comparison of the pyrigarnite and eclogite mineralogies	181
b. Amphibolite eclogite, eclogite amphibolite	137	5. Transitional types between eclogite and pyrigarnite	181
c. Amphibolite, hornblende gneiss, chlorite gneiss	138	6. Leptynites	182
8. Pegmatoid veins	139	7. Calc-silicate rocks	183
9. Chemistry and metamorphic facies	140	8. Garnet-biotite gneisses	183
10. Summary and conclusions	143	9. Post-metamorphic gabbro	185
B. Paragneisses	143	B. The Candelaria Amphibolite Formation	185
1. Banded Gneiss Formation	143	1. Pyrigarnites, amphibolites retrograde after pyrigarnite, and associated calc-silicate rocks	185
a. Occurrence	143	2. Metagabbros and amphibolites secondary after metagabbro	186
b. Mineralogical composition and textural relations	144	3. Amphibolites of uncertain origin	189
c. Behaviour of metasediments under eclogite-facies conditions	147	C. Chemistry and metamorphic facies	189
d. Eclogitic inclusions: the Masanteo geological section	150	1. Magmatic versus sedimentary descent	189
e. Non-eclogitic basic and ultrabasic inclusions	151	2. Metamorphic facies	190
2. Cariñogneiss Formation	153	IV. Structural geology	191
a. Occurrence	153	A. Evidence of folding during the oldest catazonal metamorphic phase (M_1)	191
b. Petrography	153	B. Deformation accompanying the catazonal retrograde metamorphic phase (M_2)	191
c. Cafemic inclusions	154	C. Deformation accompanying the mesozonal metamorphic phase (M_3)	192
3. Chimparragneiss Formation	156	D. Structural features of post-Hercynian age (M_4)	193
a. Occurrence	156	V. Mineralogy	194
b. Petrography	156	A. Garnet	195
c. Cafemic inclusions	158	1. Calculation of garnet analyses	195
4. Gneisses and blastomylonites from the Carreiro zone of tectonic movement	159	2. Chemical and physical data	195
a. Occurrence, general description, petrography	159	B. Clinopyroxene	197
b. Basic and ultrabasic inclusions	161	1. Nomenclature	197
5. Chemistry	162	2. Calculation of clinopyroxene analyses	197
a. Sedimentary versus magmatic descent	162	3. Chemical and physical data of clinopyroxenes	198
b. Metamorphic facies of the paragneisses	163	4. The isochemical nature of symplectitization	199
C. Purrido amphibolite formation	163	C. Hornblende	199
1. General description	163	1. Nomenclature	199
2. Petrography	164	2. Chemistry of the analyzed amphiboles	200
3. Chemistry and metamorphic facies	165	D. Plagioclase	200
D. Carreiro zone of tectonic movement	165	E. Zircon	200
1. General description	165	VI. Geological history of Cabo Ortegal	201
2. Structural and petrographical features	165	A. Pre-metamorphic events	201
a. Serpentinites	165	B. Precambrian orogeny: main phase (M_1)	201
b. Purrido-type amphibolites	166	1. Rocks of gabbroic composition	201
c. Calc-silicate rocks	168	2. Paragneisses	202
3. Metamorphic facies	168	3. Ultrabasic rocks	202
4. Precambrian isograds	202	C. Precambrian orogeny: minor phase (M_2)	203
5. Retrogradation of the eclogites	203	1. Retrogradation of the eclogites	203
6. Bacariza Formation	203	2. Bacariza Formation	203
7. Candelaria Amphibolite Formation	203	3. Candelaria Amphibolite Formation	203
8. Paragneisses and ultrabasites	203	4. Paragneisses and ultrabasites	203
9. Post-Precambrian, pre-Hercynian events	203	D. Post-Precambrian, pre-Hercynian events	203
10. Hercynian orogeny (M_3)	204	E. Hercynian orogeny (M_3)	204
1. Eclogites	204	1. Eclogites	204
2. Capelada Complex	204	2. Capelada Complex	204
3. Ultrabasic rocks	205	3. Ultrabasic rocks	205
4. Paragneisses	205	4. Paragneisses	205
5. Pre-Hercynian intrusions	205	5. Pre-Hercynian intrusions	205
6. Carreiro zone of tectonic movement	206	6. Carreiro zone of tectonic movement	206
11. Post-Hercynian geological events	206	F. Post-Hercynian geological events	206
12. Concluding remarks	206	G. Concluding remarks	206
III. The Capelada Complex	176		
A. The Bacariza Formation	176		
1. Nomenclature of the granulite facies rocks	176		
2. Petrography	176		
3. Retrograde metamorphism of the pyrigarnites	177		
a. Hornblende-clinopyroxene-almandine sub-facies retrograde metamorphism	177		
b. Amphibolite facies retrograde metamorphism	178		
c. Mineral sequences in the pegmatoid injections	180		

Samenvatting	207
Sumario	207
References	208
Appendices:	
1. Figures	
2. Tables	

3. Localities of specimens mentioned in the text
4. Qualitative mineralogical composition of chemically analyzed samples

Enclosures:

Plate 1. Geological map
Plate 2. Masanteo geological section
Plate 3. Synoptic Table
Plate 4. Geological cross-section of Cabo Ortegal

INTRODUCTION

A short history of the Dutch research at Cabo Ortegal. — The Galician part of the Hercynian massif, which covers most of the western part of the Iberian peninsula, was selected by Prof. W. P. de Roever as a suitable area for petrological field work by undergraduate and post-graduate geology students of Leiden University. In 1952, during studies undertaken for the University of Amsterdam in the northern-Portuguese part of this massif, Prof. de Roever made the acquaintance of Dr. I. Parga-Pondal. Together they visited the alkaline complex of the Galifeiro; the mapping in this area, started in 1956 by P. Floor, has since resulted in the publication of a thesis (Floor, 1966). Dr. Parga-Pondal's comprehensive knowledge of Galician geology and his large sample collection, kept at the Laboratorio Geológico de Lage, enabled Prof. de Roever to select a few promising areas for further investigation during a visit to Lage in 1956. As a result of this visit, mapping at Cabo Ortegal was started in the same year by P. A. J. Coelewijn. Under the supervision of Prof. de Roever, mapping was started in 1957 by E. Romijn and the author, who were joined in 1958 by H. de Miranda. In 1959 Prof. de Roever was succeeded at the University of Leiden by Prof. E. den Tex, under whose guidance J. P. Engels and A. G. Ho Len Fat started working in the area in 1959 and 1964, respectively.

These investigations were to lead to the publication of two Ph.D. theses, of which the present study, covering the northern part of the area, is the first. The primary aim of both studies is to provide a description of the rock-types and structures encountered. In view of the great resemblance between the rocks from the northern and southern areas, however, the emphasis will be placed here on mineralogical and chemical analysis, and on structural analysis in the thesis under preparation by J. P. Engels.

As part of his undergraduate training, the author mapped the western part of Cabo Ortegal, supervised in the summers of 1957 and 1958 by Prof. W. P. de Roever and in the summer of 1959 by Prof. E. den Tex. The field work for this thesis was entirely directed by Prof. den Tex and was carried out in the summers of 1961 and 1962. Short additional visits were made in the summers of 1965 and 1966. Since the investigations covered areas previously mapped by P. A. J.

Coelewijn, E. Romijn, and H. de Miranda, grateful use was made of their maps, samples, thin sections, and internal reports (Coelewijn, 1959; Romijn, 1959; de Miranda, 1964).

A. GEOGRAPHICAL INFORMATION

Cabo Ortegal, the area under discussion in this paper, is situated in the extreme North of the province of La Coruña, one of the four provinces (La Coruña, Lugo, Pontevedra, and Orense) constituting the former kingdom of Galicia in northwestern Spain. The mapped area is limited on the North and the West by the Atlantic Ocean, on the East by the Ria de Santa Marta de Ortigueira, and on the South by the Ria de Cedeira and the roads between Cedeira and Campo del Hospital and between Campo del Hospital and Puente de Mera.

As a basis for the geological map (Plate 1), which also covers the areas mapped by J. P. Engels and A. G. Ho Len Fat, the following 1 : 25,000 topographical maps, edited by the Cartografía Militar de España, were used: Sheet 1, quadrants I (Cabo Ortegal), II (Ortigueira), and III (Pontigás); Sheet 2, quadrant III (Puerto de Espasante); Sheet 7, quadrants I (Feria), II (San Ramón), III (Neda), and IV (Cedeira). The 1 : 50,000 topographical maps edited by the Instituto Geográfico y Catastral, Madrid: Sheets 1 (Ortigueira), 2 (Ríobarba), and 7 (Cedeira), cover the same area but were found to be less accurate. Geographical data were limited as much as possible on the geological map; for more detail, the reader is referred to the above-mentioned topographical maps. The locality of villages and hamlets is schematically indicated, and only geographical names to which reference is made in the text have been entered on the map.

The presence of a bitumen road along the southern border of the area and of two paved roads and one bitumen road crossing the area from South to North, considerably expedited the work. The recent improvement of unpaved roads used for reforestation purposes now makes it possible to arrive by car at less than an hour's walking distance from any destination within the area. All these roads and some of the more important tracks are indicated on the geological map.

B. GEOLOGICAL SETTING

The crystalline rocks of western Galicia and northern Portugal are situated in the Galician-Castilian zone (Lotze, 1945, a and b) which forms the axial part of the Hesperian massif.

The Galician part of the Galician-Castilian zone is divided by a NNE-SSW-striking fault-zone into an eastern and a western sector. The eastern sector — called “*grupo Oriental*” by Parga-Pondal (1963) and “*domaine externe*” by Capdevila (1965) — is composed mainly of Paleozoic rocks that were folded and metamorphosed during the Hercynian orogeny (Capdevila, 1965). The grade of metamorphism was epizonal in the northern and mesozonal in the southern part of this zone (Capdevila, 1965).

The western part as a whole is composed of frequently polymetamorphic crystalline rocks and was designated by Capdevila (1965) as “*domaines internes*”. It is with these areas that the studies of Leiden University are mainly concerned. A fourfold geotectonic subdivision, as proposed by Parga-Pondal (1956), was taken as a basis for mapping, although it has been slightly altered and amended (den Tex, 1966). This classification embraces the following units (names used by Parga-Pondal are given between brackets):

1. The Ordenes basin (*Grupo de rocas básicas del lopolito*)
2. The Hercynian migmatite front in western Galicia (*Grupo occidental de Lage*)
3. The blastomylonitic graben (*Grupo gneissico del complejo antiguo*)
4. The epi- and late-Hercynian plutonic massifs (*Rocas graníticas*)

The area around Cabo Ortegal (see Fig. i-1) occupies an exceptional position in this geotectonic framework, for while it is physically situated in the *domaine externe*, it is geologically, structurally, and petrographically part of the *domaines internes* and compares more specifically with the Ordenes basin.

The close association of retromorphosed high-grade metabasites with ultrabasites and paragneisses found at Cabo Ortegal, is also found repeatedly in the Ordenes basin (den Tex, 1966) and in areas lying outside the Ordenes basin, to wit: The Rebordelo-Vinhais region (Portugal V. Ferreira, 1965) and the Morais region (Anthonioz, 1966) in northern Portugal. The presence of an abnormal tectonic contact with rocks of Paleozoic age is another feature shared by the Cabo Ortegal area and the Rebordelo-Vinhais region, the Morais region, and the *domaines internes* as a whole (Capdevila, 1965; Portugal V. Ferreira, 1966; Anthonioz, 1966).

C. OUTLINE OF THE GEOLOGY OF CABO ORTEGAL

1. Review of previous studies at Cabo Ortegal

In the earliest known (Parga-Pondal, 1966) geological description of Galicia, Schulz (1835, p. 146 ff.) men-

tions the occurrence of garnet-hornblende gneisses, leptynites (cf. Chimparragneiss), chlorite schists (cf. greenschist), amphibolites, serpentinites, and marble from the area around Cabo Ortegal. Not until late in the nineteenth century was Cabo Ortegal again honoured by a visit from a geologist; this time Macpherson (1881) renewed our acquaintance with serpentinites and associated carbonate rocks in the neighbourhood of Moeche, and also mentioned the occurrence of a garnet amphibolite with pyroxene- and biotite-bearing varieties (cf. Bacariza Formation) from the Sierra de la Capelada. A plutonic rock found near Puente de Mera and called diabase by Macpherson was not recovered during the present investigation, but probably concerns a rock that can be compared with the post-metamorphic gabbroic inclusions found in both the Concepenido and the Capelada Complexes (see p. 152 and p. 185). Fourty years later, the Cabo Ortegal area was visited by Carlé (1945), who thought the serpentinite bodies (cf. Limo & Herbeira) to be magmatic on the basis of their nickel content. He also refers to the occurrence of eclogites and amphibolites associated with biotite gneisses and mentions (p. 19) the presence of gabbropegmatite (cf. metagabbro) with garnetiferous (garnet 2 cm \varnothing) varieties (cf. garnet chlorite schist, p. 164). He ends with the following statement about Cabo Ortegal (p. 26): “*Die verwickelten petrographischen und tektonischen Verhältnisse machen eine genaue Aufnahme dieses Bezirkes in kleinem Massstab dringend notwendig*”, a need which, it is hoped, is partly alleviated by the publication of this thesis.

Since 1945, publications by Parga-Pondal (1956, 1963, 1966), den Tex (1961, 1966), den Tex & Vogel (1962), Vogel & Bahezre (1965), Engels & Vogel (1966), Vogel (1966a and b, 1967), and Vogel & Warnaars (1967) have dealt with problems concerning the Cabo Ortegal area.

2. Rock-types represented on the geological map

Recent deposits. — The only recent deposits indicated on the map are beach sands. Apart from this one exception, it is a bedrock map showing solid only.

Crystalline rocks. — Only the rock-types encountered in the northern area discussed in this paper will be mentioned. To stress the contrast between a mainly meta-sedimentary and a mainly metaigneous group of formations, they have been assigned to two complexes, the Concepenido Complex and the Capelada Complex, with the ultrabasites forming a group apart. The Concepenido Complex comprises eclogites, paragneisses, and Purrido amphibolites; the Capelada Complex covers the Bacariza Formation and the Candelaria amphibolites. The various rock-types will be discussed in the order in which they are mentioned in this paper.

The eclogites are found as foliated, roughly westward-dipping bodies consisting principally of pyralmandine garnet and omphacitic clinopyroxene, with in most

cases either α -zoisite, kyanite, or carinthine as additional constituents. Their retrogradation — in three consecutive phases — into (garnet)amphibolites will be described extensively.

Eclogites or pyrigarnites reported from other areas in western Galicia were mostly found in the Ordenes basin in association with polymetamorphic paragneisses, ultrabasites, and amphibolites. Similar associations were also reported from northern Portugal (Portugal V. Ferreira, 1965; Anthonioz, 1966). Small quantities of eclogite, however, were also reported from the part of the blastomylonitic *graben* lying North of the road between Mugia and Negreira, where they were found associated with orthogneisses (Rubbens, 1963; Geul, 1964; Collée, 1964).

The paragneisses. — Because of textural and mineralogical differences as well as differences in location, the paragneisses have been subdivided into four different formations which are nevertheless considered to be different metamorphic stages of one large metasedimentary unit. These formations are: the Banded Gneiss Formation, the Cariñogneiss Formation, the Chimparragneiss Formation, and the gneisses and blastomylonites from the Carreiro zone of tectonic movement.

The Banded Gneiss Formation occurs interstratified with the eclogites in such a way as to make it impossible to map them separately. This situation led to the assignment of the eclogites to the Banded Gneiss Formation. That the eclogites are nevertheless discussed separately is due to their relative abundance and their importance in clarifying the metamorphic history of Cabo Ortegal.

The banded gneisses themselves are mainly garnet-biotite gneisses with kyanite, β -zoisite, or muscovite as possible additional constituents. Their textures range from glandular to mylonitic; their polymetamorphic nature is reflected in their petrography.

The Cariñogneiss Formation lies East of the Banded Gneiss Formation. The Cariñogneisses can be distinguished from the banded gneisses by their even-grained texture; glandular and mylonitic types do not occur in this formation. Banding caused by differences in the ratio of leucocratic to melanocratic minerals is thought to represent an original sedimentary banding. Garnet-biotite gneiss is the most frequently encountered type of rock in this formation. The polymetamorphic nature of the Cariñogneiss is demonstrated in some of the more pelitic types by the overprinting of a kyanite-bearing association on a staurolite-bearing one. Metabasite inclusions are not so abundant as in the Banded Gneiss Formation; they are common amphibolites.

The gneisses from the *Chimparragneiss Formation* are very similar in appearance to the banded gneisses; they are mainly garnet-biotite gneisses occasionally containing

kyanite. Their textures also range from glandular to mylonitic. A major difference with respect to the Banded Gneiss Formation is found in the metamorphic grade, as reflected by the mineral association of the metabasite inclusions: eclogites in the Banded Gneiss Formation, plagiopyrigarnites in the Chimparragneiss Formation. For the Chimparragneiss too, a polymetamorphic nature was established.

Small quantities of *orthogneiss* of granitic to granodioritic composition, giving evidence of the last (Hercynian) metamorphic phase only, were found locally between the paragneisses of the Chimparragneiss Formation. The orthogneiss is so intimately intermingled with paragneiss that it has been omitted from the geological map (Plate 1), but the places where orthogneiss was found are indicated on a smaller-scale map (Fig. I-18).

The gneisses and blastomylonites from the Carreiro zone of tectonic movement are also polymetamorphic garnet-biotite gneisses (sometimes containing kyanite) which have been severely mylonitized. As metabasite inclusions, heavily amphibolized (plagio)pyrigarnites were found.

The Purrido Amphibolite Formation. — The Purrido Amphibolite Formation consists predominantly of SE-dipping schistose amphibolites with a nematoblastic habit. These amphibolites are composed of hornblende, (saussuritized) plagioclase, and epidote. Relic streaks showing metagabbroic characteristics and bands of garnet-chlorite schist with garnets measuring some centimetres are occasionally found. No catazonal relics were found. Probably the Purrido amphibolites are genetically related to a *metagabbro* body found E of San Julian del Trebol; this body has been amphibolized but not tectonized and shows no traces of polymetamorphism.

The Carreiro zone of tectonic movement. — The Carreiro zone of tectonic movement is a tectonic unit composed of rock-types derived from various complexes. Microfolded Purrido amphibolite, tectonized ultrabasic rocks, and blastomylonitic paragneisses (s.a.) are found in this E-dipping (60°) zone.

The ultrabasic rocks. — Ultrabasic rocks were found in various places. In spite of this dispersion, they are thought to have originally been part of a single large ultrabasic body which was split up by tectonic action and by erosion. Their petrological history involves catazonal metamorphism (formation of garnet and clinopyroxene), mesozonal metamorphism (formation of amphibole and chlorite), and epizonal metamorphism (formation of serpentine).

The Bacariza Formation. — The heading Bacariza Formation covers a complex group of basic rocks consisting of interbanded (plagio)pyrigarnites and (garnet) amphibolites (with or without (\pm) clinopyroxene relics) found in association with calc-silicate rocks,

small amounts of garnet-biotite paragneiss, and leptynites of uncertain origin. The formation as a whole undoubtedly has a polymetamorphic nature.

The Candelaria Amphibolite Formation. — The Candelaria Amphibolite Formation consists of foliated, non-schistose, banded amphibolites composed of hornblende, plagioclase, epidote, and in most cases also garnet and quartz. They proved to be secondary after either garnetiferous metagabbro or (plagio)pyrigarnite. Relics of these two rock-types can still be found between the amphibolites.

Vein quartz. — Several deposits of sterile vein quartz, segregated in fault zones, were large enough to be indicated on the map. In one particular instance — on the peninsula immediately North of Puente de Mera — a fault zone responsible for penetration of paragneiss by multitudes of smaller quartz veins has been mapped entirely as vein quartz.

For readers interested in visiting the area an excursion program describing six short trips in the Cabo Ortegal area has been drawn up (Vogel, 1967).

3. *Dating of major geological events.*

Since no radiometric age determinations have yet been made for the area around Cabo Ortegal, an attempt has been made to correlate some of the major geological events in this area with comparable events in the southern part of West Galicia for which dates are available (Floor, 1966).

Thus, it has been assumed that the latest major orogeny found at Cabo Ortegal — the one that led to severe tectonization accompanied by almandine amphibolite facies (retrograde) metamorphism in all formations — could be directly identified with the latest orogeny in the area SE of Vigo (Floor, 1966), although it there concerns cordierite amphibolite facies metamorphism. This orogeny was dated as Hercynian (about 300 m.y.) on the basis of the radiometric ages of the biotite, lepidomelane, and microcline crystals that were formed by the accompanying metamorphism. This figure of about 300 m.y. is based on the following data:

293 ± 17 m.y. for biotite from a micaschist of Villalba (Capdevila & Vialette, 1965).

292 ± 15 m.y. for biotite from biotite orthogneiss (Vigo) (Priem *et al.*, 1966).

277 ± 14 m.y. and 278 ± 14 m.y. respectively for lepidomelane and microcline from a lepidomelane- and astrophyllite-bearing riebeckite gneiss (Vigo) (Priem *et al.*, 1966).

On the grounds of various whole-rock Rb/Sr ages of epi- to late-Hercynian granites (Bonhomme *et al.*, 1961; Priem *et al.*, 1964, 1965; Capdevila & Vialette, 1965), Floor (1966) places the upper limit of the Hercynian orogenesis in West Galicia at 274—283 m.y.

Similarly, the orthogneisses found as intrusives in the Chimparragneiss Formation may be correlated with

the orthogneisses found E of Vigo (dated on whole-rock Rb/Sr at 500 ± 25 m.y. by Priem *et al.*, 1966), since both were affected by the Hercynian metamorphism, while neither shows evidence of polymetamorphism (cf. Floor, 1966; see also p. 157 ff.). Whole-rock Rb/Sr age determinations provided a comparable age (486 ± 24 m.y.; Priem *et al.*, 1966) for a lepidomelane- and astrophyllite-bearing riebeckite gneiss from the Vigo area.

If it is assumed that the data obtained for southern Galicia apply to the geological events at Cabo Ortegal as well, the following radiometric ages are at our disposal:

1. ± 500 m.y. for the intrusion of orthogneisses affected not by catazonal metamorphism but only by the Hercynian amphibolite-facies metamorphism.
2. ± 300 m.y. for the Hercynian amphibolite-facies metamorphism.
3. 274—283 m.y. for the waning stages of the Hercynian orogenic cycle.

These data indicate that the pre-Hercynian orogeny, which was accompanied by catazonal (eclogite- and high-pressure granulite facies) metamorphism at Cabo Ortegal, took place more than about 500 million years ago. In view of the reported absence of an Assynthian and Taconic phase in NW Spain, a Precambrian age seems acceptable for the orogeny that was accompanied by catazonal metamorphism (see also Floor, 1966 and den Tex, 1966).

In the following pages, the term Precambrian will be used for all geological events connected with the earliest (catazonal) metamorphism, and the term Hercynian will be applied to all geological events connected with the latest (mesozonal) metamorphism. If radiometric age determinations in rocks and minerals from Cabo Ortegal should prove possible, they will decide whether this nomenclature is correct.

4. *The framework of this study*

In Chapters I, II, and III, the petrographical and chemical data of the different rock formations and complexes are presented and compared. In Chapter IV, the structural features deduced from petrological observations and field work are given. The mineral chemistry of garnets, clinopyroxenes, and hornblendes from Cabo Ortegal rocks is discussed in Chapter V. In Chapter VI, the geology of Cabo Ortegal will be recapitulated chronologically on the basis of a synoptic table of geological events (Plate 3).

Explanation of the meaning of sample numbers. — Each locality in the field was provided with a number, and the same number was assigned to the sample(s) taken in that locality. Consecutive samples from one locality are numbered a, b, etc. To prevent confusion with other samples collected in the same area by undergraduate students, the letters Coe (= Coelewijn), E (= Engels), M (= de Miranda), R (= Romijn), and V (= Vogel)

precede all sample numbers. Samples with numbers preceded by G1 or G7 were personally collected by Prof. E. den Tex and are used here with his kind permission.

In the Appendix, the locations of samples mentioned in the text are defined by longitude (W of Madrid) and latitude. In another column their approximate position on the map is given by a codification in which the first number corresponds to the number of the pertinent 1 : 50,000 topographical sheets (1 and 7 for Cabo Ortegal), and the second refers with a letter (A—D)-number (1—5)-combination to one of 20 congruent rectangles (quadrants) into which the 1 : 50,000 map has been divided. This quadrant-system, which was introduced by Dr. I. Parga-Pondal, is now also used in the Galician work done by the Department of Petrology at Leiden University. The positions of the quadrants in the Cabo Ortegal area are indicated in the margin of the geological map (Plate 1).

All the described samples will be included in a collection to be kept at the *Rijksmuseum voor Geologie en Mineralogie* in Leiden. The museum registration numbers can be found in a Table in the Appendix under st.

Explanation of terms and abbreviations used. — To prevent misunderstanding, the sense in which a number of terms and abbreviations is used in this paper will be given below.

For the *grain-sizes* the following subdivision is used:

3 cm.	very coarse-grained	
5 mm.—3 cm.	coarse-grained	
1—5 mm.	medium-grained	
1/3—1 mm.	fine-grained	
1/100—1/3 mm.	microcrystalline	} aphanitic
1/100 mm.	cryptocrystalline	

For *crystallographic properties*, the following abbreviations are used: n_D for the refractive index of isotropic minerals and n_{Dx} , n_{Dy} , and n_{Dz} for refractive indices of uni- and biaxial minerals, in which the suffix D indicates that measurement was made in Na-light.

The symbols a, b, and c are used for crystallographic axes; c/z stands for the angle between the crystallographic c-axis and the optical z-axis; Δ is used for the birefringence ($n_z - n_x$).

Anorthite percentages for plagioclase were determined according to the Fouqué method (Tröger, 1956, p. 101) unless stated otherwise.

Terms for the description of *migmatization* are used in the sense of Mehnert (1960).

Terms concerning metamorphic facies follow Turner & Verhoogen (1960) unless stated otherwise.

The term amphibolite has been used in the sense of de Lapparent (1923): i.e. a rock composed essentially of amphibole and plagioclase. For rocks containing only amphibole, the term amphibole rock or amphibole schist was used.

For the description of *rock textures* the following terms are employed:

banding	— for structures with layers of more than a decimetre.
lamination	— for structures with layers of less than a decimetre.
foliation	— for parallelism of minerals in non-fissile rocks.
schistosity	— for parallelism of minerals in fissile rocks.

The terms *anticline* and *syncline* (anticlinal and synclinal) are used without reference to the stratigraphical position and sequence of the folded rocks (i.e. instead of synform and antiform).

5. Acknowledgements

Prof. W. P. de Roever guided my first steps in the geology of the Cabo Ortegal area; his keen interest in Cabo Ortegal, which did not diminish after his move to Amsterdam, has greatly stimulated my own activities. I am also greatly indebted to him for his valuable advice and for his willingness to read, correct, and criticize large parts of the manuscript.

Prof. L. U. de Sitter, Dr. P. Hartman, and Dr. A. C. Tobi were so kind as to read and evaluate parts of the manuscript. Dr. P. Hartman also gave valuable advice on crystallographical matters.

I wish to extend my thanks to the *Consejo Superior de Investigaciones Científicas* and to the *Comisión Nacional de Geología* for authorizing and patronizing this study; and to Dr. I. Parga-Pondal of the *Laboratorio Geológico de Lage* for all his valuable mediations and his never-failing interest in the geology of Cabo Ortegal.

I am also greatly indebted to Mr. R. Capdevila and Mr. P. Matte, both of Montpellier University, and to Mr. A. Ribeiro of Lisbon University, for their permission to use unpublished material for the simplified geological map of NW Galicia (Fig. i-1).

The preparation of this paper has benefited greatly from the experienced guidance of Prof. E. den Tex. The way in which he always found time to listen to my problems, large and small, made it a pleasure to work under his supervision.

Many discussions with my colleagues, especially Dr. P. Floor, Dr. F. Kalsbeek, Dr. L. van der Plas, Dr. H. G. Avé Lallemand, Dr. J. A. Oele, Mr. H. Koning, Mr. C. F. Woensdregt, Mr. J. P. Engels, Mr. J. R. Möckel, Mr. F. W. Warnaars, and Mr. P. J. C. Nagtegaal, were a great help during the preparation of this paper.

Mrs. I. Seeger corrected the English text and Mrs. M. A. Woensdregt translated the summary into Spanish.

The publication of this paper in its present form would have been impossible without the advice, support, and help of many other persons, especially the members

of the technical and administrative staff of the Leiden Institute for Geology.

All illustrations, maps, and sections were prepared by Mr. J. Bult. The chemical analyses were done by Mrs. H. M. I. Bult-Bik under the supervision of Mrs. Dr. C. de Sitter-Koomans up to June, 1965. After that date they were done by Mrs. A. de Best-Giesbert and Mr. L. F. M. Belfroid under the supervision of Mr. K. M. Stephan. Mrs. B. C. Romijn-van der Plas prepared the Tables for printing. Mr. A. Verhoorn

prepared the X-ray photographs; Mr. C. F. Woensdregt and Mr. R. O. Felius identified them and calculated the a_0 -values. Mr. J. Hoogendoorn made all the photographic illustrations. Mr. M. Deijn and Mr. C. J. van Leeuwen made all the thin sections.

The friendship and hospitality of the García and Piñon families at Cedeira made my stay there an unforgettable one.

CHAPTER I

THE CONCEPENIDO COMPLEX

A number of mappable units of different composition and also differing as to grade of metamorphism are taken together as the Concepenido Complex. These units are, from East to West, the Cariñogneiss, the banded gneiss, the eclogite, the Chimparragneiss, the Carreiro zone of tectonic movement, and the Purrido amphibolite.

Despite their differences in metamorphic history and the resulting differences in texture and mineralogical composition, Cariñogneiss, banded gneiss, Chimparragneiss, and blastomylonite are considered, on the basis of the geological, petrographical, and chemical evidence, to be different modifications of one and the same metasedimentary unit. This metasedimentary unit was successively subjected to a mainly catazonal metamorphic phase and to a mesozonal metamorphic one.

The gabbroic and granitic intrusions in the metasediments are also considered to belong to this basically metasedimentary unit, whether (like the eclogites and the pyrigarnites) they have undergone both metamorphic phases or only the mesozonal metamorphic phase (like the Purrido amphibolites, the metagabbro at San Julian del Trebol, and the granitic rocks found as intrusions in the Chimparragneiss and the Banded Gneiss Formations).

A. ECLOGITES

1. Occurrence

Large outcrops of eclogite are found in a zone running from Punta Aguillones in roughly south-westerly direction. Because eclogite has a greater resistance to weathering than banded gneiss and retrograde eclogite, the outcrops are found as peaks and ridges. The most important of these are, going from north-east to south-west: Aguillón, Peña de Faroleiro, Monte Castrillon, where the eclogite is being quarried for the construction of a breakwater, Miranda (photograph I-1), Concepenido, Alto da Foxo, and Sierra de Moles. The outcrops show a marked schistosity which is generally steeply inclined, predominantly westward (photograph I-2). Banding resulting from differences in mineralogy and grain-size lies parallel to the schistosity.



Photo I-1 Eclogite, outcropping in three separate ridges on the Miranda (centre), looking North. Background, left: Limo; background, right: Masanteo.



Photo I-2 Easternmost (right) and central (left) eclogite ridges of the Miranda, showing the steeply westward-dipping schistosity plane.

A host of much smaller fragments of eclogite and retrograde eclogite occurs in the Banded Gneiss Formation. A general geological description of these rocks will be given in Chapter I, B 1. For the sake of convenience, however, their petrography is incorporated into this chapter. The gneiss intercalations between the eclogites will be described in Chapter I, B.

2. Nomenclature

According to Häuy (1882), eclogite is an essentially biminerale rock consisting of garnet and clinopyroxene; with kyanite, "*epidote blanc vitreux*" (zoisite?), quartz, and amphibole as additional constituents. The presence of a mineral other than garnet, clinopyroxene, quartz, or one of the accessories, occurring as a stable phase in an eclogite, is indicated in the name (for instance "kyanite eclogite"). In this connection, use of the term carinthine¹ eclogite for eclogites with a stable hornblende is considered preferable to that of amphibole eclogite to avoid confusion with the term hornblende eclogite, which can then be reserved for eclogites with 10–25% secondary hornblende.

The ubiquitous effects of retrograde metamorphism have given rise to a nomenclature in which the extent of the amphibolization is expressed. The original nomenclature of Hezner (1903) as amended by Eigenfeld-Mende (1948) was adopted and supplemented by Lange (1963). The classification of Lange will be used for the Cabo Ortegal eclogitic rocks. That is to say: rocks with less than 10% secondary hornblende will be called eclogite. Rocks with more than 10% secondary hornblende but with less than 5% secondary plagioclase are called hornblende eclogite. Rocks with more than 10% secondary hornblende and more than 5% secondary plagioclase are called amphibolite eclogite if they carry more omphacite than secondary hornblende, and eclogite amphibolite if they carry more secondary hornblende than omphacite.

3. Varieties of eclogite

The investigated area was found to contain α -zoisite eclogite and carinthine eclogite. Kyanite was present in retrograde eclogites only; this indicates that, although none were found, unaltered kyanite eclogites were once and may still be present.

Carinthine eclogite. — The best example of an unmodified carinthine eclogite in our series is sample V 1023. At location 1023, carinthine eclogite occurs together with a meta-olivine gabbro (sample V 1023a, for description see Ch. I, B 1 e) in a 2 × 5 m concordant lens in the Banded Gneiss Formation.

Sample V 1023. Macroscopically, the rock is fine-grained and non-oriented, and has a spotted appearance caused by dark clusters (\varnothing 0.3–1 cm) of carinthine set in a pale mass of garnet and omphacite.

Microscopically, the colourless euhedral garnet grains (\varnothing 0.05–0.10 mm) are arranged in ring- and lath-shaped forms. The garnets are free of inclusions. The interstices of this garnet-mesh are filled with aggregates of clinopyroxene (omphacite, \varnothing 0.05 mm)² or amphibole (carinthine, \varnothing 0.12–1 mm)², which are mutually exclusive.

The anhedral colourless omphacite grains are riddled with minute inclusions of rutile, whereas the rutile in the carinthine occurs as larger isolated grains or in clusters. The anhedral to subhedral carinthine, which macroscopically has

a reddish-brown colour, is colourless in thin section but where it borders on omphacite it shows a very faint pleochroism in tones of light-brown. Some of the carinthine aggregates still show the outline of the idiomorphic olivine that they have replaced. Aggregates of sericite, an occasional plagioclase grain (An. 18%), and some pyrite occur only within the patches of carinthine. They are considered to be relics, not yet transformed into eclogitic minerals.

In sample V 1023 as well as in other metabasites from Cabo Ortegal (Engels & Vogel, 1966), metamorphism has caused the growth of garnet between the mafic minerals and plagioclase. Consequently, in the totally metamorphosed rock the distribution of the garnet reflects the original texture of the metabasite, provided no deformation has occurred. Figure I-1 shows the ophitic pattern of the olivine gabbro simulated by the pattern of the garnet-growth as it can be seen in sample V 1023; for comparison, an example of a more corona-like palimpsest texture of garnet in an eclogite from Martinsreuth (Düll, 1902) has been included (Fig. I-2). The close association of carinthine eclogite with meta-olivine gabbro and the presence of blastophytic texture in sample V 1023 are considered to constitute strong evidence in support of the hypothesis that eclogitic rocks can be formed by metamorphism of basic igneous rocks.

Another carinthine eclogite (sample V 1323) comes from a concordant lens in the Banded Gneiss Formation. Macroscopically, the rock has a dense, fine-grained appearance with a faintly-developed foliation. Microscopically, the rock is seen to consist principally of garnet (colourless, subhedral to euhedral, \varnothing 0.05–0.12 mm, no inclusions), carinthine (x colourless < y = z light reddish-brown, anhedral to subhedral, \varnothing up to 0.4 mm), and clinopyroxene (colourless, anhedral, with a dusty appearance caused by inclusions). Minor constituents are quartz, rutile sometimes showing a rim of titanite, and some ilmenite. The preferred orientation of the carinthine causes a weakly-developed foliation, but the patchy arrangement of carinthine and omphacite between ring- and lath-shaped garnet aggregates is totally disturbed.

α -zoisite eclogite. — The vast majority of the eclogite outcrops are composed of α -zoisite eclogite and its products of retrograde metamorphism. All the samples show some signs of amphibolization. The α -zoisite content varies from 0.1% (sample V 1050) to 22.6% (sample V 1016).

Sample V 1050, from one of the large outcrops (175 × 125 m) on the Miranda, is the best-preserved α -zoisite eclogite found.

Macroscopical appearance: the rock is medium-grained, equigranular, and unoriented. The red garnet-crystals lie in a green mass composed of omphacite.

Microscopical appearance: the rock is virtually biminerale, garnet (euhedral to subhedral, \varnothing \approx 1 mm, extremely light-pink) and omphacite (anhedral, slightly elongate, light-green, non-pleochroic) constitute 90% of the total mineral content. The remaining 10% is shared by strain-free interstitial quartz, anhedral α -zoisite, apatite, and rutile intergrown with ilmenite as primary constituents; blue-green pleochroic hornblende, plagioclase, pistacite, and titanite

¹ For a discussion of the name carinthine, see Chapter V, C.

² For chemical and physical properties, see Table V-5.

as secondary minerals; prehnite and adularia as minerals occurring in dilatation veins (0.1 and 0.06 mm wide respectively). In addition to quartz, rutile, omphacite, and ilmenite, a light-brown pleochroic carinthine-like amphibole forms inclusions in garnet. Rutile and α -zoisite are the only minerals included in omphacite.

The secondary minerals (hornblende, plagioclase, pistacite, and titanite) are concentrated around the veins of adularia, although hornblende occurs elsewhere in small quantities, patchily replacing omphacite or as 0.01 mm-wide kelyphitic rims between garnet and omphacite.

Also virtually biminerally is sample M 459 (medium-grained eclogite). Usually, the colours of the garnet and omphacite in the eclogites are so light that they appear to be almost colourless in thin section. In thin section M 459, however, the garnet³ is definitely pink and the clinopyroxene³ is pleochroic in shades of bluish-green. A well-developed foliation is caused by the preferred orientation and parallel arrangement of elongate clinopyroxene and garnet crystals. Amphibolization is little advanced (less than 3% is secondary hornblende) as is symplectitization (stages 1, 2, and 3). The α -zoisite is present as an occasional inclusion in omphacite. Additional constituents are: strained quartz, some secondary plagioclase, rutile, apatite, zircon, and opaque matter (magnetite, ilmenite).

The properties of the minerals from the α -zoisite-rich eclogite of sample V 1016 resemble those of sample V 1050. However, the modal composition and texture differ a great deal. The amphibolization is better developed and the omphacite shows incipient stages of symplectitization. The texture is strongly oriented as a consequence of the parallel arrangement of omphacite, aggregates of α -zoisite-prisms with rounded edges, and elongate pockets of slightly undulose quartz.

4. Amphibolization

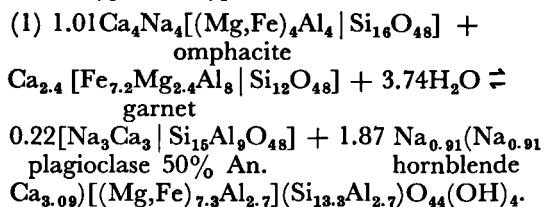
The gradual retrograde replacement of eclogite by amphibolite has been demonstrated by Hezner (1903) and Sahama (1935) to be isochemical except for the addition of H₂O. This replacement is the result of two different processes: the formation of kelyphitic rims around garnet and the substitution of common hornblende for omphacite.

The formation between garnet and omphacite of kelyphitic rims with a radial or concentric texture has been reported for a large number of eclogite occurrences, though according to Coleman *et al.* (1965) it does not occur in eclogites associated with glaucophane-schists. These rims are believed to be caused by the interaction of garnet and omphacite with addition of H₂O. The hornblende of the kelyphite generally has a more intensive pleochroism than the hornblende that replaces omphacite. The following types of kelyphite have been described from eclogites:

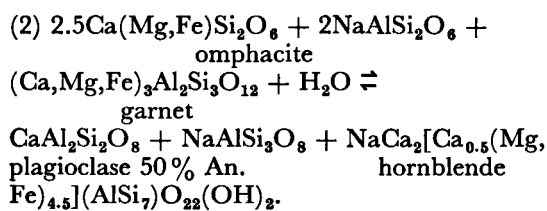
1. Hornblende.
2. Hornblende + plagioclase (Düll, 1903; Alderman, 1936; Wang, 1939; Forster, 1947). This plagioclase has an anorthite content of 26–55%, according

³ For the chemical and physical properties, see Tables V-2 and V-5.

to Wang (1939). The following reaction equation given by Forster (1947) accounts for the formation of this type of kelyphite:



Other equations are also possible, however, for instance:



3. Hornblende + plagioclase + quartz (Eigenfeld-Mende, 1948).
4. Diopsidic clinopyroxene + plagioclase + quartz (Eigenfeld-Mende, 1948).
5. Hornblende + plagioclase + magnetite (Hezner, 1903; Alderman, 1936).

In the eclogitic rocks at Cabo Ortegal, types 1, 2, and 5 have been found. Here, the initial stage of kelyphitization is the formation of an extremely narrow rim of hornblende between omphacite and garnet. As the rim grows in width the hornblende can be seen to be homoaxially intergrown with its neighbouring omphacite. Small plagioclase flakes locally lie between hornblende and garnet. As the kelyphite grows further inwards, replacing the garnet, the hornblende keeps the same orientation but is intergrown with elongate plagioclase crystals arranged roughly perpendicular to the circumference of the garnet crystal, thus giving the kelyphite a radial character. In this stage the kelyphite grows not only where garnet borders on omphacite but also where it borders on other minerals. If magnetite is present it lies as anhedral grains dispersed in the kelyphitic rim. Photograph I-3 shows a kelyphite rim in an α -zoisite-hornblende eclogite (sample V 1238); the bordering omphacite has been totally replaced by blue-green hornblende. Starting from within, first a rim of hornblende with radially arranged plagioclase, then a rim of hornblende with unevenly distributed plagioclase, and then a narrow rim of hornblende without inclusions, can be seen surrounding the garnet. The outer rim passes into the hornblende secondary after omphacite with which it is homo-axially intergrown and from which it can be distinguished by its greater c/z angle and its more intense pleochroism.

The conversion of omphacite into blue-green hornblende starts with the growth of patches of hornblende homoaxially intergrown with the clinopyroxene.

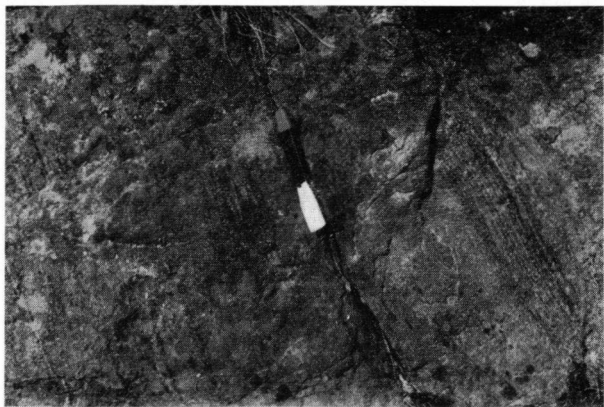


Photo I-6 Locality V 1050. Patches enriched with hornblende crystals arranged parallel to the foliation; probably caused by a (hidden) pegmatoid vein.

The patchy enrichment with hornblende crystals with an arrangement parallel to the schistosity, as observed at locality V 1050, probably had a similar origin (photograph I-6).

The role of differential movements in facilitating the circulation of infiltrating solutions is illustrated, for instance, at locality V 1271, where a 45 cm-thick layer of deformed α -zoisite-bearing eclogite amphibolite lies in undeformed α -zoisite-bearing hornblende eclogite (photograph I-9).

These phenomena, acting separately or in combination on a larger scale, could conceivably have converted vast eclogite bodies into amphibolite.

5. Symplectitization

A very characteristic phenomenon in the retrograde metamorphic transformation of eclogite is the formation of a diablatic intergrowth of clinopyroxene with sodic plagioclase secondary after omphacite. Such symplectitic intergrowths of clinopyroxene and plagioclase will hereafter be referred to as p.p. symplectite. The symplectitization process of the clinopyroxenes from eclogites at Cabo Ortegal proceeds in four different stages in exactly the same way as described by Eskola (1921) for the eclogites of Norway.

Stage 1. Small dusty zones form along the rims of the crystals and along cracks (Fig. I-3). The p.p. symplectite in the rims has the same optical orientation as the clinopyroxene crystal it surrounds; the p.p. symplectite formed in the cracks has an optical orientation that differs from that of its host and is obviously a penetration optically continuous with a neighbouring clinopyroxene crystal.

Stage 2. On its inner side the dusty zone has a thread-like pattern forming a gradual transition to the stage 3 p.p. symplectite. Sometimes, if this stage is absent, the dusty zone is separated by a sharp boundary line from the more advanced p.p. symplectites.

Stage 3. Further inwards, the p.p. symplectite becomes coarser and a cauliflower-like single plagioclase crystal is seen to be dendritically intergrown with the clinopyroxene (Fig. I-4).

Stage 4. As the symplectitization process advances, the cauliflower-like growth is changed into a coarser granular impingement structure giving the clinopyroxene a poecilitic appearance (Fig. I-5).

The following properties of the p.p. symplectites were observed:

1. The newly-formed plagioclase rods are part of a single crystal throughout one p.p. symplectite individual.
2. The newly-formed clinopyroxene is optically continuous with its mother-crystal of omphacite.
3. The symplectitic front penetrates lobularly (Fig. I-4) into neighbouring clinopyroxene crystals (see Eskola, 1921).
4. The p.p. symplectite is separated by a roughly 0.01 mm-wide monomineralic clinopyroxene rim from the neighbouring quartz (Fig. I-7), into which it penetrates (see Forster, 1947).
5. The measure of symplectitization increases in the neighbourhood of narrow zones of differential movement.

The observations support the statement by Forster (1947) and Lange (1965) that amphibolization and symplectitization are two mutually independent processes, since:

1. The nature of the two processes is different; symplectitization operates as a chemically closed system (see Ch. V, B 4), whereas for amphibolization the addition of H_2O is necessary.
2. The fractures along which p.p. symplectite penetrated can be seen to continue in the neighbouring garnet crystals, but they are not continued in the neighbouring hornblende crystals (Fig. I-3).
3. Hornblende often grows pseudomorphously after p.p. symplectitic forms.

Because the unmixing of plagioclase from omphacite results in the formation of a stable association of clinopyroxene, garnet, and sodic plagioclase, the reaction is thought to have taken place under conditions of the clinopyroxene-almandine subfacies of the granulite facies (de Waard, 1965).

6. Mineralogy

To facilitate the microscopical description of the retrograde eclogites, significant characteristics and mutual relations of some of the minerals occurring in eclogite and retrograde eclogite will be discussed in this Chapter (see also Table I-4).

Garnet. — The inclusions found in the eclogite garnets are manifold. Some of them (blue-green hornblende, β -zoisite, quartz, plagioclase, epidote, magnetite, ilmenite, and pyrite) are younger than the garnet and are probably products of selective alteration; others (omphacite, α -zoisite, apatite) are considered to be contemporaneous with the garnet. Inclusions of a light-brown pleochroic, often euhedral, carinthine-like hornblende are thought to represent an early stage in the formation of eclogite. The most frequent

inclusions, however, are quartz and rutile; they are considered to be a residue and a by-product, respectively, of the formation of garnet from pre-eclogitic minerals. The quartz inclusions are small grains ($\varnothing < 0.02$ mm), often so numerous as to give the garnet a poecilitic appearance. The rutile inclusions occur as single crystals (\varnothing up to 0.1 mm), in clusters as sagnetite, or in dusty clouds of minute crystals (Fig. I-8). Some lie in the core, leaving the rim free of inclusions, others lie in a ring between a "clean" core and a "clean" outer rim. In the garnets of sample V 1100 (α -zoisite-hornblende eclogite) they are arranged in such a way that they enclose a rutile-free core with the outlines of a euhedral garnet (Fig. I-8). In sample V 1102a (biotite-garnet amphibolite mylonite, retrograde after eclogite) the dusty zones have outlines suggesting that they are pseudomorphous after some titaniferous pre-eclogitic mineral (biotite?, titanite?, Fig. I-9), which more or less agrees with Düll's (1902, pp. 88—89) observation: "*In fast allen Granaten zeigen sich die nicht assimilierbaren Substanzen, TiO_2 und überschüssiges SiO_2 , als Rutil und Quarz, meist in Form von Mikrolithenscharen als häufigste Einschlüsse. Die Rutilmikrolithe finden sich im Granat häufig noch in der gleichen Orientierung, wie die Titanerzinterpositionen in Gabbro-Pyroxen.*"

Nowhere does the arrangement of the inclusion suggest a relic-schistosity, and no helicitic textures have been found.

Similar rutile inclusions have also been described by Riess (1878), Düll (1902), Hezner (1903), Brière (1920), Sahama (1935), Forster (1947), Eigenfeld-Mende (1948), and Smulikowski (1960, 1964); which is not remarkable, since Ti^{4+} cannot enter the lattice of the eclogite-garnet (see Ch. V, A).

The importance of these rutile inclusions is that they occur in nearly all eclogites, that they do not occur in pyrigarnites (see Ch. III), and that they are preserved in the garnet relics in retrograde eclogites. Consequently, it is possible to separate the amphibolites retrograde after eclogite from those retrograde after pyrigarnite, on the basis of rutile inclusions, provided that relic garnet is present.

Formation of second-generation garnets in eclogites under amphibolite or granulite facies conditions will be discussed in Chapter V, A.

Epidote-group minerals. — α -zoisite is the only member of the epidote-group found as a stable phase together with omphacite and garnet in the Cabo Ortegal eclogites. That it is not a secondary mineral is apparent from the fact that it occurs as inclusions in omphacite and garnet; moreover, the minerals sparingly included in α -zoisite are all of a primary nature, viz. rutile, garnet, and zircon.

Optically, the α -zoisite is characterized by a low birefringence with anomalous interference colours, parallel extinction, and the orientation of the axial plane parallel to (010). The positive optic axial angle was measured on a universal stage; it varied from 73° in sample V 1055a (α -zoisite-hornblende eclogite) to 37°

in sample V 1016 (α -zoisite eclogite), with in both cases a $r \ll \ll v$ dispersion of the optic axes.

A second generation of α -zoisite occurs in post-eclogitic pegmatoid veins; here it often encloses a zoisite with $2V^*$ large, $r \gg \gg v$, and Δ lower than α -zoisite, provisionally called γ -zoisite (see Vogel & Bahezre, 1965). This variety of zoisite may be even richer in Fe^{+3} than α -zoisite (0.34—0.38 per 25 O as against 0.28 per 25 O for α -zoisite with $2V^* = 70^\circ$), if Myer's (1966) data concerning the relation between Fe content and axial angle for zoisite are extrapolated for the above-mentioned γ -zoisite. Owing to later phases of deformation, these veins sometimes appear as extremely deformed leucocratic streaks in the eclogite still carrying α -zoisite (occasionally with enclosed γ -zoisite), which sometimes makes it difficult to distinguish primary α -zoisite from the α -zoisite introduced as a vein mineral.

Other members of the epidote group are all post-eclogitic. The combinations in which they occur permit a determination of their relative ages as well as a rough estimation of the facies conditions under which they were formed.

The formation of β -zoisite may be connected with a granulite-facies retrograde metamorphic phase, for at lower metamorphic conditions, surplus Fe^{+3} stored in α -zoisite (Myer, 1966) may be more easily accommodated by other minerals (garnet, hornblende). β -zoisite may replace α -zoisite, kyanite, and garnet; it could be distinguished from α -zoisite by the different orientation of its optic axial plane: \perp (010), by a higher birefringence (0.007^* in sample V 1053), and by the dispersion of the optical axes ($r > v$). The positive optic axial angle usually varies around 46° ; the following values were measured on the universal stage: 43.5° (sample V 1227), 44.5° (sample V 1053), 46.5° (sample V 1145), and 48.5° (sample V 1146c), with in all cases $r > v$. The β -zoisite in sample Coe E 1 has a much smaller optic angle: $2V^* = 19.5^\circ$ with $r \gg v$. The formation of *epidote* is thought to be related to the amphibolite-facies retrograde metamorphic phase. As an alteration product, epidote may replace α -zoisite, β -zoisite, kyanite, garnet, clinopyroxene, or hornblende. Individual epidote crystals often have a zoned structure; the $HCa_2Fe_3Si_3O_{13}$ content increases — according to optical observations — from the core towards the rim, varying from 5 to 15%. Post-amphibolitic epidote is found in hydrothermal veins in association with adularia, prehnite, pistacite, and pumpellyite. Solutions emanating from these veins may promote the formation of *pistacite* crystals.

The occurrence of a metamict, occasionally zoned *orthite* ($2V^* = 80—90^\circ$, $r > v$) in retrograde eclogite is related to the presence of pegmatoid veins. Orthite is frequently found as inclusions in epidote and hornblende but never in the eclogite minerals or in β -zoisite.

Kyanite. — Like α -zoisite, kyanite is found in the Cabo Ortegal eclogites not only as a typomorphic phase but also as a post-eclogitic mineral. The typomorphic kyanite is anhedral and has rounded elongate forms

oriented parallel to the foliation; it is often broken or bent (sometimes 90°). Usually, it is surrounded by rims of sericite (paragonite?), β -zoisite, or both (photograph I-8), and was gradually being replaced by these minerals. In some cases kyanite is surrounded, together with its alteration products, by a rim of sodic plagioclase. Kyanite enclosed in garnet does not show signs of alteration. The anhedral post-eclogitic kyanite occurs in the pegmatoid veins associated with the post-eclogitic β -zoisite by which it is often surrounded. Solutions emanating from these veins have caused the growth of a second kyanite generation in the altered eclogitic rocks (sample V 1058, see p. 137). These kyanites can be discerned from the typomorphic variety by their random orientation, their poiciloblastic texture, and the absence of sericite or β -zoisite rims. Their occurrence indicates that the pressure at the time of their formation was higher than 6 kb (Fonteilles, 1965). A similar distinction between typomorphic and post-eclogitic kyanite has been made by Scharbert (1954).

Hornblende. — The hornblende in the eclogites can be classified in five types with different optical properties. Their colour changes from brown to blue-green with decreasing metamorphic grade, a phenomenon known from many regionally metamorphosed areas (Shidó, 1958; Miyashiro, 1958; Engel & Engel, 1962a; Kalsbeek, 1962; Layton, 1963; Binns, 1965).

Types 1 and 2 occur as stable phases in eclogite and are considered to be carinthines. Carinthine is chemically a common hornblende, but it is distinguished by a high $Mg/\Sigma(X+Y)$ ratio (see Ch. V, C), by a pleochroism in brown colours (Angel, 1929) or by the virtual absence of pleochroism in thin section (Düll, 1902; Eigenfeld-Mende, 1948; Smulikowski, 1960, 1964; Lange, 1965).

Type 1 has a light reddish-brown colour macroscopically; in thin section it is colourless. It is found as fine-grained anhedral to subhedral grains in eclogite. For its chemical and optical properties the reader is referred to Tables V-4 and V-5.

Type 2 shows an extremely light shade of brown microscopically; it occurs as rims around colourless carinthine. In nearly all eclogitic rocks it is found as small (\varnothing up to 0.1 mm) subhedral to euhedral grains included in garnet. In sample V 1030 (a carinthine amphibolite eclogite) it is found as a separate phase together with garnet, symplectitic clinopyroxene, and plagioclase. The optical properties are: $2Vz = 85-90^\circ$, $r > v$, $\Delta = 0.16-0.18$, $c/z = 18-20^\circ$, x colourless $< y$ reddish-brown $\leq z$ brown.

Type 3 is more widely distributed. It is pleochroic in greenish-brown and brownish-green colours. When zoned, the greenish-brown hornblende is surrounded by the brownish-green kind. Inclusions of β -zoisite prove it to have been formed later than that mineral. Growths pseudomorphous after p.p. symplectite show that it replaces omphacite and that its formation occurred after symplectitization. Its colour is dark blue-green where it borders on garnet. Its optical

properties are: $2Vx = 80-90^\circ$, $r > v$, $\Delta = 0.19-0.20$ $z/c = 19-21^\circ$.

Type 4 is the common blue-green hornblende occurring in kelyphitic rims around garnet or as pseudomorphs after omphacite or p.p. symplectite; it is also found selectively replacing garnet. Its optical properties are: $2Vx = 80-90^\circ$, $r > v$, $\Delta = 0.020-0.022$, $c/z = 17-19^\circ$, x extremely light yellowish-green $< y$ olive green = z green or bluish-green, with a higher absorption where it borders on garnet. Habit and effects of post-crystalline deformation are similar to those of the type 3 hornblendes, but because it forms rims around the brownish-green hornblendes, the blue-green hornblende is considered to be younger.

Type 5 occurs where the blue-green hornblende is cut by veins carrying epidote, adularia, or prehnite; here, a pale bluish-green actinolitic hornblende, homoaxially intergrown with the blue-green hornblende, takes the place of the vein minerals. It is characterized by its lower absorption and higher birefringence ($\Delta = 0.022-0.024$). It also occurs in combination with albite replacing omphacite and blue-green hornblende. It has never been found showing signs of deformation. Thus, the hornblendes can be seen to change with the facies conditions, types 1 and 2 having been formed under eclogite facies conditions, type 3 under hornblende-clinopyroxene-almandine subfacies conditions, type 4 under amphibolite facies conditions, and type 5 under greenschist facies conditions.

Accessory minerals. — Zircon was found in almost every sample. It occurs as small (length 0.03 mm), clear, rounded grains and as larger (length 0.2 mm), turbid euhedral crystals. It is not an unusual mineral in eclogites (cf. Düll, 1902; Sahama, 1935; Eigenfeld-Mende, 1948; and Smulikowski, 1964).

Apatite is always fine-grained (\varnothing up to 0.5 mm). The grains are usually subhedral or anhedral with rounded forms, and often lie concentrated in aggregates or, in deformed rocks, in streaks of undulose grains. Needle-shaped inclusions arranged parallel to 001 are sometimes present in such quantities that the apatite has a dusty appearance, but apatite without any inclusions is also found.

Rutile is fine-grained and anhedral when not included in garnet. Usually, it has a honey-brown colour, but violet-coloured rutile also occurs. The latter type, according to Chensnokov (1964), indicates a reductive environment. It is often intergrown with *ilmenite*; the conversion to *titanite* is seen to have been simultaneous with the amphibolization. Due to this relation, titanites almost always carry a core of rutile.

In rare instances secondary *calcite* was found.

The opaque minerals include *ilmenite*, *magnetite*, *pyrite*, *hematite*, and *limonite*.

7. *Retrograde eclogite*

Several retrograde metamorphic phases have, at different times and under different facies conditions, transformed originally eclogitic material into hornblende eclogite, amphibolite eclogite, eclogite amphib-

olite, or amphibolite. Retrograde metamorphism took place under hornblende-clinopyroxene-almandine subfacies, amphibolite facies, and greenschist facies metamorphic conditions, and was sometimes accompanied by deformation. The eclogite generally shows a distinct foliation (M_1)⁴ due to and characterized by parallel orientation of prismatic α -zoisite and elongate crystals of omphacite and kyanite. Quartz lies in irregularly-shaped aggregates of non- or only slightly undulose crystals.

Deformation (M_2) under hornblende granulite facies conditions probably re-activated the older foliation plane, since various fabric elements, i.e. newly-formed omphacite lobes and β -zoisite crystals, are now arranged parallel to it and to each other. The irregularly-shaped quartz aggregates were transformed into lenticular ones, which (together with similar aggregates of β -zoisite) are disposed parallel to the foliation.

Under amphibolite-facies conditions, another deformation (M_3) took place, but because the resulting foliation plane has no characteristic elements by which it can be distinguished from the earlier foliations, it is often difficult to distinguish and to determine its relation to the previous planes. Locally occurring narrow zones of blastomylonite with an amphibolite facies mineral composition cut the old foliation (M_2) at an angle, but it is not certain whether these blastomylonites resulted from the same stress field as M_3 .

Extremely narrow mylonitic zones without any recrystallization (M_4) are correlated with the greenschist retrograde metamorphic phase; they also cut older foliation planes at an angle.

Since the degree to which the eclogites are tectonized or amphibolized may differ between zones ranging widely in size, and since the different phases of deformation and amphibolization may be superimposed upon each other, the retrograde eclogites of course vary widely in appearance.

a. Hornblende eclogite.

In the majority of the hornblende eclogites, α -zoisite occurs as a minor constituent; some also contain kyanite, either alone or in combination with α -zoisite or (post-eclogitic) β -zoisite. Hornblende eclogites without minor constituents also occur.

Sample V 1278 is an example of an α -zoisite-hornblende eclogite with a random orientation of the con-

stituent minerals that was not affected by post-eclogitic deformations.

Microscopically, the rock is fine- to medium-grained with a random orientation of the constituent minerals. The subhedral to euhedral garnets contain inclusions of quartz, rutile, brown pleochroic hornblende, and α -zoisite. Hornblende (type 3, x yellowish to colourless < y brownish-green < z bluish-green) occurs as isolated poeciloblasts or aggregates of poeciloblasts measuring up to 1 cm in diameter. Where it borders on garnet the hornblende has a more intensive pleochroism, and it often forms a kelyphitic rim together with plagioclase. Anhedral clinopyroxene crystals (\emptyset up to 1.2 mm) were only locally transformed into hornblende; stage-1 p.p. symplectites occur regularly along their boundary planes, and more advanced stage-3 p.p. symplectites can be seen penetrating as lobes into neighbouring clinopyroxene crystals. The α -zoisite crystals (length up to 0.25 mm) have rounded subhedral forms and are surrounded by dusty rims. Plagioclase is only found as a by-product of amphibolization or symplectitization. Quartz has crystallized in the interstices and shows straight or slightly undulose extinction.

Sample V 1238 is a medium-grained α -zoisite-hornblende eclogite with a macroscopically visible foliation due to M_1 . Microscopically, it resembles sample V 1278, except for the distinct foliation, the greater dimensions of the garnet (\emptyset up to 2.5 mm), and the slightly undulose extinction of omphacite and hornblende.

In sample V 1040, which is a medium-grained hornblende eclogite, post-eclogitic deformation has led to a secondary foliation (due to M_2) characterized by parallel arrangement of lobes of p.p. symplectite and wavy streaks of undulose quartz. Microscopical observations show that the deformation post-dated the pegmatoid injection, since the pegmatoid minerals (quartz, plagioclase, biotite⁵, and kyanite) occur in streaks of bent and broken crystals. The deformation also occurred later than the kelyphitization, because the hornblende-plagioclase-magnetite kelyphite is preserved only in the stress-shadow of the garnet, whereas at the stressed sides hornblende and plagioclase have disappeared, leaving a rim of small magnetite grains as the only remnant of the pre-existing kelyphite. However, the deformation must have taken place at an early stage in post-eclogitic history, since it promoted the symplectitization of the omphacite (only 10% of the original omphacite is not altered into p.p. symplectite). If the facies conditions are assumed to have declined gradually after the eclogitic stage had been reached, the kelyphitization must have taken place under PT conditions corresponding at most to the hornblende-clinopyroxene-almandine subfacies of the granulite facies.

⁵ Biotite occurs symplectitically intergrown with plagioclase. Similar biotite-plagioclase symplectites were observed by Forster (1947) and Spry (1963). At Cabo Ortegal their occurrence is restricted to narrow leucocratic zones (pegmatoid injections), in which they are not infrequently found. There is no reason to suppose that their growth was pseudomorphous after p.p. symplectite. In some places they surround muscovite or kyanite crystals, and often they are themselves surrounded by a narrow rim of plagioclase (widths of up to 0.1 mm) optically continuous with the neighbouring plagioclase from the biotite-plagioclase symplectite.

⁴ To distinguish between these deformational phases and between the resultant foliations, they have provisionally been termed M_1 , M_2 , etc. to indicate that their recognition is largely dependent on the occurrence of recognizable metamorphic associations. The use of the symbols S_1 , S_2 , etc. has been avoided because the results of a detailed investigation into the structure and fabric of the Cabo Ortegal area, which is now being carried out by J. P. Engels, is likely to yield a different meaning for these symbols.

At location V 1007 a fine- to medium-grained α -zoisite eclogite with a well-developed M_1 is encountered. Parallel to the foliation there is a 75 cm-wide band consisting of medium- to coarse-grained α -zoisite eclogite which passes into a medium- to coarse-grained β -zoisite-hornblende eclogite.

In sample V 1007a, which was taken from this band, the transition is seen to be abrupt (photograph I-7); the hornblende content suddenly increases from less than 5% in the eclogite to well over 15% in the hornblende eclogite. The secondary foliation in the hornblende eclogite is more pronounced than the primary one in the eclogite. Microscopically, the β -zoisite-hornblende eclogite contains subhedral to euhedral light-pink garnet poeciloblasts (\varnothing up to 1 cm) with numerous inclusions of the same brownish-green hornblende that replaces omphacite. This suggests the continuation of garnet growth during the granulite-facies retrograde metamorphic phase. This hypothesis is supported by the equality of the grain-size of the omphacite crystals (fine- to medium-grained) to that of the neighbouring α -zoisite eclogite. The kelyphite rims surrounding every garnet crystal consist of radially arranged, dark blue-green pleochroic

hornblende crystals sometimes accompanied by plagioclase and magnetite.

When compared with the α -zoisite eclogite, the β -zoisite-hornblende eclogite shows the following differences:

1. Kelyphitization and amphibolization have reached more advanced stages in the hornblende eclogite.
2. The α -zoisite is only found as relic. Its place as the stable form of Ca-Al silicate is taken by β -zoisite, which occurs as fine-grained subhedral crystals in lenticular aggregates.
3. The percentage of omphacite converted into p.p. symplectite increases from under 5% in the eclogite to over 80% in the hornblende eclogite.
4. A post-eclogitic deformation (M_2) has overprinted the primary eclogite deformation (M_1).

Therefore, the retrograde metamorphism of an eclogite in the clinopyroxene-almandine subfacies of the granulite facies not only involved the formation of kelyphite and brownish-green hornblende but also the replacement of α -zoisite by β -zoisite.

In a sample of medium-grained kyanite-hornblende eclogite (V 1051), the kyanite undoubtedly grew contemporaneously with omphacite and garnet; it is oriented parallel to M_1 , together with omphacite and α -zoisite. The rock was somewhat affected by post-eclogitic deformation: all birefringent minerals are visibly strained, and kyanite is sometimes even bent or broken. The quartz still occurs in irregularly-shaped pockets and not in lenticular aggregates. The symplectitization has affected only about 30% of the

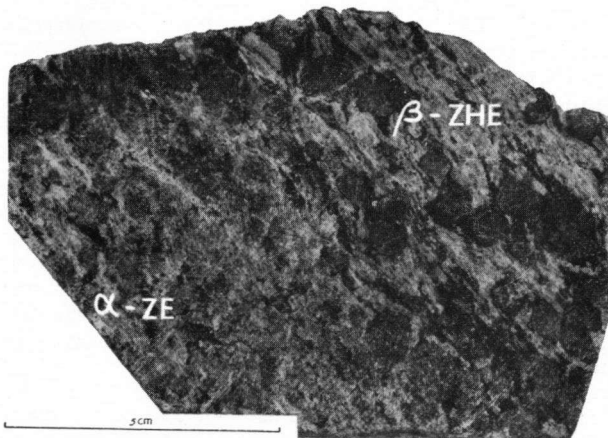


Photo I-7 Sample V 1007a. Sudden transition of medium- to coarse-grained α -zoisite eclogite (α -ZE) into medium- to coarse-grained β -zoisite-hornblende eclogite (β -ZHE). Note sudden change in texture, grain size, and hornblende content.



Photo I-9 Locality V 1271. Contact between fine- to medium-grained α -zoisite eclogite (top) and medium- to coarse-grained β -zoisite-hornblende eclogite (bottom); note parallelism of M_1 , M_2 , and contact.

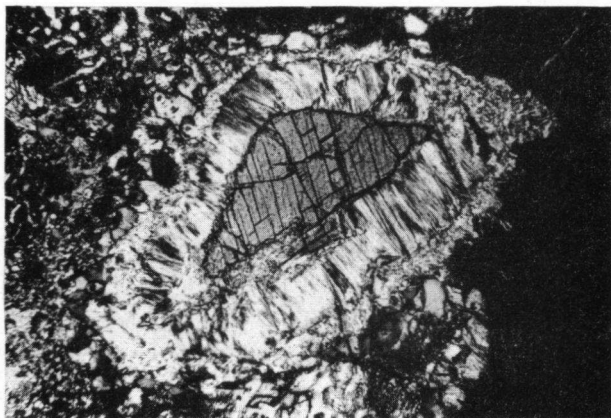


Photo I-8 Slide Coe 61. Kyanite (centre), surrounded by a corona of sericitic matter. (— nic, $\times 50$).

original omphacite content. Small lobular p.p. symplectites (stages 1, 2, and 3) are seen penetrating from one crystal into another. Signs of kelyphitization and amphibolization occur on a limited scale: 0.02 mm-wide rims of blue-green hornblende surround the subhedral light-pink garnets. The brownish-green hornblende, which is secondary after omphacite, is sometimes intergrown with sodic plagioclase in a coarsely symplectitic manner. α -zoisite is present as an accessory mineral.

b. Amphibolite eclogite, eclogite amphibolite.

The essential difference between hornblende eclogites, amphibolite eclogites, and eclogite amphibolites is that in the latter two rock-types plagioclase is present in notable quantities as individual crystals. Since the eclogite amphibolites and the amphibolite eclogites differ only in their proportions of hornblende and omphacite, they will be described together. As a rule, the retrograde metamorphic processes (amphibolization, alteration of α -zoisite or β -zoisite into epidote, etc.) have reached more advanced stages in the eclogite amphibolites than in the amphibolite eclogites. Beside types with brownish-green hornblende and β -zoisite, formed by advanced retrogradation under hornblende granulite-facies conditions, types with dark blue-green hornblende are also found in which α - or β -zoisite is partly replaced by epidote; these types are formed by retrograde metamorphism under amphibolite-facies conditions. Retrograde metamorphism under greenschist-facies conditions caused additional conversion of hornblende into actinolite and of omphacite into albite + actinolite.

Sample V 1220, which is an α -zoisite amphibolite eclogite, is an example of an eclogite showing retrograde metamorphism in two successive stages.

A retrogradation under hornblende granulite-facies conditions caused the formation of brownish-green hornblende, β -zoisite, and p.p. symplectite as stable phases. The original M_1 is overprinted by M_2 , whose foliation is characterized by a subparallel arrangement of β -zoisite and lenticular aggregates of quartz. The omphacite is completely converted into p.p. symplectite (stage 4, occasionally with stages 1, 2, and 3).

During the ensuing retrogradation under amphibolite-facies conditions, blue-green hornblende replaced omphacite and garnet; occasional relics of brownish-green hornblende in the blue-green type show that it was also formed secondary after brown-green hornblende. The α - and β -zoisites were partly replaced by epidote. Unaltered plagioclase (24% An.) occurs as isolated grains, unaffected by deformation. Its formation has been related to the amphibolite-facies step of retrograde metamorphism (p. 131).

As a result of these two retrograde metamorphic phases, the original eclogite has changed into a fine-grained amphibolite eclogite in which the garnet (equidimensional, with corroded outlines, \varnothing up to 2 mm) lies in a mass composed of p.p. symplectite, blue-green hornblende, plagioclase, α - and β -zoisite, and flat-lenticular quartz aggregates (\varnothing up to 1 mm). Hornblende and plagioclase are post-kinematic; the plagioclase shows a random orientation, but the hornblende inherited its preferred orientation from either the omphacite or the brownish-green hornblende that it replaced. Epidote grows as crystalline or dusty rims around zoisite; rutile is sometimes surrounded by a small rim of titanite.

In sample V 1207, an α -zoisite amphibolite eclogite, the original M_1 has been preserved. Under hornblende granulite-facies conditions, retrograde metamorphism caused the formation of brownish-green hornblende, blue-green kelyphitic hornblende around garnet, and some β -zoisite, but without an accompanying deformation since the characteristic flat-lenticular texture of the quartz aggregates is completely absent. No signs of retrograde metamorphism under amphibolite-facies conditions were observed, i.e. blue-green hornblende is absent except in the kelyphitic rims and rutile is not altered into titanite. But under greenschist-facies conditions, retrograde metamorphism continued to take place, this time accompanied by deformation. A 0.2–0.3 mm-wide ultramytonitic zone cuts M_1 at an angle of 40–50°. Undulose extinction of all earlier minerals (omphacite, brownish-green hornblende, α -zoisite, and quartz) and the formation of fissures, perpendicular to M_1 , in the garnet, were all caused by this deformational phase (M_4). Due to the greenschist-facies metamorphism (quartz-albite-epidote-almandine subfacies) the garnet was altered along cracks into chlorite and most of the omphacite was replaced by albite and actinolitic hornblende.

The resulting rock is a fine-grained α -zoisite amphibolite eclogite with equidimensional subhedral garnets, partly surrounded by hornblende-kelyphite rims, and altered into chlorite along cracks. The garnets are enveloped by a mass consisting of omphacite (mostly altered into actinolitic hornblende and albite), α -zoisite (subhedral), β -zoisite, brownish-green hornblende, and irregularly-shaped pockets of quartz. The symplectitization of omphacite has not proceeded beyond stages 1 and 2 as far as could be ascertained, and has affected only a small part (less than 10%) of the omphacite fraction.

β -Zoisite eclogite amphibolite from the Banded Gneiss Formation; sample V 1146a.

Macroscopical appearance: black hornblende and pink garnet (\varnothing 4–5 mm) lie as eyes in a mass consisting predominantly of fine-grained hornblende and plagioclase; flat-lenticular bodies of quartz (up to 1.5 cm long) are also present.

Microscopical appearance: the complete process of retrograde metamorphism took place under hornblende granulite-facies conditions. The newly-formed (type 3) hornblende is pleochroic in shades of greenish-brown, and β -zoisite is present instead of α -zoisite. The garnet is cracked and has corroded outlines; no kelyphite rims are present, but a small amount of the garnet has altered into hornblende. Hornblende-porphyroblasts are arranged more or less parallel to the poorly-developed secondary foliation (M_2), just as are the rounded prismatic β -zoisite crystals. Stage-3 p.p. symplectite, plagioclase (20% An., \varnothing about 0.3 mm), and insignificant amounts of quartz lie dispersed between hornblende and garnet.

In sample Coe 107, a fine- to medium-grained α -zoisite amphibolite eclogite, the original foliation M_1 and the irregularly-shaped bodies of quartz have been preserved throughout the hornblende granulite-facies (brownish-green type 3 hornblende, kelyphite), and amphibolite-facies (blue-green hornblende, epidote) steps of retrograde metamorphism. Deformation under amphibolite-facies conditions caused the formation of a blastomytonitic zone — cutting M_1 at an angle of 30° — composed of blue-green hornblende, epidote, plagioclase, and titanite. Grain-sizes in this zone vary from 0.01 to 0.2 mm.

Sample V 1058, a fine-grained eclogite amphibolite with pegmatoid veins, illustrates the occurrence of second-

generation kyanite. In thin section the eclogite amphibolite has a distinct foliation; omphacite has been transformed into p.p. symplectite, most of which was altered into blue-green hornblende. Small subhedral garnets, free of inclusions, lie dispersed in the rock. Spongy kyanite in aggregates or single crystals, sometimes surrounded by a seam of plagioclase, lie at an angle to the foliation; they are considered to have crystallized from pegmatoid emanations.

The veins run parallel to the foliation; their boundary planes with the eclogite amphibolite are irregular and they consist of slightly undulose quartz in lenticular aggregates, and plagioclase (14–20% An.) which borders or rims kyanite crystals, muscovite aggregates, and fragments of enclosed eclogite amphibolite. Biotite, chlorite, epidote, pyrite, and rutile are additional constituents. A narrow vein filled with prehnite and adularia cuts through both eclogite amphibolite and pegmatoid vein.

c. Amphibolite, hornblende gneiss, chlorite gneiss.

In these rocks, the amphibolite- (or greenschist-) facies retrograde metamorphism, whether or not accompanied by deformation, has almost completely replaced the eclogitic mineral association by an amphibolitic or greenschist paragenesis.

Since pre-amphibolitic deformation and retrogradation have also left their marks on the rock, the different types of amphibolite vary a great deal as to texture and mineral composition.

Blue-green hornblende, (chlorite), plagioclase, epidote, and quartz are the most frequent stable minerals. Relics of α -zoisite, kyanite, p.p. symplectite, or hornblende-plagioclase kelyphite; corroded garnets containing the cloudy accumulations of rutile needles typical of eclogitic garnets, and blue-green hornblende pseudomorphous after p.p. symplectite, are considered to be indicative of an eclogitic descent of the amphibolites in which they are found. These indications are extremely useful in cases where there is no apparent relation between the amphibolite and eclogite (for instance an amphibolitic band or lens in paragneiss). The term amphibolite is used in the sense of de Lapparent (1923) (see Cherotzky, 1963); amphibolite whose composition shows more than 50% leucocratic minerals and which has a gneissose texture is called hornblende-gneiss.

Sample V 1055, an epidote amphibolite, is a dense, fine-grained, black amphibolite with a faintly-developed foliation in which hornblende, epidote, and an occasional garnet can be recognized macroscopically (slide V 1055-I). It occurs as a 30 cm-wide concordant band in α -zoisite hornblende eclogite. In the centre of this band, a 3 to 5 cm-wide zone of amphibolite interspersed with streaky leucocratic bands and lenticular plagioclase porphyroclasts (measuring up to 2 cm in length), indicates that pegmatoid injection took place (slide V 1055-II; for description, see Ch. I, 8). Slide V 1055-I, *microscopical appearance*: the texture is panxenomorphic, inequigranular. Blue-green hornblende (ranging in size from 0.01 to 0.6 mm), epidote (\varnothing 0.3–0.4 mm), and plagioclase (\varnothing 0.05–0.3 mm) are the principal constituents. Accessory minerals are quartz, garnet, titanite with cores of rutile, apatite, and opaque matter. Since the amphibolite occurs as a band in hornblende eclogite and, moreover, the few corroded garnet relics enclose aggregates

of rutile needles, the epidote amphibolite is considered to be a retrograde eclogite.

The weak preferred orientation of hornblende and epidote in the epidote amphibolite is thought to be mimetic after M_1 , because neither in the neighbouring hornblende eclogite nor in the epidote amphibolite could signs of post-eclogitic deformation be detected.

Sample V 1374: β -zoisite-garnet amphibolite.

Macroscopically, the strongly-developed schistosity and the porphyroclasts of black hornblende and of pink garnet, both surrounded by rims of hornblende kelyphite, are clearly visible. Tectonized leucocratic bands (up to 1 cm in width) with eyes of plagioclase, lie parallel to the foliation.

Microscopically, the hornblende is seen to belong to the greenish-brown and brownish-green variety (type 3); no blue-green hornblende or epidote was found, so that it can be safely concluded that the conversion of eclogite to amphibolite took place under hornblende granulite-facies conditions. The eclogitic descent of the amphibolite is evident from the p.p. symplectite relics and the typical rutile inclusions in the garnet.

The medium- to coarse-grained garnets have corroded outlines and are full of fissures. Along these fissures and along the rims, the garnet has altered into brownish-green hornblende. Subhedral porphyroclasts of greenish-brown hornblende are surrounded by a rim of brownish-green hornblende; they are found lying together with garnet, as eyes, in a mass consisting of brownish-green hornblende, stage 4 p.p. symplectite (sometimes altered pseudomorphously into hornblende), β -zoisite, plagioclase, and quartz.

Coarse-grained plagioclase porphyroclasts, probably of pegmatoid origin, are surrounded by mortar rims; they lie parallel to M_2 , as do hornblende and β -zoisite. Accessories are: amoured relics of kyanite enclosed in β -zoisite or garnet; metamict orthite enclosed in brownish-green hornblende; small amounts of muscovite, chlorite, and sericite; rutile, sometimes with rims of titanite; apatite, zircon, and opaque matter.

Sample M 473: a fine-grained diablastic garnet amphibolite from the Banded Gneiss Formation, is an unusual type of amphibolite, in which the principal constituents, i.e. blue-green hornblende and garnet, are accompanied by relics of brownish-green hornblende and plagioclase. Epidote, muscovite, titanite with cores of rutile or opaque matter, apatite, and opaque matter, occur in minor amounts.

The absence of inclusions in the garnet and the textures of the hornblende pseudomorphs are conspicuous. The corroded garnets (\varnothing up to 0.8 mm) are surrounded by hornblende kelyphite or by radial hornblende-plagioclase kelyphite. Oblong garnets lie arranged with their length parallel to the faintly-developed foliation. A few small relics of brownish-green hornblende are surrounded by a rim of blue-green hornblende; the rest of the hornblende is of the blue-green variety and is either pseudomorphous after p.p. symplectite or diablastically intergrown with plagioclase. These diablastic intergrowths consist of parallel systems of small hornblende laths, which may cut each other at an angle (*Retikularstruktur*, Hezner, 1903, p. 535); the interstices between the laths are filled with plagioclase.

Sample V 1170a, a medium-grained α -zoisite-garnet amphibolite, sample V 1197, a fine-grained garnet amphibolite, and sample V 1088, a fine-grained garnet-hornblende gneiss, constitute a series characterized by an increasing amount of leucocratic components and an increasing degree of deformation.

Sample V 1170a was taken from a lens (50 × 300 cm) in the banded gneiss. The garnets lie as eyes in the foliation; they are surrounded by kelyphite rims, have corroded outlines, and show replacement by blue-green hornblende. The blue-green hornblende has undulose extinction and mortar textures; it lies, together with flat-lenticular quartz aggregates, parallel to M_3 . The α - and β -zoisite, sometimes with rims of epidote, also lie parallel to M_3 . Granular, fine-grained, plagioclase and an occasional p.p. symplectite relic are found dispersed in the rock.

In sample V 1197, the M_3 is strongly developed, and *schlieren* composed of fine-grained hornblende and sericitized plagioclase alternate with wavy, flat-lenticular aggregates of undulose quartz \pm plagioclase. Relics of garnet with pink cores and colourless rims, kyanite with rims of β -zoisite, and α -zoisite with rims of epidote, lie as rounded clots or lenticular eyes in the foliation. Clouds of rutile needles, enclosed in the garnet, and an occasional p.p. symplectite relic, indicate the eclogitic descent of the rock.

Sample V 1088, from a 15 cm-wide lens in the banded gneiss, presents the same picture as sample V 1197, but here the *schlieren* of hornblende + plagioclase are outnumbered by the flat-lenticular aggregates of slightly undulose quartz \pm plagioclase. The M_3 weaves around heavily corroded garnet-eyes (with non or slightly undulose quartz crystallized in stress-shadows) and around kyanite relics surrounded by lenticular aureoles of plagioclase. Small grains of orthite (metamict) are thought to be, like the kyanite, of pegmatoid origin.

Sample V 1312, a fine-grained epidote-chlorite gneiss, derives from a lens measuring 20 to 30 m in length and of unknown width, occurring in the Banded Gneiss Formation. Chlorite aggregates with small inclusions of titanite and opaque matter, plagioclase partly altered into sericite, quartz, and some biotite, are the principal constituents. Strongly corroded and diablastic garnets, some α -zoisite cores in zoned epidote crystals, and intergrowths of chlorite and plagioclase probably pseudomorphous after p.p. symplectite, are the only indications of the eclogitic origin of this rock. The foliation plane, indicated by a parallel orientation of garnet, epidote, and flat-lenticular quartz aggregates, is partly obliterated by transversely-oriented chlorite and biotite. Muscovite, rutile, titanite, apatite, zircon, and opaque matter, are accessory minerals.

Types of chlorite gneiss transitional to all types of eclogite amphibolite or amphibolite eclogite are also found.

8. Pegmatoid veins

Post-eclogitic injection of pegmatitic or siliceous material is described for a number of eclogite occurrences by Joukowsky (1901), Düll (1902), Kieslinger (1928), Aldermann (1935), Fiedler (1936), Forster (1947), Eigenfeld-Mende (1948), Lappin (1960), and Lange (1965). These pegmatoid veins are characterized by a low content or lack of potassium and by the sodic nature of their plagioclase. Quartz, kyanite, zoisite, or epidote may also be present. A second type of post-eclogitic pegmatoid intrusion, described by Eskola (1921) from the eclogites of Norway, is equally poor in potash but the plagioclase is of a calcic rather than a sodic type.

Erdmannsdorfer (1931) demonstrated the chemical resemblance between these two types. Roughly speaking, part of the anorthite content of the plagioclase is represented by zoisite or epidote in the types with sodic plagioclase.

The pegmatoid veins encountered at Cabo Ortegal are all of the type in which the plagioclase, if present, is sodic. They are found not only in the eclogites but also in some of the other rocks of the Concepenido Complex and in the rocks of the Capelada Complex. The petrographic evidence indicates that injection of pegmatoid mixtures took place during the granulite-facies as well as during the amphibolite-facies retrograde metamorphic phase.

Because the eclogite is a rigid rock, the penetration of pegmatoid matter took place mostly along the foliation, though discordant veins injected along joints or tension gashes are also found. In the concordant and discordant veins alike, small fragments detached from the country rock lie embedded in the vein minerals. The composition of the veins varies widely. Potash feldspar is either absent or occurs in the form of antiperthite lamellae in the plagioclase. The plagioclase: quartz ratio may vary a great deal, and in some places quartz occurs to the exclusion of plagioclase. The additional minerals include: kyanite, sometimes surrounded by muscovite, β -zoisite, or plagioclase; α -zoisite, occasionally with cores of γ -zoisite and rims of epidote; metamict orthite; muscovite; and tourmaline. The muscovite is often surrounded by biotite or biotite-plagioclase symplectite.

Solutions apparently emanating from these veins played an important role in the retrograde metamorphism of the eclogite; they also caused the formation of a second generation of kyanite (see Ch. I, 6). Solutions carrying K-ions led to the formation of post-eclogitic biotite (see also Eigenfeld-Mende, 1948; Spry, 1963) or the alteration of the ferromagnesian minerals into biotite.

Sample G 7-2, a quartz-zoisite vein in garnet amphibolite, was found as an unattached fragment. Fortunately, some country rock still adhered to the vein and the relations between vein and wall rock could be studied in thin section. Macroscopically as well as microscopically, the boundary plane is irregularly formed: quartz tongues penetrated into the garnet amphibolite and pried loose several fragments that lie now enclosed by quartz.

The garnet amphibolite has the aspect of being completely recrystallized; hornblende pseudomorphs after stage-4 p.p. symplectite indicate an eclogitic descent. Garnet lies in clusters of fine-grained anhedral crystals and is free of inclusions. Blue-green hornblende is coarse-symplectitically intergrown with plagioclase (13% An.). Neither in the garnet amphibolite nor in the vein are signs of deformation observable, although the presence of p.p. symplectite texture relics indicates that a pre-amphibolitic deformational phase probably affected the rock. The retrograde metamorphism under amphibolite-facies conditions, which caused the formation of a second garnet generation and the complete replacement of omphacite by hornblende + plagioclase, are seen as consequences of the intrusion of the quartz-zoisite vein.

The vein itself is composed of fine- to medium-grained strain-free quartz forming a mosaic texture with little interlocking of the grains, subhedral to euhedral α -zoisite crystals (up to 5 cm in length) with cores consisting of γ -zoisite (for optical and chemical properties see Vogel & Bahezre, 1965) and coarse-grained rutile. Along the rims and in cracks a small amount of the α -zoisite has altered into epidote. Similar quartz veins with α -zoisite crystals of several centimetres length have also been described by Brière (1920, p. 109).

In another unattached fragment, this one consisting of zoisite-muscovite pegmatite (sample V 1351), the fabric is dominated by flat-lenticular aggregates of strain-free quartz. Lenticular patches, embedded in plagioclase and consisting of bent muscovite and streaks of granular plagioclase, alternate with these discoid quartz aggregates. Euhedral α -zoisite (up to 3 cm in length) with cores of γ -zoisite having a lower birefringence, lie dispersed throughout the vein. These zoisite crystals show replacement along their rims by epidote in the following way: the α -zoisite is surrounded by a turbid rim, roughly 1 mm wide, of β ?-zoisite, in which droplets of epidote with optically identical orientation have formed. The β -zoisite is separated from the vein material by a 0.1 mm-wide rim of — sometimes spongy — epidote. The birefringence of this secondary epidote increases slowly from the core outwards. Relics of corroded kyanite, which are sometimes extremely cataclastic but mostly are not deformed at all, lie included in the patches of muscovite. β -zoisite aggregates are likewise surrounded by muscovite.

Because the zones with pegmatoid veins constitute an inhomogeneous element in the eclogite, they weakened the resistance of the eclogite to deformation. As a consequence, they were predestined to be used as planes of differential movement by subsequent deformational phases. An example is provided by slide V 1014.

At location V 1014, a 2 cm-wide pegmatoid vein that can be traced over about 20 metres, has intruded into an amphibolite eclogite with blue-green hornblende, from which it is separated by a 10–15 cm-wide amphibolized zone.

In thin section (slide V 1014) this amphibolized zone appears as a fine-grained epidote amphibolite with an indistinct foliation. Differential movements occurring along the boundary between the vein and the epidote amphibolite have caused mylonitization in a 13–15 mm-wide zone. This zone can be separated into three different parts: one belonging to the vein, one belonging to the epidote amphibolite, and one intermediate zone in which the deformation has mixed the epidote amphibolite with the penetrating tongues of vein matter and thus formed a tectonic hybrid.

The pegmatoid vein consists of a fine-grained mass of plagioclase and quartz (\varnothing about 0.3 mm) with a distinct lattice orientation ($z' //$ foliation). Dispersed in this mass lie subhedral crystals of epidote (up to 1.5 mm long, $\Delta > 0.030$, 2V*) and isolated porphyroclasts of plagioclase (17% An.), hornblende, and tourmaline. In the mylonitized part of the vein (6 mm wide) the grain-size of the ground mass diminishes to 0.05 mm and the epidotes are bent or broken. In the hybrid and amphibolitic parts of the mylonite the grain-size of the matrix — in which small hornblende fragments are now present — is even smaller ($\varnothing < 0.01$ –0.03). The number of hornblende porphyroclasts and the grain-size of the matrix gradually increase as the distance to the undeformed epidote amphibolite decreases.

In sample V 1055 the pegmatoid veins have been injected along several planes, thus enclosing a number of fragments of epidote amphibolite. With their streaky textures, the veins give the impression of having been tectonized.

Microscopically (slide V 1055-II), a gradual transition between pure pegmatite and pure epidote amphibolite can be seen. It is remarkable that, although the plagioclase porphyroclasts (15% An.) have a strong undulose extinction and mortar textures, the hornblende and epidote fragments embedded in pegmatitic zones are not bent, and the fine-grained (mean \varnothing 0.1 mm) mass of pegmatitic quartz and plagioclase (17% An.) surrounding the porphyroclasts in mosaic texture shows no signs of post-crystalline deformation. The sequence of events was probably as follows: a fluid pegmatoid mixture containing megacrysts of plagioclase was forcibly injected into the rock. During this process, the large feldspar crystals became strained or broken along the contact with the wall rock. The liquid part of the intrusion disengaged particles of hornblende (varying in length from 0.01 to 1.4 mm) and epidote (length 0.5–1.2 mm) from the enclosing country rock and its fragments.

A more intensive type of penetration, ultimately leading to hybridization, is represented by samples V 1394 and V 1042.

Sample V 1394 is a fine- to medium-grained β -zoisite-garnet amphibolite. In thin section the rock seems to be “soaked” with quartz + plagioclase. At least part of the plagioclase (20% An.) and the quartz had a pegmatoid origin since metamict orthite and some biotite are present as accompanying minerals. The hornblende is a brownish-green pleochroic variety (type 3) sometimes enclosing metamict orthite, which indicates that pegmatoid injection preceded retrograde (hornblende granulite facies) metamorphism.

A more intensive “soaking” resulted in a kind of maceration of the host rock, as is the case in sample V 1042, a fine- to medium-grained eclogite amphibolite.

Microscopically, clusters of mafic minerals (garnet, blue-green hornblende, and some p.p. symplectite) seem to float in a fine-grained mass of quartz and plagioclase (24% An.). Cores of metamict orthite in epidote and small-scale biotitization indicate the pegmatoid nature of the quartz-plagioclase mixture.

9. *Chemistry and metamorphic facies*

Chemical analyses of eclogites and retrograde eclogites were made with two objects in mind: to determine whether the descent of the eclogites was magmatic or sedimentary and to obtain from these analyses, in combination with analyses of the constituent minerals, an insight into the relations of the different mineral associations present.

Table I-1 shows the results of 29 analyses of mafic rocks from the Concepenido Complex. Numbers 6, 15, 20, 21, 22, and 25 will be referred to in later chapters; the remaining analyses, representing either eclogites or retrograde eclogites, were subdivided in two groups. One of these groups is composed of analyses 1, 2, 5, 16, 23, and 26, for which post-eclogitic admixture of extraneous matter seemed probable after examination of thin sections and hand-specimens. In the other group, composed of analyses 3, 4, 7–14, 17–19, 24,

and 27—29, no traces of such admixture were found in either hand-specimens or thin sections.

To distinguish between a magmatic or sedimentary nature of the eclogites, the Niggli values were plotted in an al-fm-c-alk concentration tetrahedron, in an (al-alk)/c diagram, and in an si/(c+alk) diagram (Burri, 1959). In these graphs the analyses of both groups plotted well within the field of the igneous rocks. In the c/mg diagram (Fig. I-11) used by Leake (1964), the analyses of the uncontaminated rocks plot along the trend-line for the differentiation of mafic igneous rocks; the contaminated rocks have a somewhat wider variation but plot close enough to the trend-line to indicate a magmatic rather than a pelite-limestone trend. Thus, the conclusion based on textural evidence (Ch. I, A 3), that the eclogites represent metamorphosed igneous rocks, is corroborated by their chemical composition.

The analyses in Table I-1 are arranged in order of diminishing normative quartz and then of increasing normative olivine. According to their catanorm, they can be classified as oversaturated tholeiites (nrs. 1—14, with normative quartz and hypersthene) and olivine tholeiites (nrs. 14—29, with normative olivine and hypersthene). Nr. 29, which lacks normative hypersthene, has the chemical composition of an olivine basalt. Alkali-basaltic types were not encountered (normative nepheline was absent in the analyzed samples). The over-all tholeiitic nature of the rocks was confirmed by the fact that all the analyzed rocks plotted in the tholeiitic field of the $\text{SiO}_2/(\text{Na}_2\text{O} + \text{K}_2\text{O})$ diagram of Macdonald & Katsura (1964).

To ascertain whether some of the samples had the characteristics of high-alumina basalts, they were plotted in an $\text{Al}_2\text{O}_3/(\text{Na}_2\text{O} + \text{K}_2\text{O})$ diagram (see Fig. I-12). The majority of the analyses plotted in the tholeiitic field, three plotted in the high-alumina basalt field and one (nr. 29) on the boundary between the high-alumina and alkali basalt fields. Since the three analyses that plotted in the field of high-alumina basalt are all suspected of having been contaminated by injection with pegmatoid material, their anomalous position in the diagram can be explained by an influx of Na and Al due to the addition of plagioclase to the uncontaminated rock. Because no normative nepheline is calculated from analysis nr. 29, the rock is considered to have a high-alumina basaltic rather than an alkali-basaltic composition.

The naming of the eclogites as volcanic rather than as plutonic rocks is not meant to imply that the eclogites are thought to have originally been effusive rocks. In fact, textural evidence seems to indicate that the eclogites are metamorphosed plutonites (quartz dolerites, hypersthene gabbros, norites, and olivine gabbros), but this evidence is so scarce that effusive rocks cannot be altogether disregarded as possible parent rocks of the Cabo Ortegal eclogites.

In the QLM diagram (Fig. I-13) the differentiation of the eclogitic rocks shows a trend in the direction of

the quartz-alkalifeldspar eutectic. This characterizes the igneous suite as calc-alkalic, which is in agreement with the generally low values for TiO_2 wt%, indicating, according to Chayes (1965), circumoceanic rather than oceanic parentage.

To explain the differences between kyanite eclogite and α -zoisite eclogite, the analyses of samples V 1278 (4.5% α -zoisite), V 1050 and M 459 (insignificant amounts of α -zoisite), and V 1023 (42% carinthine), were plotted in an ACF diagram together with their respective omphacite-garnet pairs. Because no Cabo Ortegal kyanite eclogites were available in which both omphacite and garnet had been chemically analyzed, the kyanite eclogite from Weissenstein (Tilley, 1937) was also plotted for comparison (Fig. I-14). Analysis V 1023 plots on the F-side of its omphacite-garnet join, the other analyses all plot on the AC-side of their omphacite-garnet joins, i.e. they lie in the field limited by kyanite, omphacite, and garnet as well as in the field limited by zoisite, omphacite, and garnet. This shows that there is a similarity between zoisite and kyanite eclogites as far as their ACF values are concerned. To verify this chemical similarity, analyses of kyanite eclogites and retrograde kyanite eclogites (nrs. 3, 7, 8, 9, 17, 29^{*}) and α -zoisite eclogites and retrograde α -zoisite eclogites (nrs. 11, 14, 18, 19, 24, 27^{*}) were plotted in a QLM diagram (Fig. I-15) together with two analyses, nr. 28 (carinthine eclogite) and nr. 13 (eclogite containing both α -zoisite and kyanite). In this graph the positions taken by plots of kyanite eclogites are distinctly different from those of α -zoisite and carinthine eclogites, which suggests that the appearance of either α -zoisite or kyanite is a function of the chemical composition of the parent-rock. In an attempt to define the compositional area in which kyanite eclogites plot, 18 analyses of kyanite eclogites (collected by Tilley, 1937) were entered in the QLM diagram (Fig. I-16). The results clearly prove the impossibility of delimiting separate fields for α -zoisite and kyanite eclogites.

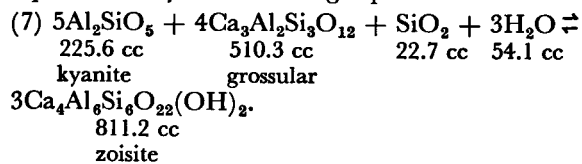
To clarify this apparent contradiction, the problem was approached in a different way, starting from the following considerations:

1. The investigation was limited to eclogites that plot on the AC-side of their omphacite-garnet join in the ACF diagram and have a K_2O content that is negligibly small (greater amounts of K_2O lead to the formation of phases such as muscovite or biotite). This means that the mineral composition of the eclogites in question is limited to omphacite + garnet \pm quartz \pm kyanite \pm α -zoisite.
2. In these eclogites, omphacite is the only phase capable of accommodating Na.
3. If omphacite is considered to be a solid solution of jadeite-acmite (Ja') on the one hand and hedenbergite-diopside (Di') on the other, its composition is determined by the PT conditions governing at the time of its formation. The amount of Di' is

* Numbers refer to Table I-1.

determined largely by T (Bautsch, 1960), the amount of jadeite by P (Coleman *et al.*, 1965; Kushiro, 1964—1965), and the amount of acmite by Po_2 (Yagi, 1966).

4. The relation between zoisite and kyanite can be represented by the following equation:



This equilibrium probably shifts to the left with an increase in T (dehydration) and to the right with an increase in P (no fluid or gaseous phases).

5. The percentage of grossular + andradite in eclogite garnets is given by Turner & Verhoogen (1960) as 12—40% depending on T, but according to the diagrams given by Yoder & Tilley (1962) it generally does not exceed 35% in the eclogite facies.

For sample V 1016 (α -zoisite eclogite), an attempt was made to reconstruct the mineralogical composition by starting from the chemical composition (Table I-2). For this purpose, the weight percentages of the oxides were recalculated to cation numbers. TiO_2 and P_2O_5 were then subtracted in the form of rutile and apatite, respectively; the other cation numbers were grouped together as follows: Si, Af (Al + Fe^{+3}), Mf (Mg + Fe^{+2} + Mn), Ca, and Nk (Na + K).

First, all the available Nk is accommodated together with proportional amounts of Af and Si in Jd'. Since the percentage of Di' in the Cabo Ortegal eclogitic clinopyroxenes lies in the neighbourhood of 65% (see Fig. V-6), Ca, Mf, and Si are subtracted in such quantities that the amount of Di' is twice the amount of Jd'. Pyralmandine is then formed with the rest of the Mf, leaving Ca, Af, and Si to be distributed over Ca-garnet + kyanite + quartz or Ca-garnet + zoisite + quartz.

Table I-2a shows how Ca-garnet and zoisite were formed from the available Ca, Af, and Si.

Now the amounts of omphacite (67% Di'), garnet (19% gross. + andr.), zoisite, and quartz were recalculated in vol.% and compared with the mode, the result showing that the calculated amount of zoisite corresponds to the amount of zoisite actually present. The discrepancies in the omphacite, garnet, and quartz percentages are ascribed to the simplification of the calculation (actually, the clinopyroxene and garnet solid solutions are of a more complex nature) as well as to the fact that 7% of secondary hornblende was disregarded in the calculation, and to possible inaccuracies in the determination of the $\text{FeO}:\text{Fe}_2\text{O}_3$ ratio. To calculate the rock as a kyanite eclogite, the same procedure is followed but after the pyralmandine is formed all the Ca is accommodated in grossular (Table I-2b), which leads to a garnet with 40% grossular + andradite molecules, a value exceeding by 10% the maximum amount of Ca-garnet observed in Cabo Ortegal eclogitic garnets (see Fig. V-1).

It is also possible to recalculate this chemical composition into a bimineralec eclogite with 75% garnet, 15% omphacite, and 10% quartz, but the compositions of garnet (42% gross. + andr.) and omphacite (38% Di'), if not irreconcilable, are in any case not realized under the PT conditions that governed the formation of the Cabo Ortegal eclogites.

To investigate the influence of the composition of the omphacite on the mineralogical composition of the eclogite, the chemical composition of sample V 1016 was recalculated to an eclogitic mineral composition for a number of different omphacite compositions (see Table I-3). The dependence of the Jd' content of the eclogitic clinopyroxene on P is also seen as an explanation for the increase of the garnet content with rising P (Green & Ringwood, 1966a), which is the principle underlying Hahn-Weinheimer's (1963) subdivision of the eclogites. For, with rising P, the Jd' content of the clinopyroxene increases, leaving more Mf to form garnet.

Because it had thus become clear that it would be possible to form a kyanite eclogite as well as a zoisite eclogite starting from one and the same chemical composition, the possibility was considered that the initial H_2O content of the rock was responsible for the difference in mineral associations. Due to both the gross inaccuracy of the H_2O determination and the different stages of amphibolization of the investigated samples, it was impossible to check this supposition accurately. Because no significant difference could be detected between the arithmetical means of the H_2O percentages of kyanite and α -zoisite eclogites, it is tentatively suggested that H_2O is present in the essentially "dry" kyanite eclogites and bimineralec eclogites in the form of fluid inclusions in quartz and as physically adsorbed water. The inactivity of the H_2O component in the "dry" eclogites can be explained by the influence of P and T on reaction equation nr. 7. Since an increase in T shifts the equilibrium towards the left and an increase in P shifts it towards the right, zoisite will be formed if the effect of P outweighs that of T, whereas kyanite and grossular will be formed if the effect of T outweighs that of P. This explains the observation of Tilley (1937) that the garnets in kyanite eclogites have high lime values. Furthermore, it suggests that within the PT-domain of the eclogite facies, H_2O remains inactive for any given T until P exceeds a certain threshold value.

The foregoing can be briefly summarized as follows:

1. Within a limited range of P and T the chemical composition of the eclogite in general and its Na_2O content in particular are determinative for the appearance of either zoisite or kyanite.
2. The conversion of zoisite eclogite to kyanite eclogite is promoted by an increasing T under constantly high P (see Table I-3), since with a rising T the Di' content of the omphacite increases.

3. The activity of H₂O is determined by the magnitude of P and T.
4. The ACF diagram is by its very nature unsuited to reflect the differences between zoisite and kyanite eclogites, because the Jd' component of the clinopyroxene is not recorded as a result of the fact that equal amounts of Na and Al are subtracted from the analysis before it is plotted.

The pyrope content of the garnet and the Di' content of the omphacite are such that the investigated eclogites can be characterized as group-B eclogites (Coleman *et al.*, 1965). That is to say, they occupy a position intermediate between eclogites associated with glaucophane schists and the so-called internal eclogites.

The close association of eclogites with rocks of the clinopyroxene-almandine subfacies of the granulite facies limits the PT field of the eclogites on one side. The boundary between the eclogite and the granulite facies is determined by the transformation of the stable association of garnet + clinopyroxene + sodic plagioclase into the eclogitic association of garnet + omphacite ± zoisite ± kyanite. The range of PT conditions under which the Cabo Ortegal eclogites could have been formed is also limited by the restricted PT area in which zoisite and kyanite can stably occur together (Pistorius *et al.*, 1962). If these data are transposed in a PT graph (Fig. I-17) in which the clinopyroxene-almandine-subfacies and eclogite-facies fields for quartz tholeiitic compositions are outlined after data of Green & Ringwood (1966b), it can be inferred that the temperature at which the Cabo Ortegal eclogites were formed must have lain between 630 and 900° C and that the pressure must have been between 14 and 19 kb.

Lately, several opinions have been put forward in favour of the abolition of the eclogite facies (Coleman *et al.*, 1965; Lange, 1965; Smulikowski, 1960). There is, however, one important criterion that links all the eclogites together: the absence of plagioclase from rocks in which it is chemically possible to form plagioclase (reappraisal of the so-called "plagioclase eclogites" containing primary plagioclase, as described by such authors as Kozłowski, 1958, and Subramaniam, 1956, will almost certainly prove these rocks to belong to the clinopyroxene-almandine subfacies of the granulite facies; see also Green & Ringwood, 1966a and b). At present it is perhaps better to abide by the status quo and to reserve judgement until more insight is obtained into the interrelationship of chemistry, mineralogy, pressure, and temperature within the eclogite facies (see also Banno, 1967).

10. Summary and conclusions

For the Cabo Ortegal eclogites the following conclusions can be drawn from the petrographic and chemical evidence:

1. These eclogites were formed by progressive metamorphism of tholeiitic igneous rocks that were

emplaced in a series of sedimentary rocks either as intrusions (gabbroic or doleritic sills and dykes) or as extrusions (basalt) prior to eclogite facies metamorphism. Düll (1902), Hezner (1903), Backlund (1936), Schüller (1945), Eigenfeld-Mende (1948), Scharbert (1954), Chenevoy (1955), and Bearth (1965) have also explained the eclogites they investigated by such a metamorphism *in situ* of mafic igneous rocks; moreover, this explanation is in accordance with the statement of Green & Ringwood (1966a and b) that eclogites can occur stably within the Earth's crust.

2. The eclogite facies metamorphism took place during or immediately after a major orogeny.
3. Symplectitization is an isochemical process representing an adaption of the eclogite-facies association of garnet + omphacite to clinopyroxene-almandine granulite subfacies conditions. The symplectitization process is promoted by deformation.
4. Within a limited range of PT conditions, the occurrence of the minor constituents α -zoisite and kyanite is determined by the chemical composition of the rock. With varying PT conditions, eclogites of identical chemical composition can differ in mineralogical composition.
5. Post-eclogitic internal deformations affected the eclogites only locally.
6. Retrograde metamorphism of eclogites is caused by penetrating solutions that emanate at least in part from pegmatoid and hydrothermal veins. The scale on which the retrograde metamorphism acted depends on the magnitude of the intrusion, the extent of the penetration of the emanating fluids (which can be greatly increased by accompanying deformation), and the PT conditions at the time of retrograde metamorphism.
7. In the eclogite bodies, hybridization in consequence of pegmatoid injection and subsequent deformation played only a minor role.
8. The local formation of coarse-grained, second-generation garnets supports the assumption of at least one post-eclogitic major metamorphic phase.

B. PARAGNEISSES

The metasedimentary units to be discussed in this chapter are, from West to East: blastomylonites from the Carreiro zone of tectonic movement, Chimparragneiss, banded gneiss, and Cariñogneiss. Although they figure at Cabo Ortegal as separate units, it can be inferred from the general geological picture in the area just South of Cabo Ortegal that they are all part of the same metasedimentary complex. In this chapter a discussion of their general properties will be followed by an attempt to correlate the types.

1. Banded Gneiss Formation

a. Occurrence.

The Banded Gneiss Formation occupies the easternmost part of Cabo Ortegal together with the Cariño-

gneiss Formation. Its western boundary was first believed to be formed by the eclogites, but closer investigation of the poorly-exposed areas between the eclogite outcrops revealed the presence of banded gneiss between — and sometimes even West of — the eclogites. Since numerous small bands and lenses of eclogite and retrograde eclogite are encountered throughout the mass of the banded gneiss, eclogite and banded gneiss were grouped together as the Banded Gneiss Formation. This formation is bordered on the West by the rocks of the Bacariza Formation and on the East by the Cariñogneiss Formation.

Small-scale compositional and textural variations set the banded gneiss apart from the more evenly textured Cariñogneiss. The divergence is such that it can be easily observed in the field, thus permitting the mapping of the eastern boundary of the Banded Gneiss Formation.

Compared to the basic and ultrabasic rocks, the gneisses are characterized by a lower resistance to erosion, resulting in a less pronounced relief.

b. Mineralogical composition and textural relations.

Fine- or medium-grained “*augen*” gneisses, planar or planoliner gneisses, mylonites, and blastomylonites alternate in bands varying in width from less than 1 mm to several metres; truly schistose types are seldom encountered. This textural banding is interwoven with a lamination resulting from fluctuations in the content of melanocratic components in the gneiss, but bands and streaks consisting of pure quartz or of quartzo-feldspatic mixtures are also frequent. In most cases banding, lamination, foliation, and schistosity are seen to run parallel to each other. Lenses and bands of eclogite or retrograde eclogite, likewise arranged in parallel, are encountered throughout the Banded Gneiss Formation.

The most frequently encountered minerals in the banded gneiss are quartz and plagioclase; garnet, biotite, muscovite, and sometimes kyanite or epidote, are found in many combinations and in varying amounts. They are sometimes accompanied by alteration products such as chlorite and sericite. Occasionally, potash feldspar (microcline), hornblende, staurolite, or β -zoisite are found. Accessory minerals include orthite, rutile, titanite, apatite, zircon, opaque matter, and tourmaline. Narrow dilatation veins discordantly cutting the foliation plane and filled with epidote, adularia, calcite, pumpellyite or prehnite indicate that post-tectonic hydrothermal activity took place.

The habit of quartz varies a great deal. Aphanitic to medium-grained quartzes, showing undulose extinction and sometimes even deformation lamellae, are found dispersed in all types of gneiss. Elongate lenticular and flat-lenticular bodies of non- or slightly undulose quartz are encountered frequently in *augen* gneisses and in planar and planoliner gneisses. In hydrothermal veins, strain-free quartz is sometimes found together with adularia.

Plagioclase porphyroclasts (predominantly oligoclase-andesine) occur as *augen* in the *augen* gneisses but also (albeit less frequently) in the planar and planoliner gneisses. The bulk of the plagioclase — varying in amount with the banding — lies dispersed throughout the rock. Twinning according to the albite and pericline laws is common; the zoned and inversely zoned structure sometimes leads to plagioclase grains with an untwinned core and a polysynthetically twinned rim. Antiperthite (or sometimes mesoperthite) is occasionally found; the presence of myrmekite is confined to gneisses with potash feldspar. Sericitization and saussuritization were at least partly caused by hydrothermal activity (solutions emanating from veins filled with adularia and epidote, respectively), since zones of sericitic (saussuritic) plagioclase can be seen to run parallel to veins filled with adularia (epidote) in rocks with otherwise unaltered plagioclase. Poecilitic plagioclase crystals enclosing parallel muscovite flakes are considered to represent recrystallized sericitic plagioclase.

Garnet is usually present as anhedral grains with outlines corroded by resorption. In rocks preserved from retrograde alterations, garnet may still show euhedral to subhedral outlines.

The garnet content changes with the banding; micaceous bands are generally richer in garnet than leucocratic ones. Pre-tectonic formation of the garnet is indicated by fissure patterns running perpendicular to the foliation throughout the slide, by the presence of garnet as *augen* in some of the gneisses, and by streaks composed of fragments of broken-down garnet crystals.

X-ray diffraction patterns (see Ch. V, A) show that separate garnet-phases of different composition occur together in one sample, and a zoned structure of single garnet crystals is sometimes indicated by slightly pink patches in the usually colourless garnet grains. Partial corrosion of such zoned garnets followed by replacement by quartz or (less frequently) plagioclase, may lead to poecilitic or atoll-like textures.

The repeated occurrence of enclosed aggregates of rutile grains and clouds of rutile dust — identical to those encountered in the eclogitic garnets — indicates that the garnet was formed under catazonal metamorphic conditions (the limited Ti-substitution in catazonal garnets will be discussed in Ch. V, A 1), and provides an argument in favour of the supposition that both paragneiss and mafic rocks have undergone eclogite facies metamorphism.

Fringes and rims of biotite around muscovite show the latter to be the older mineral. There is usually a distinct difference in grain-size, since medium-grained muscovite crystals are associated with fine-grained biotite. The age relation also appears from their deformation, for muscovite is nearly always bent or strained and biotite only occasionally so. Concentration of the micas in streaks causes lamination. Muscovite (except for muscovite secondary after kyanite) always lies parallel to the foliation plane. Biotite plates varying in colour from $n_{y,z}$ reddish-brown to $n_{y,z}$

brownish-black, generally conform to the foliation but are occasionally disposed at an angle to it.

Chlorite replaces biotite together with some opaque matter and so inherits most of the textural relations and habit of the biotite. Slide V 1394f shows a newly-formed chlorite which has crystallized as fine-grained vermicular aggregates in zones impregnated with adularia.

Kyanite is found as fine- to medium-grained relics, often bent or broken and sometimes altered into and surrounded by muscovite; this alteration preceded, at least in part, the crystallization of biotite, for fringes of biotite have formed along the muscovite rim. A second kyanite generation is often present in the form of groups of microcrystalline needles (length about 0.02 mm, width about 0.003 mm) lying predominantly along the borders of plagioclase crystals. Like the mafic minerals, kyanite is often concentrated in the dark bands.

The epidote-group minerals found in the banded gneiss include fine-grained, more or less metamict *orthite* crystals with oblong rounded forms; *epidote* (Δ up to 0.020), which occurs as a minor constituent and forms rims around the orthite when the two minerals occur together; and β -*zoisite* lying in aggregates together with muscovite and epidote. These aggregates sometimes enclose kyanite fragments; they are rare, and are thought to have been formed by the retrogradation of kyanite, just as in the eclogitic rocks.

Untwinned *potash feldspar* porphyroclasts are at times present in leucocratic lenses and bands. The infrequent and strictly localized occurrence of *microcline* porphyroblasts seems to indicate that potassium was a relatively mobile constituent. Accessory constituents are: brownish-green hypidiomorphic *tourmaline* (ϕ up to 2 mm); *zircon*, occurring as large (ϕ up to 0.1 mm) turbid well-rounded crystals, or as small (ϕ about 0.02 mm) clear subhedral or euhedral crystals; golden-brown (sometimes violet), mostly euhedral *rutile*; *titanite*, replacing rutile; and opaque matter (*pyrite*, *ilmenite*, *hematite*, and *limonite*). *Apatite*, mostly with rounded forms, is often broken; sometimes it contains numerous needle-shaped inclusions lying parallel to 0001.

Garnet-biotite gneiss samples representative of the types of gneiss encountered in the Banded Gneiss Formation are: V 1199, V 1340, Coe 251, and M 474.

Foliated garnet-biotite gneiss; sample Coe 251. Porphyroclasts of garnet and plagioclase are the only macroscopically distinguishable constituents; they lie embedded in an extremely fine-grained, dark-grey to violet-grey matrix. Lamination is caused by a varying garnet content and by differences in the grain-size of the garnet in the various laminae. The lamination is parallel to the foliation and schistosity planes.

In thin section the foliation becomes more prominent: two blastomylonitic laminae measuring 2.5 and 6 mm in width consist of a microcrystalline (ϕ not exceeding 0.07 mm) mass of undulose quartz, plagioclase, biotite, and opaque matter (estimated at 3 vol%). Dispersed through this mass

are anhedral garnet porphyroclasts (ϕ up to 0.6 mm). No signs of *augen* texture are present.

These blastomylonitic zones alternate with laminae (up to 12 mm wide) having a flat lenticular, "flaser"-like texture. In these laminae porphyroclasts of garnet and plagioclase (ϕ up to 1 cm) lie in a matrix consisting of microcrystalline to fine-grained quartz, plagioclase, and biotite. A distinct foliation is caused by streaks rich in biotite, parallelism of elongate porphyroclasts, flat lenticular bodies of undulose quartz, and wavy shear planes (causing schistosity) marked off by biotite. Preferred orientation of biotite is moderately developed. Catazonal formation of the garnet is indicated by included clouds of rutile dust. Narrow dilatation veins filled with adularia cut through blastomylonite and *flaser* gneiss alike.

Planar garnet-biotite gneiss; sample V 1340. Macroscopically, the rock appears greyish-brown. The foliation is made conspicuous by the presence of wavy flat-lenticular bodies (up to 5 cm long) consisting of plagioclase and a little quartz. The biotite-rich matrix between these plagioclase streaks is strewn with light-pink garnet crystals which can be as large as 1 cm (photograph I-10).

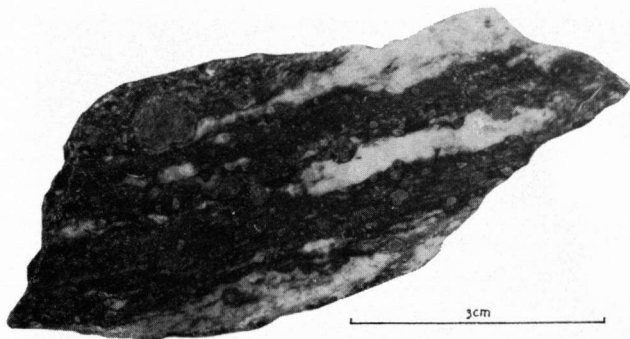


Photo I-10 Sample V 1340. Garnet porphyroclasts in planar garnet-biotite gneiss. Flat-lenticular bodies of plagioclase + quartz lie parallel to the foliation.

Microscopically, the picture is much the same. The garnets often include clouds of rutile dust; they have corroded outlines and are often surrounded by a zone rich in biotite, indicating a replacement of garnet by biotite. Medium-grained quartz-plagioclase streaks and — sometimes elongate — garnet crystals are arranged in parallel in a fine-grained matrix consisting of quartz, plagioclase, and biotite. Biotite streaks conform to the foliation plane and are woven around plagioclase streaks and garnet crystals. The anorthite content of the plagioclase in the streaks (21% An.) is equal to that of the plagioclase in the matrix.

Planilinear garnet-kyanite-biotite gneiss; sample M 474. Macroscopically, the wavy lenticular bodies of quartz and plagioclase appear more numerous than in sample V 1340 (they constitute about 50 vol% of the total rock composition), but garnet is less conspicuous (photograph I-11).

Microscopically, the rock differs greatly from sample V 1340: anhedral medium-grained garnet (with included rutile microlites), reddish-brown pleochroic biotite aggregates with a multitude of microcrystalline stubby prismatic kyanite crystals — almost to the exclusion of quartz and plagioclase — are disposed in streaks alternating with the quartz-feldspar bodies (photograph I-12). These leucocratic bodies consist of medium-grained interlocking quartz crystals,

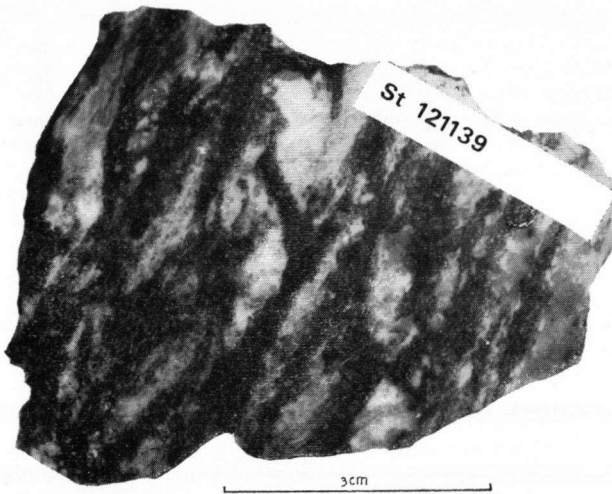


Photo I-11 Sample M 474. Planilinear garnet-kyanite-biotite gneiss. Abundant quartzo-feldspathic lenses between melanocratic streaks constitute evidence of earlier migmatization.

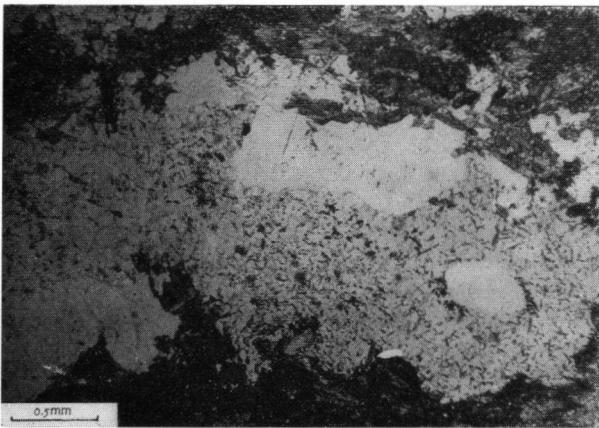


Photo I-12 Slide M 474. Part of a quartzo-feldspathic lens. The difference between medium-grained (clear) quartz and fine-grained recrystallized plagioclase strewn with small kyanite needles, is quite distinct (— nic).

fine-grained plagioclase (20% An.), and an occasional medium- to coarse-grained untwinned potash feldspar. Within these leucocratic lenses, quartz and plagioclase are rigidly separated; both occur grouped in aggregates. Small amounts of biotite and kyanite are found, but only in the feldspathic parts.

Medium-grained relics of sericitized plagioclase and the similarity in optical orientation of groups of neighbouring plagioclase crystals⁷ suggest that an originally medium-grained plagioclase component underwent strain and thereafter recrystallized together with the quartz. This supposition is more or less corroborated by the bent and broken nature of some of the crystals of biotite, garnet, and kyanite, and by the absence of undulose extinction in quartz and plagioclase.

Similar findings were made in a *microfolded garnet-two-mica gneiss*; sample V 1199. Macroscopically, the isoclinally-folded lenticular leucocratic bodies have a crumpled aspect in a section perpendicular to the tectonic b-axis, whereas they appear as thinly drawn-out parallel streaks in sections // b (photograph I-13).

Microscopically, quartz and plagioclase (20% An.) show only slight undulose extinction. The micas, accumulated in elongate concentrations, all lie subparallel to the axial plane except in the hinges of the folds where they also lie transversely. Because the micas are only occasionally bent, a late syn-tectonic to post-tectonic recrystallization of quartz, plagioclase, muscovite, and biotite is assumed to have taken place.

Small whisps of microcrystalline prismatic kyanite crystals, occurring enclosed in or at the rims of plagioclase crystals, point to a simultaneous growth of kyanite, whereas some garnet is still present as fine-grained corroded relics.

Lepidoblastic types such as that in sample Coe 126 (a chlorite-muscovite schist), in which flat-lenticular bodies of fine-grained interlocking undulose quartz alternate with drawn-out streaks composed of bent — chlorite-rimmed — muscovite, seldom occur in bands wider than several millimetres.

⁷ This similarity in optical orientation is made conspicuous by insertion of a comparator: even when the slide is rotated on a universal stage, the similarity in optical orientation remains striking.

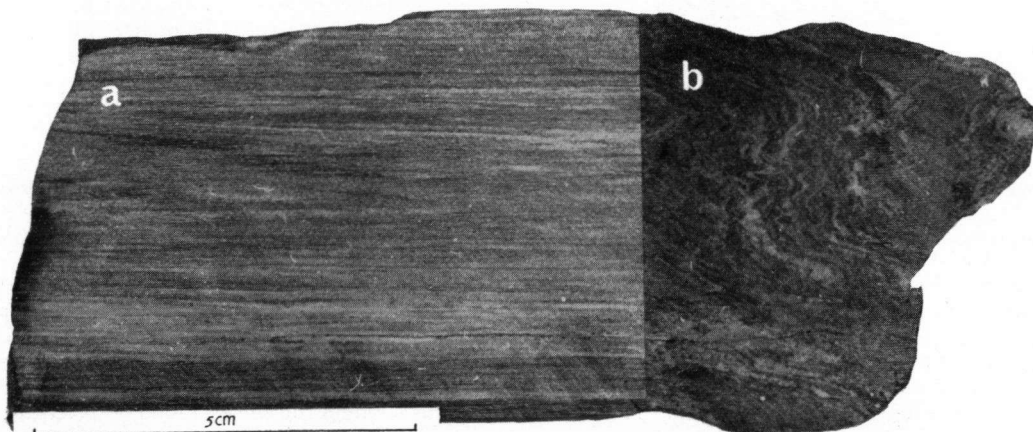


Photo I-13 Sample V 1199. Garnet-two-mica gneiss. Sections parallel (a) and perpendicular (b) to the tectonic b-axis, illustrating the difference in appearance of the leucocratic bodies in different sections.

Differences in texture interacting with compositional differences on a scale ranging from millimetres to decametres, in addition to the presence of lenses and bands of eclogite in all stages of retrograde metamorphism, gave rise to the characteristic appearance of this extremely variable series of rocks. The recrystallization of quartz, plagioclase, biotite, and muscovite, and the formation of second-generation kyanite microlites, coupled with deformation (especially intensive folding) indicate that the gneisses underwent a mesozonal phase of regional metamorphism. After this mesozonal metamorphic phase, the gneisses underwent only fracturing and local alterations caused by solutions emanating from hydrothermal veins. The fracturing caused the local formation of tectonic breccias, as for instance in the fine-grained garnet-chlorite gneiss of sample Coe 163.

In thin section the foliation plane — indicated by a sub-parallel orientation of chlorite, broken garnet, and small elongate leucocratic bodies — is repeatedly cut at an angle of about 20° by 0.06–0.3 mm-wide mylonitic zones, in which angular fragments of quartz, plagioclase, and garnet lie embedded in a cryptocrystalline matrix. In another zone (varying in width from 4 to 10 mm), which cuts the foliation at the same angle, mylonitization is not so far advanced. Here, polyminerally angular gneiss fragments (\varnothing up to 1.2 mm) are embedded together with prehnite-rimmed aggregates of newly-formed calcite (\varnothing up to 2 mm) and angular fragments of quartz, plagioclase, and garnet, in a matrix composed of calcite cement and microcrystalline fragments.

The discordant nature of the deformation, the lack of recrystallization of quartz and plagioclase, and the occurrence of hydrothermal minerals such as calcite and prehnite, lead to the conclusion that this highly localized mylonitization may be correlated with the E-W fault pattern (see Ch. I, B 4).

The most probable paragenesis of the gneisses and the eclogites is that of a geosynclinal sedimentary series with many graywackes and intercalations of mafic igneous rocks (either plutonic or volcanic). This implies that if the mafic rocks were exposed to eclogite-facies metamorphic conditions, the same should hold for the associated sedimentary rocks.

Due to the drastic changes inflicted by the post-eclogitic amphibolite facies metamorphism, however, little evidence of the catazonal metamorphic phase has been preserved in the metasedimentary rocks.

The best example of a catazonal gneiss is sample V1104 (β -zoisite-kyanite-biotite-garnet gneiss). Its position in the tectonic lee of the Faroleiro eclogite bodies probably sheltered it from deformation, which might explain its preservation from excessive retrograde metamorphism.

Macroscopically, its high content of light brownish-pink garnet causes — especially when it is covered by lichen — a close resemblance to eclogite. Closer inspection, however, reveals the absence of omphacite and an abundance of leucocratic constituents.

Microscopically, medium-grained anhedral to subhedral garnet — rich in included rutile microlites — is again much

in evidence. Together with kyanite, β -zoisite, staurolite, biotite, and muscovite, it seems to float in a fine-grained mass composed of interlocking, slightly undulose quartz and plagioclase (inversely zoned: core 25% An., rim 30% An.). Accessory minerals are rutile, often accompanied by some ilmenite or titanite, apatite, and zircon (subhedral grains showing lengths of up to 0.3 mm). Garnet, kyanite, and β -zoisite are interpreted as having been formed during the catazonal metamorphic phase. The garnet is fissured and has lost its euhedral form. Kyanite has corroded outlines, and has undulose extinction or is bent or kinked. It is often surrounded by a biotite-fringed alteration rim of sericite. Derelict β -zoisite is surrounded by epidote rims.

The minerals connected with the mesozonal metamorphism, to the contrary, show few or no signs of deformation. Staurolite forms idiomorphic unbent crystals. Second-generation kyanite is likewise unbent and takes the form of small (up to 0.35 mm in length) subhedral to euhedral needles. Biotite, muscovite, quartz, and plagioclase do not seem to be affected by post-crystalline deformation of any consequence. As a result, the foliation is poorly developed in the more leucocratic parts of the rock.

Laminae of similar composition — varying in width from several millimetres to several centimetres — are also found in other parts of the banded gneiss, although there they are rendered nearly indistinguishable by retrograde metamorphism, as shown, for instance, by sample V 1031, in which laminae having widths of up to 6.5 mm, composed of leucocratic kyanite- β -zoisite-garnet-biotite gneiss, alternate with 1.5–2 mm wide zones of garnet-biotite schist.

c. Behaviour of metasediments under eclogite-facies conditions.

The conflicting facies evidence concerning the eclogites and their associated rocks, the extremely wide spread of P and T of the eclogite facies, and the restriction of rocks with an eclogite-facies mineral association to basic and ultrabasic compositions, have all contributed to the creation of the "Eclogite Problem". In their threefold division of the eclogites, Coleman *et al.* (1965) stress the contrast between their group B and C eclogites⁸ on the one hand and the associated rocks on the other. They state: "Groups B and C are difficult to assess properly because they seem to be geologically out of place in their associated rocks, assuming of course that all eclogites represent the highest grade of metamorphism".

Indeed, the association of group B eclogites with gneisses or schists has been reported from many localities. It is remarkable that in all those occurrences — whether they concern paragneisses (Düll, 1902; Brière, 1920; Alderman, 1935; Lange, 1965), orthogneisses (Düll, 1902; Eskola, 1921), "Injektionsgneise" (Wang, 1939), or migmatitic gneisses (Smulikowski, 1964) — no "eclogitic" mineral associations have been found in the associated gneisses.

One of the principal reasons for this discrepancy is

⁸ Group B: eclogites from migmatite gneissic terrains; group C: eclogites from metamorphic rocks in alpine-type orogenic zones.

that the susceptibility of the gneisses to retrograde metamorphism is greater than that of the eclogites (Watznauer, 1964). This is conceivably due in part to the differences in tectonic competence between leucocratic and melanocratic rocks in respect of deformation (Sørensen, 1953; Engel & Engel, 1962), differences which are only enhanced by the inhomogeneous nature of the banded gneisses at Cabo Ortegal. The concentrations of garnet, kyanite, and biotite observed in sample M 474, which are virtually melanosomes and closely resemble the so-called "restites" in wet migmatitic rocks, in conjunction with the repeated occurrence of feldspathic and quartzofeldspathic laminae, lenses, and streaks in the banded gneiss, appear to justify the supposition that the banded gneiss was at one time subject to a certain measure of anatexis. Such partial melting of metamorphosed sedimentary rocks, resulting ultimately in the formation of a series of banded or veined gneisses, was predicted by Winkler & von Platen (1961a and b) on the basis of experimental metamorphism of graywackes. From field and petrographic evidence the same was inferred by Engel & Engel (1962) and by Seitsaari (1962) for catazonal terrains in the Adirondacks and SW Finland, respectively.

Experiments conducted at high temperatures and pressures by Khitarov & Pugin (1962) have shown that the temperature of incipient fusion of a sandy shale lies at 550° C for pressures exceeding 10 kb. The absence of orthoclase tends to raise the temperature at which the first melt forms by about 40° C (Winkler, 1965). According to Winkler (1965), the amount of melt formed, its composition, and the temperature of formation also depend on the amount of H₂O present, the anorthite content of the plagioclase, and the possibly incongruent melting of muscovite and biotite. The lack of exact data, however, largely reduces these factors to imponderables. Nevertheless, it is assumed that under the PT conditions inferred for the Cabo Ortegal eclogites (630–900° C; 14–19 kb), partial melting of the associated sedimentary rocks is possible. For sample M 474 (see p. 145), the composition of the metatekt was determined by modal analysis. After counting 1584 points, the volumetric ratio of restite to metatekt could be determined as 48.1 : 51.9. Within the metatekt, quartz, plagioclase (20% An.), and potash feldspar were found in the following volumetric ratio: Q : Ab : Or : An = 50.4 : 38.6 : 1.4 : 9.6. It is possible that the value given for quartz is somewhat too high, since quartzes properly belonging to the restite may have been counted as part of the metatekt.

The important role played by the presence or absence of H₂O is illustrated by the experiments of Green & Lambert (1965), who report that in a dry rock of granitic composition, plagioclase can occur as a stable phase at a temperature of 950° C under pressures of up to 22.5–25 kb. At these PT conditions, the plagioclase in H₂O-bearing rocks at Cabo Ortegal is either no longer a stable phase or is incorporated into a

eutectic melt. On the basis of Winkler's statement "*Unter höheren Drucken, bei denen Almandin-Granat beständig ist, wird auch dieser weitgehend als ein Mineral des kristallinen Restes erhalten bleiben*", the following picture — which is largely conjectural — can be drawn for the catazonal metamorphism of the Cabo Ortegal sedimentary rocks.

The rocks were divided into two contrasting components by partial anatexis. The first component is an anatectic melt for which quantity and composition are determined by physical (P, T) and chemical (H₂O content, chemical and mineralogical composition of the rock) conditions. The mineralogical composition of the second (solid) component is expected to reflect eclogite-facies conditions; it would presumably be composed of garnet, accompanied by either kyanite or zoisite or both. Muscovite, which melts incongruently at 645° and 10 kb (v. Platen & Holler, 1966), may have entered into the anatectic melt. Since incongruent melting of biotite at 10 kb requires a still higher temperature, biotite is seen as a possible constituent of the restite. If tectonic action did not press out the melt so that it intruded elsewhere (Winkler & v. Platen, 1961a), it would recrystallize more or less *in situ*, thus forming migmatitic, arteritic or, if deformed, banded gneisses.

From the evidence of sample M 474 (p. 145) it would appear that during the post-eclogitic amphibolite-facies metamorphism, P, H₂O and T were too low to permit renewed partial anatexis but high enough to permit recrystallization of quartz and plagioclase and also large-scale alteration of eclogitic mineral associations into amphibolitic ones. The rarity with which migmatitic textures are encountered in the banded gneiss is probably attributable to obliteration by the extensive deformation accompanying the amphibolite facies metamorphism.

It is now possible to account for the metamorphic history of the rock represented by sample V 1104 (p. 147). During eclogite-facies metamorphism, partial anatexis gave rise to a quartzofeldspathic melt, while the restite became composed of a mineral association (garnet + kyanite + omphacite?) which is stable under eclogite-facies conditions. Formation of zoisite at this stage is less probable, because the garnet can accommodate all the available lime (see Table I-4). It is conceivable that β -zoisite — which is greatly altered but shows no signs of deformation — formed during the post-eclogitic (bent kyanite, broken garnet) M₂ deformation under granulite facies conditions.

During the amphibolite-facies metamorphic phase the gneiss was subjected to retrograde metamorphism, since the eclogite-facies mineral association is now found in a state of transformation into an amphibolite-facies association. Biotite and muscovite have (re?)crystallized, partly at the expense of the garnet, zoisite is altered into epidote or anorthite, quartz and plagioclase and even some kyanite have recrystallized. Staurolite has been formed as an additional phase.

In this context it will be useful to describe another example of banded gneiss showing the effects of partial anatexis

(sample V 1037). In this rock, leucocratic laminae of varying width are folded along with the garnet-biotite gneiss in which they occur.

Microscopical appearance: the garnet-biotite gneiss consists of fine-grained anhedral garnet (with included rutile micro-lites) which is embedded together with small flakes of biotite in a mass consisting of fine-grained plagioclase (11% An.) and imperfectly developed lenticular bodies of slightly undulose quartz. Accessory constituents are: rutile, apatite, zircon, and some opaque matter.

The amount of garnet in the leucocratic bands is smaller than that in the garnet-biotite gneiss, but the aspect of the garnet is the same. The medium-grained muscovite is considerably bent; biotite has crystallized along its rims and its parting planes. Newly-formed, fine-grained, unbent muscovite often adheres to these bent crystals as a kind of fringe (photograph I-14); this younger muscovite is not rimmed by biotite. Lenticles of slightly undulose quartz are better developed here than in the gneissic part. Plagioclase (11% An.) occurs as severely bent, medium-grained porphyroclasts surrounded by fine-grained mortar rims. Accessories are: kyanite (occurring as sheafs of small needles in aggregates of fine-grained plagioclase), apatite, zircon, and minute amounts of rutile and opaque matter.

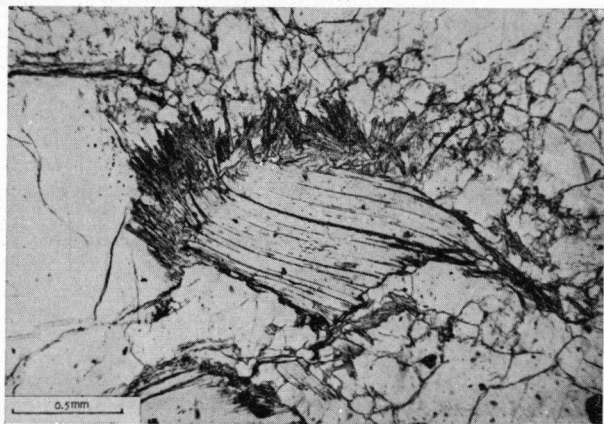


Photo I-14 Slide V 1037. Bent biotite-rimmed muscovite porphyroclast in a leucocratic band in garnet-biotite gneiss. Fringes of newly-formed fine-grained muscovite without biotite rims, probably formed contemporaneously with the biotite rims.

The occurrence of garnet in the leucocratic band and the abundance of quartz and plagioclase in the garnet-biotite gneiss, make it probable that the relation between the gneiss and the leucocratic band is not that of restite and metatekt⁹ but rather that of layers originally differing in composition and therefore reacting differently to migmatization.

The microscopical evidence suggests that muscovite was present in the leucocratic band prior to the amphibolite-facies metamorphism. Either it was already present in the metasedimentary rock, which would mean that the reaction muscovite + quartz \rightleftharpoons orthoclase component + sillimanite + H₂O (Winkler, 1965) did not take place while anatexis occurred, or it was formed when the anatectic melt recrystallized; but it might also have formed part of an "eclogite-facies" association together with garnet while the remainder of the rock became molten.

During the amphibolite-facies metamorphic phase, in any case, the rock was refolded, muscovite and plagioclase were

⁹ In the sense of Mehnert (1960).

deformed (less severely than in sample M 474), and biotite was formed at the expense of garnet and crystallized around muscovite. Small amounts of muscovite and kyanite were also formed. Quartz recrystallized entirely, and possibly plagioclase partially.

Evidence of the emplacement of granitic rock prior to the mesozonal metamorphic phase has also been found in the Banded Gneiss Formation. Parallelism of textures with the surrounding gneiss indicates that the granitic rocks were subjected to the Hercynian deformation.

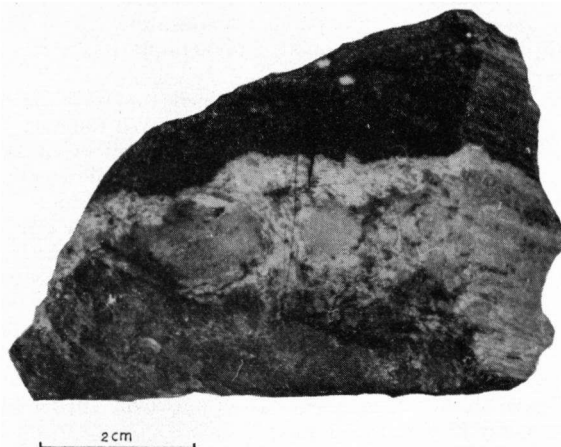


Photo I-15 Sample V 1020a. Parallelism of linear textures in garnet-biotite gneiss and tectonized granitic body. In the plane perpendicular to the tectonic b-axis (lefthand side), the borderline is erratic and poorly defined; in the plane parallel to b (righthand side) the borderline is sharp and parallel to b.

At location V 1020, a 20 cm-wide leucocratic band was found in a garnet-biotite gneiss (sample V 1020a, photograph I-15). The textures of the gneiss and the leucocratic band are parallel to each other and have a strongly linear character. The boundary between the gneiss and the leucocratic band is sharp and runs parallel to the lineation in sections taken parallel to the tectonic b-axis, but follows an erratic pattern in sections taken perpendicular to b. Large porphyroclasts of potash feldspar (up to 3 cm in length) are the most conspicuous elements of the leucocratic band; small quartz blades lie arranged parallel to their contours. Microscopically, the leucocratic band presents a picture similar to that of the leucocratic *flaser* in sample M 474. The potash feldspar porphyroclasts are xenomorphic, show no microcline twinning, have a strongly undulose extinction, and show partial replacement by muscovite. Flat lenticular bodies of medium-grained, slightly undulose quartz follow the contours of the porphyroclasts or lie arranged parallel to the contact with garnet-biotite gneiss. Fine-grained plagioclase (20% An.) is concentrated in aggregates with a similar optical orientation, suggesting — as in the case of sample M 474 — a recrystallization from pre-existing medium-grained plagioclase. Relics of medium-grained plagioclase were not found. Clusters of muscovite, partly replacing potash feldspar or plagioclase, are numerous. The unstrained nature of the muscovite suggests a late crystallization contemporaneous with the recrystallization of quartz and plagioclase.

It is difficult to explain the presence of veins of only slightly deformed tonalitic rock of magmatic appearance that are found over a distance of some 50 metres in the neighbourhood of location V 1025. These veins vary in width (some of them being as narrow as 1 cm) and cut across the surrounding gneisses. The gneisses dip 5° to the SW, the veins dip 25° to the ENE. The tonalitic rocks are, in turn, cut by veins of epidote (widths of up to 8 mm) accompanied — but not cut — by narrow veinlets of chlorite.

Hornblende-quartz diorite (sample V 1025). Macroscopically, no foliation can be observed. The hornblende is distributed irregularly; in some patches it constitutes about 80% of the rock, but in the bulk of the sample it appears in amounts less than 10%.

Microscopical appearance: medium-grained (up to 5 mm in length) plagioclase grains (3% An.) are surrounded by narrow mortar rims; they are sometimes bent or broken. Quartz grains have an amoeboid form and undulose extinction. Potash feldspar is untwinned and perthitic. The brownish-green to blue-green pleochroic hornblende is hypidiomorphic; its terminal faces are not developed. It is surrounded by rims of identically oriented actinolitic amphibole. The alteration into actinolitic amphibole (and sometimes also in chlorite) was probably caused by hydrothermal action related to a 5 mm-wide vein that cuts through the diorite and is filled with prismatic epidote and some quartz and chlorite. Accessory minerals are: muscovite enclosed by plagioclase, biotite, and titanite.

The discordant nature of the hornblende-quartz diorite in relation to the gneiss indicates that it intruded after the amphibolite-facies metamorphism and therefore cannot be correlated with the above-mentioned tonalitic anatectic melts. The hydrothermal alterations and the discordant epidote veins in this rock provide an indication about its upper age-limit.

The formation of potassium-poor anatectic melts in the banded gneisses occurred at a time immediately preceding the injection of similar melts in the neighbouring eclogites. It seems a plausible inference to consider the pegmatoid veins occurring in the eclogites (see Ch. I, A 8) as anatectic melts that were pressed out of the rocks in which they originated into the eclogites, along zones of minimum resistance.

d. Eclogitic inclusions: the Masanteo geological section.

The bulk of the mafic rocks found as inclusions in the Banded Gneiss Formation can be considered to be of eclogitic descent on the basis of their characteristic minerals or textures. These inclusions occur either as bands or as lenses (varying in length from less than 1 m to well over 200 m); their petrography is discussed in detail in Chapter I, A. Only the biggest lenses are shown on the map; the presence of great numbers of smaller inclusions is indicated by a symbol because of difficulties with respect to scale and quality of exposure.

A well-exposed section measuring 268 m in length and running roughly perpendicular to the general strike of the Banded Gneiss Formation is located on

the southern shore of the Masanteo peninsula. This section was first sampled in 1959 by E. Romijn. In 1961, J. P. Engels took some additional samples and sketched the geological relations on a series of photographs of the section. The capricious course of the coastline and the highly irregular variations in width, composition, and texture of the gneissic and mafic bands along the strike, make a great deal of simplification unavoidable and prohibit correlation of the various bands and lenses.

The geological section (Plate 2), which is based on data of Romijn and Engels, should therefore be seen as a simplified illustration of the complicated way in which gneisses and mafic rocks are associated in the Banded Gneiss Formation.

The gneisses in this section (samples Ma 1, Ma 5, Ma 17, H, 61P2, and 61P3) can be roughly divided into three types:

1. A granitic type (sample H) composed of a quartz-plagioclase (10% An.)-microcline mass containing sub-parallel oriented muscovite flakes and occasional grains of broken garnet, biotite, chlorite, and orthite.
2. A type of *augen* gneiss (samples Ma 5, 61P2, and 61P3). In this type, biotite and muscovite lie in elongate streaks, separated by flat-lenticular, medium-grained quartz bodies and fine-grained, elongate aggregates of plagioclase and muscovite. The eyes are either lenticular quartz bodies (61P2), recrystallized plagioclase porphyroclasts (Ma 5), or potash feldspars with mortar rims (61P3). The migmatic appearance is most clearly perceptible in samples 61P2 and Ma 5. Sample 61P3 is transitional between the *augen* gneisses and the planar gneisses, i.e. lenticular porphyroclasts are still present, but the rest of the fabric is planar.
3. In some of the planar gneisses (type Ma 1) the porphyroclastic eyes are absent; the lenticular bodies of quartz and plagioclase are flattened and the streaks of biotite and muscovite have been stretched into an indistinct lamination. The presence of small microfolded relics of *augen* gneiss in these planar gneisses (see Plate 2, 0-13 m) supports the assumption that the planar gneiss is formed by further deformation of the *augen* gneisses. Another type of planar gneiss is represented by sample M 17; here there is no evidence of earlier migmatization; the texture is equigranular. Medium-grained lenticular bodies of quartz are imperfectly developed. There is no strict separation between quartz and plagioclase (20% An.). The melanocratic minerals lie dispersed and are not concentrated in streaks or laminae.

The mafic rocks in this section (Ma 5a, Ma 6, Ma 9, Ma 10, Ma 12, Ma 13, Ma 15, Ma 16, Ma 19, B, C, D, E, G, I, J, L, and 61P1) present a widely varied appearance although they are all of eclogitic descent. They have been subdivided into three groups: hornblende eclogite, amphibolite eclogite + eclogite amphibolite, and garnet amphibolite + amphibolite. A further subdivision is made into types with greenish-brown or blue-green hornblende, because the colour of the hornblende is indicative of the facies conditions during amphibolization (see Ch. I, A).

1. *Hornblende eclogite (sample Ma 13)*. — The garnet in this β -zoisite-hornblende eclogite is poor in inclusions but occasionally shows included clouds of rutile dust. It is arranged in a honeycomb-like pattern (cf. sample V 1023). Biotite-plagioclase intergrowths, symplectitization of omphacite (90% of the omphacite is altered into p.p. symplectite, stages 1, 2, and 3), and the presence of porphyroblasts of light greenish-brown pleochroic hornblende and of β -zoisite aggregates with enclosed kyanite relics, indicate a granulite facies retrograde metamorphism coupled with pegmatoid activity (K-supply). During the ensuing amphibolite-facies retrogradation, narrow rims of light blue-green hornblende formed around garnet and greenish-brown hornblende. Additional constituents are: α -zoisite, quartz, calcite, rutile, titanite, apatite, zircon, and some opaque matter.

2. *Amphibolite eclogite + eclogite amphibolite (samples Ma 9, Ma 15, Ma 19, and J)*. — Amphibolite eclogite (sample Ma 15): the garnet is medium-grained and poecilitic; inclusions of rutile and epidote are sometimes arranged parallel to the crystal faces. Along the rim and cracks it alters into blue-green hornblende. Omphacite is totally converted into p.p. symplectite as well as partly altered into blue-green hornblende. Kyanite is bent and rimmed with sericite and epidote. Quartz occurs in flat-lenticular bodies of undulose grains. Additional constituents: plagioclase, biotite, rutile, apatite, zircon, and some opaque matter.

Eclogite amphibolite (sample Ma 19): garnet, poor in inclusions except for rutile, is fine-grained and anhedral. Omphacite was totally converted into stage-3 p.p. symplectite and thereafter altered into blue-green hornblende. Sericite masses containing a few relics of kyanite are rimmed with epidote. Quartz occurs in wavy flat-lenticular bodies of slightly undulose grains. Additional constituents: plagioclase, biotite, chlorite, rutile, apatite, zircon, orthite, opaque matter, and some adularia in veinlets.

Eclogite amphibolite (sample Ma 9): the garnet is fine-grained, subhedral and profuse in rutile inclusions. Only a few relics of p.p. symplectite are present; the rest of the omphacite has been altered into fine-grained subhedral crystals of greenish-brown hornblende with a weak preferred orientation. Quartz and plagioclase (12% An.) are dispersed. Additional constituents: titanite-rimmed rutile and ilmenite; apatite, zircon, chlorite, and epidote. Discordant veins filled with adularia cut veins filled with prehnite.

Eclogite amphibolite (sample J): the garnet is fine-grained, anhedral, and is rimmed with greenish-brown hornblende. Omphacite was converted into stage-3 p.p. symplectite and thereafter altered into blue-green hornblende. Quartz and plagioclase lie dispersed or in imperfect lenticular bodies. Additional constituents: chlorite, sericite, epidote, titanite-rimmed rutile, apatite, zircon, and opaque matter.

3. *Amphibolites + garnet amphibolites*. — Garnet amphibolite (samples I and L): these samples resemble the eclogite amphibolite of sample J in every respect except for the alteration of all p.p. symplectite into blue-green hornblende. This alteration has given rise to the formation of a reticulate or mesh texture of hornblende and plagioclase (cf. sample M 473, Ch. I, A).

Garnet amphibolite (samples Ma 5a and Ma 10): in these samples, garnet is fine-grained, anhedral, and rich in rutile inclusions. The hornblende is reddish-brown pleochroic. Blue-green hornblende has grown pseudo-

morphously after p.p. symplectite. Quartz and plagioclase are dispersed. The texture of the rock is compact, seemingly without preferred orientation. Additional constituents: biotite, rutile, titanite, apatite, and opaque matter.

Garnet amphibolite (sample G): this rock resembles the eclogite amphibolite of sample Ma 19, but here all the omphacite has been replaced by greenish-brown hornblende. No kyanite relics are found in the nests of sericite, β -zoisite, and epidote. Well-developed flat-lenticular quartzes lie parallel to the foliation.

Sample C is the totally amphibolized counterpart of the amphibolite eclogite of sample Ma 15.

Samples Ma 6, Ma 16, D, and 61P1 are all equigranular medium-grained amphibolites (composed of hornblende and plagioclase) with occasional garnet relics. Eclogitic palimpsests were not found in these rocks.

The rocks indicated in Plate 2 as hybrid are eclogitic rocks, first impregnated with pegmatoid matter and subsequently tectonized. The ensuing alternation of mafic and leucocratic bands gives these rocks the aspect of laminated mafic rocks. Thus, the hybrid rocks between 99 and 124 m, at 138 m, between 142 and 153 m, and between 171 and 184 m are composed of alternate bands of pegmatoid material and amphibolite (type 61P1).

The hybrid rock between 246 and 254 m is composed of alternating bands of pegmatoid matter and amphibolite eclogite (type Ma 15).

e. Non-eclogitic basic and ultrabasic inclusions.

Inclusions of ultramafic rocks and of mafic rocks of non-eclogitic descent are scarce; this is surprising, because in the area south of Cabo Ortegual large serpentinite lenses are regularly found enclosed in the paragneiss.

Of special interest is a meta-olivine gabbro occurring together with a carinthine eclogite in a concordant lens with a width of 2 m and at least 5 m long (see p. 129). Judged by its texture, the carinthine eclogite must have been formed by catazonal metamorphism of a gabbroic rock (see Ch. I, A 3). In the meta-olivine gabbro (sample V 1023a), however, this metamorphism did not advance beyond an initial stage.

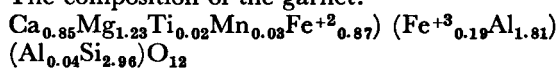
Macroscopically, the rock is compact with an ophitic texture. White plagioclase laths and black olivine (\varnothing up to 4 mm) can be identified.

Microscopical appearance: the meta-olivine gabbro is fine-grained; its original constituents, olivine, augite, plagioclase, and brown spinel, are randomly oriented. The olivine ($2V^Z = 89^\circ$) is hypidiomorphic to idiomorphic and has a forsterite content of 88% (determined by the X-ray diffraction method according to Yoder & Sahama, 1954). Opaque dust occurs as inclusions in the olivine, leaving a rim which is clear of inclusions. The xenomorphic colourless augite ($2V^Z = 48^\circ$, $r > v$ inclined, $n_{Dv} = 1.694 \pm 0.002$) has a well-developed diallage parting, and crystallized after both plagioclase and olivine. In some places, the augite is rendered semiopaque by the presence of irregularly-distributed minute inclusions of opaque matter (ilmenite). Although the plagioclase has retained its original form, it has been completely transformed into albite with numerous micro-crystalline inclusions (up to 0.02 mm long) of zoisite (epidote?).

The decalcification of the plagioclase was caused partly by the formation of the zoisite inclusions, partly by the formation of rims of colourless garnet between the mafic constituents and the plagioclase, and partly by the formation of amphibole and clinopyroxene(?) as a result of metamorphism. The amphibole lies in 0.05 mm-wide rims of radially-arranged prisms around olivine as well as around augite. Its optical properties are $2V^z$ large, $\Delta = 0.010-0.012$, $n_{Dz} \approx 1.675$, extinction oblique. Along the rims of the plagioclase crystals, cryptocrystalline aggregates of anhedral clinopyroxene(?) grains (\varnothing up to 0.01 mm) have grown at the expense of plagioclase. Their extremely small size permitted only a rough approximation of the optical properties; $2V$ could not be determined, $n_{Dxyz} \approx 1.675$, $\Delta < 0.012$. At the outside of the amphibole-rims, 0.03–0.04 mm-wide rims of colourless garnet formed. These garnet rims, which are not wholly continuous, may border on plagioclase or on the cryptocrystalline clinopyroxene aggregates. Sometimes, narrow rims of cryptocrystalline clinopyroxene are found between the garnet and the amphibole. In consequence of the strict localization of the garnet formation, the garnet is disposed in a honeycomb pattern.

The following evidence has led to the assumption that the formation of garnet, amphibole, and clinopyroxene, is to be interpreted as a first step in the transformation of the olivine gabbro into a carinthine eclogite.

1. The association of the meta-olivine gabbro with a carinthine eclogite of gabbroic composition in the same lens.
2. The similarity between the newly-formed minerals in the meta-olivine gabbro (amphibole, garnet, clinopyroxene) and those found in the carinthine eclogite (carinthine, garnet, omphacite).
3. The arrangement of the garnet in the carinthine eclogite in the same honeycomb pattern that is also found in the meta-olivine gabbro.
4. The fact that the decalcification of the plagioclase is caused not only by the formation of Ca-bearing minerals such as amphibole, clinopyroxene, and garnet, but also by transformation of the anorthite component into an epidote-group mineral. This indicates that the prevailing pressure was so high that the plagioclase could not even accommodate the anorthite that was not used in the formation of amphibole, clinopyroxene, or garnet (see also Engels & Vogel, 1966).
5. The composition of the garnet:



(see Vogel & Warnaars, 1967) is definitely eclogitic and closely approaches that of the garnet in the carinthine eclogite (Table V-1, nr. 6).

The hypersthene gabbro cutting across the banded gneiss at location V 1077 as a 30 cm-wide dyke (at least 40 m long) must have intruded after the amphibolite-facies metamorphic phase, since it lacks any signs of metamorphic alteration.

Hypersthene gabbro (sample V 1077).

Microscopical appearance: the medium-grained rock has a holocrystalline panxenomorphic texture with a random

orientation of the grains. Non-pleochroic hypersthene ($2V^x = 80-90^\circ$) is invariably rimmed by and altered into a yellowish augite. Plagioclase (67% An.) shows abundant albite-Carlsbad twins, sometimes with added pericline lamellae. Small quantities of intricately intergrown plagioclase and potash feldspar, sometimes accompanied by quartz, have crystallized along the rims of the plagioclase crystals or as feathery concentrations in interstices. These concentrations are considered to have been formed by late crystallization from a residual melt. As accessories, brown pleochroic basaltic hornblende with green pleochroic rims, and some opaque matter are found. Small-scale hydrothermal alteration has caused partial sericitization of plagioclase and partial alteration of mafic minerals into chlorite and biotite.

Owing to the discordant nature of the dyke and its hydrothermal alterations, the time of intrusion of the gabbro can be determined as roughly coincident with the intrusion of the quartz diorite of location V 1025 (see p. 150).

Along the northern shore of the Masanteo peninsula, the banded gneiss has an appearance not unlike that of the Carreiro zone of tectonic movement (see Ch. I, C). Severely deformed gneiss curves around variably sized tectonic fish of basic and ultrabasic composition. The gneiss is composed of alternating bands of mylonite and of *augen* gneiss. In shear zones, chlorite schists are found. Samples were taken from three lenses of ultra basic rock (numbers V 1308, V 1309a and V 1309b), of which V 1309a showed the least alteration.

Biotite-hornblende pyroxenite (sample V 1309a).

Macroscopical appearance: the rock is coloured a clear green due to the preponderance of light-green clinopyroxene over the other constituents. Dispersed in this green matrix lie dark-green prisms of medium-grained hornblende and brownish aggregates in which biotite is the only macroscopically identifiable mineral.

Microscopical appearance: the colourless, fine-grained, xenomorphic clinopyroxene ($2V^z = 58-59^\circ$, $c/z = 40-44^\circ$) is little altered, although small patches of hornblende in the clinopyroxene indicate replacement by hornblende. Clinopyroxene relics enclosed in the medium-grained hypidiomorphic porphyroblasts of greenish-tinged hornblende ($2V^x = 80-90^\circ$, $c/z = 14-15^\circ$) indicate that the porphyroblasts were also formed at the expense of clinopyroxene.

Iddingsite has grown together with bowlingite, α -chrysolite, or sericite as a secondary product after hypersthene ($2V^x = 80-90^\circ$). These alteration products are gathered in clusters of pseudomorphs in which fine-grained light-brown biotite also occurs; the biotite is sometimes intergrown with chlorite (x light-green $< y = z$ dark blue-green; $2V^x$ small; Δ low), which locally also replaces clinopyroxene. The chlorite was investigated microchemically for Ni, but no traces of this element could be detected. Pyrite, rutile, titanite, apatite, and calcite occur as accessories.

Biotite-hornblende pyroxenite (sample V 1309b).

The clinopyroxene is medium-grained; its patchy alteration into hornblende is more advanced than in sample V 1309a. Blastesis of hornblende, however, is not so pronounced. The pseudomorphs after hypersthene are lacking, as is chlorite.

Hornblendite (sample V 1308).

This rock consists wholly of the same slightly green hornblende as that forming the porphyroblasts in sample V 1309a and b. No relics of clinopyroxene have been found. Minute amounts of biotite are present.

2. Cariñogneiss Formation

a. Occurrence.

Although the Cariñogneiss is chemically and mineralogically very similar to the banded gneiss, it differs so much in general appearance and fabric that it can be easily distinguished in the field. The banded gneisses, which are characterized by a wide variation in rock-types differing in both structure and composition, form a strong contrast with the even-grained, uniformly textured, non-laminated Cariñogneiss. The latter shows a banding dependent on compositional differences, but this banding is more an inherited sedimentary feature, in contradistinction to the layering and lamination in the Banded Gneiss Formation, which is the result of tectonic and metamorphic differentiation. Further distinctions are provided by the smaller number of mafic inclusions in the Cariñogneiss and by the decidedly non-eclogitic nature of these inclusions. The boundary plane between the banded gneiss and the overlying Cariñogneiss to the E is gradual rather than sharp. Nevertheless, in a well-exposed section its position can be located within a distance of about 20 metres.

b. Petrography.

In the field, two types could be discerned: a psammitic type having a granoblastic texture and reacting competently to folding, and a pelitic type having a lepidoblastic texture and reacting incompetently to folding (photograph I-16).



Photo I-16 Locality Coe 220. Isoclinal folds in the Cariñogneiss, which is banded due to compositional differences. The leucocratic (quartz-rich) bands have reacted competently to the folding; the melanocratic (quartz-poor) types have reacted incompetently and have been pressed into the cores of the folds. Photo: P. A. J. Coelewijn.

On the basis of their mineralogical composition, the psammitic types may be qualified as quartz-gray-

wackes and normal graywackes (Huckenholz, 1963). They contain 35—70 % quartz, 5—50 % feldspar, and 12—30 % other constituents. The pelitic types contain 15—45 % quartz, 0—40 % feldspar, and 40—80 % other constituents. According to the classification of Huckenholz, they may be considered as metamorphosed normal and quartz-poor graywackes.

Within these two types, variation is caused by differences in mineral associations. Two-mica gneisses, often garnetiferous, are the most commonly encountered types; melanocratic types of two-mica gneiss may contain kyanite and staurolite in addition to garnet. Less common are biotite (\pm garnet) gneiss, muscovite (\pm garnet) gneiss, and muscovite (\pm biotite) schist.

Texture. — With few exceptions, the mutual relations of the minerals resemble those of the banded gneisses. Quartz and plagioclase occur as equant interlocking grains, sometimes undulose or bent (kinked twin lamellae). Liquid and two-phase inclusions in quartz are often found in trains running perpendicular to the foliation. Plagioclase is inversely zoned; alteration into saussurite and sericite occurs in the neighbourhood of narrow veins filled with epidote and adularia, respectively.

The garnets are corroded and have anhedral outlines; they have a turbid, pitted appearance, and alter into biotite. Two generations of muscovite are found. The oldest muscovite is fine- to medium-grained, sometimes has corroded outlines, and is often bent or broken. Small flakes of homoaxially-oriented biotite occur along cleavages and rims of these muscovite crystals. The second muscovite generation is fine-grained, undeformed, and lacks rims of biotite. Biotite itself is fine-grained and undeformed; its size is usually smaller than that of the leucocratic constituents. Both kyanite and staurolite occur as fine-grained, rounded or corroded, sometimes altered relics. Bent or otherwise strained crystals are common. Evidence of a second kyanite (or staurolite) generation is lacking.

A common accessory is epidote (intermediate birefringence, $2V^z = 80^\circ$ — $2V^x = 80^\circ$), which is always surrounded by a turbid rim of epidotic matter. Occasionally, potash feldspar is found, either with Carlsbad or microcline twinning and sometimes with myrmekitic plagioclase along the rims. Alteration products are: chlorite (secondary after garnet and biotite) and sericite (secondary after plagioclase, staurolite, and kyanite). As in all the rocks of the Concepenido Complex, there is a close relation between the occurrence of these alteration products and that of narrow veins filled with adularia and epidote. Accessory minerals are: rutile, titanite, apatite, zircon, and opaque matter (all occurring in the same manner as in the banded gneisses) and rounded metamict orthite and tourmaline. The tourmalines are zoned, with greenish-brown cores and green rims. As demonstrated by broken crystals and the alignment of prismatic crystals parallel to the foliation, the tourmalines are older than the Hercynian metamorphism.

There is a continuous series of transitional types between the psammitic and the pelitic types of Cariñogneiss. It will suffice to describe only the extreme types in detail.

Garnet-muscovite-biotite gneiss (sample V 1081).

This rock is chosen as a representative of the psammitic type. The ratio quartz to feldspar to other constituents (60 : 18 : 22) is that of a quartz graywacke.

Macroscopically, the rock has a greyish to brown colour. The faintly expressed foliation is marked by parallel alignment of feldspars and micas. A maze of hydrothermal veins cutting across the foliation is conspicuous because the veins and their surrounding, hydrothermally influenced, areas (about 1 mm on both sides) have a light greenish colour. Microscopically, the rock is inequigranular and fine-grained. The minerals lie evenly dispersed and show no tendency toward concentration in streaks. Interlocking, faintly undulose quartz with trains of liquid and two-phase inclusions is the principal component. A strong preferred orientation of quartz could be determined with the comparator. Inversely zoned, amoeboid plagioclase (core 20% An., rim 25% An.), is slightly saussuritized. Strongly corroded garnet relics with a dusty appearance have been partially replaced by reddish-brown biotite. The grain-size of biotite and muscovite is in general much smaller than that of quartz and plagioclase. The typical biotite rims around muscovite are found only around the bigger muscovite crystals. It is remarkable that the micas seem to be located along the boundaries of quartz and plagioclase grains, whereas micas wholly or partially enclosed in quartz or plagioclase are rare; consequently, the preferred orientation of both biotite and muscovite is poorly developed.

Further constituents are: chlorite (secondary after biotite), rounded microcrystalline grains of metamict orthite, rutile, apatite, zircon, and opaque matter.

Kyanite-staurolite-garnet-muscovite-biotite gneiss (sample V 1401).

This rock corresponds in composition (quartz 18%, feldspar 12%, other constituents 70%) to a quartz-poor graywacke. The severely microfolded rock has a dark-brown colour and a strongly developed lepidoblastic texture. Biotite, muscovite, and garnet can be discerned macroscopically.

Microscopically, garnet, kyanite, and staurolite appear as corroded and altered grains. Garnet has a pitted appearance but sometimes still shows euhedral outlines. Staurolite is converted into biotite or chlorite along fissures. Elongate crystals of all three minerals are aligned parallel to the foliation, but no signs of bending or straining could be found. Plagioclase (28% An.), potash feldspar (twinned according to the Carlsbad law and lightly sericitized), and non-undulose quartz lie in a mosaic pattern frequently interrupted by micas. The micas, muscovite, and reddish-brown biotite are situated preferentially in the steep limbs of the microfolds, thus causing a kind of tectonic banding. Biotite, slightly altered into chlorite, is once again the younger of the two minerals, since it occurs in rims around muscovite. Only in shear-zones are bent micas found. The absence of bending or straining in muscovite and biotite as well as in feldspar and quartz is considered to be an indication of post-kinematic or late-kinematic (re?) crystallization of these minerals.

According to the petrographical evidence, the Cariñogneisses have been twice affected by regional metamorphism. Evidence of the earliest metamorphic

phase is present only in the form of relics of garnet, muscovite, kyanite, and staurolite. In all types of Cariñogneiss the association garnet \pm muscovite \pm kyanite is quite common. Staurolite occurs only in the more pelitic lepidoblastic types as an additional constituent. The presence of staurolite makes it possible to establish the facies conditions during the Precambrian metamorphic phase as those of the staurolite-almandine subfacies of the almandine-amphibolite facies (Turner & Verhoogen, 1960). During the Hercynian metamorphic phase, the association garnet \pm muscovite \pm kyanite \pm staurolite was replaced by the association biotite \pm muscovite (\pm garnet?). Because the plagioclase is predominantly an oligoclase-andesine, the possibility that a greenschist-facies association is involved can be disregarded. Moreover, the presence of an amphibolite-facies association is confirmed by the amphibolization, during the Hercynian metamorphic period, of the mafic inclusions (for instance at San Julian del Trebol, see Ch. I, B 2 c).

c. Cafemic inclusions.

The sparse inclusions found in the Cariñogneiss, though diverse, are all of a Cafemic nature and include amphibolite, calc-silicate rock, and metagabbro.

The amphibolites were found exclusively on the peninsula just North of Puente de Mera. They closely resemble the amphibolites of the Peña Escrita type (Engels, in preparation) and occur as concordant lenses up to 70 m wide in leucocratic brecciated gneisses. That is to say, the body of the amphibolite lies parallel to, but its foliation perpendicular to, the foliation of the gneisses.

Macroscopically, the amphibolite (sample V 1067) is compact and aphanitic; an abundance of hornblende causes its black colour. The foliation is faintly visible, being marked by the parallel orientation of hornblende crystals and tiny white elongate specks of plagioclase. Veins of light-green epidote have penetrated the amphibolite along fissures. Microscopically, the texture of the rock appears as microcrystalline and nematoblastic. The chief constituents are: an intensely dark-green hornblende (x yellow brown < y dark olive-green = z dark blue-green) locally altered into chlorite, sericitized plagioclase (15–17% An.), and colourless epidote. Quartz, titanite (sometimes rutile), zircon, and opaque matter occur as accessories. The epidote found in the veins is of a faintly pleochroic pistacite-like variety. Its colour and its higher birefringence set it apart from the clinzoisite-like variety found in stable association with hornblende and plagioclase.

A remarkable inclusion was found at location V 1083, where a microfolded kyanite-staurolite-garnet-two mica gneiss (sample V 1083a) with fold axes plunging S 20°E/35°, is bordered by — and passes along the strike into — a planar garnet-biotite gneiss. In the planar gneiss lies a concordant lens measuring 6 × 15 cm, with a zoned structure (sample V 1083). Its brownish-red, 3 cm-wide core, which is surrounded by a 1 cm-wide white rim, consists mainly of garnet. The

white rim is in its turn surrounded by a 0.5 cm-wide black rim rich in hornblende. The boundary between the gneiss and the lens is a sharp one, but between zones the borderlines are ill defined.

Microscopically, the garnetiferous part of the lens consists of garnet, epidote, clinopyroxene, and undulose quartz. Apatite, titanite, and zircon occur as accessories. The minerals have a random orientation and an even distribution. The garnet is anhedral — though at times crystal faces are still present — and slightly brownish-pink in colour. According to X-ray and optical data ($\bar{a}_0 = 11.883 \pm 0.002$, $n_D = 1.761 \pm 0.005$), its composition is that of a grossular-rich grossular-andradite mixture (Frietsch, 1957). The clinopyroxene is colourless in thin section; its optical properties ($\Delta = 0.022'$; $2V^z \approx 60^\circ$; $c/z \approx 41^\circ$) do not allow determination of its composition, which is probably diopsidic. Anhedral epidote ($2V^x = 80-90^\circ$, $r > v$) appears as a mineral secondary after garnet (and clinopyroxene?).

The leucocratic zone is almost entirely composed of zoisite and quartz with minor amounts of epidote. Hornblende, sericite, light-pink pleochroic titanite, apatite, zircon, and opaque matter are accessory constituents. Three varieties of zoisite are present: α -zoisite ($2V^z$, $r < v$) and γ -zoisite ($2V^x$, $r > v$) in the form of heavily zoned cores are surrounded by a rim of β -zoisite ($2V^z$, $r > v$). Remarkably, the epidote occurs as separate crystals and not as rims around zoisite. Small prisms of subhedral to euhedral, extremely light pleochroic hornblende ($\Delta \approx 0.023$, $c/z \approx 19^\circ$) have a random orientation in contrast with the zoisite, which has a weak preferred orientation.

From the garnetiferous part outwards, the zoisite-epidote content diminishes and quartz, hornblende, and sericite become more prominent. Gradually, the hornblende becomes more intensively pleochroic and the sericite patches grade into sericitized plagioclase. In this way, the leucocratic rim gradually passes into the outer rim, which has the composition of a hornblende gneiss. In this latter part, epidote has completely disappeared. Hornblende, quartz, sericitized plagioclase, and muscovite are the principal constituents. Titanite (still faintly pleochroic), zircon, apatite, metamict orthite, and opaque matter are accessories. The hornblende is of a common blue-green variety with slightly brownish cores and has a strongly-developed preferred orientation ($c //$ to the contours of the lens). The abrupt appearance of garnet, biotite, and mesoperthite instead of hornblende and sericitized plagioclase, marks the boundary line with the garnet-biotite gneiss. In the gneiss, the garnet content slowly diminishes with increase of the distance to the inward boundary, and at the same time the antiperthitic nature of the plagioclase gradually disappears.

The origin of the calc-silicate rock remains just as obscure as the origin of its zoned appearance. Metamorphism has eradicated all evidence of earlier textures; the parallelism of the zones with the outer boundary of the lens suggest that the zoned appearance was probably caused by metamorphism, possibly accompanied by reaction-metasomatism with the surrounding gneiss.

The metagabbro body situated East of San Julian del Trebol (locations V 1085, V 1086) differs in size as well as in petrography from the other inclusions in the Cariñogneiss. Its true size is unknown, since it lies on a promontory and is thus surrounded on three sides by

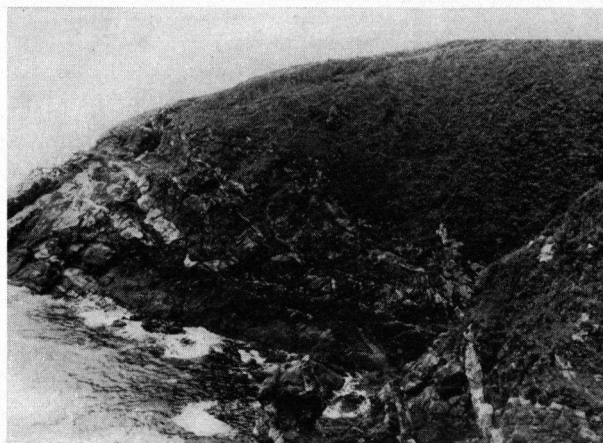


Photo I-17 Pegmatite veins in the metagabbro near San Julian del Trebol, looking South.

water. However, its minimum observable thickness is 125 m and its minimum length 375 m. In a 5 to 10 m-wide zone, pegmatites have intruded into the metagabbro (photograph I-17); they bear the imprint of deformation and locally are definitely schistose. Their composition is inhomogeneous. They may be pink and rich in potash feldspar, greenish and rich in plagioclase, or white and gneissic with coarse-grained muscovite and an occasional garnet.

In the metagabbroic rock, two types can be discerned: a fine-grained type (sometimes with ophitic texture) and a locally occurring coarse-grained, pegmatoid type in which the plagioclase lies in aggregates (photograph I-18). The random orientation of the grains, the spheroidal type of weathering, and the presence of an undisturbed system of joints in which tourmaline and chlorite sometimes occur, constitute convincing evidence, together with the palimpsest textures, of the igneous origin of the metagabbro.

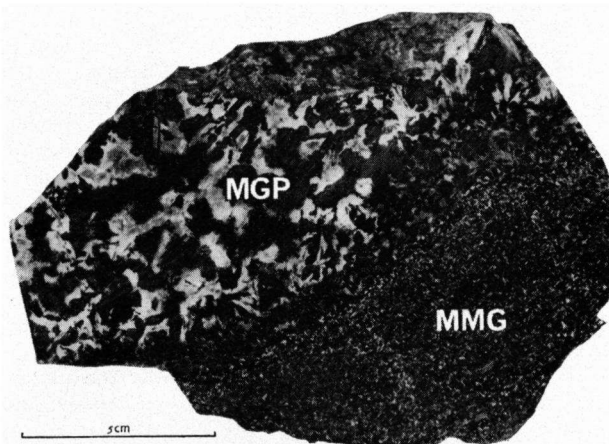


Photo I-18 Sample V 1085. Contact between medium-grained metagabbro (MMG) and metagabbro pegmatite (MGP).

The microscopic evidence indicates that coarse-grained pegmatite of granitic (samples V 1085a, V 1085c) or albititic (sample V 1085b) composition has undergone a thorough post-crystalline deformation.

In the albitite of *sample V 1085b*, corroded apatite, and bent, biotite-rimmed muscovite appear to be the oldest constituents. Muscovite must have crystallized earlier than apatite, because it is idiomorphic relative to apatite. Recrystallized porphyroclasts of poicilitic albitite and the grain-size of the apatite (medium) testify to the originally coarse-grained nature of the albitite. Fine-grained recrystallization of albitite (0% An.), muscovite, and interlocking grains of strain-free quartz give the rock its present fine-grained appearance. Deformation has caused narrow microcrystalline mylonitic zones, but no preferred orientation of muscovite was found. Macroscopically, the granite pegmatite of *sample V 1085a* consists of white, rounded crystals of potash feldspar (up to 1 cm in \varnothing) lying in a matrix of sugary, pink potash-feldspar. Muscovite is scarce and concentrated in irregular streaks, thus accentuating a poorly-developed foliation. Quartz is aggregated without any visible relation to the foliation.

Microscopically, the white grains of potash feldspar appear to be untwinned perthitic porphyroclasts surrounded by mortar rims. The pink matrix consists almost exclusively of microcline (twinned), with scattered grains of plagioclase. Muscovite occurs isolated or in streaks and is usually somewhat bent. The quartz aggregates consist of coarse-grained, interlocking slightly undulose crystals.

Between these virtually monomineralic rocks occur more gneissic types of pegmatite (*sample V 1085c*). These types have a well-developed foliation, are rich in muscovite, and are composed of both potash feldspar and plagioclase, while quartz lies in flat-lenticular bodies parallel to the foliation.

Microscopically, untwinned perthitic potash feldspar and plagioclase (0% An.) twinned according to the albitite-law — both rich in microcrystalline muscovite inclusions — occur together with bent muscovite as medium-grained porphyroclasts. The matrix is formed by a mosaic-patterned aggregate of albitite and microcline. Streaks of muscovite and flat-lenticular aggregates of slightly undulose quartz in the matrix weave around the porphyroclasts.

The medium-grained metagabbro (*slide V 1085k I*) and the metagabbro pegmatite (*slide V 1085k II*) have both been completely converted into amphibolite. The originally medium-grained gabbroic rock has recrystallized as a fine-grained amphibolite. The seemingly lath-shaped plagioclase crystals have been replaced by pseudomorphous aggregates of fine-grained plagioclase (37% An.), locally altered into saussurite. The ferromagnesian minerals have been transformed into spongy blue-green hornblende with quartz inclusions, which is diablastically intergrown with a hornblende free of inclusions. Dusty clouds of opaque matter (ilmenite?) occurring in the hornblende are probably inherited from gabbroic olivines or pyroxenes (see description of *sample V 1023a*, Ch. I, B 1 e). Rutile grains are surrounded by rims of ilmenite and titanite. Garnet has grown incidentally along the border between hornblende and plagioclase. Epidote, biotite, chlorite, rutile, apatite, zircon, and opaque matter are minor constituents.

Except for the grain-size, *slide V 1085k II* is identical to *slide V 1085k I*. The spongy hornblende crystals with quartz inclusions can reach lengths of well over 5 mm. They show the same diablastic intergrowths with inclusion-free hornblende. The plagioclase (32% An.) lies in clusters of medium-grained crystals, but its recrystallization in fine-grained aggregates is less pronounced than in *slide V 1085k I*. Garnet occurs more frequently between hornblende and

plagioclase. Clusters of chlorite with rounded outlines are possibly pseudomorphs after olivine. Additional constituents are: epidote, orthite, biotite, muscovite, chlorite, sericite, prehnite (rounded and cracked), rutile, apatite, and opaque matter.

Near the contact with the Cariñogneiss, the metagabbro (*sample V 1086*) lacks the ophitic texture. It has the aspect of an unoriented biotite amphibolite. The presence of 5–7% biotite in the rock may perhaps be ascribed to contamination with potassium from the pegmatite. Garnet does not occur in *sample V 1086*.

Vein minerals deposited in the vertical joint system are (*samples V 1085d, V 1085f*): idiomorphic schorlrite ($2V^x = 0^\circ$, $\Delta = 0.025-0.027$, $1.650 < n_{y,z} < 1.658$; pleochroism: x light pinkish-brown < y = z dark brown), idiomorphic prochlorite ($2V^z = 0-14^\circ$, $1.592 < n_{x,y} < 1.606$) in booklets, ilmenite, and alternatively quartz or adularia. Hydrothermal solutions have caused alteration of the wall-rock.

3. Chimparragneiss Formation

a. Occurrence.

Tectonic contacts separate the Chimparragneiss Formation from the Uzal serpentinite to the East and from the underlying Candelaria amphibolite to the West. The reasonably well-exposed eastern boundary of the gneiss could be mapped with an accuracy of about 20 metres, but most of the western boundary is hidden under the alluvials of the Rio Condomiñas. Like the other gneisses, the Chimparragneiss is poorly exposed. Consequently, the study of the relations between the different types was severely hampered.

b. Petrography.

The most common type of gneiss is a planar to planolite, sometimes mylonitic or blastomylonitic, garnet-biotite or garnet-two mica gneiss poor or lacking in potash feldspar. Its macroscopical appearance is reminiscent of the banded gneisses. Eyes and elongate lenses consisting of quartz and plagioclase alternate with streaks consisting predominantly of mafic minerals (see photograph I-19). Although the mineralogi-



Photo I-19 Locality V 358. Glandular texture of the Chimparragneiss. The leucocratic eyes consist of quartz or quartz-plagioclase mixtures.

cal composition and the relations between the minerals are largely identical to those in the banded gneisses, some differences, albeit small ones, indicate that the Chimparragneiss had a slightly different metamorphic history.

The minerals found in this common type of Chimparragneiss are: quartz, plagioclase, garnet, biotite (chlorite), and muscovite as principal constituents, and tourmaline, orthite, rutile, apatite, zircon, and opaque matter as accessory constituents. Staurolite was not found. Garnets are found as anhedral, fissured, and corroded grains; the rutile inclusions so characteristic of garnets in eclogites and banded gneisses are lacking in the Chimparragneiss garnets. As in the banded gneisses, two generations of kyanite are found. The older kyanite occurs as fine-grained, rounded crystals concentrated in the melanocratic streaks; the younger generation is found as groups of microcrystalline needles lying predominantly at the borders of plagioclase crystals. Neither bent nor altered kyanites were found. The relations between the phyllosilicates are identical to those in the banded gneisses, i.e. fine-grained unstrained biotite often rims medium-grained bent muscovite. Chlorite was formed secondary after biotite.

The separation of the minerals into leucocratic and melanocratic streaks suggests that the Chimparragneisses, like the banded gneisses, underwent partial anatexis accompanied or followed by deformation and recrystallization under mesozonal conditions.

In the fine- to medium-grained kyanite-garnet-two mica gneiss of sample V 300, for instance, streaks consisting of biotite, garnet, muscovite, and kyanite alternate with elongate disks of medium-grained, slightly undulose quartz and lenticular aggregates of fine-grained plagioclase (10—18% An.). The rigid separation of quartz aggregates from plagioclase aggregates suggests that, as in sample M 474 (p. 145), recrystallization of a coarser-grained metatekt has taken place. Extreme deformation has given rise to (blasto) mylonites in which the metatekts have been drawn out into narrow bands (photograph I-20).

In a few localities (see Fig. I-18) parts of the gneiss have escaped partial anatexis. Irregularly-formed fish of a fine-grained, compact garnet-biotite gneiss — closely resembling, both macroscopically and microscopically, the psammitic type of Cariñogneiss (see p. 153) — lie in a matrix of *augen* gneiss (photograph I-21). Presumably, the level at which these Cariñogneiss-like fragments are found represents the “upper” limit of partial anatexis. As such, it is comparable to the transition zone between the Banded Gneiss and Cariñogneiss Formations.

Orthogneisses. — Potash feldspar-rich rocks of granitic composition frequently lie within the above-mentioned potassium-poor gneiss. Relics of virtually undeformed granite and the existence of an intrusive relationship between granite and Chimparragneiss are indicative

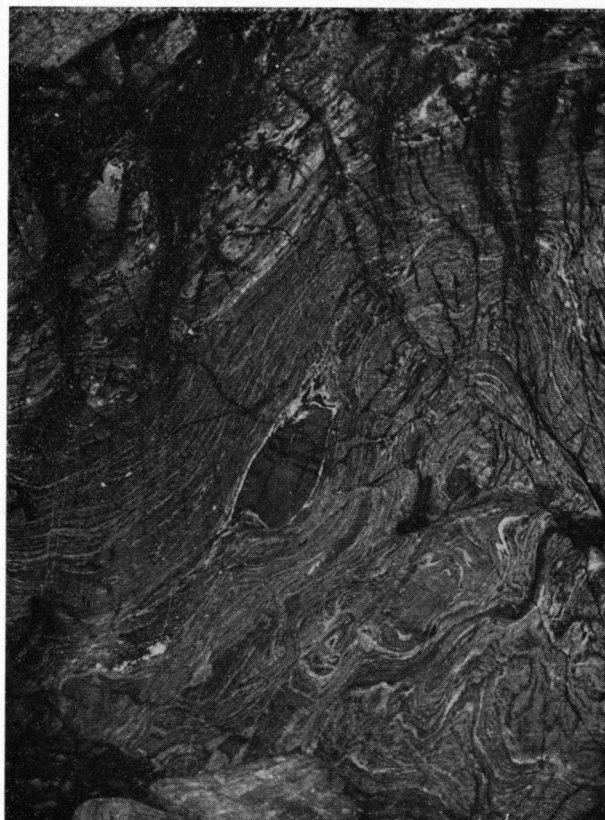


Photo I-20 Locality V 366. Mylonitic texture of the Chimparragneiss at Playa de Cartés. The metatekt has been drawn out into narrow streaks which bend around included pyrigarnite lenses.

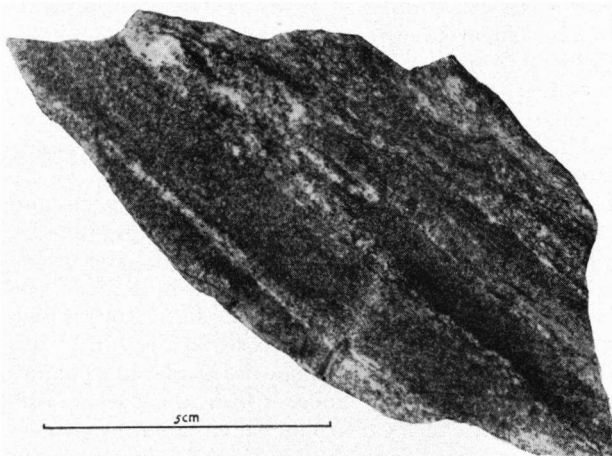


Photo I-21 Sample V 307. Fish of non-anatectic Chimparragneiss in glandular gneiss which has been subjected to partial anatexis.

of the igneous origin of the potassium-rich types of gneiss. Although progressive and retrograde metamorphism have often altered the original granitic mineral composition, it can still be seen that muscovite granites as well as two-mica granites have intruded. Since the muscovite-rich types of granitic gneiss may



Photo I-22 Locality V 352. Granitic vein in the Chimparragneiss, folded after intrusion.

be found as bands in the types rich in muscovite and biotite, it is inferred that the muscovite granite is younger than the two-mica granite.

Their intrusive relation to the Chimparragneiss (see photograph I-22) and the absence of migmatic features, suggest that the granites intruded after the catazonal metamorphic phase. However, the imprints of mesozonal metamorphism and deformation suggest that the granites intruded prior to the mesozonal metamorphic phase.

The textures of the potash-rich rocks vary according to the degree to which they have been affected by deformation. Virtually undeformed rocks with a medium-grained granitic texture and random orientation of the constituent minerals (samples V 41, V 208); *augen* gneisses (samples V 307a, M 249) with a linear or planoliner texture, and planar gneisses (samples V 266a, M 140) with a strong preferred orientation of quartz and micas, are all found. An attempt to correlate the degree of deformation with the position of the gneisses relative to the large-scale tectonic features remained inconclusive.

The absence of deformation in some granitic rocks and the whitish colour of the biotite-poor orthogneisses are generally useful criteria for distinguishing the ortho- from the paragneisses, although potash-poor muscovite gneisses have also been found (sample M 100). However, if potash feldspar is macroscopically unidentifiable, it is impossible to distinguish the planar or planoliner biotite-rich orthogneisses from the paragneisses in the field. The localities at which granitic gneisses were encountered are shown in Fig. I-18. Several areas in which no potassium-poor gneisses were found between the granitic gneisses have been provisionally outlined.

The constituent minerals of the granitic rocks are: quartz, plagioclase, potash feldspar, muscovite, and sometimes biotite. Mesozonal metamorphism caused the growth of kyanite, garnet, second-generation biotite, and sometimes second-generation muscovite. Accessory minerals are: apatite, zircon, and opaque

matter; sometimes rutile, titanite, and brownish-green or blue-green tourmaline are also found.

The *potash feldspar* of the granitic rocks is untwinned or twinned according to the Carlsbad law; it is often perthitic. It has been partially replaced by cross-hatched microcline. In the gneissic types the untwinned potash feldspar is found as porphyroclasts lying as eyes surrounded by mortar rims, parallel to the foliation. An abundance of small grains of myrmekitic plagioclase around these porphyroclasts indicates replacement of potash feldspar by plagioclase. In the matrix, all the potash feldspar is present in the form of cross-hatched microcline.

Antiperthitic *plagioclase* is more frequently found than in the potash-poor gneisses. The anorthite content of the plagioclase ranges from 9 to 26%. The development of sheaves of *kyanite* needles at the rims of or enclosed in feldspar crystals, the formation of *biotite* rims around *muscovite* and of *garnet* rims around primary biotite, and the replacement of potash feldspar by microcline and myrmekitic plagioclase, are all regarded as effects of mesozonal metamorphism. Chloritization, saussuritization, and sericitization are effected by hydrothermal veins filled with epidote, prehnite, or adularia. In sample V 283, a light-green pleochroic pumpellyite ($2Vz = 40^\circ$, $r < < v$, $n_x = 1.67$, $\Delta = 0.010-0.015$) is found in aggregates with epidote and in narrow dilatation veins.

c. Cafemic inclusions.

The few inclusions in the Chimparragneiss can be separated into two groups. The first group includes calc-silicate rocks, the second metabasites.

The calc-silicate rocks are garnet-zoisite-quartz rocks with an indistinct foliation. The predominant zoisite is of either the α - or β -variety (samples V 1157 and V 33b, respectively). Of the two, β -zoisite seems to be the latest phase, since it always rims α -zoisite.

Sample V 33b, a fine-grained garnet-zoisite-quartz rock, was taken from a lens (length 0.5–1 m) in the Chimparragneiss. Microscopically, it consists of slightly-strained quartz, xenomorphic colourless grossular-rich garnet ($\bar{a}_0 = 11.787$, $n_D = 1.753 \pm 0.002$), and anhedral to subhedral β -zoisite ($2Vz \approx 30^\circ$, $r > v$, $\Delta \approx 0.008$) with cores of α -zoisite, as principal constituents. Accessory constituents are: chlorite, sericite, titanite, apatite, zircon, and opaque matter.

The distinction between the Banded Gneiss Formation and the Chimparragneiss Formation is based predominantly on the mineral associations encountered in their respective metabasite inclusions. Whereas plagioclase is only found as a product of retrograde metamorphism in the metabasites from the Banded Gneiss Formation, it occurs as a stable phase associated with garnet and clinopyroxene in the metabasites of the Chimparragneiss Formation, which should therefore be called (plagio)pyrigarnites (for definition see Ch. III, A 1) or retrograde (plagio)pyrigarnites, rather than eclogites or retrograde eclogites.

The (plagio)pyrigarnite inclusions were all found at the Playa de Cartés, where the Chimparragneiss is well exposed over a distance of about 50 metres, lying with their longitudinal axis parallel to the schistosity. Drawn-out leucocratic streaks weave around the lenses, and segregations of leucocratic material are found in their stress-shadows. Dark-green hornblende-rich rims around the light-green lenses (photograph I-23) show that amphibolization proceeded from the rim inwards.



Photo I-23 Locality V 366. Pyrigarnite lenses with amphibolized rims, found as inclusions in mylonitized Chimparragneiss at Playa de Cartés.

Microscopically, the (plagio)pyrigarnitic rocks (samples V 366, V 366a, V 366b) are distinguishable from eclogite by the distinctly green colour of their clinopyroxene, the absence of p.p. symplectite, the pink colour of the garnet, the absence of rutile inclusions in the garnet, and the presence of plagioclase as a stable phase in addition to garnet and clinopyroxene.

Their composition is simple; garnet, clinopyroxene, plagioclase (16—19% An.), biotite, and quartz are the principal constituents. Orthite, titanite-rimmed rutile, apatite, zircon, and opaque matter occur as accessories. Growth of epidote and brownish-green or blue-green pleochroic hornblende secondary after garnet and clinopyroxene caused the transformation of the biotite-(plagio)pyrigarnites into (garnet)-biotite amphibolites (samples V 302 and V 366c).

Another plagiopyrigarnite (sample V 367), also occurring as a lens in the Chimparragneiss at Playa de Cartés, differs

microscopically from the samples described above. Here, virtually colourless garnet with numerous rutile inclusions, and colourless clinopyroxene are found in stable association with plagioclase (36—40% An.) and quartz. Reddish-brown pleochroic hornblende and biotite appear as secondary products. No signs of symplectitization were found. Accessory constituents are: rutile, titanite, apatite, zircon, and opaque matter. Parallelism of quartz-plagioclase aggregates with elongated crystals of biotite, hornblende, clinopyroxene, and garnet causes a distinct foliation, in contrast to the other (plagio)pyrigarnite inclusions, which lack a preferred orientation of the minerals.

The metamorphic history of the Chimparragneiss can be briefly summarized as follows (see also Plate 3). A geosynclinal sedimentary series of graywackes with a few mafic intercalations of gabbroic composition was subjected to catazonal metamorphic conditions (which are inferred to be those of the clinopyroxene-almandine subfacies of the granulite facies, on the basis of the mineral association found in the mafic inclusions). The catazonal metamorphism was accompanied or closely followed by essentially dry anatexis of the meta-sediments, so that only the mineral association in the restite (garnet, kyanite, muscovite?, biotite?) reflects the high PT conditions. The mafic inclusions were converted into (plagio)pyrigarnites at the same time.

A later mesozonal metamorphic phase, which was accompanied by mylonitization, destroyed most of the evidence of anatexis and caused the growth of a second kyanite generation and the replacement of garnet by biotite; the mafic inclusions were tectonized and wholly or partially amphibolized. Intrusion of stocks and veins of granite took place before the mesozonal deformation.

After the mesozonal phase, the gneisses were dislocated along faults and locally brecciated. Small-scale alteration connected with the emplacement of hydrothermal veins also occurred subsequent to the mesozonal metamorphic phase.

4. Gneisses and blastomylonites from the Carreiro zone of tectonic movement

a. Occurrence, general description, petrography.

Metasedimentary rocks with a graywacke type of chemical composition (see Ch. I, B 5) are also found in a zone of tectonic movement about 300 m wide (see also Ch. I, D) which underlies the Candelaria amphibolites to the West. Intensive tectonization caused an intermingling of the rocks in this zone (metasediments, basic and ultrabasic rocks), so that isolated fragments of garnet-biotite gneiss may be encountered in several parts of the zone. However, along the eastern boundary of the Carreiro zone of tectonic movement there are blastomylonitic garnet-biotite gneisses with an approximately 60° eastward dip, which lie, as far as could be ascertained from the scattered exposures, as an uninterrupted horizon, about 30 m wide, below the western border of the Candelaria amphibolites.



Photo I-24 Locality V 402. Isoclinal recumbent similar folds in the blastomylonites at Punta del Carreiro.

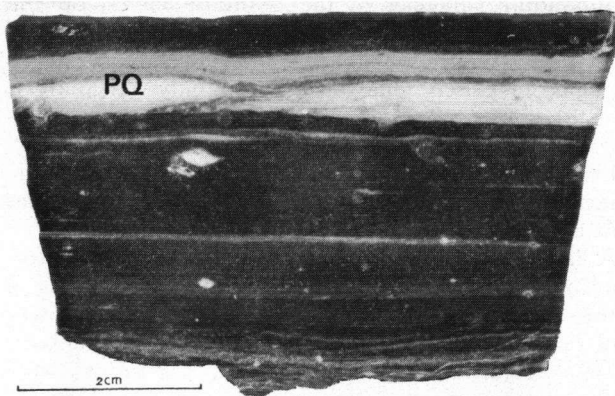


Photo I-25 Sample V 402. Boudinage in plagioclase-quartz bands (PQ) in blastomylonite, caused by mylonitization. Lenticular porphyroclasts, occurring isolated or trailed by narrow leucocratic streaks are also considered to be remnants of such plagioclase-quartz bands.

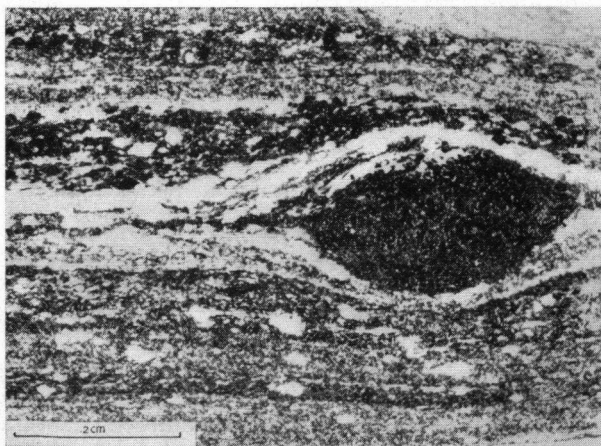


Photo I-26 Sample V 70d. Lens of garnet-hornblende rock, trailed by melanocratic fragments and flanked by rows of plagioclase porphyroclasts and leucocratic streaks. The small-scale alternation of blastomylonitic bands, melanocratic bands, and leucocratic bands is largely caused by the flattening ultimately leading to tectonic hybridization.

The mylonitic habit of the metasediments can best be observed macroscopically, especially at the cobble beach of Punta del Carreiro, where two isoclinal recumbent folds with $S 20^{\circ} W$ -trending fold axes that plunge $15^{\circ} S$ are exposed (photograph I-24). The blastomylonites have an *augen* gneiss or banded structure. Leucocratic, feldspar-rich bands are often thickened and microfolded in the hinges of larger folds, and flattening in the limbs caused boudinage (photograph I-25) and thinning out of the bands, which ultimately led to their total disruption. In extreme cases the prior existence of such leucocratic bands can be inferred from rows of small feldspar eyes (varying in \varnothing from less than 1 mm up to 2 cm) lying parallel to the foliation (photograph I-26). The same extension of the limbs relative to the hinges can be seen in the bands of garnet-biotite blastomylonite. The mafic inclusions have also been severely tectonized; lenses of garnet-hornblende rock trailed by trains of hornblende and garnet fragments, bear witness to the slow disintegration of the metagabbroic inclusions. Thus, the mylonitization led to tectonic hybridization because it ultimately reduced the leucocratic as well as the mafic bands to trains of inclusions in the meta-sedimentary component.

In the blastomylonites exposed at the boulder beach located 100 m East of the Faro de Punta Candelaria, the same evidence of flattening and resultant tectonic hybridization were observed. Here, some of the bigger basic and ultrabasic inclusions were broken up into fragments which were then rotated by differential movements on the *s*-plane (photograph I-27, see also Ch. I, B 4 b).



Photo I-27 Locality V 324. Lens of amphibolite, broken and rotated by differential movements in the blastomylonites at the boulder beach near the lighthouse at Punta Candelaria.

Microscopically, much of the evidence of mylonitization appears to have been obscured by the recrystallization of quartz, plagioclase, biotite, and perhaps garnet. Only the microcrystalline grain-size, the extremely bent nature of relics of plagioclase, hornblende, and kyanite, and the texture of the rock as a whole bear witness to the severity of the deformation undergone by these rocks.

Sample V 402 (photograph I-25) was taken from the common limb of the two folds shown in photograph I-24. Its foliation is macroscopically apparent from the drawn-out leucocratic bands representing pegmatoid potassium-poor injections, concentrations of tonalitic anatectic melt, or veins of granitic composition as is the case in sample V 402a, in which microcline porphyroclasts of 2 cm \varnothing were found.

Microscopically, these bands run parallel to the bands or laminae (which are sometimes as thin as 0.03–0.06 mm) caused by variations in the ratio of melanocratic to leucocratic constituents. Garnet, kyanite, and an occasional relic of undulose plagioclase (25% An., photograph I-28) appear to be prekinematic relics. The garnets are anhedral to subhedral, traversed by fissures perpendicular to the foliation, and poor in inclusions. The kyanite crystals have rounded anhedral shapes and are often undulose or bent (sometimes up to 50°). Lenticular undulose plagioclase relics are surrounded by mortar rims.

Small flakes of reddish-brown unstrained biotite (length about 0.1 mm), equant grains of clear plagioclase (20% An.), slightly undulose quartz (\varnothing about 0.1 mm), and strained skeleton crystals of biotite-rimmed muscovite have crystallized post-kinematically. Accessory constituents are rutile, titanite, apatite, zircon, tourmaline, and opaque matter.

The leucocratic bands consist of plagioclase (sometimes also microcline), muscovite, kyanite, and quartz. Minute amounts of biotite, garnet, rutile, and zircon may also be present. The kyanites are rounded and bent; the bigger (synkinematic?) muscovite crystals are also bent; the smaller ones, which are probably postkinematic, have straight extinction. Plagioclase has the same mode of occurrence as in the melanocratic bands, and quartz is arranged in small disk-like microcrystalline aggregates which are larger (up to 2 cm in length) and coarser-grained in zones of minimum compression (between two boudins or in stress-shadows).

In sample V 402b, taken from the hinge of the biggest fold, the deformational evidence is not quite so clear. The kyanites are rounded but scarcely undulose. Most of the garnets have retained their idiomorphic form. The preferential orientation of the newly-formed biotite lies at an angle to the compositional banding, which supports the assumption that biotite crystallized after the folding.

Sample V 70f is an example of tectonic hybridization. Relic lenses composed of biotite, inclusion-free garnet, and spongy hornblende with brownish-green cores and blue-green rims carry rutile, quartz, slightly metamict orthite, and opaque matter as accessory constituents. They are trailed by melanocratic tails in which garnet porphyroclasts and undulose hornblende porphyroclasts appear as eyes. Streaks of hornblende fragments and biotite flakes lying parallel to the foliation bend around the lenses and the eyes. On a microscopic scale, such garnet-hornblende streaks alternate with garnet-biotite blastomylonite streaks or bands and with narrow bands of microcrystalline quartz and plagioclase in which heavily bent plagioclase porphyroclasts (photograph I-28) are still found. This provides a good illustration of how the composition of the blastomylonites may change within a distance of millimetres.

The evidence of an earlier catazonal metamorphic phase is scarce: the mafic inclusions have been completely amphibolized (hornblende is clearly a secondary mineral) where they were not completely elimi-

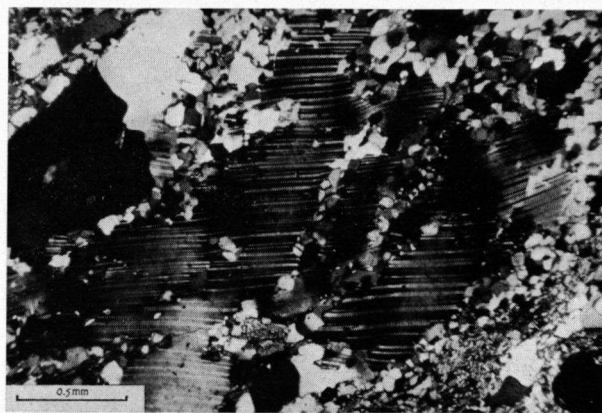


Photo I-28 Slide V 70f. Broken and bent coarse-grained plagioclase porphyroclast with recrystallized mortar texture, found in a blastomylonite from Punta del Carreiro (+ nic).

nated by the mylonitization. The generally inclusion-free nature of their garnets and their over-all resemblance to the amphibolized mafic inclusions in the Chimparragneiss lead to the assumption that the original nature of the biotite-garnet-hornblende rock inclusions was pyrigarnitic rather than eclogitic, which would imply a correlation of the blastomylonites with the Chimparragneiss Formation and not with the Banded Gneiss Formation.

Evidence of a pre-mylonitic metamorphic phase in the metasedimentary rocks is limited to the relics of fissured garnet, bent kyanite, and bent plagioclase. All textural evidence has been eradicated by mylonitization. Comparison with the other metasedimentary formations yields the same picture of a catazonal association of garnet + kyanite arrested in the process of replacement by a mesozonal association of garnet + biotite + muscovite.

b. Basic and ultrabasic inclusions.

In addition to the small lens-like biotite-garnet-hornblende rock inclusions, banded or foliated amphibolites are also found as inclusions in the blastomylonites. Although they may be remnants of original mafic intercalations, it also seems possible that they are fragments torn from the adjacent Candelaria amphibolite during deformation.

Photograph I-29 illustrates how such a fragment is broken down by mylonitization. The more or less plastic mylonite was driven into tiny fissures and thus tore off small parts of the fragment, which were then sometimes drawn-out further into melanocratic streaks.

The ultrabasic inclusions in the blastomylonite were all found at the exposure near the Faro de Punta Candelaria. One instance of an ultrabasic fragment shows boudinage coupled with rotation; it was fractured perpendicular to its length, after which the fragments were rotated (counterclockwise, when looking in the direction of dip of the blastomylonites) while they were drawn away from each other by the de-



Photo I-29 Boulder from the boulder beach near the lighthouse at Punta Candelaria, showing fragment of foliated amphibolite enclosed in blastomylonite. Penetration along cracks of the incompetent blastomylonite (centre) ultimately caused the ripping-off of isolated amphibolite fragments.

formational movements. Thus, three roughly rectangular blocks with dimensions of 23×24 , 30×20 , and 20×13 cm (their longitudinal axes rotated from 30 to 60° relative to the foliation of the blastomylonite) occur on the same level at mutual distances of 150 and 60 cm, respectively. What was originally the upper side of the ultrabasic blocks consists of an oblong plate, about 8 cm wide, of compact, black microcrystalline garnet peridotite. What was originally the under side consists of black serpentinite with a platy cleavage parallel to the longitudinal axis of the fragment. The tough peridotitic part (sample G 1—5) consists of olivine, relic garnets, enstatite, pargasitic colourless amphibole ($2V^z$ large, $c/z = 24^\circ$), and picotite. The peridotite is traversed by a network of narrow veins filled with α -chrysotile and magnetite. In the serpentinitic part of the blocks (sample G 1—6), only small, slightly altered peridotite remnants embedded in serpentinite are indicative of its former nature.

At another level of the blastomylonite there are serpentinite fragments which are surrounded by a more or less radial rim (about 1 cm wide) consisting of a colourless anthophyllite ($n_y \geq 1.63$, $\Delta \approx 0.22$, $2V^x = 63^\circ$). The optical diagnosis of anthophyllite was confirmed by an X-ray diffraction photograph (nr. 2645). Where the anthophyllite-rim borders on the blastomylonite, a macroscopically light-green actinolitic amphibole ($2V^x \approx 60^\circ$, $n_x = 1.618$, $\Delta = 0.024 \pm 0.001$) was found lying with its longitudinal axis parallel to the contours of the fragment. A lens about 50 cm long and consisting entirely of talc was found near the contact with the Candelaria amphibolite.

5. Chemistry

a. Sedimentary versus magmatic descent.

From each of the gneiss formations discussed in this chapter, different types were selected for chemical

analysis, principally to determine whether they represent igneous or sedimentary rocks.

With the exception of nr. 12 (see Table I-4) — to be discussed separately below — their nature is sedimentary rather than igneous for the following reasons:

1. They plot outside the field of igneous rocks in the al-fm-c-alk tetrahedron, the $+T/-T/c$ triangle and the $si/(c+alk)$ diagram (cf. Burri, 1959).
2. They have a large excess of aluminium, $t = al - (c+alk)$, also expressed by the presence of sp and hz in the basis, which in fresh, uncontaminated rocks is a strong indication of a sedimentary descent.
3. Their composition does not agree with any one of the magma types of P. Niggli (cf. Burri, 1959) but it does agree with the chemical characteristics of graywacke (Pettijohn, 1957).

Preponderance of Na_2O over K_2O is considered by Pettijohn (1957) to be a feature that distinguishes graywacke from argillite and also from arkose. The first nine analyses in Table I-4 show such a preponderance of Na_2O over K_2O , but analyses 10 and 11, representing normal and quartz-poor graywacke, respectively, according to their mineralogical composition, contain more K_2O than Na_2O . This is possibly caused by a high mica-content in the original graywacke, for both rocks contain over 50% melanocratic constituents. However, gneisses with the composition of a mafic graywacke, represented by analyses 10 and 11, constitute only a fraction of the total amount of paragneiss found at Cabo Ortegal.

In Fig. I-19, 17 graywacke analyses have been plotted in a QLM diagram together with the gneiss analyses, to illustrate their similarity. It is of course impossible to ascertain to what extent the chemical composition of the gneisses changed during migmatization, due to the loss of metatekt or gain of melanosome. However, all gneisses (except nr. 12) plot in positions between those of nrs. 2 and 11 relative to M. It is therefore assumed that in general no significant loss of metatekt has occurred, since nrs. 2 and 11 are Cariñogneisses unaffected by partial anatexis.

The divergent chemical composition of analysis nr. 12 requires some explanation, because according to its Niggli-values the rock has a gabbroic composition. Plotting of the Niggli-values in the al-fm-c-alk tetrahedron, the $+T/-T/c$ triangle, and the $si/(c+alk)$ diagram, reveals an igneous rather than a sedimentary composition. However, in contrast to the other gabbroic rocks found as inclusions in the gneisses (Table I-1), its $t = al - (alk+c)$ has a positive value, albeit a small one as compared with the other gneisses. The possibility that its divergent chemistry arose from pressing-out of an amount of anatectic melt during the eclogite-facies metamorphism was investigated as follows: SiO_2 , Al_2O_3 , Na_2O , and K_2O (totalling 100 wt%), taken in amounts proportional to those of a eutectic melt containing alkalifeldspar and quartz,

were added to analysis nr. 12. The analysis was then recalculated to 100 wt%. Obviously, the result is that the projection-point in the QLM diagram (Fig. I-19, 12') shifts towards the eutectic point along a straight line connecting the projection point of analysis 12 with the eutectic point. Although the analysis now plots in the midst of a number of graywacke analyses, its Niggli values still indicate an igneous composition rather than a sedimentary one. The rock simply has a quartz-dioritic rather than a gabbroic composition. Therefore, the possibility that sample V 1104 represents a graywacke whose chemical composition was changed by the pressing-out of a certain amount of eutectic melt, may be discarded. If the rock is not considered to be a normal gabbro changed in composition by metasomatism or by contamination with graywacke material, it must be assumed that sample V 1104 represents a mafic graywacke of unusual chemical composition. For comparison, the QLM projection-point (Fig. I-19, nr. 29) of a Miocene sandstone also lacking sedimentary characteristics, is given.

b. Metamorphic facies of the paragneisses.

During the catazonal metamorphic phase, the banded gneisses (analyses 1, 3, 4, 6—9) were subjected to eclogite-facies metamorphism. Since most of the K_2O and Na_2O was then incorporated into a eutectic melt, the mineralogical composition of the restite can be read from an ACF diagram (Fig. I-20a). Garnet + kyanite, and in sample Ma 17 (analysis 3) kyanite + zoisite, are most probably the minerals formed at that time. During the mesozonal metamorphic phase, potassium and soda again became available for mineral formation, which necessitates plotting in the A'KF diagram, since the rocks have excess Al_2O_3 as well as excess SiO_2 . In the A'KF diagram (Fig. I-20b) the analyses plot both on the A'- and on the K-side of the almandine-muscovite join. Because staurolite is not found as a constituent in the banded gneisses lying on the A'-side of this join, it must be concluded that the metamorphic conditions during the mesozonal metamorphic phase were those of the kyanite-almandine-muscovite subfacies of the almandine amphibolite facies.

For the Chimparragneisses (analysis 5) and the blastomylonites (analysis 10), a similar picture can be envisaged. Conditions during the catazonal metamorphic phase were those of the clinopyroxene-almandine subfacies of the granulite facies. Consequently, at that time garnet and kyanite were formed in the gneiss together with an amount of eutectic melt (see Fig. I-20c). The projections of analyses 5 and 10 in the A'KF diagram permit no decision about the metamorphic grade of the mesozonal metamorphism, because both analyses plot within the almandine-muscovite-biotite field (Fig. I-20b). It is assumed that the PT conditions at that time were those of the kyanite-almandine-muscovite subfacies of the almandine amphibolite facies, because no staurolite was found either in the Chimparragneiss Formation or in the blastomylonites.

The Cariñogneisses (analyses 2 and 11) did not undergo partial anatexis. From their mineralogical composition it can be deduced (sample Coe 204) that during the catazonal metamorphism of the other gneiss formations, the Cariñogneisses were metamorphosed under PT conditions of the staurolite-almandine subfacies of the amphibolite facies. The A'KF diagram (Fig. I-20d) explains why staurolite is only found in the darker types of meta-graywacke. The disappearance during the ensuing mesozonal metamorphic phase must have been due to a shift in the PT conditions from those of the staurolite-almandine subfacies to those of the kyanite-almandine-muscovite subfacies of the almandine amphibolite facies (Fig. I-20b).

C. PURRIDO AMPHIBOLITE FORMATION

1. General description

The Purrido amphibolites, which grade towards the East into the zone of tectonic movement (Ch. I, D), are bordered on their western side by the Atlantic Ocean. They are characterized by the absence of compositional banding and the presence of a well-developed foliation due to a planar nematoblastic texture parallel to the schistosity, which causes it to split up into slabs. No internal folding was found; the foliation has a dip varying roughly from 40—50° in an approximately southeastern direction.



Photo I-30 Locality V 172. Tectonized metadiorite with lenticular porphyroclasts of magmatic plagioclase, lying as a concordant zone between the Purrido amphibolites.

2. Petrography

Hornblende and plagioclase are the only macroscopically identifiable minerals in the Purrido amphibolites. The medium-grained amphibolite is black due to its great abundance of hornblende; in this black mass, white oblong specks of plagioclase lie arranged parallel to the *s*-plane. The monotonous texture is sometimes interrupted by a zone of alternating streaks of coarse-grained plagioclase and hornblende porphyroclasts lying parallel to the schistosity (photograph I-30).

In a 1 to 2 m-wide zone on the western slope of Monte Purrido, 10 to 20 cm-wide bands consisting of coarse-grained garnet-chlorite schist (sample V 131a) — with idiomorphic garnets of over 1 cm \varnothing — are found. Identical garnet-chlorite schists are also found in this formation south of the Ria de Cedeira (Engels, internal report, 1963).

According to its physical properties (Table V-3), the microscopically light-pink garnet found in this garnet-chlorite schist is an almandine with an admixture of pyrope and grossular (Frietsch, 1957). It is slightly altered into chlorite (— pennine) and contains numerous inclusions of opaque matter (ilmenite?). Although the abundant bent prochlorite ($2V^z$ small, $\Delta < 0.005$, $n_D > 1.62$) may at times replace garnet or biotite, it is not found as an alteration product of the blue-green hornblende but rather as a stable phase in addition to garnet and hornblende. Small-scale alteration of the hornblende can be seen in the form of rims of colourless actinolitic amphibole around the blue-green hornblende and also in the form of a patchy replacement of hornblende by a plagioclase(albite?)-actinolite mixture. Undulose quartz, saussuritized plagioclase (20% An.), rutile, apatite, and opaque matter occur in minor amounts.

In the surrounding amphibolites, garnet does not appear as a constituent; their mineralogical composition is much simpler.

Sample V 125 (a medium-grained amphibolite) is composed principally of amphibole and plagioclase. The amphibole, a common hornblende (x light yellowish-green $<$ y olive green $<$ z bluish-green; $c/z = 23^\circ$; $\Delta = 0.022-0.023$; $2V^x = 84^\circ$), is subhedral and has a strong dimensional orientation. The unaltered plagioclase is inversely zoned (core 29–31% An., rim 35–38% An.) and is twinned according to the albite and pericline laws; it lies dispersed in the maze formed by the hornblende. Slightly undulose quartz, epidote sometimes showing a core of little-metamict orthite, apatite, and titanite with cores of rutile, occur in minor amounts.

Slight differences in the chemical composition of the rock may result in associations of the same minerals but in different proportions, as for instance in sample V 118 (medium-grained epidote amphibolite), which is richer in both subhedral hornblende and subhedral epidote and poorer in plagioclase than sample V 125. The plagioclase in sample V 118 has been totally altered into a semi-opaque woolly mass of saussurite. This complete alteration of the anorthite component of the plagioclase — leaving only the albitic part vaguely visible through the woolly saussurite cloud — is present in almost every investigated sample of the Purrido amphibolites (photograph I-31).

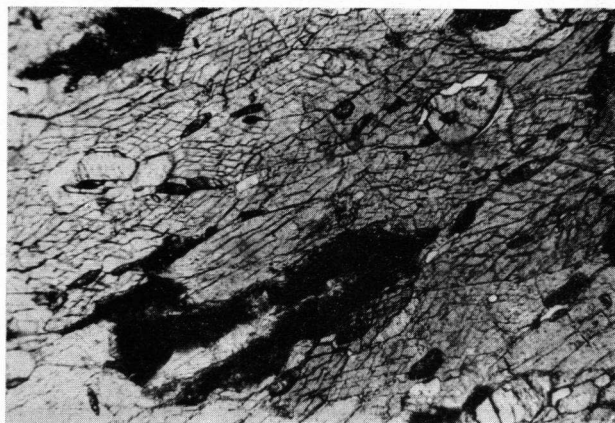


Photo I-31 Sample V 122. Nematoblastic texture of the Purrido amphibolite. In addition to hornblende, there are heavily saussuritized plagioclase (bottom centre, top left), epidote (colourless, high relief), quartz (white), and titanite (dark, shadowy rims) (— nic, $\times 50$).

It is clear from the petrographic evidence that the association hornblende + oligoclase-andesine (\pm epidote) — representing amphibolite-facies metamorphic conditions — has undergone greenschist-facies retrogradation. It is remarkable that only plagioclase shows the effect of retrograde metamorphism (saussurization); neither hornblende nor epidote has a zoned structure; only along hydrothermal dilatation-veins (filled with quartz, prehnite and epidote) are zoned epidote, and actinolite secondary after hornblende found. That the saussurization of the plagioclase was not restricted to the immediate neighbourhood of the hydrothermal veins may have been brought about by the extremely well-developed schistosity of the Purrido amphibolite, which permitted large-scale circulation of hydrothermal solutions.

Evidence of catazonal metamorphism has not been encountered in the Purrido Amphibolite Formation, but the zones rich in plagioclase- and hornblende-porphyroclasts (sample V 172) give an indication of the nature of the Purrido amphibolites prior to mesozonal metamorphism.

Microscopical investigation of sample V 172 shows that the rock must be considered as a slightly metamorphosed mafic diorite (gabbro?). It is composed mainly of medium- to coarse-grained hornblende (\varnothing up to 1 cm) and plagioclase (\varnothing up to 6 mm). The coarse-grained hornblende is bent and has lost most of its idiomorphic shape, although medium-grained idiomorphic hornblende is frequently found enclosed by the coarse-grained individuals. Crystallization of unstrained euhedral to subhedral medium-grained hornblende, together with clinoclone and epidote along rims and cracks of the coarse-grained crystals, is ascribed to metamorphism. The plagioclase most clearly reveals the igneous origin of the rock by the occurrence of Carlsbad-albite twins (pericline twinning is also found) and by its zoned structure (core 56% An., rim 40% An.); it is also slightly bent due to deformation.

3. Chemistry and metamorphic facies

The petrographically almost uniform nature of the Purrido amphibolites is reflected in their similarity in chemical composition (Table I-1, analyses 20—22). Their igneous descent is confirmed by their chemical similarity to gabbroic rocks and by the proximity of their projection points to the trend-line for igneous rocks in the *c/mg* diagram (Fig. I-11) and the QLM diagram (Fig. I-13).

The chemical characteristics of the garnet-chlorite schist are quite different. According to its positive *t*-value, the position of its projection point in the *alm-c-alk* tetrahedron and the $+T/-T/c$ triangle, and its lack of similarity to any of the magma types of P. Niggli (Burri, 1959), its chemical characteristics are those of a sediment or a weathered igneous rock. This contrast with the associated amphibolites is also illustrated by the *c/mg* plot (Fig. I-11), where the projection point of the garnet-chlorite schist lies well away from the differentiation-trend of the igneous rocks.

The mineral association found in the Purrido amphibolites, i.e. oligoclase-andesine (+ epidote) + hornblende, is indicative of amphibolite-facies metamorphic conditions and probably in particular those of the kyanite-almandine-muscovite subfacies as is the case for the mesozonal metamorphism of all the rocks of the Concepenido Complex.

In the ACF diagram (Fig. I-21) of the kyanite-almandine-muscovite subfacies of the almandine amphibolite facies, the amphibolites (nrs. 20—22) plot as expected in the anorthite(epidote)-hornblende field, whereas the garnet-chlorite schist (25) plots in the anorthite(epidote)-almandine-hornblende field. The explanation of the presence of prochlorite as an apparently stable phase in the garnet-chlorite schist should perhaps be sought in the extremely low *al : fm* ratio, which prohibited accommodation of all available Fe-Mg in garnet and hornblende. The total lack of potassium explains why this *fm* surplus is expressed in the presence of prochlorite instead of biotite.

The greater abundance of epidote in sample V 118 as compared to samples V 125 and G 1—7 may be explained by the lower Na₂O content of sample V 118; with less Na available to form albite, less Ca and Al could be accommodated in anorthite. This left a greater surplus of Ca and Al to form epidote.

The evidence of sample V 172 leads to the assumption that the Purrido amphibolites represent metamorphosed diorites of gabbroic composition that were emplaced prior to the mesozonal metamorphic phase but most probably subsequent to the catazonal metamorphic phase.

D. CARREIRO ZONE OF TECTONIC MOVEMENT

1. General description

Metagraywackes (garnet-biotite gneiss, blastomylonite, see p. 159), ultrabasic rocks, and Purrido-type¹⁰ amphibolites are the components welded into a mappable unit by severe deformation. This unit lies concordantly as a roughly 50—60°/SE-dipping sheet, about 250 m wide, between the Candelaria amphibolites and the Purrido amphibolites. Tectonized Purrido-type amphibolites in the zone of tectonic movement grade towards the West into the schistose types of Purrido amphibolite (Ch. I, C). The metagraywackes (Ch. I, B 4) are found predominantly along the eastern margin of the zone of tectonic movement, immediately West of the Candelaria amphibolites. Serpentinite occurs as tectonic lenses between the metagraywackes and the Purrido-type amphibolite. At the Allado de Algoda, for instance, it is found only as a succession of small lenses.

Except for the sea-level exposures of Punta Candelaria, Punta del Carreiro, and Allado de Algoda, the Carreiro zone of tectonic movement is poorly exposed, especially between the Allado de Algoda and Punta Felgueira. Nevertheless, it was possible to locate its boundaries within approximately 50 metres in these poorly-exposed areas.

2. Structural and petrographical features

An attempt will be made in this section to give an impression of the tectonic and petrographic complexity of the Carreiro zone of tectonic movement by the description of a few selected exposures exemplifying how the deformation and the metamorphism affected the Purrido-type amphibolites and the serpentinites in this zone (see Ch. I, B 4 for a description of the metagraywackes). Despite the abundance of petrographic and structural details, the nature and significance of the zone of tectonic movement are not yet fully understood. Much work remains to be done in this zone, which undeniably merits further investigation.

a. Serpentinites.

The serpentinite layer in the Carreiro zone of tectonic movement has been split up by deformation into a number of large-scale lenses (varying in length from 30 m to over 1.5 km). On a smaller scale, the effects of the deformation are expressed in an internal lenticular texture (photograph I-32) of the serpentinite boudins. Slickensides adorn the boundaries of individual lenses. This lenticular texture can sometimes — at the rims of lenses — even be observed on a microscopic scale, as for instance in sample V 216.

¹⁰ These amphibolites are petrographically similar to the Purrido amphibolites, but more intensive tectonization has given them a different texture.

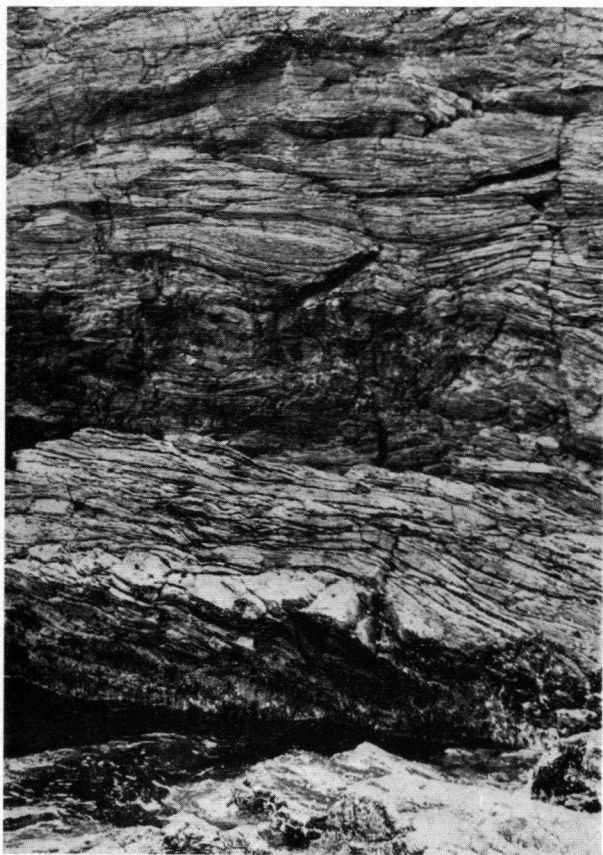


Photo I-32 Lenticular texture of internally-deformed serpentinite at Punta del Carreiro. Photograph Prof. W. P. de Roever.

In thin section, two sets of shear-planes — which are marked by clinocllore and (sometimes) talc — intersect at an angle of about 40° , thus enclosing roughly lenticular fragments of the serpentinite (a bastite serpentinite with abundant relics of olivine, orthopyroxene, and a probably pargasitic colourless amphibole).

Olivine ($2V^z = 80-90^\circ$) has been altered into serpentine and shows a well-developed mesh texture; orthopyroxene ($2V^x = 80-90^\circ$) is partially altered into bastite. Both olivine and orthopyroxene have undulose extinction; the orthopyroxene is sometimes surrounded by a mortar rim. Olivine crystals, more than 75% of which are altered into serpentine, still show identical optical orientation of the olivine remnants, even when the olivines lie next to, or are cut by, one of the shear planes. This may be an indication that serpentinization occurred post-tectonically.

In two exposures on Punta del Carreiro (V 250—V 219 and V 271—V 74), the deformation was so severe that part of the ultrabasites was totally transformed into chlorite schists or chlorite-amphibole schists that probably acted as a lubricant during the deformation.

Sample V 250c, an amphibole-chlorite schist, is composed of alternating bands of chlorite schist — composed entirely of clinocllore ($2V^z = 20^\circ$, $\Delta = 0.006-0.007$, $n_{Dz} = 1.582$, $x = y$ light-green $> z$ colourless) with some pyrite — and amphibole-chlorite schist, in which the same chlorite is associated with a macroscopically colourless amphibole

($2V^x = 85-90^\circ$, $c/z \approx 19^\circ$, $n_{Dz} = 1.63$, $\Delta = 0.021$) and some pyrite. Although microfolding is evident in both hand-specimens and thin sections, the chlorites are only slightly bent and the amphiboles do not show any sign of deformation.

Embedded in these amphibole-chlorite schists lie lenses — several metres long — of serpentized peridotite with accessory pargasitic amphibole and chlorite (sample V 250), of amphibole pyroxenite (sample V 219a), or of epidote-amphibole schist (samples V 250a, V 250b).

These medium-grained epidote-amphibole schists have a strongly nematoblastic texture. Their composition is 90% subhedral amphibole (x colourless to light yellowish-green $< y$ light-green $< z$ light bluish-green, $2V^x = 85-86^\circ$, $c/z = 16-18^\circ$, $n_{Dz} = 1.67$) and 10% subedral epidote ($2V^x = 85-90^\circ$). Plagioclase is totally absent. A set of fissures running perpendicular to the foliation is partly filled with cryptocrystalline serpentine. Whether the epidote-amphibole schists represent metamorphosed late-ultrabasic or early gabbroic differentiates is not clear.

At location V 217—V 74, which is situated 75 m North-west of location V 250, the same alternation of lenses of serpentinite and serpentized harzburgite with chlorite-schist lubrication zones is again encountered. It is curious that the chlorite schists, which are composed largely of clinocllore and lenticular chloritized bastite-remnants, contain apatite and zircon as accessories.

As in location V 250, the strike and dip of the deformation zone are roughly parallel to the strike and dip of the zone of tectonic movement as a whole. For convenience' sake, the petrography of the ultrabasites will be discussed more extensively in Chapter II.

b. Purrido-type amphibolites.

West of the serpentinites, Purrido-type amphibolites are the dominant rock-type in a metagraywacke/



Photo I-33 Locality V 320—V 403 near the lighthouse at Punta Candelaria. Folded amphibolite-boudins lying in a schistose amphibolite matrix. Lenses of hornblende-garnet-chlorite gneiss (top right) also lie in a matrix of schistose amphibolite.

amphibolite alternation in which the proportion of the metagraywackes dwindles rapidly towards the West. As in other parts of the Carreiro zone of tectonic movement, the evidence of severe deformation is ubiquitous. Especially at Punta Candelaria, some interesting examples of boudinage and folding of the Purrido-type amphibolites could be studied, for instance at location V 320 — V 403 (photograph I-33, Fig. I-22). Both the folded boudins (samples V 403, V 403a, and V 320 m) and the incompetent matrix (sample V 320n) consist of nematoblastic Purrido-type amphibolite.

Sample V 320n can be macroscopically discerned from the competent amphibolites by its more schistose nature. It consists of hornblende (z blue-green), plagioclase (25% An.), and clinocllore ($2V^z$ small, $x = y$ light-green $> z$ colourless) as principal constituents and quartz, apatite, rutile, zircon, and opaque matter (mainly ilmenite) as accessories. The long prismatic hornblende lies subparallel to the foliation; it is sometimes bent, and as a rule is traversed by multitudes of fissures lying perpendicular to the foliation. Together with the bent chlorite it weaves around the lenticular, bent, partly saussuritized plagioclase crystals and around isolated lenticular aggregates of weakly undulose quartz.

Sample V 403a consists of hornblende (z blue-green) and plagioclase (25–27% An.) as principal constituents, and quartz, clinocllore, apatite, rutile, zircon, and opaque matter (mainly ilmenite) as accessories. Compositionally, it differs from sample V 320n by a slightly higher plagioclase content and the virtual absence of clinocllore. The hornblende lies subparallel to the slightly vaulted s-plane (see Fig. I-22) but is only lightly strained, and fissures perpendicular to the s-plane are absent. The slightly saussuritized plagioclase is not strained and does not occur as lenticular isolated crystals but lies concentrated in irregular streaks running parallel to the foliation.

The type of folding of the boudins is concentric; hornblendite is formed in the cores of the folds (sample V 403), where lack of space probably caused the migration of plagioclase to zones of minimum tension. In fact, the plagioclase is concentrated in lenticular bodies along the concentric shear-planes (see Fig. I-22 and thin section V 403a). This tendency of plagioclase to migrate to zones of minimum compressive stress was also observed for a nearby lens of amphibolite, where plagioclase had crystallized in tension cracks (photograph I-34).

A thin section from one of the compressed fold-cores (sample V 403), in which the angle between the limbs of the fold diminishes from 50° at the outside of the fold-arc to 30° in the core of the fold, reveals that hornblende lies arranged sub-parallel to the limbs. Only in the compressed core are hornblendes found lying subparallel to the axial plane. The absence of broken hornblende in the hinges is striking; in general, broken or fissured hornblende-crystals are rare in sample V 403. From these phenomena it is inferred that (re)crystallization of hornblende took place during the folding.

Eastward from this amphibolite zone there is a zone about 1 m wide in which competent lenses of chloritiz-



Photo I-34 Locality V 320—V 403. Plagioclase-filled tension cracks in an amphibolite lens.

ed hornblende-garnet-biotite gneiss lie in an incompetent matrix of amphibolite (photograph I-33).

Sample V 320o was taken from such a lens, which measured about 150×35 cm; the principal components are quartz, plagioclase (inversely zoned; core 22% An., rim 32% An.), hornblende (z bluish-green), biotite, and garnet. Chlorite secondary after biotite, epidote, metamict orthite, apatite, zircon, rutile, and opaque matter occur as accessories. Internally, the lens has a glandular texture; corroded anhedral garnet relics appear as eyes and were partially replaced by quartz. Hornblende, biotite, and chlorite are bent and lie in streaks. Quartz and plagioclase show only slight undulose extinction and often lie concentrated in lenticular aggregates.

It is curious that at location V 320—V 403 the relative competence between metasediment and amphibolite is the reverse of that shown by the blastomylonites.

The incompetent amphibolite (sample V 320p) is composed chiefly of hornblende (z blue green) and plagioclase (24–27% An.), with quartz, anthophyllite ($2V^z = 72^\circ$, $c/z = 0^\circ$), clinocllore, biotite, epidote, rutile, apatite, and opaque matter as minor constituents. The rock has a pronounced flat-lenticular texture. The plagioclase crystals are slightly bent and have a lenticular shape. The melanocratic minerals are all bent or strained, hornblende as a rule more so than the others. They lie in streaks which are woven around the plagioclase.

c. Calc-silicate rocks.

At the Allado de Algoda (location V 410), calc-silicate rocks are interstratified with metasedimentary hornblende-garnet-biotite gneisses. Several bands of plagioclase-bearing epidote hornblende schist, 10 to 15 cm wide, lie concordantly in the hornblende-garnet-biotite gneiss. A 20 to 25 cm-wide band, bordered on both sides by gneiss, consists of two yellowish-green boudinaged bands of calc-silicate rock bedded in an orange to pink, medium- to coarse-grained calcite marble. Tension cracks in the boudins are filled with plagioclase, which is remarkable in view of the fact that they are surrounded by marble.

The boudinaged band (sample V 410d) consists of a pan-xenomorphic garnetiferous diopside-epidote rock. Garnet, diopside (for analysis see Table V-4), and epidote are the principal constituents; calcite, chlorite, titanite, apatite, and opaque matter are minor constituents. The garnet occurs in skeletal forms because it is being replaced by calcite. The diopside is bent and small amounts are locally altered into chlorite; in other cases it is replaced by calcite. Both garnet and diopside were once coarse-grained, to judge from the size of their remnants. The epidote occurs both as medium-grained crystals and as coarse-grained spongy individuals. Before boudinage occurred, the band probably consisted of plagioclase-epidote-garnet-diopside rock from which the plagioclase migrated during the boudinage-process, leaving the boudins composed of epidote, garnet, and diopside. The substitution of calcite for garnet and diopside occurred later than the boudinage, and is probably related to the greenschist-facies metamorphic phase.

3. *Metamorphic facies*

The conclusions reached in Chapter I, B 4 concerning the facies conditions during the deformation responsible for the development of the Carreiro zone of

tectonic movement, are confirmed by the petrography of the Purrido-type amphibolites found in the western part of this zone. The presence of calcic oligoclase or sodic andesine as a stable phase, the paratectonic (re)crystallization of hornblende, and the formation of anthophyllite, indicate that in this part of the Carreiro zone of tectonic movement, PT conditions were those of the almandine amphibolite facies. This inevitably leads to the conclusion that the chlorite schists and the amphibole-chlorite schists were also formed by tectonization of ultrabasic rocks under amphibolite facies conditions. Considering that chlorite may be formed at 10 kb at temperatures as high as 825° C, according to Yoder & Chinner (1958—1959), this conclusion seems justified.

About the metamorphic state of the rocks prior to the mesozonal metamorphism, little can be said. In the Purrido-type amphibolites, no magmatic or catazonal relics were found. It is assumed, in view of their great resemblance to the neighbouring Purrido amphibolites, that they were also formed directly from igneous rocks emplaced after the catazonal metamorphism. The relic-association garnet-diopside-(plagioclase)-epidote in the calc-silicate rocks is not incompatible with the granulite-facies metamorphism (Ch. I, B 5) that is here considered to have affected the metasediments and their inclusions.

Greenschist-facies metamorphism, post-dating both the catazonal and the mesozonal metamorphic phases, occurred on a limited scale. No explanation can be given for the fact that in the Purrido amphibolites nearly all plagioclase has been altered into saussurite, whereas in the equally schistose Purrido-type amphibolites from the Carreiro zone of tectonic movement saussuritization played only a minor role.

CHAPTER II

THE ULTRABASIC ROCKS

A. OCCURRENCE; GEOLOGICAL SETTING

A large number of isolated, partially serpentinized, ultrabasic bodies are found at Cabo Ortegal, the largest of them at the Limo, the Herbeira, and the Uzal. Smaller units of ultrabasic rock lie as lenses in the Carreiro zone of tectonic movement (see p. 161) and at the tectonic contact between the Candelaria amphibolite and the Chimparragneiss; others are found as a host of small scattered occurrences on the Sierra de la Capelada.

The key to the correlation between the various ultrabasic occurrences is found at the Uzal, where the ultrabasic can be seen concordantly overlying the rocks on the western side of the Capelada Complex (photograph II-1). Towards the West, the Uzal serpentinite borders, with a steeply-dipping tectonic contact, on the Chimparragneiss. The same conformity



Photo II-1 Uzal ultrabasic overlying rocks of the Bacariza Formation (looking East); the s-plane of the ultrabasic and the contact are indicated.

of structures is found on the Sierra de la Capelada, where the isolated ultrabasic bodies occur in the synclinal depressions in the folding pattern of the rocks of the Capelada Complex. Their form and dimensions are determined by the topography, the amplitude of the underlying folds, and the direction and plunge of the fold axes. This concordance is confirmed by the agreement in plunge and direction of the fold axes constructed from the interpolation of outcrop and topography with those observable in the neighbouring rocks of the Capelada Complex. The ultrabasic massifs of the Limo and the Herbeira are — especially at their southern sides — confined by steep, roughly NW-SE-lying fault planes. On their eastern sides they can be seen to overly the rocks of the Capelada Complex with a tectonic contact. Constructed profiles bear out the conclusion that the bottom planes lie parallel to the structures of the underlying rocks.

From the foregoing, it requires little imagination to suppose that the ultrabasites of the Limo, the Herbeira, and the Uzal are all part of one ultrabasic body. This body must once have continuously overlain the rocks of the Capelada Complex and is now only found where it was protected from erosion. At the Uzal, the ultrabasic disappears under the Chimparragneiss, only to reappear again — as scattered fragments — along the boundary between the Chimparragneiss and the Candelaria amphibolite. The Candelaria amphibolites show no erosional relics, but the ultrabasic ultimately reappears in the Carreiro zone of tectonic movement, where it has been heavily tectonized.

The thickness of the ultrabasic body diminishes from the Limo and the Herbeira (where it measures well over 500 m) towards the West (about 300 m at the Uzal and a maximum of 200 m in the Carreiro zone of tectonic movement). After allowing for tectonic thinning, the ultrabasic can be envisaged as a flat-lenticular body that reaches its maximum thickness in the neighbourhood of the Herbeira and becomes slowly thinner towards the rims.

B. PETROGRAPHY

Since the petrography and the chemistry of the ultrabasites of Cabo Ortegal will be the subject of a separate study by P. Maaskant, they are here discussed only summarily. However, a number of phenomena require mention because they provide indications about the time of emplacement of the ultrabasites in this area.

Different types of ultrabasic; nomenclature, field-relations. — Although the ultrabasic rocks have twice undergone metamorphosis, the names dunite and peridotite are used regardless of their metamorphic origin or of the degree of serpentinization. The presence of typically metamorphic minerals such as garnet, amphibole, or chlorite is indicated in the name. The higher-grade metamorphic associations may have been partly or wholly obliterated by serpentinization, which occurred

on a large scale. Since the serpentinization can be seen as an independent process with respect to the catazonal and mesozonal metamorphism, it will be discussed separately.

In the field the ultrabasic can be readily distinguished from the other rocks by the reddish-brown colour of its weathered surface. The scenery on the ultrabasic bodies is desolate: peridotite blocks several metres high seem to lie haphazardly in a terrain profusely covered with gorse (photograph II-2). Most of the rocks must be attached to the bedrock, however, in view of the recurrence of three sets of joint-planes. These joint-planes lie either subhorizontally in varying directions or subvertically in N-S or WNW-ESE directions.



Photo II-2 Ultrabasic outcrop at the Limo; in the background the Ria de Santa Marta de Ortigueira. Looking SE. Photograph: E. Romijn.

The most common type of ultrabasic at Cabo Ortegal is an amphibole peridotite often containing chlorite. Its serpentinized counterpart, a (chlorite)-amphibole-bastite serpentinite, is also frequently encountered. In some places, dunites or chlorite peridotites without any amphibole are also found. In a fresh hand-specimen, details of mineralogical composition and texture are difficult to discern, but on weathered surfaces minerals such as orthopyroxene (bastite), spinel, amphibole, and chlorite can be easily identified. Especially spinel and amphibole (and sometimes chlorite) may cause a linear or planar texture of the peridotite by their preferred orientation. Exact measurement by compass of these directions was virtually impossible, because the magnetite content of the ultrabasites causes a strong local disturbance of the terrestrial magnetic field.

If banding occurs, it lies parallel to this planar texture. In the neighbourhood of the basal plane of the ultrabasic body, it can also be seen to lie parallel to this basal plane. The banding is caused by compositional variation and is seldom continuous over great distances, but near the summit of the Herbeira, concordant, gently westward-dipping pyroxenite bands

sions which, in the relic, lie in rows strictly parallel to (010), are coarser in the recrystallized rim, and their orientated pattern has disappeared. The second generation of orthopyroxene is unstrained and is free of exsolution lamellae and oriented spinel inclusions. It is formed either by recrystallization of first-generation orthopyroxene or as a by-product of the transformation of garnet into amphibole.

The *amphibole* likewise occurs in two generations. The older generation is found as extremely light-green, corroded crystals which are strained, bent or broken. It contrasts strongly with the newly-formed colourless second-generation amphibole, which is unstrained and subhedral with well-developed {110} faces. The first-generation amphibole often contains spindle-shaped spinel inclusions lying parallel to the crystallographic c-axis. It has a large negative optic axial angle ($80-90^\circ$), a c/z of $13-16^\circ$, and a higher birefringence than the younger amphibole.

For the second-generation amphibole, the following optical properties were determined in an amphibole peridotite (sample R 85): $2V^z = 87^\circ$, $c/z = 21^\circ$, birefringence low. It greatly resembles — both in optical properties and in its occurrence — the pargasitic amphibole found by Green (1964) in the Lizard peridotite. For this reason it will be provisionally called pargasite. Occasional remnants of pargasite-spinel symplectite indicate that garnet, although it is now rare, was once a common constituent. Pargasite aggregates, richer in spinel inclusions than the rock in which they occur, are likewise interpreted as replacement products of garnet. The pargasite and the first-generation amphibole both show a preferred orientation, thus imparting a foliation to the rock.

Olivine is always anhedral; it appears curiously unstrained as compared, for instance, with ortho- and clinopyroxene. This is in accordance with Greens' (1964) observation that it "... is apparently the most readily recrystallizing mineral..." (see also Rost, 1963). In sample G 1—5 (see p. 162) first- and second-generation olivine are found together. The first generation occurs as strained, medium-grained porphyroclasts in a recrystallized matrix of fine-grained unstrained olivine crystals.

Chlorite is only found as a constituent of the mesozonal secondary paragenesis. Its optical properties ($2V^z = 28^\circ$, $n_{Dy} = 1.581$, $\Delta \approx 0.010$) were determined in a chlorite from sample R 9 (chlorite-amphibole peridotite). Usually it appears to be colourless, but in thick sections it is a faintly yellowish-green. Twins according to [001] are frequently found. The chlorite has been analyzed chemically by Cardoso and Parga-Pondal (1951), who called it kotschubeite on the basis of its chrome content of 1.88 wt %. According to their analysis, its composition in terms of end-member molecules is approximately: 73.4% amesite, 7.8% daphnite, 11.5% antigorite, 1.2% ferro-antigorite, 6.1% k ammerite.

The *spinel* is invariably greenish-brown to brown. Quantitative chemical analysis has proven it to be chromiferous. Although it generally occurs interstitially (\varnothing up to 0.4 mm) in trains parallel to the foliation,

it has been found included in all minerals except garnet.

To summarize the foregoing, it may be said that the association garnet + clinopyroxene + orthopyroxene + olivine \pm amphibole \pm spinel relics, indicative for catazonal metamorphic conditions (O'Hara & Mercy, 1963), has been replaced by the association of olivine + orthopyroxene \pm amphibole \pm chlorite + spinel under mesozonal metamorphic conditions.

2. Pyroxenites and garnet pyroxenites

Nomenclature; distinction between bands and veins. — Following Peters & Niggli (1964), we shall use the names (spinel) pyroxenite and garnet pyroxenite instead of ari egite and eclogite for the bands and veins of corresponding composition found in the ultrabasic rocks at Cabo Ortegal, thus emphasizing the differences in chemistry, petrogenesis (Bearth, 1965; Vogel & Warneers, 1967), and possibly also in metamorphic facies, between garnet pyroxenites and eclogites.

The distinction between bands and veins was made on the basis of the position of the pyroxenite bodies relative to the foliation of the surrounding peridotites. Concordant bodies were considered to be bands, discordant ones to be veins. This interpretation is dubious, because the peridotites have twice undergone regional metamorphism accompanied by deformation, and consequently the presence of primarily concordant veins cannot be excluded. Nevertheless, the following differences in mineralogy and appearance seem to warrant the distinction:

1. The bands are generally devoid of spinel, whereas it is always present in the veins.
2. The mineralogy of the bands is much simpler than that of the veins. They are almost entirely composed of clinopyroxene, orthopyroxene, amphibole, and sometimes olivine, whereas the veins may carry chlorite \pm biotite (phlogopite?) in addition to these common minerals.
3. The contact between the vein and its wall-rock is sharp, both macroscopically and microscopically, whereas the bands usually show a gradual transition.

Mineralogy of the pyroxenites. — The pyroxenites are medium-grained panxenomorphic rocks. Colourless orthopyroxene and clinopyroxene are the principal constituents of both bands and veins. They usually occur in about equal quantities, but preponderance of one of the two is also seen. In most cases the pyroxenes are severely bent, but sometimes they are surrounded by mortar rims.

The *orthopyroxene* has a positive optic angle of about $80-90^\circ$. Severely bent orthopyroxenes with clinopyroxene exsolution lamellae parallel to {010} and spinel inclusions parallel to the crystallographic c-axis (see p. 170) are occasionally found in the pyroxenites.

The *clinopyroxene* has $2V^z = 58^\circ$, $c/z \approx 41^\circ$ (measured in a spinel pyroxenite from a vein, sample V 1403b); its replacement by a light-green amphibole is interpreted as a result of mesozonal retrograde metamorphism.

The *amphibole* is pleochroic in extremely light-green colours; and has $2V^x = 88^\circ$, $c/z = 28^\circ$ (also measured in sample V 1403b). It is probably a common hornblende. Its occurrence seems to be influenced mainly by external factors, since completely amphibolized veins and bands are found as well as virtually non-amphibolized ones. Even in a single band the distribution of the amphibole appears to be haphazard. In some of the orthopyroxenites, the pyroxenes may locally alter into an amphibole of a probably cummingtonitic type (see p. 175), but in other parts the pyroxenitic nature of the body persists unchanged.

Olivine is found in both the veins and bands in small quantities.

The *chlorite*, which is found mostly in the veins, has the same optical properties as the chlorite found in the peridotites (see p. 171); occasionally, a chlorite with a positive elongation ($2V^x \approx 20^\circ$, both n and Δ higher than that of the kotschubeite) is also found.

Spinel is lacking in most of the investigated bands; in the veins it is frequently found as brown grains (up to 1 mm) with rounded forms, in quantities up to 1 vol%.

Biotite (*phlogopite?*), *zircon*, and *apatite* occur in small quantities in some of the veins.

A spinel pyroxenite from a vein (sample R 378) made conspicuous by its divergent mineralogical composition may be briefly described here.

Its composition is about 80% clinopyroxene; orthopyroxene and olivine occur in minor amounts. The spinel is not the customary brown picotite with rounded forms; instead, it is bright green and occurs interstitially with spine-like protuberances which lie wedged between neighbouring crystals. The amphibole that has grown in small amounts secondary after the clinopyroxene is not of the light-green variety found in the other pyroxenites but rather a pale-brown one with a $2V^z$ of about 90° . Further investigation will be necessary to determine why this pyroxenite differs from the others and why garnet is not one of its constituents.

Mineralogy of the garnet pyroxenites. — Garnet pyroxenites were found in all the major ultrabasic bodies at Cabo Ortegal. They are most abundant at the Limo, on a lateral ridge running from the top in an approximately northern direction. They are heavily tectonized and appear in the peridotite as thin (up to 5 cm wide) partially retrograde veins folded on subhorizontal, roughly northward-plunging fold axes (Fig. II-2). As a consequence of the folding, the veins have undergone thinning and boudinage. Garnet, as the most rigid mineral, may therefore appear as sausage-shaped crystals (or aggregates), up to 7 cm long, with newly-crystallized amphibole in the stress-shadows.

The mineralogy of the garnet pyroxenites shows little variation; it will therefore be discussed by description

of a single sample. The selected sample, number R 70, was chosen because it provides a good illustration of the petrogenetical processes involved in the formation of the garnet.

The rock is heterogranular. Spinel and chlorite may be coarse-grained; the other constituents, i.e. clinopyroxene, orthopyroxene, amphibole, and garnet, are fine-grained. Macroscopically, the black spinel surrounded by coronas of light-pink garnet present the most striking feature.

Microscopically, the *spinel* appears to be a bright green. It is invariably rimmed with garnet. According to its refractive index ($n_D = 1.737 \pm 0.002$) and the size of its unit cell ($a_0 = 8.11 \pm 0.01$), it is a virtually pure spinel with an admixture of about 8% picrochromite. The crystals are xenomorphic and some are still as large as 7 mm. The *garnet* is colourless in thin section and, according to its optical and physical properties (see Table V-2), is rich in the pyrope molecule. The rim it forms around the spinel is an aggregate of small crystals rather than a single crystal. In the core, it is interspersed with fine-grained remnants of spinel which disappear gradually as the distance from the spinel-core increases while at the same time their colour changes to browner shades of green. This change in colour, which is illustrated even better by sample R 1 (spinel-garnet pyroxenite), is thought to be the expression of a selective use of the aluminous spinel for the formation of garnet, whereby the remaining spinel is enriched in the chromiferous end-members (cf. Bamba, 1958). Another mineral enclosed in the garnet has the following optical properties: $n_D > 1.75$, $\Delta \approx 0.030$, $2V^x = 0^\circ$, $y = z$, dark brown $> x$ clear yellow-brown; and has been tentatively identified as *högbomite*. Confirmation of this determination by X-ray analysis was impeded by the extremely small size of the grains (\varnothing up to 0.10 mm) and the difficulty of obtaining sufficient material from them. Spinel + garnet lie embedded in a fine-grained mass consisting mainly of anhedral *clinopyroxene* ($2V^z = 62^\circ \pm 2^\circ$, $n_D = 1.647 \pm 0.002$, $c/z \approx 40^\circ$). Small quantities of anhedral *orthopyroxene* and *olivine* are also found, although in other garnet pyroxenites these minerals are often absent. As accessories, *apatite*, *rutile*, and *zircon* (all lacking in sample R 70) may be found. Clinopyroxene, orthopyroxene, and olivine occur in exactly the same way as in the pyroxenites without garnet.

The *paragitic amphibole* is subhedral with well-developed prismatic faces, and is extremely light-coloured, with x_1 colourless $< y = z$, extremely light grayish-green, and $2V^x = 80-90^\circ$. It was formed secondary after either clinopyroxene or garnet. In the latter case it occurs as part of a kelyphitic rim of fine-textured amphibole-green spinel symplectite — which is sometimes coarser towards the periphery — around the garnet. Like the amphibole, the *chlorite* is seen as a product of mesozonal retrograde metamorphism. It is found predominantly in the neighbourhood of the garnet (sometimes lying between garnet and spinel) where it forms subhedral crystals, sometimes as long as 5 mm. Its optical properties are equal to those of the chlorites found in the peridotites ($2V^z = 20-30^\circ$, $\Delta \approx 0.010$): twinning parallel to $\{001\}$ occurs regularly.

The deformation that affected the veins is microscopically evident from the strained or broken appearance of clinopyroxene and orthopyroxene. On the other hand, amphibole and chlorite rarely exhibit a strong undulose extinction.

Similar garnet pyroxenites with relic hercynite are described by Portugal V. Ferreira (1966) from the Vinhais region (Portugal).

C. SERPENTINIZATION

The study of the successive metamorphic assemblages was greatly hampered by the considerable serpentinization undergone by all the ultrabasic rocks at Cabo Ortegal. In spite of a varying degree of susceptibility to serpentinization (olivine and orthopyroxene are more easily transformed than, for instance, clinopyroxene and amphibole), wholly serpentinized ultrabasites were found regularly, especially in the neighbourhood of the quartz-bearing E-W fault forming the southern boundary of the Herbeira.

In anticipation of the description of its effects on the various minerals in the ultrabasite, the following statements can be made concerning the serpentinization:

1. It proceeded without any significant amount of accompanying tectonization.
2. It post-dates both the catazonal and the mesozonal metamorphic phases.
3. In view of the previous metamorphic history of the ultrabasites, it is improbable that it was a deuteric or autometasomatic process, so that the required water must have been supplied by extraneous sources (Rost, 1959).
4. No significant increase of volume occurred as a consequence of the serpentinization.

Effects of serpentinization on the minerals. — α -Chrysotile ($2V^x = \text{small}$, $z = y$, greenish, $> x = \text{yellowish}$), antigorite ($2V^x = \text{small}$, yellowish-green, Δ lower than α -chrysotile), iddingsite, bowlingite, talc, and carbonate all play a role in the serpentinization *s.l.* of the ultrabasites.

The serpentinization of the *olivine* invariably started with the development of a mesh-texture due to the formation, along cracks, of a central train of magnetite grains or needles flanked on both sides by α -chrysotile. The α -chrysotile fibres are always arranged perpendicular to the wall of the fissure in which they have formed. Since the isolated remnants of the altered olivine crystal always show a groupwise identical optical orientation and because these olivine relics are in general unstrained, it is concluded that the serpentinization post-dates the mesozonal metamorphism and proceeded unaccompanied by tectonization. After the formation of the mesh texture, some of the olivine remnants were ultimately transformed into a non-oriented mass of antigorite with cryptocrystalline inclusions of magnetite.

Isomorphous substitution by a single antigorite crystal is the most common form of replacement for the *orthopyroxene*. The resulting *bastite* can often be easily identified macroscopically.

The *pargasite* is usually only slightly affected by the serpentinization, although small amounts of α -chrysotile have generally been formed along the cleavage planes of the amphibole. In cases of advanced serpen-

tinization, the pargasite alters pseudomorphously into a cryptocrystalline aggregate of antigorite.

The *spinel* is altered into chromite + magnetite (see also den Tex, 1955); this feature can be clearly observed in a spinel band that has been altered into chromite (sample R 18). In the serpentinized peridotites, however, its alteration takes the form of opaque magnetite concentrations at the rim of translucent brown picotite grains. The amount of magnetite around the spinel increases with the degree of serpentinization of the rock in which it is found.

The *chlorite* itself is never altered, but it is invariably rimmed by magnetite, some of which also penetrated along the cleavages. Small lenticular grains of carbonate may also be found lying along the cleavage of the chlorite.

The consistency of the serpentinization patterns of olivine, orthopyroxene, and amphibole permits recognition of these minerals even after the completion of serpentinization. Thus, it is often possible to determine the erstwhile nature of completely serpentinized ultrabasites.

Serpentinite veins. — Serpentine-(\pm carbonate)-filled veins post-dating the above-mentioned serpentinization, can be divided into two categories.

The older veins can be quite complicated in texture. They are assumed to have partly the character of dilatation veins and partly that of replacement veins. They can be seen to cut through the peridotite minerals (including pargasite and chlorite). They also cut across pre-existing serpentine patterns, sometimes leaving intact the texture of the magnetite. In the pyroxenite and garnet pyroxenite bands and veins they have the character of dilatation veins, as for instance in sample R 1 (spinel-garnet pyroxenite). Here, a 0.15 mm-wide peripheral rim consisting of α -chrysotile (fibres perpendicular to the vein wall) encloses a 0.01 mm-wide rim of γ -chrysotile (+ elongation, higher Δ) with a similar orientation. The central part of the vein may be filled with either aggregates of spherulitically-developed antigorite (Δ very weak) or carbonate.

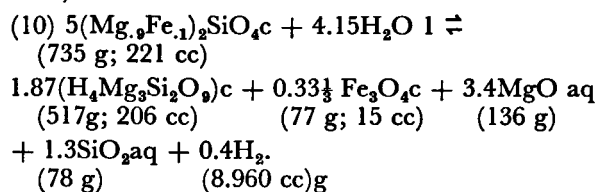
The younger veins are smaller and have the character of filled tension fissures. They often cut the older veins at roughly right angles and are seldom longer than several millimetres. They are filled with γ -chrysotile, once again with a cross-fibre texture.

At the Playa de Cartés, cavities filled with a radial outer rim of anthophyllite and a core of randomly-oriented γ -chrysotile were found. Their relation to the two above-mentioned types of veins is not clear.

Nature of the serpentinization process. — Since the serpentinization seems to have occurred later than the amphibolite facies metamorphism (it cuts through textures formed by the amphibolite facies metamorphism and is unaffected by deformation), it remains to place it in the context of the post-metamorphic geological events in the neighbouring rock formations. In this

connection it is expedient to take the nature of the serpentinization-process into consideration. As has already been stated (p. 173), autometamorphism as well as any serpentinization process involving an increase in the volume of the ultrabasite can be disregarded as a possible explanation for the serpentinization of the Cabo Ortegal ultrabasites.

Serpentinization without significant increase in volume is possible according to the following equation (Thayer, 1966):



This process is dependent on the supply of large amounts of H_2O (Turner & Verhoogen, 1960), and the evacuated MgO and SiO_2 must be accounted for. In this case, hydrothermal fluids circulating along fissures and fault-planes are thought to be responsible for the serpentinization, since:

1. The rocks of both the Concepenido Complex and the Capelada Complex show evidence of hydrothermal activity.
2. This hydrothermal activity has been shown to post-date the mesozonal metamorphic phase.
3. The hydrothermal fluids form an obvious source of the necessary water.
4. In the field, serpentinization appears to have been more intensive in the neighbourhood of the quartz-filled vein South of the Herbeira (p.173).
5. The hydrothermal veins filled with epidote, prehnite, or adularia, frequently encountered in the rocks of the Concepenido and Capelada Complexes, are not found in the serpentinites.

If it is assumed that the serpentinization was caused by the same hydrothermal activity that was responsible for the formation of the hydrothermal veins in the country rocks, one point remains to be explained. In the gneisses and the basic rocks, the alterations caused by the hydrothermal veins (sericitization, saussuritization, actinolitization) occur on an extremely limited scale (1—2 mm on either side of the vein). In the ultrabasic bodies, on the other hand, the hydrothermal activity has succeeded in transforming more than 50% of the rock into serpentinite. The reasons for these differences are probably twofold:

1. Circulation was less limited in the ultrabasites than in the other rocks. That this is an important factor is proved by the extensive saussuritization of the Purrido amphibolites, where the hydrothermal fluids could indeed circulate freely owing to the extremely well-developed schistosity plane.
2. The susceptibility to alteration of certain ultrabasic constituents is greater than that of the minerals in the other rocks. This is not improbable, since differences in susceptibility were observed

(see p. 173) between the minerals of ultrabasic rocks. Marked differences in the state of serpentinization between the peridotites and the (spinel) pyroxenites may also be ascribed to this phenomenon.

The only problem remaining is to account for the MgO and SiO_2 that should have been carried off in solution. It seems logical to expect the SiO_2 to be deposited elsewhere as quartz in veins; the MgO would be deposited in the form of magnesite according to the reaction equation:



That such a process indeed took place is demonstrated by the frequent occurrence of encrustations of dolomite on serpentinite (samples R 180 and R 303) and by the presence of small amounts of magnesite in calcite veins (sample R 17). Nevertheless, large amounts of MgO must have been transported elsewhere, because the amount of dolomite found is much too small to account for the amount of the MgO that would have been liberated by serpentinization.

D. CHEMICAL COMPOSITION

Chemical analyses of some selected ultrabasic rocks are presented in Table II-1. Too little is known as yet about the composition of the constituent minerals to draw any conclusions concerning modality from the chemical composition of the serpentinized peridotites (analyses 6—10). The low CaO content of the heavily serpentinized rocks (analyses 6, 9, 10) suggests that besides MgO and SiO_2 , CaO was also removed at the stage of serpentinization in which the pargasite was replaced by antigorite. In comparison with the pyroxenites (analyses 1, 3, 4), the serpentinized peridotites are low in Al_2O_3 , CaO , K_2O , Na_2O , and TiO_2 , but high in MgO and H_2O . The heavily serpentinized nature of the peridotites, implying a change in chemical composition (see above), unfortunately does not permit a conclusion to be drawn concerning the possible magmatic consanguinity of the peridotites and the veins.

In the case of the pyroxenites, no serpentinization has taken place, and it may therefore be assumed that their chemical composition did not change significantly after their formation. The modal interpretation of their chemical composition is again hampered by lack of mineral data. Nevertheless, there is a relation between their ACF values and their mineralogical composition, as shown by Fig. II-3. This Figure is a slightly amended version of the Al-Mg+Fe-Ca triangle for the granulite facies given by O'Hara & Mercy (1963). Their field for the orthopyroxene monomineralic composition had to be enlarged to include the projection-point of analysis 3 (a pyroxenite composed of about 90% orthopyroxene with some secondary chlorite and amphibole). The high percentage of Al_2O_3 (see Table II-1) suggests that the orthopyroxene is highly aluminous, which is not unexpected for

orthopyroxenes formed under catazonal metamorphic conditions (Boyd & England, 1960).

As microscopical observations have shown, these orthopyroxenites are replaced under amphibolite facies conditions by chlorite hornblendites. To test the reliability of these textural interpretations, a chemical analysis was made of such a chlorite hornblendite (analysis 4, sample R 348), about 90% of which is amphibole. In the ACF diagram this analysis plots well within the orthopyroxene field, thus confirming the assumption based on optical grounds. The position of the projection point of this hornblendite and the high MgO content of the rock suggest that the amphibole is extremely rich in the cummingtonite molecule.

Except for differences in their MgO and CaO content, analyses 1 and 2 show a remarkable similarity in chemical composition. Due to the aforementioned differences, they plot far apart on the ACF diagram (Fig. II-2). No conclusion can be drawn, however, from their different positions, because neither association (in both of which clinopyroxene, orthopyroxene, garnet, and spinel are found together; see also p. 172) can be deemed to represent a state of equilibrium, since in both the conversion of spinel into garnet has been arrested midway in the process.

Because the trends of the tie-lines in the F-corner of the ACF triangle are almost identical in the eclogite facies and in the clinopyroxene-almandine subfacies of the granulite facies and too little is known as yet about the associations found in catazonally metamorphed ultrabasic rocks, it is impossible to establish precisely the metamorphic facies conditions of the Cabo Ortegal ultrabasites. However, in view of the close association in the field of the ultrabasites with rocks that have undoubtedly undergone granulite facies metamorphism, it is tentatively suggested that the metamorphic conditions were those of the clinopyroxene-almandine subfacies of the granulite facies rather than those of the eclogite facies.

E. EMPLACEMENT OF THE ULTRABASITES

Speculations about the origin of the ultrabasites are doomed to be fruitless in view of the various geological processes to which these rocks have been subjected. Mineralogical, chemical, and textural evidence concerning their emplacement has been obscured, either by metamorphism or by serpentinization. An attempt will be made, however, to approximate the nature of the ultrabasites on the basis of the scanty data collected. These are:

1. Intrusions or inclusions of gabbroic rock are not found in the ultrabasic bodies.

2. Inclusions of ultrabasic are found in the meta-sedimentary rocks, as for instance in the banded gneiss (p. 152) or the blastomylonite (p. 162).
3. The nature of these inclusions indicates that the ultrabasic was emplaced prior to the mesozonal metamorphic phase (p. 162), and the petrography of the ultrabasites shows that they were present even earlier, to wit at the time of the catazonal metamorphism.

From this evidence it is tentatively concluded that the ultrabasic was introduced after the intrusion of the earliest gabbroic rocks but before the catazonal metamorphism.

Since the geological setting seems to indicate that the Cabo Ortegal ultrabasites are alpinotype rather than stratiform, their $Fe/(Mg + Fe)$ ratio was compared with the values given by Miyashiro (1966) as typical for stratiform (0.15) and alpinotype (0.10) ultrabasites. As can be seen in Table II-1, the $Fe/(Mg + Fe)$ values of the Cabo Ortegal ultrabasites agree well with those of the alpinotype ultrabasites, and even more so if the removal of MgO during serpentinization is taken into consideration.

The close association between alpinotype peridotites and rocks of gabbroic composition has been widely reported, and Miyashiro's (1966) statement that "... the spatial association appears too close to be fortuitous" may well be applied to the ultrabasites of Cabo Ortegal. To account for their presence, a choice can be made among several mechanisms of emplacement suggested by various authors; for instance: *extrusion of ultramafic lava* (Miyashiro, 1966; Clark & Fyfe, 1961; Dubertret, 1959; Brunn, 1956), *intrusion of primary peridotite magma* (Hess, 1955, 1938; Vogt, 1923), *intrusion of a "crystal mush"* (Bowen & Schairer, 1935), *intrusion in solid state* (Bowen & Tuttle, 1949), and *solid intrusion of mantle-derived ultrabasic* (de Roever, 1957). Since the time of emplacement of the ultrabasites may be taken to be later than the intrusion of the earliest basic rocks that crystallized (at least partially) as gabbros (p. 151), it seems improbable that they represent effusive rocks; this is the more likely because any sign of associated spilites or radiolarites is lacking. The most attractive theory in this case seems to be that of intrusion of a "crystal mush" or a solid body — possibly formed together with the basic magma by zonal melting (Udintsev, 1965) — which may have had its source in the mantle or in the deeper crust. The absence of contact metamorphism at its borders (as described by Green, 1964b) is not seen as being in contradiction with this concept. Any contact metamorphic association would in all likelihood have been replaced by a regional metamorphic one, in view of the time of emplacement of the ultrabasites with respect to the orogenic and metamorphic phases.

CHAPTER III

THE CAPELADA COMPLEX

Two mappable rock units — the Bacariza Formation and the Candelaria Amphibolite Formation — both consisting predominantly of metabasites, have been taken together as the Capelada Complex. Although they occur separated in the field and differ in aspect, their close relationship is evident from the geological (Plate 1) and petrographical as well as the chemical evidence.

All the rocks of the Capelada Complex first underwent catazonal metamorphism (high-pressure granulite facies) and then mesozonal metamorphism (almandine amphibolite facies). Their differences in appearance can be explained by differences in intensity of the mesozonal metamorphic phase (which left few catazonal relics in the Candelaria amphibolites) and the catazonal metamorphic phase (which failed to completely alter some of the mafic rocks of the Candelaria Amphibolite Formation). Whereas plagiopyrigarnite (see below) relics are scarce in the Candelaria Amphibolite Formation, the (plagio)pyrigarnitic descent can be easily proved for most of the rocks of the Bacariza Formation.

A. THE BACARIZA FORMATION

The Bacariza Formation occupies the central part of Cabo Ortegal. It consists predominantly of metabasic rocks with a streaky or banded appearance, but it also contains small amounts of calc-silicate rock (e.g. on the western side of the Formation) and paragneiss (mainly on the eastern side of the Formation).

To the West, the Bacariza Formation is separated from the metasedimentary rocks of the Chimparragneiss Formation by the Uzal serpentinite. The eastern boundary is not so conspicuous; here, a gradual transition from the predominantly metasedimentary Concepenido Complex into the mainly metabasic Bacariza Formation, seems to coincide with a gradual change in metamorphic grade (from eclogite-facies for the rocks of the Concepenido Complex to high-pressure granulite-facies for the rocks of the Bacariza Formation).

1. *Nomenclature of the granulite facies rocks*

The stable mineral association present in some of the mafic rocks of the Bacariza Formation comprising pyralmandine garnet + clinopyroxene + plagioclase \pm quartz, is critical for the granulite facies (clinopyroxene-almandine subfacies, de Waard, 1965; high-pressure granulite, Gjelsvik, 1952; Green & Ringwood, 1966a and b). The only other facies in which clinopyroxene is known to co-exist stably with a pyralmandine garnet is the eclogite facies. This, and the hitherto rather doubtful status of the high-pressure granulite facies, has led many authors to use the terms

eclogite, feldspar eclogite, or plagioclase eclogite for rocks in which pyralmandine garnet and clinopyroxene are stably associated with plagioclase (Eskola, 1921; Davidson, 1943; Subramaniam, 1956; Kozłowski, 1958, 1965; Saravanan, 1960; Church, 1964 and Coleman *et al.*, 1965). Although there is undoubtedly a strong affiliation between the eclogites and the high-pressure granulites, the term plagioclase (feldspar) eclogite seems unfortunate, since it implies that plagioclase can exist as a stable phase in an eclogite. This is in contradiction with the definition of eclogite given by Haüy (1882), as well as with Eskola's (1921) concept of the eclogite facies (see also O'Hara, 1960). The terms granulite, pyroxene granulite or garnet-clinopyroxene granulite (Lovering, 1964; Lovering & White, 1964; Smulikowski, 1964) seem equally unfortunate, because the name granulite implies a fine grain-size and has been strictly reserved by Scheumann (1961) for specifically-textured rocks with mineral associations appertaining to the low-pressure granulite facies (see also Scharbert, 1963); and the latter objection may also be levelled against the use of the names (clino)pyribolite or (clino)pyriklasite (Berthelsen, 1960), for which the presence of orthopyroxene as a stable phase is mandatory. Since these are the only names available for rocks of gabbroic or dioritic composition and their use is apparently restricted to rocks belonging to the low-pressure granulite facies, the Cabo Ortegal granulite-facies rocks could not be accommodated by Scharbert's (1963) nomenclature.

To circumvent the use of so cumbersome a name as garnet-clinopyroxene-plagioclase rock or granofels, the name pyrigarnite is tentatively suggested for rocks belonging to the high-pressure range of the granulite facies in which garnet and clinopyroxene occur in stable association. Rocks in which plagioclase is present as an additional stable phase could then be called plagiopyrigarnite, and the presence of a stable amphibole (hornblende) can be indicated in the name (see Table III-1). These terms are used throughout this paper. Quartz and zoisite may be present as additional phases; potash feldspar is absent. Orthopyroxene, which may, according to de Waard (1965), occur together with garnet and clinopyroxene, has not been found in the Cabo Ortegal parageneses. The texture of the pyrigarnite may be either granoblastic or schistose; its chemical composition is gabbroic or dioritic.

2. *Petrography*

As a consequence of extensive amphibolization accompanied by deformation, true pyrigarnites (with less than 5% secondary hornblende) are found only as

relics in the form of "tectonic fish". That these fish have survived severe tectonization does not mean that they have altogether escaped amphibolization by "fluids" penetrating from the rim of the fish inwards, as in the pyrigarnite lenses found in the gneisses (see p. 159 and photograph I-23). Small lenses of pyrigarnite may thus be completely converted into garnet amphibolite or garnet-hornblende rock; only in the larger ones is pyrigarnite still found relatively unaltered.

The petrography of the (plagio)pyrigarnites will be discussed on the basis of one of the least amphibolized samples (V 1234).

In the field the plagiopyrigarnite appears to be a massive, greenish-black, tough rock dotted with red garnets. On a fresh saw-cut, however, bright-green clinopyroxene and bluish-white plagioclase can be discerned. No trace of lamination or preferred orientation of the minerals could be observed, either in the field or under the microscope.

Microscopical appearance: the rock is fine-grained (grain-sizes up to 1 mm \varnothing) and panxenomorphic. Its principal constituents are clinopyroxene, garnet, and plagioclase. Minor constituents are quartz, rutile, apatite, zircon, and opaque matter (pyrite, magnetite, and ilmenite). Small quantities of alteration products (together under 1 vol%) include blue-green hornblende, biotite, chlorite, epidote, and titanite.

The *clinopyroxene* shows amoeboid forms and is light-green in thin section and weakly pleochroic (x light-green > y light yellowish-green < z light bluish-green). Its sometimes slightly strained crystals are partially replaced by hornblende with a blue-green z-colour that may appear along the rim or in patches in the centre of the crystals. Chemical analysis shows the clinopyroxene to be a diopside-hedenbergite-jadeite-acmite mixture with a preponderance of acmite over jadeite (see Table V-5).

The pink *garnet* is anhedral to subhedral with poorly-developed crystal faces. Large amounts of microcrystalline quartz inclusions, producing a sieve texture, unfortunately prevented reliable chemical analysis of the garnet. Small amounts of rutile and opaque matter were also found included in the garnet, but the rutile did not show any of the patterns so distinctive for rutile inclusions in the eclogite garnets (see p. 133).

The *plagioclase* is an oligoclase (19% An.); it occurs intergrown to a mosaic with small quantities of quartz. Both minerals are slightly strained. Garnet and clinopyroxene lie fairly evenly dispersed throughout the rock. Quartz and plagioclase, however, are more abundant in some spots than in others. These small quartzofeldspatic concentrations have completely irregular, more or less amoeboid outlines. Of the secondary minerals, a common blue-green variety of hornblende is the most important. *Chlorite*, *biotite*, *epidote*, and *titanite* occur only in insignificant amounts.

That (plagio)pyrigarnite relics are found in the Candelaria Amphibolite Formation as well as in the Bacariza Formation is considered proof of a close genetic relationship between the two rock-units. It therefore seems justified to include them in one complex: the Capelada Complex.

3. Retrograde metamorphism of the pyrigarnites

The retrograde metamorphism of the pyrigarnites is closely related to the injection of pegmatoid matter.

The resemblance of the pegmatoid injections in the Bacariza Formation to those found in the eclogites is apparent from their mineralogical composition (in addition to plagioclase and quartz there may also be kyanite, zoisite, orthite, and epidote), from their chemical composition (extremely little potassium), and from the way in which they affect the invaded rocks. Since the retrograde alterations caused by these injections are also almost exactly identical to those caused by the injections in the eclogite, it is assumed that there are no fundamental chemical differences between the two. Differences in nature and geological situation between the pyrigarnite and the eclogite could be responsible for the following distinctions:

1. Pegmatoid injection in the pyrigarnites occurs on a wider scale than in the eclogites. As a result, a more complete age relation between the different pegmatoid phases could be established in the pyrigarnites.
2. Injection along the foliation is absent because the pyrigarnite is a non-schistose rock.
3. Deformation accompanying the mesozonal metamorphism affected the pyrigarnites more strongly than the eclogites, so there is little evidence of the original nature of the older injections. They now appear as streaks or laminae.

The age relations between the different phases of pegmatoid injection could be established on the basis of the relations between their minor constituents. These age relations are in accordance with the grade of metamorphism effected by the injection (as indicated by the colour of the secondary hornblende) and they tally with the observations that could be made in this respect on the retrograde metamorphism of the eclogites (see p. 139). A schematic outline of these relations is given in Table III-2.

The retrogradation of the rocks in which the pegmatoid matter was injected occurred in two ways. In the first place, fluids emanating from the injection could have caused retrograde alterations in the immediate neighbourhood of the injection; in the second place, penecontemporaneous deformation of injected matter and wall-rock may widen the scope of retrogradation considerably.

a. Hornblende-clinopyroxene-almandine subfacies retrograde metamorphism.

Retrograde alterations involving the formation of a brown, greenish-brown or brownish-green hornblende in a (plagio)pyrigarnite, are related to injections of kyanite-, γ -zoisite-, α -zoisite-, β -zoisite-, and sometimes to orthite-bearing pegmatoid veins. The supposition that these retrograde metamorphic phases occurred under hornblende-clinopyroxene-almandine subfacies metamorphic conditions is made largely on the basis of analogous retrogradations observed in the eclogites (see p. 135), where symplectitization occurred in this stage, accompanied or closely followed by the forma-

tion of greenish-brown or brownish-green hornblende secondary after omphacite.

Retrograde plagiopyrigarnite with brown hornblende. —

Only one sample of hornblende-plagiopyrigarnite with a brown (secondary) amphibole (sample V367) was found (for description, see p. 159). Judged from the colour of the hornblende, the retrograde metamorphism shown by this sample must have taken place at higher PT conditions than for those containing greenish-brown or brownish-green (secondary) amphibole (see p. 14). Consequently, the retrograde phase that caused the growth of this brown amphibole is thought to be the oldest retrograde metamorphic phase (see Table III-2).

Retrograde (plagio)pyrigarnite with greenish-brown or brownish-green hornblende. — This stage of retrograde metamorphism has been found in tectonized as well as in non-tectonized rocks. The pegmatoid injections were unfortunately found only in a tectonized state.

An example of a non-tectonized hornblende pyrigarnite is given by sample V 1181. Macroscopically, the rock appears to be a garnet-hornblende rock without preferred orientation of the constituent minerals (medium-grained pink garnet and medium- to coarse-grained black hornblende).

Microscopically, garnet and greenish-brown pleochroic hornblende are accompanied by a light-green clinopyroxene. Quartz and plagioclase are lacking.

In thin section, the light-pink garnet shows mostly euhedral outlines. According to its optical and physical properties (see Table V 2), it is a pyralmandine garnet. It is practically free of inclusions; only rutile (sometimes violet) is found included in minor amounts.

Although the xenomorphic clinopyroxene is partially replaced by hornblende, garnet still appears to be a stable phase because no hornblende-rims between garnet and clinopyroxene (so common in amphibolized eclogites) are found in this sample. Rutile, apatite, and zircon are found as accessory constituents; they are thought to form the original constituents of this sample together with garnet and clinopyroxene.

The occurrence of strongly-zoned, slightly metamict orthite and the idioblastic nature of the secondary hornblende (x extremely light yellow < y greenish-brown > z light greenish-brown) indicate that circulating fluids probably emanating from pegmatoid matter were the immediate cause of the retrograde alterations. Small amounts of β -zoisite were probably also formed at this stage.

The occurrence of chlorite, calcite, and pistacite in cavities is related to a narrow sub-continuous 1–2 mm-wide prehnite veinlet rimmed on both sides by an irregularly-bordered actinolized zone, about 1 cm in width.

The absence of secondary titanite (after rutile), the greenish-brown colour of the secondary hornblende, and the presence of β -zoisite as a stable phase (Schüller, 1948) are taken to be indications that the amphibolization of this pyrigarnite occurred under granulite-facies conditions (hornblende-clinopyroxene-almandine subfacies).

For sample M 643, a medium-grained, foliated zoisite-hornblende pyrigarnite, the retrogradation proceeded according to the following pattern:

The clinopyroxene-almandine subfacies association is probably represented by garnet, clinopyroxene, zoisite, rutile, and apatite (+ plagioclase?). The anhedral to subhedral garnet is light-pink and contains only a few inclusions, mainly

rutile. The clinopyroxene is anhedral, light-green, and slightly strained. The zoisite is zoned; its cores are composed of γ -zoisite (Δ extremely low, $2V^x$ large, $r \gg \gg v$), its rims of α -zoisite with an extremely large optic axial angle ($2V^z = 80-90^\circ$, $r \ll \ll v$). The zoisite is anhedral and has rounded outlines. It is not found as inclusions in garnet and clinopyroxene, but it may occur included in hornblende. Large zoisite crystals may contain clinopyroxene inclusions. During retrograde metamorphism under hornblende-clinopyroxene-almandine-subfacies conditions, epidote and hypidiomorphic brownish-green, slightly strained hornblende were formed as additional phases, while plagioclase (29% An.) (re?) crystallized interstitially. It is remarkable that epidote and zoisite are not intergrown but instead occur as separate phases.

b. Amphibolite facies retrograde metamorphism.

The pyrigarnites and hornblende pyrigarnites, weakened by continuous intrusion of pegmatoid matter, were extensively tectonized and folded during the mesozonal metamorphic phase. The combination of pegmatoid injection and tectonization has caused a large-scale amphibolite facies retrogradation which left only a few relics unaffected. Therefore, any transitional type between (plagio)pyrigarnite and (garnet)-amphibolite may be encountered in the field.

The age relation between the hornblende granulite-facies and amphibolite-facies retrograde metamorphic stages are illustrated at location V 1155 (photograph III-1), where the foliation of a zoisite-hornblende pyrigarnite (sample V 1155) is cut off by the well-developed foliation of a garnet amphibolite (sample V 1155a).



Photo III-1 Locality V 1155. The weakly-developed foliation of a zoisite-hornblende pyrigarnite (right) is cut by the well-developed foliation of a garnet amphibolite (left) that has formed retrograde after the zoisite-hornblende pyrigarnite. Discordant veinlets in the pyrigarnite are cut off by the foliation of the garnet amphibolite.

In sample V 1155, the foliation is marked by parallelism of greenish-brown hornblende and zoisite. This foliation and the strained nature of the amphibole are interpreted as indications of deformation penecontemporaneous with the hornblende granulite-facies retrograde metamorphism.

The anhedral hornblende has replaced almost all the clino-

pyroxene, which is found as colourless, partially altered relics. The almost colourless, subhedral, inclusion-free *garnet* appears to be unaffected by the amphibolization. The *zoisite* has elongate forms with rounded outlines; it may be either α -zoisite, α -zoisite rimmed by β -zoisite, or β -zoisite. *Plagioclase* (28% An.) and *quartz* are completely anhedral with dented forms; they are both either strained or bent. Interrupted streaks of strained *scapolite* ($2V^x = 0^\circ$, $\Delta = 0.025 \pm 0.03$), lying longitudinally parallel to the foliation, indicate that the scapolite was probably formed under granulite facies conditions (cf. Davidson, 1943; v. Knorring & Kennedy, 1958; Lovering & White, 1964). *Rutile*, *apatite*, *zircon*, and *opaque matter* are found as accessory constituents.

Solutions emanating from discordant veins (see photograph III-1) caused the growth of rims of *blue-green hornblende* around the greenish-brown type. At the same time, turbid rims of *epidote* were formed around *zoisite* and *rutile* was locally altered into *titanite*. The injection of these veins antedated the deformation that caused the formation of the foliation in the neighbouring amphibolite, because the veins are cut off by this foliation.

In sample V 1155a, brownish-green hornblende and *zoisite* have been replaced by *blue-green hornblende*, *epidote*, and small amounts of *biotite*. *Garnet* and *scapolite* are still found as constituent minerals, but have corroded outlines and are full of cracks. *Scapolite* has been altered into *sericite* along the cracks. Undulose *quartz* and bent *plagioclase* (27% An.) also occur as principal constituents. *Rutile*, *titanite*, *apatite*, *zircon*, and *opaque matter* are found as accessories.

The texture of the rock is streaky; melanocratic fragments of amphibolized pyrigarnite alternate with leucocratic streaks which have incorporated small particles of the dark fish as a result of the tectonization. Garnet-rimmed *kyanite* crystals in these leucocratic streaks show that they are, at least in part, remnants of the pegmatoid veins accompanying the hornblende granulite facies retrograde metamorphism in the neighbouring rock (see above, sample V 1155).

The relation between injected pegmatoid material and amphibolization is illustrated by a non-tectonized barren pegmatoid vein in amphibolized plagiopyrigarnite (sample V 1197a).

The vein itself is coarse-grained; it is entirely composed of *quartz* (\varnothing up to 1.5 cm) and *plagioclase* (18% An., \varnothing up to 3 cm) with small flakes of *sericite*. Fragments of the wall-

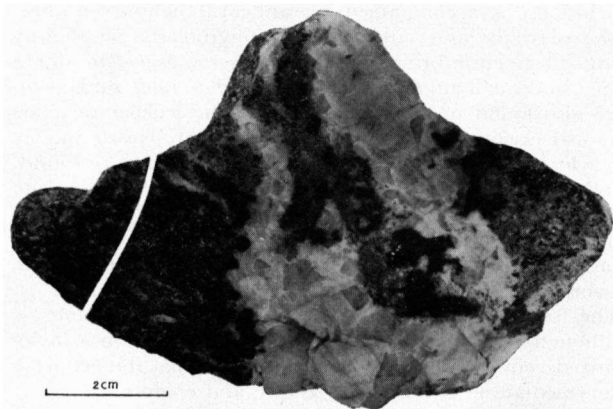


Photo III-2 Sample V 1197a. Non-tectonized barren pegmatoid vein in amphibolized plagiopyrigarnite. The line indicates the distance from the vein at which the first completely amphibolized relics occur.

rock, which were disrupted during the injection of the vein, are surrounded on all sides by pegmatoid matter. The contact of vein and wall-rock is irregular. The part of the wall-rock bordering on the vein has been completely altered into garnet amphibolite by the solutions emanating from the vein. However, the limited range of action of these solutions is demonstrated by the appearance of the first clinopyroxene relics at a distance of only 1.5 cm from the vein (see photograph III-2). It is also demonstrated by the differences in grain-size of the secondary hornblende in different parts of the rock. For, whereas the amphiboles in the disrupted fragments may reach a length of 1 cm, the amphiboles at the border of the vein are no larger than 3–4 mm, and this maximum size rapidly dwindles to 1 mm as the distance to the vein increases.

The deformation that accompanied the mesozonal metamorphic phase on a regional scale left few of the veins unaffected and developed locally narrow mylonitic zones in rocks weakened by pegmatoid injection; a good example of this is found in sample V 1214 (see photograph III-3).



Photo III-3 Sample V 1214. Barren pegmatoid vein transformed into a mylonitic streak by the Hercynian deformation (— nic, $\times 20$).

Microscopical appearance: the barren leucocratic veins have been changed into microcrystalline mylonitic streaks. In these streaks, isolated garnets and severely bent plagioclase (20% An.) and hornblende-porphycroclasts are found as eyes, trailed and rimmed by trains of microcrystalline hornblende and biotite fragments (possibly indicating potassium metasomatism). Non-mylonitized, medium-grained, fragments of epidote-garnet-hornblende rock with mylonitized rims lie as lens-shaped bodies parallel to the foliation, as do the disc-shaped bodies of fine-grained recrystallized quartz. A few relics of light-green clinopyroxene (indicating a pyrigarnitic descent), patchily replaced by blue-green hornblende, are still found in the epidote-garnet-hornblende rock fragments. No clinopyroxene was found in the mylonitized part of the rock.

This mylonitic type of deformation is typically linked to the mesozonal metamorphic stage; it was never found connected with granulite facies retrograde metamorphism.

The few examples described above are only a selection from the host of different types of rock that can occur

in a metamorphic formation where retrograde metamorphism proceeded in such a complex manner as in the Bacariza Formation. In fact, every conceivable gradation in composition between (plagio)pyrigarnite and (garnet) amphibolite has been found.

c. Mineral sequences in the pegmatoid veins and streaks.

The general paucity of leucocratic components and the random orientation of the melanocratic constituents give the (plagio)pyrigarnites a certain amount of tectonic rigidity. (Plagio)pyrigarnites veined with pegmatoid matter are, however, likely to offer far less resistance to internal deformation. This is probably the reason why veins of the older sequence (connected with hornblende granulite-facies retrograde metamorphism) are only found as tectonized bands and streaks in the rocks of the Capelada Complex.

The effects of metamorphism and tectonic hybridization preclude a thorough investigation of the original mineralogical and chemical composition of the veins. Nevertheless, it was possible to establish some age relations on the basis of the textural relationships between certain minor constituents when present (see Table III-2). For instance, the age relations between kyanite, γ -zoisite, α -zoisite, and epidote can be inferred from the way in which they occur in the leucocratic laminae of a partially amphibolized, streaky plagiopyrigarnite (sample V 1185).

The streaks consist of a plagioclase (24% An.)-quartz mosaic that probably recrystallized post-kinematically, as judged from the virtual absence of undulose extinction and bending. Minor constituents are kyanite, γ -zoisite, α -zoisite, and epidote. Apatite and zircon are found as accessories. The fine-grained kyanite is anhedral and has rounded outlines. Its occurrence as inclusions in α -zoisite proves that it crystallized before that mineral (see photograph III-4). It has been slightly altered into sericite along cracks and along the rims. The medium-grained α -zoisite has $2V^Z \approx 60^\circ$ and $r \ll \ll v$. Besides kyanite, its anhedral elongate crystals may contain inclusions of quartz, rutile, zircon, or garnet, which indicates that it crystallized after the emplacement of

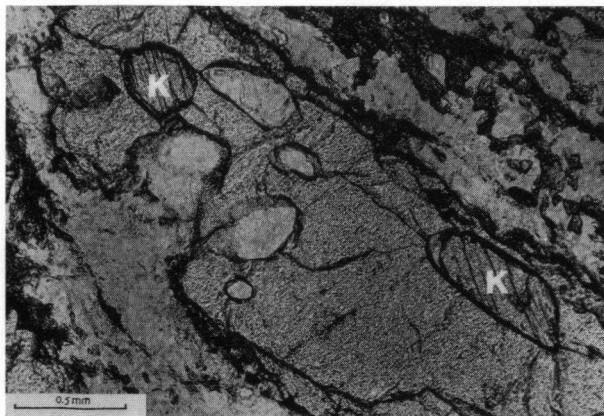


Photo III-4 Sample V 1185. Kyanite relics (K) enclosed in α -zoisite in a pegmatoid streak in plagiopyrigarnite (— nic).

the vein. In some places the α -zoisite has a zoned appearance caused by patches of γ -zoisite (lower Δ) occurring in the centre of the α -zoisite crystals. In the melanocratic laminae, epidote may be found as separate crystals. In the leucocratic streaks it is found only in the form of discontinuous rims around zoisite. Its appearance is considered to be an effect of mesozonal retrograde metamorphism.

The presence of kyanite as the oldest phase gives an indication of the PT conditions at which the pegmatoid material originated. Sobolev and Bazarova (1963) give the approximate pressure and temperature of crystallization of kyanite in pegmatites as 12 kb and 600° , respectively.

At some places the injection seems to have soaked the rock into which it penetrated, as for instance in sample M 217, where melanocratic patches of hornblende plagiopyrigarnite seem to float in leucocratic matter (photograph III-5).

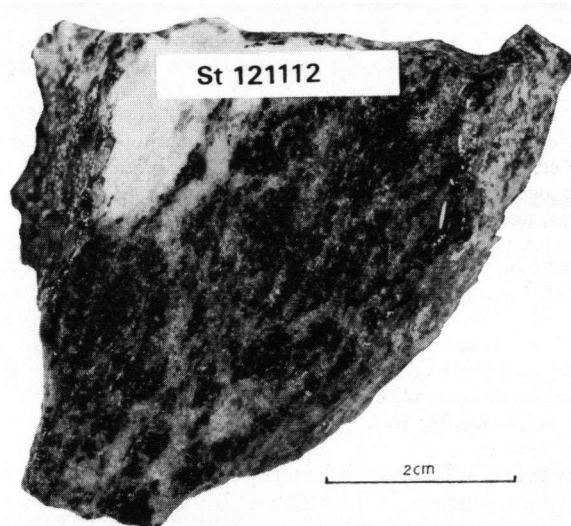


Photo III-5 Sample M 217. Pegmatoidally-soaked hornblende plagiopyrigarnite.

In the dark patches, light-pink euhedral garnet, poor in inclusions, is accompanied by anhedral light-green clinopyroxene relics and subhedral prophyroblasts of slightly strained greenish-brown hornblende. Quartz, plagioclase (30% An.), and small amounts of α -zoisite, titanite, rutile, and apatite are also found in the dark patches. The leucocratic mass consists essentially of a plagioclase (32% An.)-quartz mosaic in which some isolated garnet and zoisite grains are found. Both α - and β -zoisite are found as separate phases. β -zoisite crystals partially enclosing α -zoisite indicate that the former are probably younger than the latter. Increments of epidote on α - and β -zoisite indicate that epidote is younger than β -zoisite.

The frequent occurrence of orthite as cores in epidote — although it is also found as rims around zoisite (in a mylonitized vein, sample M 639) — indicates that the orthite is intermediate in age between zoisite and epidote.

The veins do not contain orthoclase or microcline; nevertheless, they must once have carried some potassium, in view of the biotitization of the pyrigarnite

within their sphere of influence. Although larger amounts of metasomatic biotite are found around the veins carrying epidote and orthite than around those carrying kyanite or zoisite, a granitic or granodioritic descent of these younger veins (as found by Scheumann, 1960, for orthite-bearing veins from the Waldheim area) is precluded on the basis of their total lack of alkali-feldspar. They may, however, very well be considered as residual liquids of post-catazonal gabbroic intrusions (cf. metagabbro at San Julian del Trebol, p. 155; Purrido amphibolite, p. 164). Whether the same supposition would be valid for the veins carrying kyanite and zoisite is not clear, since they might also be considered to have been formed by partial anatexis of deeper-lying, potash-poor rocks (sedimentary or magmatic). Subsequent squeezing could have caused migration of these partial melts into the overlying rocks. Formation of the leucocratic streaks by migmatization *in situ* of the parent rock of the pyrigarnites seems less likely, in view of the relation between retrograde alterations in the pyrigarnites and the occurrence of the pegmatoid matter.

4. Comparison of the pyrigarnite and eclogite mineralogies

Except for the presence of plagioclase as a stable phase in (plagio)pyrigarnite, the resemblance of this rock to eclogite is so close that it is sometimes difficult to distinguish one from the other. This similarity is only enhanced by amphibolization, because plagioclase may be present in retrograde eclogites as well as in retrograde (plagio)pyrigarnites. To map the boundary between eclogite- and granulite-facies rocks as accurately as possible, distinguishing mineral features had to be sought. These features had to be of such a nature that the amphibolized rocks with only a few catazonal mineral relics could still be recognized as belonging to one group or the other. Although several distinguishing features could be found for minerals of eclogite and (plagio)pyrigarnite, it should be borne in mind that these criteria are by no means infallible and that, in view of the close association of eclogite and (plagio)pyrigarnite in the field, transitional types are to be expected.

In thin sections the *garnet* in the granulite-facies rocks generally has a distinct light-pink colour, but in the eclogites (except sample M 459, see p. 130) it is nearly colourless. It is virtually free of inclusions. Although small amounts of quartz or rutile may be found included in garnet, they never occur in such abundance and with such characteristic patterns as in eclogite garnets (see p. 133). The formation of well-developed hornblende-plagioclase-magnetite kelyphite, a quite common phenomenon in the eclogites, was not found in the pyrigarnites with the exception of sample V 1250 (for description see below).

In thin section the *clinopyroxene* of the (plagio)pyrigarnites is light-green and slightly pleochroic, whereas the omphacite found in the eclogites is (again with the exception of sample M 459) nearly colourless. While alteration into hornblende proceeds in exactly the

same way as in pyrigarnite and eclogite, the formation of p.p. symplectite from omphacite (as described on p. 132), must be considered characteristic for clinopyroxenes from eclogitic rocks. Nevertheless, this separation of plagioclase from clinopyroxene is also found in rock-types of the Bacariza Formation considered here to be transitional between eclogite and pyrigarnite (sample V 1250, see below).

In contradistinction to the eclogites, *kyanite* does not occur as a stable phase in the (plagio)pyrigarnites, which is in accordance with the stable joins in de Waard's (1965) ACF diagram for the clinopyroxene-almundine subfacies of the granulite facies (Fig. III-6). Its presence in the leucocratic veins and streaks, where it is invariably rimmed by zoisite or epidote, must be ascribed to early crystallization from an alumina-supersaturated melt at a time when this melt still operated as a separate system (R. D. Schuiling, personal communication).

Zoisite may have formed in the (plagio)pyrigarnites as an additional phase for surplus Ca or Al that could not be accommodated in clinopyroxene, garnet, or plagioclase. Its occurrence as a typomorphic mineral, however, is much more restricted than in the eclogites.

To summarize the foregoing, it may be stated that, in general, the presence of garnet or clinopyroxene with a pronounced colour and the absence of inclusions in the garnet are indications for a pyrigarnitic descent. Typical for eclogites and retrograde eclogites are virtually colourless clinopyroxene and garnet crystals, the occurrence of p.p. symplectite and of kelyphitic rims around garnet, the presence of kyanite as a stable phase together with garnet and clinopyroxene, and the occurrence of garnet with many inclusions (especially rutile). A structural indication that frequently proved helpful is the pre-Hercynian foliation (M_1), which is in most cases well-developed in eclogites but always absent in (plagio)pyrigarnites.

5. Transitional types between eclogite and pyrigarnite

Especially near the border between the Bacariza Formation and the eclogites, rock-types are found with both eclogitic and pyrigarnitic properties. The classification of these rocks was arbitrarily based on the properties of the minerals as well as by the location of the sample. An example of an eclogite with pyrigarnite-like qualities has already been mentioned in Chapter I (sample M 459, p. 130); an example of a pyrigarnite with eclogite-like qualities is given by a hornblende pyrigarnite (sample V 1250) found at a distance of about 500 m West of the boundary between the Bacariza Formation and the eclogites of the Sierra de Moles.

Macroscopically, the most conspicuous mineral in this non-schistose rocks is a euhedral, medium- to coarse-grained, brownish-red garnet. The garnet is surrounded by a dark-green clinopyroxene mass in which medium- to coarse-grained black hornblende can be readily identified. Microscopically, the *garnet* appears as perfectly euhedral as in the hand-specimen. Although it is rich in inclusions (of

quartz, inversely-zoned plagioclase, clinopyroxene, hornblende, rutile, apatite, titanite, and opaque matter), it lacks the patterned rutile inclusions so characteristic of eclogite garnets. Amphibolization caused the formation of rims around the garnet consisting of fine-grained magnetite, dark hornblende (x yellow < y brown > z brownish- to bluish-green) and some plagioclase. The minerals in the kelyphitic rim show no sign of a "radial" or other oriented pattern. The zoned appearance of the garnet realized by a difference in colour between its dark orange-pink 0.06–0.20 mm wide outer rim and its pink core is probably a result of the kelyphite formation. The colour-zoning is reflected in compositional differences, the rims being richer in grossular and poorer in almandine than the cores (Vogel & Bahezre, 1965; see also Table V-2).

The anhedral *clinopyroxene* is medium-grained, light-green, and slightly pleochroic. Its optical properties are: $2V^z = 77^\circ \pm 2^\circ$, $r < v$, $c/z = 38-40^\circ$, $\Delta = 0.022-0.024$, $n_{Dy} = 1.706 \pm 0.002$. The occurrence of p.p. symplectite (predominantly stage 4, but also stages 1, 2, and 3; see p. 132) is seen as an indication that the transition between pyri-garnite and eclogite is gradual rather than abrupt. The clinopyroxene is altered into hornblende where it borders on garnet; clinopyroxenes found as inclusions in garnet are often unaltered.

The anhedral secondary *hornblende* is dark-green (x yellow < y brownish-green = z green) and often has a dark blue-green z-colour where it borders on garnet. Inclusions of fine-grained metamict orthite surrounded by pleochroic halos show that the formation of the hornblende is connected with a pegmatoid intrusion of the younger type (see Table III-2). The optical properties of this hornblende are: $2V^x = 72^\circ \pm 2^\circ$, $c/z = 18-20^\circ$, $n_{Dy} = 1.680 \pm 0.002$.

Plagioclase (oligoclase) and *quartz* occur only in minor amounts; *orthite*, *rutile*, *titanite*, *apatite*, *zircon*, and *opaque matter* occur as accessories.

6. *Leptynites*

Very conspicuous because of their light colour are rocks for which the name leptynite seems appropriate (Cogné & v. Eller, 1961). Although these leptynites occur in rather subordinate amounts, they are of interest because of their aberrant composition (garnet \pm plagioclase + quartz + epidote \pm orthite) and puzzling petrogenesis.

They are found as bands of variable width (up to 50 cm) in retrograded (plagio)pyrigarnites, and show the following characteristics:

1. The boundary of the leptynite cuts through textures in the retrograde (plagio)pyrigarnite (see photograph III-6).
2. Although garnet is the principal ferromagnesian mineral in the leptynite, hornblende (in amounts of under 1%) may be found as small whisps or in protected places, and small fragments of clinopyroxene may occur in the same way.
3. Epidote, sometimes with well-developed cores of orthite, is the only minor constituent in the leptynites.
4. Zircon is more abundantly present in the leptynites than in the neighbouring rocks.
5. The garnet in the leptynites lies evenly distributed and shows no inclination to form clusters or streaks.

Its composition (py 14–20%, alm + sp 54–60%, Ca-garnet 26%, as determined for the garnets from samples V 1193 and V 1243a; see Ch. V, A) is indicative of formation at amphibolite facies metamorphic conditions.

These characteristics are well illustrated by a sample of retrograde plagiopyrigarnite with a band of leptynite found as an unattached fragment near Francoy (Sample G 7–2, photopgraph III-6; see also den Tex & Vogel, 1962).

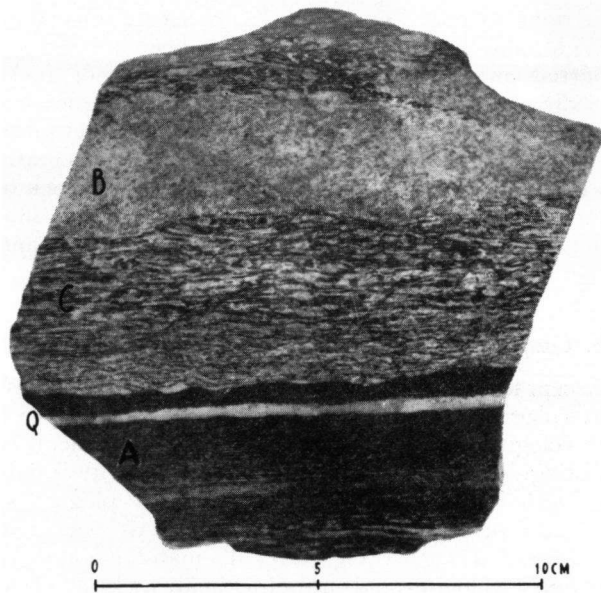


Photo III-6 Sample G 7-2. Leptynite (B), discordantly cutting through the foliation of a streaky garnet amphibolite (C), (for description see below).

The non-leptynitic part of the sample consists macroscopically of two rock-types, A and C, both with a well-developed foliation lying parallel to their contact but cut discordantly at a small angle by the leptynitic part (B).

Type A is a garnet amphibolite with occasional relics of light-green clinopyroxene. The hypidiomorphic garnets are poor in inclusions and have a light-pink colour. The xenomorphic hornblende is zoned with green-brown cores and blue-green rims. Quartz, plagioclase (20% An.), and epidote are additional constituents. Apatite, titanite-rimmed rutile, and opaque matter (mainly ilmenite) occur as accessories. The texture of band A is characterized by parallelism of amphibole and by a more or less even distribution of the minerals over the sample. The leucocratic band, marked Q on photograph III-6, consists of quartz with deformation lamellae. Epidote crystals with zoisite cores and isolated grains of garnet, amphibole, or apatite are also present in this quartzband.

In type C, the macroscopically-visible planilinear texture is caused by parallelism of rod-shaped leucocratic aggregates. These aggregates consist mainly of medium-grained epidote, occurring singly or in clusters, with cores of α -zoisite. The occasional occurrence of included muscovite aggregates may indicate that kyanite was once also present. The other constituents of these leucocratic rods, which are thought to be tectonized streaks, are quartz and plagioclase (19% An.),

but small amounts of garnet and rutile are also found (mostly as inclusions in epidote). The melanocratic streaks consist of a garnet amphibolite resembling type A except for the absence of clinopyroxene relics and the rather euhedral habit of the fine-grained garnet crystals.

In the leptynite (B), subhedral corroded light-pink garnet, sometimes with darker spots, is the most conspicuous mineral. Quartz, plagioclase (20% An.), and epidote are the other principal constituents. Rutile, titanite, apatite, zircon, and opaque matter are found as accessories. Chlorite occurs secondary after either garnet or the blue-green hornblende present in small amounts (well under 1 vol%). Foliation is caused by parallelism of epidote and elongate garnet. Plagioclase seems to occur in two generations, one medium-grained and the other fine-grained. The latter (older) plagioclase lies in elongated aggregates parallel to the foliation. For both, the anorthite content was 20 per cent. If the mineralogy of types B and C is compared, it appears that B is richer in garnet (21 vol% against 12.7 vol% in C), quartz, zircon, and plagioclase, but poorer in epidote (zoisite is lacking completely) and amphibole.

Discordance can also be observed at location V 1193, where leptynite bands about 1 cm wide are disposed at an angle to planes of penetrative deformation formed during catazonal retrograde metamorphism (sample V 1193a). Other leptynite bands in this exposure may have a considerable width, as for instance the 50 cm-wide band from which sample V 1193 was taken. This leptynite is extremely rich in anhedral to subhedral medium-grained garnet (≈ 50 vol%) which is distinctly zoned (dark-pink cores, light-pink rims). Other principal constituents are epidote-rimmed orthite (sometimes bent over 40°) and strongly undulose interlocking quartz with a distinct preferred orientation. Plagioclase occurs in small amounts. Accessory constituents are: biotite, rutile, titanite, apatite, zircon, and opaque matter. Investigation of the zircon from this sample by Hoppe (1966) revealed that 44 per cent of the zircon contained older cores, separated from newly-grown rims by a zone rich in tiny vesicular inclusions. Unfortunately, no conclusive evidence about the magmatic or sedimentary descent of these older cores could be drawn, because, as Hoppe states, p. 75: "*Die Formen der älteren Teile sind nur mit grosser Vorsicht auswertbar. Mit der Annahme eines sedimentären Ausgangszustandes scheint das Erscheinungsbild der älteren Teile nicht in Widerspruch zu stehen*".

The discordant nature of the catazonally-formed foliations and the frequent occurrence of epidote \pm orthite as minor constituents, seem to indicate that the formation of the leptynites is connected with the mesozonal metamorphic phase. This supposition is in accordance with the almandine-rich nature of their garnets (see Table V-2). However, their ultimate origin remains obscure (see also Ch. III, C 1; p. 190).

7. Calc-silicate rocks

Calc-silicate rocks were found only in the eastern part of the Bacariza Formation, near the contact with the Uzal ultrabasite (see Fig. III-1). They occur interbanded with pyrigarnites and retrograde pyrigarnites. Except for the epidote-rich types, which have a pistachio-green colour, they are difficult to recognize in the field because their principal constituents are similar to those of the pyrigarnites and retrograde pyrigarnites: garnet, clinopyroxene, epidote (and

hornblende). Microscopically, they differ from the pyrigarnites by containing accessory titanite instead of rutile, which is the stable titaniferous phase in most granulite facies associations. The mineral associations are: clinopyroxene + epidote (sample M 158a) and garnet + clinopyroxene + epidote (sample R 329).

The garnet-epidote-clinopyroxene rock (sample R 329) is macroscopically identical with a pyrigarnite. It is a dark, medium-grained rock with a weakly-developed foliation. Garnet and black clinopyroxene can be identified in the hand-specimen.

Microscopical appearance: anhedral clinopyroxene is the most important constituent; it is green and distinctly pleochroic (x yellowish green < y blue-green > z blue-green). Its optical properties — $2V^Z = 70^\circ \pm 2^\circ$, $c/z \approx 44^\circ$, $\Delta = 0.024 \pm 0.002$, $n_{Dx} = 1.701 \pm 0.001$, $n_{Dy} = 1.709 \pm 0.001$, $n_{Dz} = 1.725 \pm 0.001$ — indicate that it probably has a diopside-hedenbergite-rich composition. It is replaced by small patches of dark-coloured secondary hornblende. The garnet is dark pink, has corroded outlines, and contains inclusions of titanite. Where it borders on clinopyroxene, a rim of secondary hornblende has been formed, and indications of replacement by epidote have also been found. Its physical and optical properties (see Table V-2 and Fig. V-3) are not characteristic for a member of the ugrandite group (cf. Winchell, 1956), although they differ distinctly from those found for garnets in normal pyrigarnites. The epidote crystals generally occur in elongate aggregates lying parallel to the foliation marked by the clinopyroxene; they occasionally contain cores of orthite. There were no signs that zoisite had at any time been a constituent mineral. The hornblende occurs in minor amounts, secondary after clinopyroxene and garnet. It is very dark, with x dark yellow < y dark brownish-green < z dark blue-green. Its optical properties are: $2V^X = 69^\circ \pm 2^\circ$, $c/z = 17^\circ$, $\Delta = 0.018 \pm 0.002$, $n_{Dx} = 1.676 \pm 0.002$, $n_{Dy} = 1.687 \pm 0.002$, $n_{Dz} = 1.694 \pm 0.002$. Quartz is found as a minor constituent; titanite, apatite, and zircon occur as accessories; adularia was deposited hydrothermally in veinlets.

The biminerale epidote-clinopyroxene rock (sample M 158a) has an extremely simple mineralogical composition. Its texture is panxenomorphic with a random orientation of the minerals. Clinopyroxene is pleochroic in distinctly green colours (x yellowish-green < y blue-green > z blue-green). It closely resembles the clinopyroxene in sample R 329 (s.a.). Epidote ($2V^X \approx 80^\circ$, $r < v$) is the only other major constituent. Apatite and titanite occur as accessories. Secondary hornblende was not found.

8. Garnet-biotite gneisses

Narrow zones of garnet-biotite gneiss 10 to 20 m wide are found predominantly in the eastern part of the Bacariza Formation (see Fig. III-1). Although they are believed to be of sedimentary descent, they are distinguished from the metasedimentary rocks of the Concepenido Complex (Ch. I) by compositional and textural differences. In the field they are found as dark, violet-brown *augen* gneisses (types with an imperfectly-developed lamination are seen only rarely) with a foliation parallel to that of the neighbouring retrograde pyrigarnites. The eyes are formed by garnet, hornblende, or large plagioclase porphyroclasts measured in centimetres. Fish of pyrigarnite or retro-

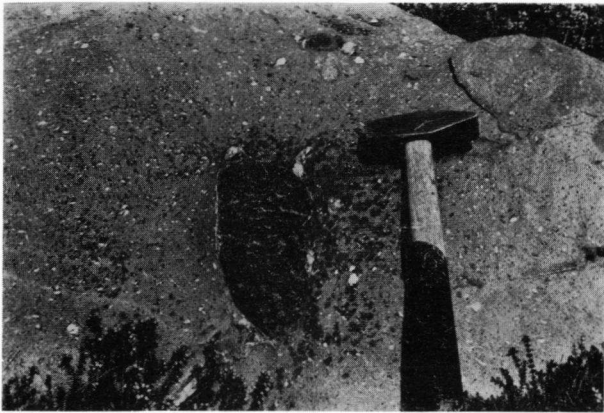


Photo III-7 Locality V 1179. Fish of garnet-hornblende rock (retrograde after pyrigarnite) in phyllonite-like garnet-biotite gneiss.

grade pyrigarnite occur frequently in the *augen* gneisses (photograph III-7).

Petrography. — In general, the mineralogical composition and petrogenesis are the same as for the banded gneisses and the Chimparragneisses, though there are some differences in detail.

Quartz, plagioclase, garnet, biotite, and epidote with cores of orthite were all found as principal constituents in these gneisses, but muscovite was present only in some of them. As accessories, rutile (sometimes altered into titanite), apatite, zircon, and opaque matter were found.

Hydrothermal veins, filled with adularia or epidote, have caused local alteration of biotite into chlorite, and the occurrence of pistacite is also related to these veins.

Kyanite is generally absent, though small kyanite relics were found in one sample (Coe 304). Crystals of hornblende and sometimes also of clinopyroxene were often found lying in streaks, or — in the case of hornblende — as isolated porphyroclasts. The plagioclase occurs as porphyroclasts and as a constituent of the matrix. In all cases the porphyroclasts had a lower anorthite content (varying from 10 to 32% An.) than the accompanying plagioclase in the matrix (varying from 12 to 42%). Both were inversely zoned. Potash feldspar is totally absent.

Differences in texture are ascribable to differences in the intensity of tectonization. Three types representative of the different stages in the continuous transition from streaky to phyllonitic types will be discussed.

Least tectonized is a planolite garnet-biotite gneiss (sample V 1255), found near the eclogite border on the Concepenido ridge. Its texture — with streaks of predominantly melanocratic minerals weaving around lenticular and flat-lenticular leucocratic aggregates — is reminiscent of the banded gneisses and Chimparragneisses for which partial anatexis was assumed to have taken place. The melanocratic streaks consist mainly of garnet, biotite, and epidote-rimmed orthite. Microcrystalline plagioclase occurs interstitially. The *garnet* is free of inclusions; it has

scalloped rims and is being replaced by biotite. The fine-grained *biotite* is of a dark-brown pleochroic variety and shows no signs of deformation. The darkorange *orthite* is almost completely metamict and has either rounded or subrounded euhedral outlines; it is surrounded by extremely narrow rims of *epidote*.

Aggregates of fine-grained *plagioclase* crystals (20% An.) with almost identical optical orientation are considered to be a recrystallization product of older coarse-grained plagioclase. They occur together with medium-grained *quartz* and isolated medium-grained plagioclase relics in the leucocratic bodies.

Replacement of garnet by biotite, recrystallization of plagioclase, and crystallization of epidote, indicate that the rock has suffered mesozonal retrograde metamorphism. The presence of an anatectic palimpsest texture and the absence of bending of biotite, orthite, and epidote testify that in this instance metamorphism proceeded unaccompanied by deformation.

Where deformation accompanied the mesozonal metamorphism, a streaky to laminated planar type of garnet-biotite gneiss (sample V 1244) was formed. Here the garnet is anhedral but lacks scalloped outlines. Except for the presence of larger leucocratic streaks, garnet, biotite, epidote-rimmed orthite, quartz, and plagioclase (27% An.) lie more or less evenly distributed over the rock. They have all become slightly strained, cracked, or bent by the deformation.

The severely tectonized types of garnet-biotite gneiss (sample V 1179d) have a phyllonite-like texture. Macroscopically, they appear as extremely fine-grained grayish-brown to violet rocks with a well-developed foliation. Porphyroclasts of medium- to coarse-grained garnet and plagioclase may lie parallel to or at an angle with the foliation together with fish of pyrigarnite or retrograde pyrigarnite.

Due to the extremely fine grain-size (porphyroclasts excepted), the texture can only be determined in thin sections. Here it appears to be caused by an accumulation of biotite-rimmed lenticular particles of quartz and plagioclase lying in parallel. The absence of fluxion-banding and the blastesis of biotite were among the reasons for calling this rock a blasto-phyllonite instead of a (proto)blastomylonite (Reed, 1964). Although fracturing, bending, and undulose extinction are common in all minerals, the effects of deformation have here been largely obliterated by recrystallization. *Garnet* occurs as light-pink rounded to subrounded crystals, and sometimes has definitely elongate shapes. Plagioclase appears in two generations. The older generation is represented by medium- to coarse-grained inversely-zoned porphyroclasts (core 21% An.; rim 27% An.), the younger one by microcrystalline lenticular biotite-rimmed grains which are also inversely zoned (core 29% An.; rim 42% An.). *Biotite* is only slightly bent and lies in two sets of shear-zones intersecting each other at an angle of about 30° (in the slide). *Epidote-rimmed metamict orthite* occurs in minor amounts. Cryptocrystalline needles of a mineral which according to its localization and habit might be kyanite, lie along the rims of the micro-crystalline plagioclase grains. *Rutile*, *apatite*, *zircon*, and *opaque matter* are accessory constituents.

The most common garnet-biotite gneisses have textures intermediate between those of samples V 1179d and V 1244.

The presence of microcline in three samples of garnet-biotite gneiss that otherwise conform in every aspect

to the above-mentioned types, is ascribed to local potassium metasomatism connected with late emplacement of granitic or granodioritic rocks (cf. Ch. I, B 3 II b, pp. 156 ff.). In the Bacariza Formation the only evidence of such intrusion was found in a small intrusive stock of coarse-grained leucocratic muscovite granodiorite (sample V 1111) at the Playa de Cartés. This granodiorite suffered only slightly from tectonization. Its plagioclase (16% An.) is partly replaced by potash feldspar.

9. Post-metamorphic gabbro

A gabbroic rock lacking any sign of metamorphism (sample V 1407) was found cutting across amphibolized pyrigarnites in the Sierra de la Capelada. Since it shows hydrothermal alterations (sericitization, chloritization), the time of its intrusion is assumed to have been roughly the same as that deduced for similar rocks found in the Banded Gneiss Formation (samples V 1025 and V 1077, p. 152), i.e. post amphibolite-facies metamorphism.

The mineralogical composition of the gabbro is simple; *augite*, sometimes with *uralite* rims, and *plagioclase* (64% An.), are the principal constituents. Brown *hornblende* with green rims and *biotite* with reddish-brown cores and blackish-brown rims are minor constituents; *olivine* and *hypersthene* are lacking. *Augite* and *plagioclase* appear to have crystallized simultaneously, since both have hypidiomorphic forms. Opaque matter, mainly *magnetite* and *ilmenite*, occurs in considerable quantities (3–5 vol%).

Eutectic crystallization of residual melt in interstices resulted in the appearance of feathery aggregates of micrographically intergrown plagioclase and quartz. Sericitization of plagioclase and alteration of the melanocratic constituents into chlorite and calcite are ascribed to hydrothermal action.

B. THE CANDELARIA AMPHIBOLITE FORMATION

The Candelaria amphibolite forms a roughly N-S-trending body, bordered on the East by the Chimparagneiss and on the West by the Carreiro zone of tectonic movement. The Candelaria amphibolites can be easily distinguished from the Purrido amphibolites by their extremely laminated and inhomogeneous nature and by the absence of fissility. Although the Candelaria amphibolites as a whole dip eastward at varying angles, local variations in dip are frequent as a consequence of small-scale folding (flow folding). Their incorporation in the Capelada Complex is based predominantly on the occurrence of a few plagiopyrigarnite relics but also on geological evidence (see Plate 1) from the area South of Cabo Ortegá to be treated by Engels in a forthcoming paper (J. P. Engels, Ph.D. thesis, in preparation): Nevertheless, the field evidence indicates that the petrogenesis of the Candelaria amphibolites is more complicated than a simple retrogradation of pyrigarnitic and plagiopyrigarnitic rocks. At least part of the Candelaria amphibolites resulted directly from gabbroic or metagabbroic rocks, as indicated by the presence of rocks with gabbroic or noritic mineral relics and with palimpsest textures (see Engels & Vogel, 1966). In both cases the end-

product of the metamorphic alteration is a common amphibolite, and because, furthermore, either gabbroic or pyrigarnitic relics are scarce, it is difficult to establish the extent to which these rock-types contributed to the formation of the Candelaria amphibolites.

1. Pyrigarnites, amphibolites retrograde after pyrigarnite, and associated calc-silicate rocks

Although some relics of plagiopyrigarnite or amphibolized plagiopyrigarnite were found in the Candelaria Amphibolite Formation, transitional types between plagiopyrigarnite and amphibolite are rare. More specifically, (garnet)amphibolites with relic clinopyroxene were never encountered. Although it is difficult to tell amphibolites derived from (plagiopyrigarnite apart from those secondary after metagabbro, it is believed that a massive, non-laminated type of garnet amphibolite — found in a zone of varying width (up to 400 m) along the western margin of the Candelaria Amphibolite Formation — has been retrotransformed from a high-pressure granulite.

A pyrigarnite relic found in this zone (sample V 28b) underwent tectonization (as testified by cracked garnet and strained clinopyroxene) and amphibolization, but it has retained its granofelsic texture with random orientation of the constituent minerals. The secondary hornblende is of a brownish-green variety; where it borders on garnet it has blue-green rims. The field relations of sample V 28b are not clear, but its petrography agrees well with that of several relics of retrograde pyrigarnite found in the Bacariza Formation.

The amphibolites in this zone are sometimes garnetiferous. Near the western border of the Candelaria amphibolites they are generally non-laminated, but lamination increases towards the East. At some 400 m from the boundary with the Carreiro zone of tectonic movement, on the NW slope of the Monte de Vilar, a small lenticular pyrigarnite-relic was found in banded and laminated, severely folded amphibolite (see photograph III 8). Alternating bands of amphibolite (with or without garnet-relics) interspersed with quartzofeldspathic laminae surround the relic.



Photo III-8 Location V 1130. Lenticular pyrigarnite-relic in laminated amphibolite.

A garnet amphibolite occurring near the western border of the Candelaria Amphibolite Formation (sample V 1125a) still exhibits its pyrigarnitic descent in spite of heavy amphibolization. It is an extremely dark, schistose amphibolite in which garnet can be clearly distinguished macroscopically.

Microscopical examination reveals a nematoblastic texture caused by parallel orientation of fine-grained subhedral hornblende crystals with a dark blue-green z-colour. Corroded relics of fine- to medium-grained poecilitic garnet are the only surviving pyrigarnitic remnants. Clinopyroxene is absent, but spongy textures in some of the hornblendes may indicate growth secondary after clinopyroxene or p.p. symplectite. Fine-grained quartz and saussuritized plagioclase occur interstitially. Epidote, apatite, titanite, and opaque matter are found as accessory minerals. Adularia, prehnite, carbonate, and chlorite occur in narrow hydrothermal dilatation veins.

In other samples of (garnet)amphibolite (V 162, V 231), the garnet content has dwindled considerably. In sample V162, the corroded garnet-relics are still fairly evenly dispersed throughout the rock; in sample V 231 all smaller garnets have disappeared and only isolated larger ones (\varnothing up to 1 cm) are still recognizable.

A non-schistose amphibolite with a well-developed foliation (sample V 28), totally lacking in relics indicative of a pyrigarnitic or gabbroic origin, has also been classified as a retrograde pyrigarnite on the basis of its occurrence in the midst of rocks of unquestionably pyrigarnitic ancestry. Its mineralogical composition is simple; subhedral hornblende with a blue-green z-colour and xenomorphic plagioclase (27% An.) are the principal constituents, and anhedral epidote is found in minor amounts. Titanite, apatite, and opaque matter occur as accessories. Veinlets filled with epidote have locally caused saussuritization and chloritization.

Catazonal retrograde metamorphic phase. — Recognition of a catazonal phase of retrograde metamorphism in analogy with the Bacariza Formation proved impossible in the Candelaria amphibolites, due to the intensity of the mesozonal metamorphic phase, which left few pyrigarnite-relics untouched. For the same reason, the presence of pegmatoid injections could not be established unambiguously. Nevertheless, leucocratic bands and laminae are frequently found in the (garnet)-amphibolites retrograde after (plagio)pyrigarnite (samples V 1130a and V 220a). They bear a striking resemblance to the tectonized pegmatoid veins and the leptynites from the Bacariza Formation, although minor constituents such as orthite and epidote are scarce and zoisite and kyanite are lacking.

Textures in the bands vary from glandular (sample V 220a) to virtually mylonitic (sample V 1130a, see photograph III-8), and the degree of tectonic hybridization is seen to increase with the intensity of the deformation, which results in a tendency to blurred boundary planes in the more intensively tectonized leucocratic bands.

The composition of the leucocratic bands is simple: quartz, plagioclase (28–31% An.), and corroded or rounded light-pink garnet are the principal constituents. Epidote-rimmed orthite occurs in small amounts,

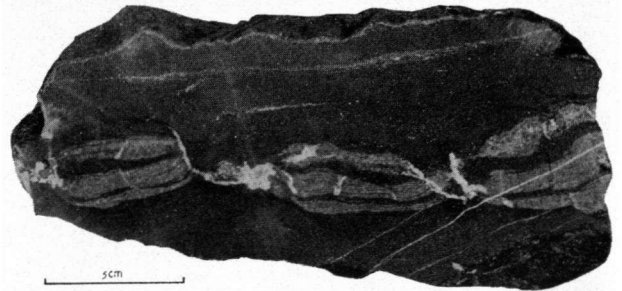


Photo III-9 Sample V 73. Boudinaged calc-silicate bands in amphibolite with plagioclase secretion in tension cracks. The direction of the lineation can be seen on the side of the sample.

and either biotite (sample V 220a) or hornblende (sample V 1130a) may also be present.

Calc-silicate rocks. — Narrow boudinaged bands of calc-silicate rock (see photograph III-9) were found in amphibolites retrograde after pyrigarnite, at a short distance from the Carreiro zone of tectonic movement. They consist either exclusively of epidote or of epidote and slightly pleochroic light-green clinopyroxene. Apatite, titanite, and opaque matter are found as accessories on both types. During deformation, the surrounding amphibolite, a plagioclase-poor, epidote-rich type, behaved incompetently with respect to the boudinaged calc-silicate laminae. Plagioclase, now heavily saussuritized, was secreted in cracks and zones of minimum tension.

2. *Metagabbros and amphibolites secondary after metagabbro*

In the central part of the Candelaria Amphibolite Formation, rocks with gabbroic palimpsest textures and relic gabbroic or noritic minerals are found together with their completely amphibolized counterparts. The petrogenesis of these rocks could be at least partially clarified by comparison with rock-types transitional between gabbro (norite) and amphibolite.

Non-tectonized types, only slightly affected by metamorphism, were not found in the investigated area, although they are known to occur in this formation in the area South of Cabo Ortegal (sample E 320, photograph III-10a).

Metamorphism caused the following changes in the norite (sample E 327b):

1. Formation of garnet (\pm hornblende) rims between the melanocratic constituents and plagioclase.
 2. Replacement of medium-grained labradorite (60% An.) by fine-grained aggregates of andesine (42% An.).
- The composition of the newly-formed garnet (see Table V 1) makes it likely that it developed under high-pressure granulite-facies conditions (see Engels & Vogel, 1966).

In the investigated area, non-tectonized types are found only in such a strongly amphibolized state that it is impossible to determine whether their original nature was noritic or gabbroic.

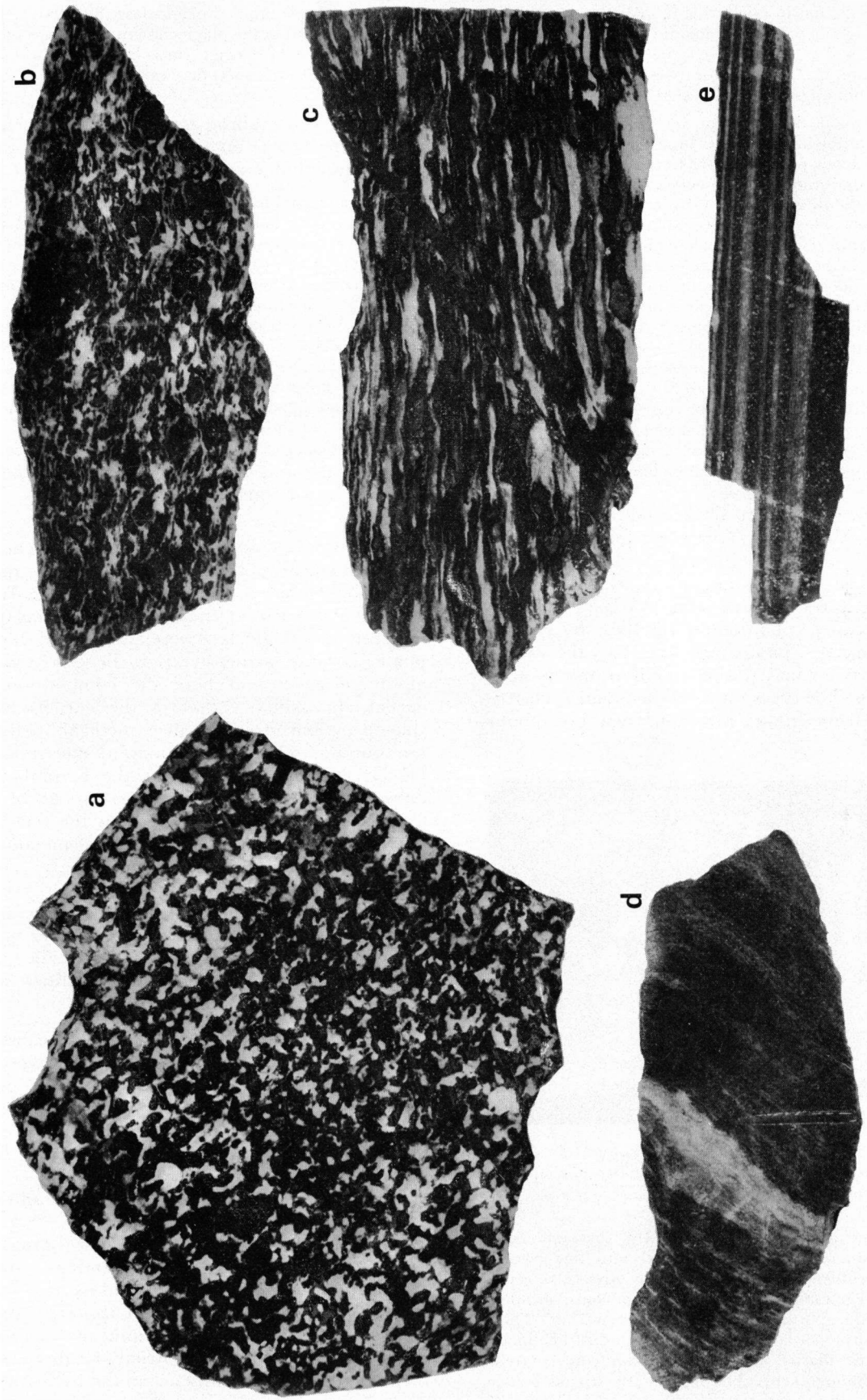


Photo III-10 Transitional stages in the metanorite/mylonite series: a. metanorite, sample E 320; b. flaser metagabbro, sample V 174b; c. metagabbro with flat-lenticular texture, sample V 1019; d. protomylonitic amphibolite, sample V 174; e. amphibolite mylonite with regular banding, sample V 199a (true size).

Sample V 1135, for instance, has a palimpsest gabbroic texture, although no gabbroic mineral relics could be found. The plagioclase has recrystallized in aggregates of fine-grained andesine (32% An.). Hornblende may have replaced the mafic minerals in two ways, to wit:

1. Pseudomorphous replacement by medium- to coarse-grained hornblende with a brownish-green z-colour; these hornblende pseudomorphs have a dusty appearance caused by multitudes of cryptocrystalline inclusions.
2. Pseudomorphous replacement by a poecilitic brownish-green hornblende with quartz inclusions. Opaque dust was not found in this type of pseudomorphs.

In both cases the hornblende pseudomorphs are surrounded by a polycrystalline rim of brownish-green or blue-green hornblende. Where this rim borders on plagioclase, a discontinuous rim of fine-grained garnet-crystals was formed. Narrow dilatation veins, filled with epidote and chlorite, caused local alteration of plagioclase into epidote and of hornblende into actinolite + albite.

In analogy with sample E 327b, it is supposed that the spongy hornblende with quartz inclusions is secondary after magmatic orthopyroxene; the hornblende with opaque inclusions is secondary after magmatic clinopyroxene.

Depending on the degree of deformation, the tectonized metagabbros may have *flaser* textures (photograph III-10b) not unlike those of the gabbro-amphibolites described by Scheumann (1954, 1956), flat lenticular textures (photograph III-10c), or even mylonitic textures (photograph III-10e). By gradual changes in texture (photograph III-10d), the various deformation types may grade over into one another, although *flaser*-like types may also be found as clearly-defined relic lenses in mylonitized metagabbro (photograph III-11).



Photo III-11 Monte de Vilar. Microfolded laminated amphibolite with a relic fragment of *flaser* metagabbro (below coin and caterpillar).

In the *flaser* metagabbro (sample V 174b), the mafic components are almost completely altered into fine-grained blue-green hornblende. The melanocratic streaks, or *flaser*, consist of aggregates of this hornblende or of coarse-grained, bent, hornblende porphyroclasts with mortar rims. These hornblende porphyroclasts are riddled with dust-like inclusions of opaque matter and often contain cores of relic (magmatic) clinopyroxene. The leucocratic streaks consist

exclusively of fine-grained plagioclase (80% An.). This high anorthite content of the plagioclase may perhaps be ascribed to the absence of garnet rims between the leucocratic streaks and the melanocratic *flaser*.

The *flaser* metagabbro passes first into a metagabbro with flat-lenticular texture and then into a protomylonitic amphibolite (sample V 174).

This microcrystalline mylonite has a weakly-developed lamination. The hornblende porphyroclasts and pyroxene relics have disappeared completely; garnet has a corroded appearance. Except for garnet, which is considered to be a relic, blue-green hornblende, spongy epidote, and slightly pleochroic clinocllore are the only melanocratic constituents. The leucocratic part of the rock consists of laminae of a plagioclase (27% An.)-quartz mosaic and of occasional flat-lenticular aggregates of quartz. A narrow band of calc-silicate rock has a central part consisting of pink garnet, epidote, and quartz, and rims consisting of epidote and quartz (see photograph III 10d).

In more extreme cases of mylonitization (sample V 199a, photograph III-10e) the streaky lamination is replaced by a regular lamination.

To summarize the foregoing, it may be concluded that all the metagabbros have undergone the mesozonal (amphibolite facies) metamorphic phase. It is not likely that the garnet rims between the melanocratic minerals and plagioclase were also formed during this phase, because garnet tends to be corroded during amphibolization and here the composition of the garnet approximates that of the garnets found in (plagio)pyrigarnites. Moreover, metagabbro fragments are found as relic lenses in amphibolite (photograph III-11), which indicates that the amphibolite was formed secondary after *metagabbro* instead of directly from gabbro. The supposition that the metagabbros were subjected to granulite facies metamorphism before they were "amphibolized" is also supported by the occasional occurrence of brownish-green hornblende formed at the expense of the melanocratic gabbro minerals. The period of time during which the gabbros could have intruded can thus be narrowed down considerably, but two possibilities are still open, to wit:

1. They were emplaced contemporaneously with the rocks that were completely converted into (plagio)pyrigarnite, but were somehow protected from the full impact of the granulite-facies metamorphism. However, this leaves unanswered the question of why they were not found in the Bacariza Formation.
2. They intruded after the main granulite facies (clinopyroxene-almandine subfacies) metamorphism but prior to the retrograde granulite facies (hornblende-clinopyroxene-almandine subfacies) metamorphic phase. This would explain why they are so incompletely metamorphosed, since the retrograde phase was geographically more restricted than the main phase. Strictly localized intrusion would explain their absence in the Bacariza Forma-

tion. A similar explanation has been given by Daniels *et al.* (1965) for the association of banded metagabbros with granulite- or amphibolite-facies rocks in Somalia.

3. Amphibolites of uncertain origin

Amphibolites without mineral relics or palimpsest textures form the bulk of the rocks in the Candelaria Amphibolite Formation. Their uniformity in texture is remarkable; their mineralogical composition differs only on minor points. They are panxenomorphic inequigranular rocks, in which hornblende with a blue-green z-colour is the most abundant mineral (50—75 vol%). Plagioclase is another major constituent, varying in composition from 25 to 50% An. Quartz and epidote are minor constituents; they occur in varying amounts. Accessories are titanite (with cores of rutile), rutile (unaccompanied by titanite), apatite, zircon, and opaque matter. Biotite, muscovite, sericite, garnet, and chlorite have been found in subordinate amounts in some of these amphibolites.

Changes in the ratio of hornblende to plagioclase or changes in grain-size may cause lamination or banding. In view of the uniformity of these amphibolites, it will suffice to describe only one of them (sample V 289) in detail.

The amphibolite is a grey, schistose rock. Black hornblende and milky white plagioclase can be discerned macroscopically. Lamination, which is caused by differences in hornblende content, is parallel to the foliation.

Microscopically, the blue-green hornblende appears to occur both as medium-grained porphyroclasts and as fine-grained crystals. Despite the occurrence of these porphyroclasts, the texture is not streaky; both the porphyroclasts and the fine-grained crystals lie evenly distributed throughout the rock. Regardless of size, the hornblendes show a well-developed planar parallelism (foliation).

A fine-grained mosaic of plagioclase (33% An.) containing some quartz, lies around and between the hornblende crystals (in other samples, e.g. sample V 195, the plagioclase is also found as rounded porphyroclasts). Titanite with cores of rutile, apatite, zircon, and opaque matter occur as accessories. In the neighbourhood of an epidote-bearing veinlet, saussurization of plagioclase and cloritization of hornblende have taken place together with crystallization of epidote. Epidote is absent from the part of the sample lacking signs of hydrothermal influence.

C. CHEMICAL COMPOSITION AND METAMORPHIC FACIES

Seventeen analyses of various rocks from the Capelada Complex were made in an attempt to determine whether they are of magmatic or sedimentary descent and also to obtain some insight into the relation between the mineralogical composition and chemistry of the various rock-types.

1. Magmatic versus sedimentary descent

Mafic rocks. — The (plagio)pyrigarnites, the retrograde (plagio)pyrigarnites, and the metagabbroic rocks (Table III-3, analyses 1—10 and 12—14; Table

I-1, analysis 6) appear to be of magmatic descent. Plots of their Niggli values in the c-fm-al-alk tetrahedron, the +T/—T/c triangle, and the si/(c+alk) diagram, all lie within the field of the igneous rocks (cf. Burri, 1959). They have no surplus aluminum over alkalis + lime ($t < 0$).

In the QLM diagram (Fig. III-2), a curve has been tentatively drawn between the projection points of the mafic rocks. This curve deviates somewhat from the differentiation trend of a circum-pacific magmatic suite, although several analyses plot within the field covered by the eclogitic rocks (cf. Fig. I-13).

The magmatic descent is confirmed by a c/mg diagram (Fig. III-3), where the analyses plot in good agreement with the trend of the Karroo dolerites (as given by Leake, 1964).

According to their normative mineral content, the mafic rocks can be classified as oversaturated tholeiites (analyses 1-7, 12, 13) and olivine tholeiites (analyses 8-10, 14), although the latter are by no means so well represented as in the Concepenido Complex (cf. Table I-1).

Analysis nr. 10 has an aberrant normative composition characterized by the presence of olivine in combination with wollastonite and the absence of orthopyroxene and diopside. This normative composition is also seen, though in a more extreme form, in the calc-silicate rock (analysis 17). This finding is considered to constitute an indication for a genetic link of contamination between the calc-silicate rocks and some of the more calcic mafic rocks (see also analysis 7, which lacks normative olivine but carries a small amount of normative wollastonite).

Paragneisses. — The sedimentary origin of the gneisses (Table III-3, analyses 15 and 16) is equally obvious. According to their Niggli values, they plot outside the field of igneous rocks in the following diagrams: c-fm-al-alk; T/c and si/(c+alk) (cf. Burri, 1959). Their composition corresponds very well with that of the gneisses from the Concepenido Complex ($\text{Na}_2\text{O} > \text{K}_2\text{O}$, absence of alkali feldspar from the mode), and like those gneisses they have surplus aluminum ($t > 0$), which is considered to constitute additional evidence for their sedimentary descent.

Their projection points in the QLM diagram lie outside the field covered by the paragneisses from the Concepenido Complex, but they lie well within the compositional field of the graywackes (Fig. III-4).

Leptynite. — The descent of the leptynites is by no means clear. The only available analysis (Table III-3, analysis 10) plots inside the igneous field in the al-fm-c-alk tetrahedron and in the T/c triangle, but outside that of the si/(c+alk) diagram. Furthermore, it has a small surplus of al over c+alk ($t > 0$), which suggests that it is either a metasediment or a contaminated igneous rock. Although the leptynite plots both within the field covered by graywackes and the field covered by the paragneisses from the Concepenido Complex in the QLM diagram, it is highly improbable, on the

basis of the observations made in the field (see p. 182), that the leptynites represent metamorphosed sediments. The problem of the leptynites evidently cannot be solved in simple terms of magmatic or sedimentary parentage. A more detailed study is required to elucidate their origin and mode of development.

Calc-silicate rock. — The parentage of the calc-silicate rock (Table III-3, analysis 17) is equally dubious. On the one hand this rock seems to be affiliated with some of the mafic rocks (cf. analyses 7 and 10), and it plots inside the igneous field of the T/c and si/(c+alk) diagrams. On the other hand, it plots in the field of the chemical sediments in the al-fm-c-alk tetrahedron, and its chemical composition does not tally with that of any known type of magma. The possibility that the calc-silicate rocks represent "residual cipolinos" (Schuiling, 1965) or perhaps the residual products of some other Ca-rich sediment, seems to deserve serious consideration. On the other hand, the possibility that these rocks represent natural high-lime silicate liquids formed by removal of phenocrysts during flowage differentiation (Drever & Johnston, 1966) cannot be totally excluded, although their normative composition (normative wollastonite) does not concur with those of natural high-lime silicate rocks as given by Drever & Johnston.

2. *Metamorphic facies*

The relative scarcity of (plagio)pyrigarnites completely unaffected by retrograde metamorphism, drastically limited the number of feasible chemical analyses in high-pressure granulite minerals. Especially clinopyroxene was often found so intergrown with secondary hornblende that it was impossible to separate the two by mechanical means. Garnet presented fewer difficulties. It was possible to delineate a compositional field for pyrigarnitic garnet in the ACF diagram (Fig. III-5), but the compositional field of the clinopyroxene had to remain largely conjectural.

Because it was difficult — even optically — to separate pyrigarnitic garnet relics from garnets stable under amphibolite facies conditions, no data were available to delineate the compositional field of garnet in the ACF diagram of the almandine amphibolite facies (kyanite-almandine-muscovite subfacies). The only analysis of blue-green hornblende (from a garnet-hornblende rock) plotted well within a wide field of possible compositions in this subfacies.

Mafic rocks. — The mafic rocks were plotted in the ACF triangle for the clinopyroxene-almandine subfacies of the granulite facies (de Waard, 1965b). They all lie within the field delimited by the anorthite (zoisite)-garnet-clinopyroxene tie-lines (Fig. III-6).

For the pyrigarnites (Fig. III-6, nrs. 9 and 10) nearly all the Ca and Al could be accommodated in garnet and clinopyroxene and little was left to form plagioclase or zoisite. In the plagiopyrigarnites (Fig. III-6, nrs. 4 and 6) surplus Ca and Al went to form oligoclase in

combination with the Na left over after the formation of the clinopyroxene; shortage of Na caused formation of zoisite instead of plagioclase in the zoisite-hornblende pyrigarnite (Fig. III-6, nr. 7). The same ACF diagram illustrates that the formation of garnet in metanorites and metagabbros (Fig. III-6, nrs. 12, 13, 14) under conditions of the clinopyroxene-almandine subfacies of the granulite facies, was inevitable.

Retrograde metamorphism at hornblende-clinopyroxene-almandine-subfacies metamorphic conditions (de Waard, 1965b) caused the growth of secondary hornblende in zoisite pyrigarnite and plagiopyrigarnite (Fig. III-6, nrs. 7 and I-6). The position of the projection points of these rocks with regard to the anorthite-garnet, anorthite-hornblende, and anorthite-clinopyroxene tie-lines explains why hornblende grows predominantly secondarily after garnet in the zoisite pyrigarnite, whereas it replaces clinopyroxene in the plagiopyrigarnite.

Judging from their position relative to the tentatively-drawn anorthite-hornblende tie-line in the ACF diagram for the kyanite-almandine-muscovite subfacies of the almandine amphibolite facies (Fig. III-7), two retrograde (plagio)pyrigarnites (nrs. 5 and 8) and two metagabbros (norites) (nrs. 12 and 14) and all analyzed (plagio)pyrigarnites would be converted at almandine amphibolite facies metamorphic conditions into amphibolites without garnet, whereas amphibolization of three retrograde (plagio)pyrigarnites (nrs. 1, 2 and 3) and one metagabbro (nr. 13) would lead to the formation of garnet amphibolite. For sample V 174b, a metanorite (analysis 14, for description see p. 188), this would mean that the garnets in the rock could not have been formed during the amphibolite facies metamorphism and should thus be considered relics of the catazonal metamorphism. However, the anorthite-hornblende tie-line shifts with a changing composition of the hornblende and, moreover, too little is known about the compositional variations of the hornblendes in the rocks of the Capelada Complex to permit prediction of the mineralogical composition of completely amphibolized (plagio)pyrigarnites or metagabbros (norites) with any certainty. But it is beyond doubt that clinopyroxene became an unstable phase under amphibolite facies metamorphic conditions in all analyzed metabasites from the Capelada Complex. This conclusion is in accordance with the microscopical observations.

Paragneiss. — The observations concerning metamorphic facies in the paragneisses of the Concepenido Complex (p. 163) can also be applied to the paragneisses of the Capelada Complex. During catazonal metamorphic conditions (clinopyroxene-almandine subfacies of the granulite facies) the gneisses suffered partial anatexis. If it is assumed that all Na and K became incorporated into the metatect, the projection-points of the gneisses (Table III-3, nrs. 15 and 16) in the ACF diagram for the clinopyroxene-almandine subfacies (Fig. III-6) will reveal the mineralogical composition of the restite. For both the analyzed

gneisses, the restite appears to have consisted principally of garnet with some additional kyanite.

During the mesozonal retrograde metamorphic phase (kyanite-almandine-muscovite subfacies of the almandine amphibolite facies), however, no partial anatexis took place, so the analyses can be plotted in an A'KF diagram (Fig. III-8). Judged from their projection points in this diagram, kyanite could not have been formed in addition to quartz, plagioclase, garnet, biotite, and muscovite during this metamorphic phase. The microscopically-observed alteration of garnet into biotite (see p. 184) seems to be a logical consequence of the fact that the metatectic part of the sample is also actively involved in mineral formation under almandine amphibolite facies conditions.

Leptynite and calc-silicate rock. — For both the leptynite (11) and the calc-silicate rock (17) it is impossible to conclude from the ACF diagram (Figs. III-6 and III-7) whether their mineral association reflects catazonal or mesozonal metamorphic conditions, because both these rocks plot in the same field in both diagrams. However, although the chemical composition of the leptynite suggests that partial anatexis would have taken place under catazonal metamorphic conditions, their texture (with the garnet evenly distributed over the rock) gives no reason to suspect that anatexis took place at any stage of their formation.

CHAPTER IV

STRUCTURAL GEOLOGY

The structural features of the Cabo Ortegual area are not yet fully understood. From the foregoing chapters it is evident that the various metamorphic phases were all accompanied by deformational phases. Because much of the information about the different tectonic phases is scattered throughout the first three chapters, a recapitulation in chronological order will be given in this chapter. A statistical approximation of the problem was not carried out because a structural analysis of the area around Cabo Ortegual will be discussed extensively in a forthcoming Ph.D. thesis by J. P. Engels.

A. EVIDENCE OF FOLDING DURING THE EARLIEST CATAZONAL METAMORPHIC PHASE (M_1)

Since the retrograde metamorphic changes in the various formations were almost always accompanied by deformation, evidence of the earliest folding must be sought in rocks that were unaffected by retrograde metamorphism.

Paragneisses. — For the gneisses that suffered partial anatexis during the catazonal metamorphism, it is not to be expected that tectonic features older than those of the Hercynian orogeny will be found. For the non-anatexitic Cariñogneiss, no convincing evidence of pre-Hercynian folding has been found in the field, although it is quite possible that it could be provided by systematic structural investigations.

Eclogites. — The W-NW-dipping foliation of the eclogites, which is marked by such primary minerals as omphacite, α -zoisite, and kyanite, developed as a consequence of isoclinal folding of the eclogite during the earliest catazonal metamorphic phase. Evidence of the isoclinal nature of these folds was found on one of the islets north of Punta Aguillones and in the Sierra de



Photo IV-1 Isoclinally-folded eclogite at the Sierra de Moles, looking SW. Photograph: Prof. E. den Tex.

Moles (photograph IV-1), where the anticlinal crests were found to be exposed. The isoclinal folds have steep, more or less westward-dipping axial planes and gently northward-plunging fold axes.

(Plagio)pyrigarnites. — No foliation has been found in the (plagio)pyrigarnites unaffected by retrograde metamorphism, nor could any trace of folding connected with their original metamorphism be detected.

Ultrabasites. — Vague indications on the aerial photographs that weathered-out bands at the Limo are disposed in the pattern of a fold with a steeply northward-plunging axis could not be verified in the field.

B. DEFORMATION ACCOMPANYING THE CATAZONAL RETROGRADE METAMORPHIC PHASE (M_2)

Evidence of the catazonal retrograde metamorphic phase was found only in the eclogites and in the mafic rocks of the Capelada Complex.

Eclogites. — In the eclogites, the foliation marked by parallelism of omphacite \pm α -zoisite \pm kyanite, is replaced by a new foliation (lying parallel to its predecessor) marked by parallelism of p.p. symplectite, β -zoisite, and brownish-green or greenish-brown hornblende (see photographs I-7 and I-9). That deformation actually played a role in the development of this new foliation is apparent from the strained nature of the older minerals.

(Plagio)pyrigarnites. — In the Bacariza Formation this phase led locally to a weakly-developed foliation (see photograph III-1) in the non-foliated (plagio)pyrigarnites.

Metagabbros from the Candelaria Amphibolite Formation. — It has been assumed (p. 188) that the metagabbros from the Candelaria Amphibolite Formation were partly metamorphosed during the catazonal retrograde metamorphic phase. In some cases the metamorphic alterations went hand in hand with development of a *flaser* texture, which is thus indicated to be a deformation belonging to the catazonal retrograde metamorphic phase.

The localized occurrence of this phase and the fact that no contemporary folds were found suggest that this was only a minor deformational phase expressed in penetrative movements along predestined zones of weakness (s-plane, pegmatoid injections).

C. DEFORMATION ACCOMPANYING THE MESOZONAL METAMORPHIC PHASE (M_2)

The Hercynian folding, which was accompanied by mesozonal metamorphism, affected all the formations at Cabo Ortegal. The imprint of the Hercynian orogeny is of a highly variable nature, probably due to differences in the lithology of the rocks and their position in relation to the major tectonic features.

Open folds (see photograph I-16) with steeply WNW- to NW-dipping axial planes and gently NE-plunging fold axes have been found in the *Cariño*gneiss as well as in the *Banded Gneiss Formation*. The *eclogites* had to adapt to the folding pattern of the surrounding banded gneisses but were themselves too rigid to be folded anew; consequently, evidence of the Hercynian deformation is found in the eclogites only in the form of disruptions along local shear-zones. Their behaviour as competent layers or bands caused them to be broken up and boudinaged on a large scale (see Plate 1) as well as on a small one (see Plate 2). This mechanism explains the curious way in which the eclogites appear in the Banded Gneiss Formation, i.e. as trains of lenses varying in dimensions from several centimetres to several hectometres.

Evidence of isoclinal folding (photograph I-22) is scarce in the *Chimparagneiss*, but evidence of intensive tectonization accompanying the mesozonal meta-

morphic phase is ubiquitous (see photographs I-19, I-20, and I-23). Here too, the metabasite bodies reacted competently to the folding.

Construction of several sections through the Chimparagneiss Formation revealed the presence of large open folds measured in hectometres (see Plate 4 as well as Fig. I-18) and gently NNE-plunging fold axes.

In the western part of Cabo Ortegal, intensive penetrative movements occurred during the Hercynian deformation in a steeply (about 60°) SE-ESE-dipping zone: the *Carreiro zone of tectonic movement*, which in all probability represents a basal thrust plane. In this zone the paragneisses were mylonitized in their entirety (see p. 159 ff.); the overridden amphibolites (Purrido type) were partly dragged and microfolded by the thrust movement (see photographs I-33 and I-34).

The part of the *Purrido amphibolite* lying outside the thrust zone acquired a nematoblastic texture and a 40–60° SE-dipping s-plane. No evidence of folding has been found in this part of the Purrido amphibolites. The *ultrabasite body* lying between the mylonitized paragneiss and the Purrido amphibolite acquired a lenticular texture due to the thrust movement. This lenticular texture can be observed both on a large scale (see Plates 1 and 4) and on a small scale (see photograph I-32).

Unlike the eclogites, the (plagio)pyrigarnites were folded internally during the Hercynian orogeny. This folding went hand in hand with retrograde metamorphism, so that the originally non-foliated (plagio)pyrigarnites were changed into foliated and folded (garnet)amphibolites. Two styles of folding were observed: open folds with amplitudes varying from 50 to several hundred metres and much smaller isoclinal folds. The relation between these two types of folding is not quite clear, but in all probability the open folds are the latest, because refolded isoclinal



Photo IV-2 Small-scale isoclinal folds in Candelaria amphibolite; fold axes plunging weakly in an approximately northward direction. Along the footpath from Cedeira to the Capilla de San Antonio, looking N.

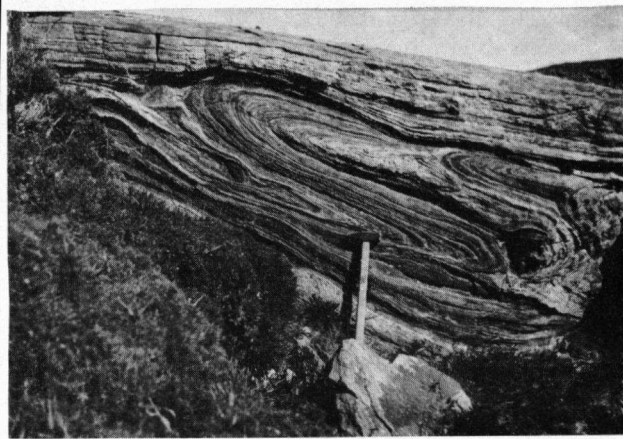


Photo IV-3 Small-scale isoclinal fold in amphibolite retrograde after pyrigarnite; fold axis plunging N 60 W/20°. On the flank of the open fold lying as a ridge between San Andres de Teixidelo, looking S.

folds occur. Both have a Hercynian age, according to the petrographical evidence. A similar sequence of isoclinal folds on which open folds are superposed has been described by Matte (1964) for Hercynically-folded rocks in eastern Galicia.

The isoclinal type of folding was found both in the Candelaria amphibolites (photograph IV-2) and in the Bacariza Formation (photograph IV-3), where many isoclinal folds are found on the flanks of a large, open style, anticlinal fold with a subvertical axial plane and a 20–60° NW-plunging fold axis. This particular anticline is topographically expressed as a SE-NW-trending ridge with dip-slopes on both flanks. It is located between San Andres and Teixidelo.

The northwesterly plunge of the fold axes (of both the open and the isoclinal folds) is only found in this part of the Bacariza Formation. The prevailing azimuth of the fold axes in the Bacariza Complex is northerly (see Plate 1).

Localization of the open folds is facilitated by the occurrence of ultrabasic erosion-remnants in the synclinal depressions of the folding-pattern at places where the boundary between the ultrabasite and the Bacariza Formation coincides with the level of erosion.

In the *ultrabasites*, evidence of small-scale folding during the Hercynian orogeny was found only occasionally (Figs. II-1 and II-2). The involvement of the ultrabasites in the folding phase that formed the open folds is evident in the Uzal serpentinite (photograph II-2).

The Hercynian isograds cannot be used to clarify the structure of Cabo Ortegal. The older mineral associations, however, are useful: the staurolite-almandine-subfacies association (of the Cariñogneiss) underlying the eclogite-facies mineral association (of the Banded Gneiss Formation) indicates that the present position of the Cariñogneiss relative to the banded gneiss is an

inversion, and that the pre-Hercynian isograds were folded during the Hercynian phase.

The following metamorphic and stratigraphical data can therefore be used to elucidate the structural pattern of the Cabo Ortegal area:

1. The normal metamorphic sequence was locally overturned, so that catazonal metamorphic rocks now overlie mesozonal metamorphic rocks that were also formed during the first — Precambrian — metamorphic phase.
2. The ultrabasites overlie the rocks of the Bacariza Formation and are themselves overlain by the Chimparragneiss Formation. This is presumed to be a normal sequence.
3. The metamorphic grade of the Precambrian metamorphism decreases upwards in the Chimparragneiss Formation, showing that the Chimparragneisses were not inverted.
4. Cariñogneiss, banded gneiss, Chimparragneiss, and the blastomylonites from the Carreiro zone of tectonic movement all form part of the same meta-sedimentary unit, occurring in different metamorphic grades and tectonic positions.

In accordance with these relations derived from petrological, geological, and chemical evidence, the structure of Cabo Ortegal may be interpreted as a domed-up culmination with overturned flanks and a sub-horizontal top (cf. "mushroom shape"; den Tex & Vogel, 1962). As yet, no evidence has been found to indicate that the overturned sequence is the consequence of nappe tectonics, as has been presupposed for similar phenomena in the Bragança-Morais region (Anthonioz, 1967a & b) and in Brittany (Cogné, 1966).

D. STRUCTURAL FEATURES OF POST-HERCYNIAN AGE (M₄)

After the Hercynian folding, tectonic activity was restricted to the movement of blocks along mainly NW-SE- or E-W-striking subvertical (rectilinear outcrops) fault-planes. In the field, only the faults causing offset or those carrying hydrothermal deposits could be mapped. On aerial photographs, such faults could be easily recognized and traced, even in localities where field evidence was lacking. Several faults for which the evidence was less clear could be drawn with some certainty after study of the aerial photographs.

It was thus ascertained that a bend in the Carreiro zone of tectonic movement at Punta Meda was caused not by folding but by repeated small displacements along a set of six possibly antithetic faults disposed *en echelon*.

Similarly, it appeared from the aerial photographs that fold axes plunging in an aberrant direction (N 60 W/20–60°) are separated by faults from blocks that azimuth readings have shown to have the same fold axes as those found over all of Cabo Ortegal (N 20–30 E/5–30°).

The post-Hercynian age of the block movements is evident from the way in which Hercynically-formed structures (e.g. the Carreiro zone of tectonic movement) were cut by and displaced along these faults (see Plate 1). This is in accordance with observations of den Tex & Floor (in press) concerning the age of the faulting in Galicia.

Brecciation and mylonitization. — Locally, the movements along the faults caused the formation of tectonic breccias, mylonites, or even ultramylonites. These deformations were contemporaneous with greenschist facies retrograde metamorphism in the immediate neighbourhood of the tectonized zone. Brecciated zones may have a width of several metres, and contain fragments measuring up to 5 cm \varnothing . The mylonitized zones are much narrower (up to 2 cm in width); in thin section they can be seen to cut through the Hercynian foliation. The diameter of the fragments can become as small as 0.01 mm in ultramylonites. The breccias are cemented either by aphanitic quartz (Chimparra-neiss, Cariñogneiss) or by carbonate (serpentinite, Candelaria amphibolite; see photograph IV-4).

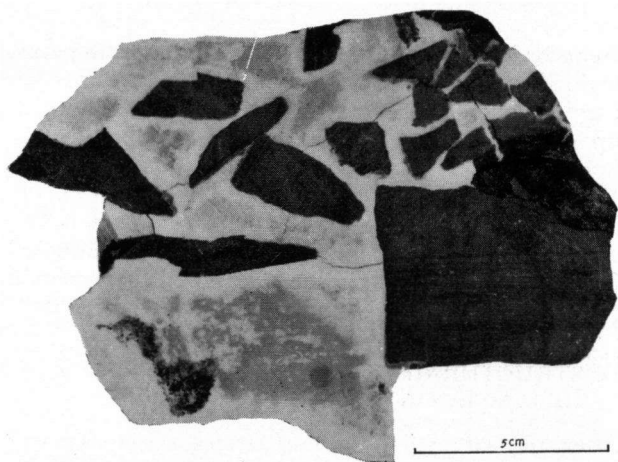


Photo IV-4 Sample V 1164. Brecciated Candelaria amphibolite in carbonate matrix. Found in the E-W-striking fault that passes along the Cedeira waterfront.

Mineralization. — In some of the faults, substantial deposits of quartz or carbonate may be present, as for instance in the WNW-ESE-striking fault bordering the southern side of the Herbeira ultrabasite. In this fault the quartz deposits sometimes reach a width of 30 to 50 m. At its western extremity, deposits of carbonate in brecciated serpentinite were found (samples

R 17, R 208, R 331, and R 332). Obviously, the nature of the deposited mineral may change along the strike of the fault.

Agate of inferior quality was found in the fault that runs from San Andres in a SSE-direction.

Deposition of hydrothermal minerals in fissures is thought to have taken place simultaneously with the mineralization in the larger faults. Except for the serpentinites in which serpentine minerals and carbonate are the dominant minerals in the veins, all rock formations at Cabo Ortegal were found to contain veinlets filled with quartz, carbonate, epidote, prehnite, adularia, and sometimes pumpellyite. Green-schist-facies retrograde metamorphic alterations — involving serpentinization of the ultrabasic rocks, saussuritization and sericitization of plagioclase, and alteration of the mafic constituents into chlorite and epidote or pistacite — were found to be unequivocally related to the mineralization of these veinlets.

Displacements along the faults. — Judging from the way in which the interformational boundaries were displaced by the movement of blocks along the fault planes, this movement must have been mainly in a vertical direction, though tilting may also have occurred in some instances.

The elevation of the bottom plane of the ultrabasites provides an indication concerning the amount of displacement in the vertical sense. For the northernmost block (Limo), the bottom plane lies at an altitude of about 200 m; in the block South of it (Herbeira) the altitude of the bottom plane is about 300 m, and the bottom plane lies at an altitude of about 500 m in the block of the Sierra de la Capelada. Provided, of course, that the bottom plane of the ultrabasite was lying subhorizontally before the faulting started, this would mean that in general the southern block was uplifted in relation to the northern one and that the amount of vertical displacement along the faults is in the order of 100–200 m. These vertical movements also provide an explanation for the differences in the apparent width of the Banded Gneiss Formation in these three blocks (0.5 km in the Limo block, 3.7 km in the Herbeira block, 4.5 km in the block of the Sierra de la Capelada).

It is uncertain whether the intrusion of post-metamorphic gabbroic rocks (see pp. 152 and 185) is connected with the formation of the post-Hercynian fault system.

CHAPTER V

MINERALOGY

Methods used. — The preparation of mineral samples for chemical analysis was carried out with a Frantz isodynamic separator. Purification of the resulting mineral fractions to obtain a sample with less than 1 %

impurities was attained by repeated gravitative separation in methylene iodide and Clerici solution. The indices of refraction (n_D) were measured in Na light with the Cargille set of index liquids in combination

with a Leitz Jelly refractometer. Values for 2V and c/z were determined with a universal stage. Birefringence (Δ) was measured with a Berek compensator where possible, and estimated in other cases.

For garnet, the unit cell-size (a_0) was determined from X-ray powder photographs (Fe K α radiation; Bradley camera \varnothing 9 cm) by measuring the distances between the 4 10 0, 2 4 10, and 8 8 0 K $_1$ reflections. The density of the minerals was determined at 24° C with a pycnometer.

A. GARNET

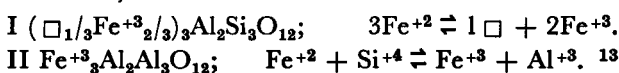
1. Calculation of garnet analyses

The garnet analyses were calculated according to the general formula $X_3Y_2Z_3O_{12}$, allotting Si $^{+4}$ and Al $^{+3}$ cations to the Z-group, Al $^{+3}$ and Fe $^{+3}$ cations to the Y-group, and Ca $^{+2}$, Mg $^{+2}$, Mn $^{+2}$, Fe $^{+2}$, and sometimes Fe $^{+3}$ cations to the X-group. If the number of cations to 12 O is less than 8, it is sometimes necessary to assume the existence of vacant sites in the lattice (represented by the symbol \square).

For the formation of the end-member molecules, the following rules were applied:

1. The cationic ratio X : Y : Z must be exactly 3 : 2 : 3.
2. The end-member molecules formed have to be electrostatically balanced.

This necessitates the formation of two hypothetical molecules, i.e.:



in which the disturbance of the charge balance brought about by the replacement of Fe $^{+2}$ by Fe $^{+3}$ is compensated for by the use of vacant lattice positions or by substitution of Al $^{+3}$ for Si $^{+4}$. These hypothetical end-members are thought to represent substitutions in the almandine molecule.

Other molecules formed are:

Pyrope	Mg $_3$ Al $_2$ Si $_3$ O $_{12}$
Almandine	Fe $_3$ Al $_2$ Si $_3$ O $_{12}$
Spessartine	Mn $_3$ Al $_2$ Si $_3$ O $_{12}$
Grossular	Ca $_3$ Al $_2$ Si $_3$ O $_{12}$
Andradite	Ca $_3$ Fe $_2$ Si $_3$ O $_{12}$

The formation of titanium garnet is omitted because earlier investigations (Vogel & Bahezre, 1965) have shown that in the eclogites and plagiopyrigarnites of Cabo Ortegal, Ti $^{+4}$ does not play the role of a garnet-forming cation (see also Eskola, 1921; Bloxam & Allen, 1958—1959; Rost & Grigel, 1964).

Since sufficient Ca was always present in the X-group to form andradite with the available Fe $^{+3}$ in the Y-group, there was no need to calculate end-members such as khoharite, skiagite, or calderite (Tröger, 1959).

¹³ Compare Y $^{+3}$ Al $_3$ Al $_3$ O $_{18}$ (Jaffe, 1951).

Certain factors contributed to inaccuracies in the chemical analysis of the garnet concentrates. These were:

1. The determination of the FeO : Fe $_2$ O $_3$ ratio (Lange, 1964; Tröger, 1959).
2. The occurrence of small inclusions (predominantly quartz and rutile) that could not be removed by physical separation.
3. Impurities in the concentrate. A very fine grain-size of garnet is required to render it more soluble in acid. The agate ball mill used for this purpose contaminated the garnet concentrate with SiO $_2$.
4. Difficulties with the preparation of garnet grains. Several of the Cabo Ortegal garnets were not completely dissolved after 12 to 48 hours in a mixture of H $_2$ SO $_4$ and HF. Consequently, small quantities of impurities which dissolved more readily than the garnet had a greater influence on the analysis than was to be expected.

The analyzed powders were examined microscopically for impurities. When quartz was relatively abundant, the determined SiO $_2$ percentage was disregarded and the garnet composition was calculated on the basis of a partial analysis. Usually, the Fe $_2$ O $_3$: FeO ratio had to be changed (keeping the total of Fe atoms constant) to suit a better distribution of cations over the X, Y, and Z groups.

2. Chemical and physical data

Table V-1 shows the results of six chemical analyses of garnets from rocks found in the Concepenido Complex and five chemical analyses of garnets from rocks found in the Capelada Complex. Other analyzed garnets have been discussed in earlier publications (Vogel & Bahezre, 1965; Engels & Vogel, 1966; Vogel & Warnaars, 1967); the chemical and physical properties of the latter are given in Table V-2.

Compositional variations of garnets within the sample. —

From one hornblende eclogite sample (V 1278), two garnet fractions with different magnetic properties were separated and analyzed (Table V-1, nrs. 9 and 10). In view of the existence of similar differences between clinopyroxene fractions from this sample (see Ch. V, B 3), the compositional differences found between these two fractions are attributed not to incipient amphibolization but to a natural compositional spread inherent in all Cabo Ortegal eclogites.

To test the presence of zonally-arranged compositional variations in the eclogite garnets, a garnet from an α -zoisite eclogite (sample V 1007b) was investigated by means of an electron microprobe (see Vogel & Bahezre, 1965). This garnet has a core and outer rim free of inclusions and separated from each other by a zone rich in inclusions of microcrystalline rutile. Nevertheless, no differences in chemical composition could be established for these three zones.

In another case, however, compositional zoning could be established for garnets from amphibolized pyri-

garnite (sample V 1250, see Vogel & Bahezre, 1965). In this sample, coarse-grained garnets with light-pink cores and dark orange-pink (0.2 mm wide) outer rims are surrounded by a kelyphitic rim of fine-grained hornblende, magnetite, and plagioclase. The differences in chemical composition (the rim being richer in grossular and poorer in almandine than the core) are thought to have been caused by the formation of the kelyphite rim.

Compositional differences between separate garnet crystals that could not be ascribed to a natural spread were observed in a partially amphibolized α -zoisite eclogite (see Vogel & Bahezre, 1965). Microscopically, it could be established that a virtually colourless inclusion-riddled garnet and a light-pink inclusion-free garnet occurred as separate phases in the same sample. In all probability the inclusion-free garnet (which is poorer in pyrope and Ca-garnet and richer in almandine than the inclusion-rich one) was formed during one of the phases of retrograde metamorphism. The occurrence of two differently-composed garnet phases within one sample is not confined to the eclogites. Some of the diffractograms made from concentrates of banded gneiss garnets showed broad lines or even doublets for 4 10 0, 2 4 10, and 8 8 0 $K\alpha_1$ reflections (see Fig. V 5). The possibility that this line-broadening could have been caused by the occurrence of zoned garnets was ruled out by redetermination of a_0 and n_D for a single garnet crystal from one of the samples concerned; in this case the reflections were found to be sharp. As for the above-mentioned sample, the existence of two separate garnet phases in one sample is attributed to incomplete breakdown of garnet that became unstable.

Compositional differences between garnets from rocks belonging to the high-pressure metamorphic lineage and those from rocks of the low and intermediate pressure metamorphic lineages. — The frequently observed association of rocks of the clinopyroxene-almandine subfacies of the granulite facies with eclogites (see p. 206) suggests that this subfacies must be considered part of a high-pressure metamorphic lineage, as contrasted with the charnockitic suite, which must belong to the low and intermediate pressure lineages (cf. den Tex, 1965). It is not unreasonable to expect the differences in metamorphic conditions between these lineages to be reflected in the composition of their garnets. To verify this, the composition of 17 garnets from rocks belonging to the charnockitic suite (Compton, 1960; Hietanen, 1943; Howie, 1955; Howie & Subramaniam, 1957; Scharbert, 1964; Subramaniam, 1962), four garnets from plagiopyrigarnitic rocks (Groves, 1935; v. Knorring & Kennedy, 1958; O'Hara, 1960; v. Philipsborn, 1930), and 14 garnets from eclogitic rocks (Lee *et al.*, 1963) were plotted together with the Cabo Ortegal garnets in an $al+sp - py - gr+an$ triangle (Fig. V-2). In this diagram they can be seen to occupy different compositional ranges, since the garnets from the low- to intermediate-pressure lineage

generally have more and those from the high-pressure lineage less than about 60% of the almandine + spessartine molecules. Although Tröger's (1959) empirically-determined compositional fields for garnets from amphibolite + glaucophane schist, granulite + charnockite, metabasite, and eclogite are indicated by dotted lines in Fig. V-2, their value appears to be limited since, for instance, only four out of 20 eclogite garnets actually plotted within Tröger's field for eclogite garnets. This wide compositional range of eclogite garnets motivated Coleman *et al.* (1965) to make a threefold subdivision in the eclogite group. In this subdivision, the Cabo Ortegal eclogites seem to fit nicely into group B, on the basis of their field relations as well as of the composition of their garnets (see Fig. V-1).

Compositional differences between garnets from eclogite and (plagio)pyrigarnite. — In Fig. V-1 it appears that garnets from Cabo Ortegal eclogites and hornblende eclogites (py 29–47%, $al + sp$ 31–46%, Ca-garnet 20–28%) occupy a rather limited field of the $al+sp - py - gr+an$ compositional triangle. Pyrigarnitic garnets were found to occupy a neighbouring field as a result of their less pyrope-rich nature (py 22–29%, $al + sp$ 45–53%, Ca-garnet 22–29%). Falling somewhat out of this range, but still close to it, are the plotted compositions of garnets from rocks supposed to be transitional types between eclogite and pyrigarnite (see p. 130). They are richer in almandine and poorer in Ca-garnet than the ordinary pyrigarnite garnets (Fig. V-1, 1250c and M 459).

The leptinite garnets (Fig. V-1, 1193 and 1243a) are still poorer in pyrope than the pyrigarnite garnets; they plot together with the second-generation garnet from sample V 1223 within Tröger's (1959) compositional field for garnets from amphibolites. This is in accordance with the statement (pp. 183 and 191) that they were formed during the Hercynian (amphibolite-facies) retrograde metamorphic phase.

As for the garnets from incompletely metamorphosed gabbros, their metamorphic affiliation appears clearly from their position in the $al+sp - py - gr+an$ compositional triangle (Fig. V-1). The garnet from metagabbro associated with carinthine eclogite (sample V 1023a, see p. 151) plots well within the eclogite field, while the garnet from a metagabbro found in the Capelada Complex (sample E 327b, see p. 186) plots within the compositional range of the (plagio)pyrigarnite garnets.

Change of a_0 and n_D with metamorphic grade. — Although the eclogite garnets tend to become less rich in pyrope with the advancement of retrograde metamorphism (Fig. V-1), it appeared impossible to fit them into the different zones for garnets associated with brown, brownish-green, and blue-green hornblende as given by Portugal V. Ferreira (1966). Nevertheless, the same trend that appears from his diagrams, i.e. an increase

of a_0 and n_D with diminishing metamorphic grade, can also be observed for the Cabo Ortegal garnets. Partial overlap of the fields covered by garnets from eclogite + retrograde eclogite, from (plagio)pyrigarnite, and from banded gneiss (cf. Figs. V-3, V-4, and V-5) tends to impair the diagnostic value of a_0 and n_D for the distinction between eclogite and (plagio)pyrigarnite garnets and makes them all but meaningless for the distinction between retrograde eclogite and retrograde pyrigarnite. Nevertheless, Behr *et al.* (1965) have demonstrated that a_0 - n_D values from high-pressure granulite facies rocks differ notably from those of low- and intermediate-pressure granulite facies rocks.

B. CLINOPYROXENE

1. Nomenclature

The clinopyroxene found in eclogites was first described by Haüy (1801) under the name of diallage, and was later termed omphacite by Werner (1812). Since that time, any clinopyroxene found in an "eclogite" — whether it concerned a true eclogite or not — has more or less automatically been labelled omphacite (cf. "closed circuit definition"; Appelman, 1966). The consequence of this procedure was that "omphacite" compositions ranged from practically pure diopside-hedenbergite to compositions of diopside-hedenbergite 20%, jadeite 80%. Until Tröger (1962) proposed a nomenclature for the clinopyroxenes on the basis of their composition with respect to end-member molecules, omphacite was, for lack of a rigid precept to be applied in the diopside-hedenbergite-jadeite-acmite compositional range, somewhat vaguely referred to as a green variety of fassaite found in eclogite (Machatski, 1953), or alternatively as a green variety of diopside found in eclogites (Winchell, 1956). As far as the nomenclature of clinopyroxenes from rocks found at Cabo Ortegal is concerned, Tröger's (1962) proposals will be followed (see Fig. V-6).

2. Calculation of clinopyroxene analyses

If the clinopyroxene formula is written as $W(X,Y)Z_2O_6$, the representation of the composition of the clinopyroxene in terms of end-member molecules along the lines proposed by Hess (1949) gives, as Bown (1964) has pointed out, no certainty about the distribution of Al over Y and Z sites. Furthermore, if the number of cations per 6 oxygens differs from 4, a surplus of cations (the nature of which depends on the last calculated end-member) remains after the last end-member has been formed. White's proposal (1964) of a preferred sequence of calculation for the different end-members only shifts the problem. Analytical errors and the possible existence of unoccupied sites in the clinopyroxene lattice are suggested by Bown (1964) as the causes of the deviation from the theoretical 4 : 6 ratio for cations to oxygen ions. Because the determination of the $FeO : Fe_2O_3$ ratio is not very reliable (Tröger, 1962), an attempt was made to determine how a change in the $FeO : Fe_2O_3$

ratio (for a constant number of Fe-atoms) would affect the cation : oxygen ratio. An increase of the Fe_2O_3 content leads to a smaller number of cations per 6 oxygens; an increase of the FeO content has the opposite effect.

A suitable division of cations over W, X, Y, and Z groups can be obtained in the following way:

1. By changing the $FeO : Fe_2O_3$ ratio (if necessary) and by assuming as many vacant positions as are required to obtain exactly 4 cations for every 6 oxygens.
2. By choosing the $FeO : Fe_2O_3$ ratio such that electrostatically balanced end-members can be formed by using all the cations. This condition is fulfilled by only a limited number of $FeO : Fe_2O_3$ ratios. From these $FeO : Fe_2O_3$ ratios, the one giving the best approximation of the actually determined values for FeO and Fe_2O_3 is chosen.

If the number of cations exactly equals 4, the partition of the Al ions no longer presents a problem, because Z is made equal to 2 by adding the required amount of Al (or Fe^{+3} if an insufficient amount of Al is present) and allotting the rest of the Al (Fe^{+3}) ions to Y.

The cations can be divided over the W, X, Y, and Z positions as follows:

W: Na^{+1} , Ca^{+2} , Fe^{+2} , (Mg^{+2}) , \square .

X: Fe^{+2} , Mg^{+2} , Mn^{+2} , Ca^{+2} , Ni^{+2} .

Y: Al^{+3} , Cr^{+3} , Fe^{+3} , Ti^{+4} .

Z: Al^{+3} , (Fe^{+3}) , Si^{+4} .

To obtain local charge balance (over-all charge balance being maintained as a result of the method of calculation; Bown, 1964) the principle of coupled substitution is used for the formation of the following end-member molecules:

1. $CaMgSi_2O_6$ diopside (Di)
2. $CaAlAlSiO_6$ Tschermak's molecule (Ts')
3. $\square TiSi_2O_6$ $Ca^{+2} + Mg^{+2} \rightleftharpoons \square + Ti^{+4}$ (I)
4. $CaTiAl_2O_6$ $Mg^{+2} + 2Si^{+4} \rightleftharpoons Ti^{+4} + 2Al^{+3}$ (II)
5. $CaFe^{+2}Si_2O_6$ hedenbergite (He)
6. $CaFe^{+3}AlSiO_6$ $Fe^{+2} + Si^{+4} \rightleftharpoons Fe^{+3} + Al^{+3}$ (III)
7. $\square_{0.5}Ca_{0.5}AlSi_2O_6$
 $0.5Ca^{+2} + Mg^{+2} \rightleftharpoons 0.5\square + Al^{+3}$ (IV)
8. $Fe^{+2}Fe^{+2}Si_2O_6$ clinoferrosilite (CFs)
9. $MgMgSi_2O_6$ clinoenstatite (CE)
10. $CaCaSi_2O_6$ wollastonite (Wo)
11. $NaAlSi_2O_6$ jadeite (Ja)
12. $NaFe^{+3}Si_2O_6$ acmite (Ac)

The end-members represented by the symbols Ts', I, II, III, and IV are hypothetical and are considered to represent substitutions in the diopside and hedenbergite molecules, because according to Zvetkov (1954), $CaAl_2SiO_6$ can replace $CaMgSi_2O_6$ up to 40 mol. per cent. Fe_2O_3 and TiO_2 can appear in solid solution up to 10 and 6 per cent, respectively, in the diopside molecule (Segnit, 1953).

Clinoferrosilite was calculated in preference to clinostatite, because structural analysis has shown that Ca^{+2} and Mg^{+2} show a preference for W and X positions, respectively, but that Fe^{+2} appears in both (Morimoto *et al.*, 1960). Only when Fe^{+2} is present in insufficient amounts is clinostatite formed.

A certain ambiguity still remains, for if the clinopyroxene formula is to be presented in the form of end-member molecules, a choice must be made between Ts' and III, and in end-member IV the place of Al could equally well be taken by Fe^{+3} . Furthermore, the question arises of the substitution by which the compensation for the surplus charges of Ti^{+4} should preferably be expressed (I or II). Although it concerns only minor amounts of Ti or a minor number of vacant sites, a preference for one substitution over the other will in the end influence the calculated jadeite : acmite ratio. If, for graphical reasons, the clinopyroxene composition has to be expressed in terms of end-member molecules, a choice between these possibilities is unavoidable.

Therefore, end-member I is only formed if insufficient Al^{IV} is present to compensate for all the Ti. End-member III is only formed if insufficient Al^{VI} is present to form Tschermak's molecule with the available Al^{IV} . Provided enough Al^{IV} is present, the Y site in end-member IV is considered to be occupied by Al and not by Fe^{+3} . Preference of the aluminous end-members (Ts' and IV) over the ferriferous ones (III and the ferriferous form of IV) is in accordance with the observation of Kushiro (1962) that " $\text{NaAlSi}_2\text{O}_6$ is incompatible with Fe^{+3} containing components excepting $\text{NaFeSi}_2\text{O}_6$ ".

The amounts of CFs, CE, and Wo are dictated by the number of Fe^{+3} or Mg ions at the W sites and by the number of Ca ions at the X sites.

Owing to the size of sample V 1023, the clinopyroxene concentrate extracted from it was too small to permit a complete analysis to be made, so only a partial analysis was done for this sample. Since the weight percentage of Al_2O_3 was unknown, the analysis had to be calculated by trial and error, dividing SiO_2 and Al_2O_3 in different proportions over the remaining 63.39 per cent until a satisfactory division of cations over the W, X, Y, and Z groups was arrived at.

3. Chemical and physical data of clinopyroxenes (see also Tables V-4 and V-5)

The intimate intergrowth of clinopyroxene with hornblende in rocks affected by retrograde metamorphism and the occurrence of inclusions in clinopyroxene crystals, were restrictive with respect to the suitability of the clinopyroxenes concerned for chemical analysis. Because of a lack of suitable material, only one analysis of a clinopyroxene from a plagiopyrigarnite is available (from sample V 1234). For the eclogites, these restrictions applied to a much smaller degree, although the number of rocks from which clinopyroxene-garnet pairs could be analyzed was again found to be small. For this reason, it is obviously necessary

that the analyses presented in this paper be supplemented with analyses performed by electron microprobe.

Compositional variations of clinopyroxenes within one sample.

— Two clinopyroxene fractions of different magnetic susceptibility were separated from a hornblende eclogite (sample V 1278) together with a p.p. symplectite fraction. They were found to show small differences in chemical composition (see Tables V-4 and V-5). Since there is no reason — on the basis of the microscopical observations — to suppose that the clinopyroxenes have a zoned structure, it must be assumed that these differences in chemical composition represent a natural compositional spread. Similar chemical differences have been demonstrated in the Silberbach eclogite (v. Wolff, 1942).

Composition of plagiopyrigarnitic and eclogitic clinopyroxenes from Cabo Ortegal.

— Seven clinopyroxene analyses from Cabo Ortegal eclogites and plagiopyrigarnites (see Tables V-4 and V-5 and Fig. V-6) are available. Of the eclogitic pyroxenes, two could be identified as omphacite and three as omphacitic chloromelanite, according to Tröger's (1962) nomenclature. The clinopyroxene from the eclogite thought to be transitional between eclogite and pyrigarnite, plots like the clinopyroxene from the plagiopyrigarnite in a field of Tröger's diagram that has as yet not received a name. They are here provisionally termed aegirine augitic chloromelanite and diopside-rich aegirine augite, respectively.

The unequivocal eclogite clinopyroxenes are characterized by a composition with a Di (+ He + Ts') content of 70% ($\pm 5\%$) and a preponderance of jadeite over acmite. Compared with eclogite clinopyroxenes from other areas (Coleman *et al.*, 1965), they lie at the same Di (+ He + Ts') level as the eclogite clinopyroxenes from the eastern Sudetes (Smulikowski, 1960) and have a roughly 15% higher Di (+ He + Ts') content than the clinopyroxenes found in eclogites associated with glaucophane schists. In the plagiopyrigarnite pyroxene (1234) and the pyroxene from the transitional type of eclogite (m 459), acmite dominates over jadeite, although the two pyroxenes have a markedly different Di (+ He + Ts') content. However, more chemical data are needed to delineate a compositional field for pyrigarnitic clinopyroxenes.

A way to distinguish between eclogite- and pyrigarnite-clinopyroxenes may have been provided by Clark & Papike (1966a), who found that omphacite crystallized in the monoclinic space group P2. Structural investigations carried out by Dr. P. Hartman and Mr. C. F. Woensdregt on Cabo Ortegal clinopyroxenes revealed that the omphacite from eclogite (sample V 1050) possessed a P2/m symmetry, whereas clinopyroxenes from plagiopyrigarnites (samples V 1234 and V 1243) had a C2/c symmetry. Investigation of the clinopyroxene from sample M 459 is still in progress.

Clinopyroxene compositions as related to facies. — From investigations made by Kushiro (1964—1965), there appears to be a correlation between the composition of omphacite (jadeite content) and the PT conditions under which it was formed. According to his curves, the eclogite pyroxenes from Cabo Ortegal (with a Na-clinopyroxene content of roughly 30%) could have formed at pressures between 18 and 20 kb and at temperatures between 700° and 1300° C. Previously inferred data about PT conditions (600—900° C, 14—19 kb), though seemingly not in contradiction with these values, were found to be more consistent with a jadeite content of 45% in omphacite (cf. Fig. I-17). Nevertheless, the chemical composition of the clinopyroxenes may prove to be of vital importance for a subdivision of the eclogite facies at a future date when more experimental data concerning omphacitic clinopyroxenes are available.

4. The isochemical nature of symplectitization

The p.p. symplectite analysis (Table V-4, analysis 5) is calculated according to the principles mentioned in Chapter V, B 2. With no change of the FeO : Fe₂O₃ ratio required, its composition proved identical to that of a clinopyroxene of the following composition:

(□_{0.03} Na_{0.32} Ca_{0.61} Mg_{0.01} Fe⁺²_{0.03}) (Mg_{0.63} Fe⁺²_{0.03} Ti_{0.01} Fe⁺³_{0.09} Al_{0.34}) (Al_{0.07} Si_{1.93}) O_{6.00}; or, written as end-member molecules: Di 52, II 1, IV 6, Ts' 5, CFs 3, CE 1, Ja 23, Ac 9. This result supports Eskola's (1921) opinion that symplectitization is an isochemical process.

If the clinopyroxene formula is written as W₄(XY)₄ Si₈O₂₄, the albite formula as Na₃Al₃Si₉O₂₄, and the anorthite formula as Ca₃Al₆Si₆O₂₄, both albite and anorthite prove to be one W-group cation short of the ideal clinopyroxene formula. Also, the number of Si ions in clinopyroxene is lower than that in albite and higher than that in anorthite. The calculated plagioclase composition in which for every 24 O ions, 8 Si ions are present, is Ab₂An₁, a figure closely corresponding to the anorthite percentage of 30 observed by Eskola (1921) and Forster (1947) for plagioclase occurring in p.p. symplectite.

To form a plagioclase of this composition (Na₂CaAl₄Si₈O₂₄) from omphacite, the following reaction is thought to have taken place:

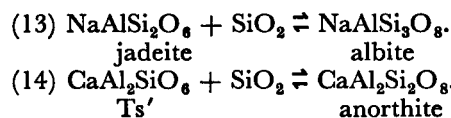


From this reaction equation it would appear that the extent of the symplectitic unmixing of plagioclase from omphacitic clinopyroxene is limited by the number of vacant sites in the clinopyroxene lattice as well as by the amount of jadeite present. The maximum volumetric ratio of plagioclase : clinopyroxene for the analysed omphacite — if all the available □ CaAl₂Si₄O₁₂ is used to form plagioclase — is about

1 : 7.5, which is lower than the ratio of 1 : 5 observed by Lange (1965) and lower than the ratio of 1 : 5.5 calculated by Forster (1947). By lowering the FeO : Fe₂O₃ ratio and thereby increasing the number of vacant sites in the lattice, the plagioclase : pyroxene ratio could be increased to about 1 : 4. A more probable explanation of the discrepancies in the plagioclase : pyroxene ratios is that they are caused by chemical dissimilarity of the investigated omphacites.

The composition of the clinopyroxene in the p.p. symplectite (Di-He 70, Ja 20, Ac 10) does not differ greatly from that of the omphacite from which it was formed (Di-He 68, Ja 23, Ac 9).

If the system becomes chemically open, the breakdown of the clinopyroxene may continue, e.g. by the following reactions:

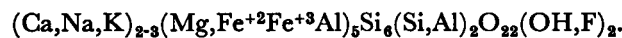


C. HORNBLLENDE

1. Nomenclature

The terms carinthine and smaragdite for amphiboles from eclogitic rocks have often been applied in the wrong sense, and it therefore seems useful to give a short elucidation of their meaning.

Chemically, all the carinthines so far described conform to the general formula for common hornblende given by Deer *et al.* (1963):



Hintze's (1897) definition of carinthine as a dark hornblende from eclogite probably led Weinschenk (1915) to determine a dark blue-green amphibole occurring in eclogite as carinthine. Murgoci (1924) and Angel (1929) considered this amphibole to be a barroisite, a name that has since been abandoned. From Weinschenk's description, this blue-green "carinthine" is probably a common blue-green secondary hornblende. Angel (1929) defined carinthine as a brown pleochroic hornblende occurring in stable association with garnet and omphacite in eclogites. Heritsch & Kahler (1960) found that carinthine is richer in magnesium and poorer in iron as compared to common green hornblende. Machatski & Walitzi (1962) compared five hornblende analyses from amphibolite, eclogite amphibolite, and eclogite, and did not find significant differences in chemical composition between blue-green and brownish-green pleochroic hornblende, but from their description it appears probable that the analyzed specimens were all of a secondary nature and therefore could not be true carinthines. In these hornblendes, the ratio of Mg : Σ(X+Y)¹⁴ varies

¹⁴ Mg being the total number of Mg cations in the X group taking part in the formation of tremolite, Σ(X+Y) the total of cations present in the X and Y groups, and (Fe⁺² + Fe⁺³) the total number of Fe cations present (see also Table V-6).

from 0.502 to 0.562 and the $(\text{Fe}^{+2} + \text{Fe}^{+3}) : \Sigma(\text{X} + \text{Y})$ ratio varies from 0.264 to 0.294.

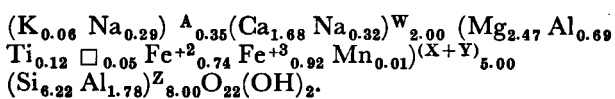
For true carinthines in the sense of Angel (1929), these values are $\text{Mg} : \Sigma(\text{X} + \text{Y}) = 0.634\text{--}0.608$ (see Table V-6) and $(\text{Fe}^{+2} + \text{Fe}^{+3}) : \Sigma(\text{X} + \text{Y}) = 0.120\text{--}0.158$. So that perhaps in addition to Angels definition, carinthine can be defined chemically as a member of the common hornblende group with an $\text{Mg} : \Sigma(\text{X} + \text{Y})$ ratio of more than 0.6 and a $(\text{Fe}^{+2} + \text{Fe}^{+3}) : \Sigma(\text{X} + \text{Y})$ ratio of less than 0.2.

In this paper the term smaragdite has not been used for the common blue-green hornblende formed after and intergrown with omphacite, although the definitions of smaragdite given by Hintze (1897) and Dana (1932) certainly warrant such a denomination. It seems better to reserve the name smaragdite for a chromiferous member of the actinolite series, as Weinschenk (1915) and Tröger (1956) have suggested.

2. Chemistry of the analyzed amphiboles

Since amphibole figures in pyrigarnites and eclogites largely as a mineral secondary after garnet and clinopyroxene, only two analyses of amphibole were made, one of a secondary blue-green hornblende present in a garnet-hornblende rock from the Bacariza Formation (sample V 1267), the other of an amphibole from a carinthine eclogite (sample V 1023). Their composition as to end-member molecules has been calculated according to the method proposed by Shidô (1957—1959) with application of the rules suggested by Phillips (1963). The cation ratios of these amphiboles were calculated on a water-free basis of 23 O, since the H_2O percentages were much too low to be included in the basis (Table V-6).

The formula of amphibole V 1267 can be written as:

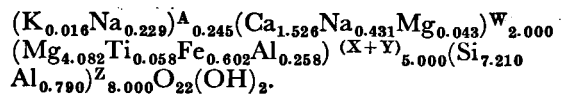


This agrees well with the formula of a common hornblende. Due to its rather high aluminum content, this hornblende plots in the ACF diagram at a point with the coordinates A 20.7, C 30.8, F 48.5 (see Fig. III-5).

The hornblende fraction from sample V 1023 was too small, due to the size of the sample, to permit a complete analysis to be made, so the weight percentages of SiO_2 , Al_2O_3 , $\text{FeO} + \text{Fe}_2\text{O}_3$, MgO , and CaO were determined with an electron microprobe by Mr. F. W. Warnaars (University of Utrecht). The percentages of MnO , Na_2O , K_2O , TiO_2 , P_2O_5 , and H_2O were

determined by Dr. C. de Sitter-Koomans and Mrs. H. M. I. Bult-Bik by means of a wet analysis.

The chemical formula of the carinthine can be written as:



The hornblende occurs in an eclogite, stably associated with garnet and omphacite (cf. Chs. V A and V B) and has a brown colour, although it is practically colourless and non-pleochroic in thin section. Its $\text{Mg} : \Sigma(\text{X} + \text{Y})$ ratio of 0.816 and its $(\text{FeO} + \text{Fe}_2\text{O}_3) : \Sigma(\text{X} + \text{Y})$ ratio of 0.120 seem to warrant the use of the name carinthine. As compared with hornblende V 1267, it plots more towards the F corner of the ACF diagram.

D. PLAGIOCLASE

The measured anorthite percentages for plagioclases found in the rocks of the different formations at Cabo Ortegal have been plotted by groups in frequency histograms (Fig. V-7).

E. ZIRCON

Zircons were separated from five different rock-types to obtain a rough impression of their nature. The concentrates were of a poor quality due to the admixture of a large amount of rutile.

From the Capelada Complex three samples were investigated:

Sample V 174b; metagabbro with *flaser* texture; no zircon found in thin section, no zircon found in the separated fraction.

Sample V 1179d; phyllonitic garnet-biotite gneiss; the majority of the zircons are subrounded; some well-rounded grains also occur.

Sample V 1234; plagiopyrigarnite; a few zircons, all subrounded.

From the Concepenido Complex two samples were investigated:

Sample V 1278; α -zoisite-hornblende eclogite; although zircon was found in thin section, none was found in the concentrate.

Sample V 1394f; muscovite-garnet gneiss; comparatively many zircons present in the concentrate, the majority of them being well-rounded although some subrounded grains are also present.

Zircon concentrates from sample V 1193, a leptynite from the Capelada Complex (see p. 183), have been studied in detail by Hoppe (1966).

CHAPTER VI

GEOLOGICAL HISTORY OF CABO ORTEGAL

This chapter gives a chronological reconstruction of the geological events at Cabo Ortegá without reference to the factual data presented in the preceding chapters. A synoptic table (Plate 3) gives the same information in a more condensed form.

A. PRE-METAMORPHIC EVENTS

The deposition, in a probably geosynclinal environment, of a layered sequence of graywackes of varying composition and having minor calcareous intercalations, is the earliest detectable geological event in the Cabo Ortegá area. During the subsidence of this eugeosynclinal basin, tholeiitic magma intruded continuously and crystallized as gabbros in various sills and possibly also in one large stock. While subsidence continued the ultrabasites were emplaced, either in the solid state or as a "crystal mush".

B. PRECAMBRIAN OROGENY: MAIN PHASE (M_1)

During the ensuing orogenesis, which was probably Precambrian, the rocks may have been forced still further downward by tectonic action while also undergoing metamorphism. The picture of the Precambrian metamorphism emerging from the various relics left unaffected by the retrograde metamorphism, is a coherent one even though its interpretation gives rise to several difficulties.

1. *Rocks of gabbroic composition*

The most direct data concerning metamorphic facies and PT conditions during this orogeny were derived from the metamorphic assemblages formed in the gabbroic rocks.

Eclogites. — The eclogites were found only as intercalations in the Banded Gneiss Formation, which is bordered on the East by paragneisses of staurolite-almandine subfacies grade and on the West by metabasites of high-pressure granulite facies grade. The metagabbroic nature of the eclogites has been inferred from their chemical composition; this assumption is confirmed by the occurrence, in one instance, of incompletely eclogitized gabbro in close association with carinthine eclogite (p. 151). Other gabbroic "relics" are the curiously patterned rutile aggregates occurring enclosed in garnet. These aggregates are thought to represent surplus Ti from gabbroic minerals (Ti-augite?) that could not be accommodated in the eclogite garnets (p. 195). The mineralogical composition of the eclogites is characterized by the stable association of pyralmandine garnet and clinopyroxene, without plagioclase but with the following possible additional minerals: kyanite, kyanite + α -zoisite,

α -zoisite, and carinthine. Quartz and rutile occur frequently as minor constituents.

The absence of plagioclase as a stable phase in eclogite-facies assemblages, the relation between the clinopyroxene composition and PT conditions (see also Kushiro, 1964—1965), and the limited capacity of the eclogite garnet to accommodate grossular + andradite, provide an explanation of the relation between the chemical composition of the Cabo Ortegá eclogites and the nature of the minerals formed in them in addition to garnet and clinopyroxene (p. 140 ff.).

From the fact that α -zoisite and kyanite can occur together in stable association, the temperature of formation of the Cabo Ortegá eclogites could be inferred (Pistorius *et al.*, 1962) to have lain within the range of 600—900° C at a pressure of between 14 and 19 kb. These figures closely correspond to those given by den Tex (1965) and Fritsch (1966) for eclogite-facies metamorphism: they indicate a geothermal gradient of about 12—14° C/km.

Dimensional orientation of eclogite minerals (omphacite, kyanite, α -zoisite) and field evidence of folding of the eclogites (p. 191) indicate that the eclogite was subjected to tectonic as well as to lithostatic pressure. Consequently, the geothermal gradient may well have been somewhat higher than the 12—14° C/km just mentioned.

Capelada Complex. — To the East, the eclogite/banded gneiss sequence borders on a complex of mainly metabasitic rocks (Capelada Complex) which seems to represent a larger gabbroic stock. It was impossible to determine whether a stock or only a sill of much larger magnitude than the eclogitized sills is concerned, because no exposure of the rocks underlying the Capelada Complex was found. The gabbroic rocks of this stock were altered by the Precambrian metamorphism into pyrigarnites and plagiopyrigarnites, i.e. rocks characterized by the stable association of pyralmandine garnet and clinopyroxene with plagioclase. β -zoisite may occur in addition to these three minerals, and in most cases small amounts of rutile and quartz are also found. On the basis of these associations, the (plagio)pyrigarnites are thought to have formed under clinopyroxene-almandine-subfacies metamorphic conditions.

The supposition that the (plagio)pyrigarnites are of magmatic descent is confirmed by their chemical composition (p. 189) and by the infrequent occurrence of gabbroic palimpsest textures (Engels, oral comm.).

No data are available that permit any definite conclusion about PT conditions during the formation of these rocks. The pyralmandine garnet-clinopyroxene association indicates a close relationship to the eclogites. The lower pyrope content of the pyrigarnite garnets as compared to eclogite garnets seems to indicate that the pyrigarnites were formed at a lower pressure. However, the field evidence indicates that the eclogite/banded gneiss sequence overlies the rocks of the Capelada Complex, which would mean that the (plagio)pyrigarnites were formed at both a higher temperature and a higher lithostatic pressure than the eclogites.

The narrow zones of graywacke situated principally on the eastern side of the complex, must have behaved similarly to those in the Banded Gneiss and Chimparragneiss Formations during the main phase of the Precambrian orogeny (see Ch. VI, B 2).

2. *Paragneisses*

The effect of the Precambrian metamorphism on the deepest part of the graywacke deposits was, due to their chemical composition, of a quite different nature. Notwithstanding their low potassium content, they became partially anatexitic because plagioclase and quartz entered into a eutectic melt. Kyanite and garnet (\pm biotite?) were formed as typomorphic minerals in the restite. This garnet-(biotite)-kyanite association was formed in all catazonally metamorphosed rocks, regardless of their grade of metamorphism. Metamorphic conditions for the various gneiss formations could only be established on the basis of the mineral associations in their metabasite inclusions. They were found to be of eclogite-facies grade in the Banded Gneiss Formation and of clinopyroxene-almandine-subfacies grade in the Chimparragneiss Formation and in the blastomylonites from the Carreiro zone of tectonic movement.

Even if the absence of potash feldspar is taken into consideration, partial melting of the graywackes can be reconciled with the PT conditions inferred on other grounds for eclogite formation (see p. 148).

In the upper part of the graywacke sequence (Cariño-gneiss Formation and upper level of the Chimparragneiss Formation), no partial melting took place. Here, facies conditions could be determined to have been those of the staurolite-almandine subfacies of the almandine amphibolite facies, on the grounds of severely bent and altered staurolite relics in some of the more pelitic types of graywacke. This conclusion is confirmed by the absence of catazonal assemblages or relics in the (few) metabasite inclusions found in this type of gneiss.

3. *Ultrabasic rocks*

Most of the traces of the Precambrian metamorphism in the ultrabasic rocks were eradicated by the Hercynian metamorphism or by serpentinization. On the

basis of mineral associations in pyroxenite veins and also from the evidence presented by mineral relics in the serpentinized peridotites, it can be demonstrated that the ultrabasic rocks have undergone catazonal metamorphism.

The chemical composition of the ultrabasites did not permit a conclusive determination of the facies conditions during this catazonal metamorphism. The association garnet + clinopyroxene + orthopyroxene + olivine \pm amphibole, found both in the peridotites and in the pyroxenite veins, could have formed equally well under eclogite- as under high-pressure granulite-facies conditions. The occurrence of ultrabasic fragments in the blastomylonites from the Carreiro zone of tectonic movement shows that at least part of the ultrabasites suffered high-pressure granulite-facies metamorphism.

Only doubtful evidence of Precambrian folding was found on aerial photographs, where isoclinally-folded structures with steeply N-plunging fold axes and steep axial planes could be discerned.

4. *Precambrian isograds*

Two Precambrian isograds could thus be discerned in the Cabo Ortegal area: the isograd separating eclogites from high-pressure granulite-facies rocks (marked by the appearance of plagioclase as a stable phase beside clinopyroxene and pyralmandine garnet) and the isograd separating partially anatexitic from non-anatexitic metagraywackes. This latter isograd also seems to coincide with the boundary between catazonal and mesozonal metamorphism in the Cabo Ortegal area.

In the Chimparragneiss Formation, the assemblages of the clinopyroxene-almandine subfacies of the granulite facies border immediately on non-migmatic gneisses, but in the eastern part of Cabo Ortegal a formation of varying width (Banded Gneiss Formation) is found between the two, which can only mean that somewhere between these areas the two aforementioned isograds cut across each other. The reason for this phenomenon is probably that addition of tectonic pressure to lithostatic pressure caused the isograd between the high-pressure granulite facies and the eclogite facies to be overstepped in the Banded Gneiss Formation, which absorbed the first impact of the tectonic pressure (cf. foliated texture of eclogites as compared to non-foliated texture of plagiopyrigarnites). Similar views on eclogite formation have also been expressed by Backlund (1936) and Cogné (1966).

The fact that at Cabo Ortegal staurolite-almandine subfacies associations are found bordering on eclogite-facies associations, does not concur with the position of the staurolite-almandine subfacies in the PT graphs of den Tex (1965) and Fritsch (1966). It does concur with the position of this subfacies in Hietanen's (1967) PT graph, although in this graph the PT conditions for the eclogite facies boundary are set rather low.

As borne out by Anderson's (1965—1966) investigations on staurolite stability, staurolite can be stable up to pressures as high as 10 kb at a temperature of about 850° C, so that enlargement of the PT field of the staurolite-almandine subfacies may have to be considered.

C. PRECAMBRIAN OROGENY, MINOR PHASE (M_2)

Relaxation of tectonic pressure after the Precambrian main phase is thought to have been followed by gabbro intrusion in the western part of Cabo Ortegal. Subsequently, just before the renewal of tectonic activity, potassium-poor pegmatoid veins penetrated along zones of weakness. The origin of these pegmatoid veins remains unsettled; they may represent part of the metatekt from the partially molten surrounding graywackes, although it seems more probable that their provenance must be sought at a deeper level, since they are more widespread in the deep-seated Capelada Complex than in the overlying Concepenido Complex. Quartz and sodic plagioclase are the principal constituents of these veins; kyanite, γ -zoisite, α -zoisite, and β -zoisite may have crystallized, in that order, as additional constituents. That these veins were only distinguished in the metabasites and not in the paragneisses is probably due to their chemical and mineralogical similarity to the latter.

Solutions emanating from these veins caused retrograde alterations in the wall-rock over short distances. The scope of these retrogradations, however, is sometimes considerably wider where the injected zone (which forms a point of weakness) was subjected to penetrative deformation.

1. Retrogradation of the eclogites

In the eclogites, the formation of p.p. symplectite secondary after omphacitic clinopyroxene is seen as the most significant alteration effected by this retrograde metamorphic phase, because it means that the association of pyralmandine garnet + omphacitic clinopyroxene became unstable and was replaced by the high-pressure granulite-facies association of pyralmandine garnet + clinopyroxene + plagioclase. At the same time, greenish-brown hornblende was formed after garnet and clinopyroxene, while α -zoisite and kyanite were replaced by β -zoisite. In tectonized samples the foliation formed by newly-grown minerals such as hornblende and β -zoisite (M_2), lie at a small angle to the original foliation (M_1) of the eclogite (marked by parallelism of α -zoisite, kyanite, and omphacitic clinopyroxene). Rutile remains unaffected by this retrogradation.

In non-tectonized parts, the veins have effected the growth of second-generation kyanite poiciloblasts; growth of second-generation α -zoisite with γ -zoisite cores may also have taken place along the veins.

2. Bacariza Formation

In the Bacariza Formation, p.p. symplectitization is only found in types of rock representing transitions to eclogite. Growth of greenish-brown hornblende secondary after (garnet and) clinopyroxene and possibly the formation of epidote and of second-generation β -zoisite represent the mineralogical changes caused by the catazonal retrograde metamorphic phase in the Bacariza Formation. Penetrative deformations have locally brought about a foliation (M_2) in the originally non-foliated plagiopyrigarnites.

The veins themselves were found only in a tectonized state; in several cases their original nature could be established by the presence of kyanite, a mineral which cannot be formed as a stable phase together with the pyralmandine garnet-clinopyroxene-plagioclase association.

It proved impossible to determine whether scapolite, which occurs in thin veinlets, was also introduced during this stage or whether it was formed by the main Precambrian metamorphism.

3. Candelaria Amphibolite Formation

So few (plagio)pyrigarnite relics were found in this formation that it was impossible to establish how they were affected by the catazonal retrograde metamorphism, but it is assumed that retrogradation took place according to the same pattern as in the Bacariza Formation.

The newly-intruded gabbros were only slightly altered by this metamorphic phase; garnet formed between plagioclase and the melanocratic constituents, and the latter were partly replaced by greenish-brown hornblende. As far as could be ascertained, the effect of tectonization was also slight, being confined mainly to the formation of *flaser* textures in some of the gabbros.

4. Paragneisses and ultrabasites

The activity of the catazonal retrograde metamorphic phase in the paragneisses could only be established on the basis of retrograde alterations in the enclosed metabasite bodies. The mineral associations in the gneisses themselves were unsuitable to reflect such subtle differences in facies conditions. The same reasoning probably applies to the ultrabasic rocks.

D. POST-PRECAMBRIAN, PRE-HERCYNIAN EVENTS

After the Precambrian orogeny, the Galician-Castilian block was uplifted. In Infra-Cambrian and Lower Cambrian times, sedimentation recommenced (deposition of *ollo de sapo* further to the East; Parga-Pondal *et al.*, 1964; Capdevila, 1966), while marine sedimentation continued virtually uninterrupted throughout the Lower Paleozoic from the Middle Cambrian onwards, proving the absence of a major orogenesis between the Precambrian and the Hercynian orogene-

ses (Capdevila, 1966) in northwestern Spain. In the Cabo Ortegal area, the intrusion of gabbroic rocks followed by an intrusion of rocks of granitic composition took place during this period. The gabbroic rocks intruded in the western (Purrido amphibolite) and eastern (metagabbro near San Julian del Trebol) parts of the area. There is abundant evidence of granite intrusion in the Chimparragneiss Formation (stocks and veins) and less in the Banded Gneiss (veins) and Cariñogneiss Formations (pegmatite emplacement at the margin of the gabbro at San Julian del Trebol). The granite intrusion is assumed to have taken place more or less simultaneously with the intrusion of similar rocks in southern Galicia, whose age has been given as 486 ± 24 to 500 ± 25 m.y. (cf. Floor, 1966).

E. HERCYNIAN OROGENY (M_3)

After renewed subsidence, the Galician-Castilian block was intensively (re)folded and (re)metamorphosed by the Hercynian orogeny. The grade of metamorphism could be established as that of the kyanite-almandine-muscovite subfacies of the almandine amphibolite facies for all formations. The differences in location and lithology of these formations, however, caused great diversity in the ways in which the Hercynian orogeny was expressed. It was during this orogeny that the structure at Cabo Ortegal acquired its "mushroom shape" as the result of the overturning of the normal stratigraphic sequence in the eastern as well as in the western parts of the area.

1. *Eclogites*

The amphibolite facies retrogradations left large parts of the eclogite massifs untouched. Like the catazonal retrograde metamorphic phase, amphibolite facies retrogradation was largely confined to zones where it was activated by penetrative movement or circulating solutions. The injected veins carrying these solutions are similar to those responsible for catazonal retrogradation. Quartz and sodic plagioclase are the principal constituents; orthite and epidote, in that order, may have crystallized as additional constituents. Small amounts of potassium are incorporated in the form of biotite or of perthite lamellae in plagioclase.

The mineralogical changes wrought by the amphibolite facies retrogradation are: replacement of garnet and clinopyroxene by blue-green hornblende, plagioclase, and magnetite (kelyphitization). Replacement of clinopyroxene by blue-green hornblende \pm quartz and replacement of garnet by blue-green hornblende + epidote. Zoisite and kyanite are no longer stable phases in the mafic associations, and rutile was altered into titanite \pm ilmenite. That garnet did not become wholly instable is apparent from the occasional finding of a second-generation garnet with a less pyrope-rich composition. Depending on the chemical composition of the eclogite, an amphibolite or a garnet amphibolite is the end-product of the amphibolization process.

Due to their rigidity, the eclogite bodies as a whole reacted competently to the Hercynian deformation (with respect to the surrounding paragneisses). As a consequence, they were boudinaged and therefore show internal signs of penetrative deformation only locally. The form in which the eclogites are now encountered in the field (as lenses and boudins in banded gneiss) is considered to be principally the effect of the Hercynian orogeny.

2. *Capelada Complex*

Retrograde (plagio)pyrigarnites. — Unlike the eclogites, the mafic rocks of the Capelada Complex were intensively amphibolized. The relationship between deformation, pegmatoid injection, and amphibolization found for the eclogites could also be established for the mafic rocks of the Capelada Complex. Owing to their similarity in chemical composition to the eclogites, the end-product of amphibolization is either an amphibolite or a garnet amphibolite. The newly-formed stable minerals are blue-green hornblende, epidote, second-generation garnet?, plagioclase, quartz, titanite, and ilmenite. Biotite was sometimes formed in the neighbourhood of pegmatoid injections. The composition of these injected veins is identical to those found in the eclogites: quartz \pm plagioclase \pm orthite \pm epidote, with epidote crystallizing after orthite.

The new foliation (M_3), marked by parallelism of blue-green hornblende and epidote, was formed as a consequence of strong penetrative deformation accompanied by small-scale isoclinal folding; in places it can be seen to cut off the M_2 plane. The effects of this deformational phase are so widespread that only a few relics of (plagio)pyrigarnite were left unscathed. The frequent occurrence of clinopyroxene relics constitutes the sole evidence of the former pyrigarnitic nature of the complex.

The M_3 foliation was later refolded into open folds of varying amplitude. Both the isoclinal and the open folds have weakly N-plunging fold axes (though deviating, steeply NW-plunging axes were also found). For the open folds, the axial planes are steep; for the isoclinal folds, they are inclined at varying angles in easterly or westerly directions.

Metagabbros. — The metagabbros from the Candelaria Amphibolite Formation were likewise transformed into amphibolites with or without garnet, in most cases indistinguishable from similar amphibolites retrograde after (plagio)pyrigarnite. The penetrative deformation changed the gabbroic textures into *flaser*-like, foliated, or even mylonitic textures. Nevertheless, metagabbros unaffected by deformation and only slightly affected by amphibolite facies metamorphism, are still present.

Leptynites. — It is uncertain whether the leptynites, which are composed principally of garnet + quartz \pm plagioclase \pm orthite \pm epidote, originated during

the Hercynian orogeny, although their discordant relations to M_2 -foliations certainly seem to indicate that this is the case. Nevertheless, the composition of their garnets is such that it indicates a genetic relationship with the high-pressure granulite facies rocks. For the time being, the provenance and the genesis of the leptynites remain obscure.

Paragneisses. — The few paragneisses found in the Bacariza Formation acquired a phyllonitic texture during the Hercynian orogeny. Garnet, biotite, plagioclase, and quartz \pm kyanite (re)crystallized in stable association.

3. Ultrabasic rocks

During the Hercynian orogeny, the catazonal mineral association of the ultrabasic rocks became overprinted by a mesozonal association. Garnet was replaced by amphibole and spinel, first arranged in kelyphitic rims, later recrystallized as amphibole aggregates with spinel inclusions. Clinopyroxene altered into amphibole; orthopyroxene and olivine recrystallized. In extremely soda- and aluminum-poor associations, chlorite has some-times partially replaced the amphibole.

Microfolded amphibole streaks demonstrate that the ultrabasites were affected by the Hercynian phase of isoclinal folding; the occurrence of ultrabasic erosion relics in the synclinal depressions of the open folding pattern of the Bacariza Formation demonstrates that the ultrabasites were also refolded in Hercynian times.

4. Paragneisses

In all the paragneisses, the association quartz + plagioclase + biotite \pm garnet \pm muscovite \pm kyanite was formed secondarily after the previous associations as a consequence of the Hercynian metamorphism. The foliation (M_3) in the gneisses is marked mainly by parallelism of the phyllosilicates (biotite \pm muscovite).

Cariñogneiss Formation. — In the Cariñogneiss, penetrative deformation played only a minor role, as shown by its non-laminated texture. Whether isoclinal folding preceded the formation of asymmetrical open folds with N-plunging fold axes and steeply westward-dipping axial planes, is uncertain.

Banded Gneiss Formation. — In all catazonally metamorphosed paragneisses, the inhomogeneous partition of the minerals, originated by partial anatexis, gave rise to the formation of a variety of textures when they were tectonized in Hercynian times. In this formation, glandular gneisses alternate with laminated or mylonitized types of gneiss, but gneisses showing hardly any effect of Hercynian deformation are also found. Although relationships between different styles of folding are not evident, it is assumed that isoclinal folding preceded the formation of open folds.

Chimparragneiss Formation. — Textures in the Chimparragneiss Formation are similar to those in the Banded Gneiss Formation. Evidence of isoclinal folding is scarce, but the presence of large open folds with amplitudes of several hectometres could be established.

Blastomylonites from the Carreiro zone of tectonic movement. — In the Carreiro zone of tectonic movement, the gneisses were mylonitized in their entirety, and simultaneously underwent isoclinal folding. The inhomogeneity of the starting material is still visible in the form of a lamination (fluxion banding) caused by compositional differences between the lamina. In the folds it could be demonstrated that biotite (re)crystallized subsequent to the isoclinal folding. Open folds were not found in this formation.

Mafic inclusions in the paragneisses. — The retrogradation of the mafic inclusions in the paragneisses proceeded according to the same pattern as in the larger metabasite bodies. Smaller inclusions were entirely amphibolized, but in the larger lenses amphibolization was mainly restricted to marginal zones and fissures. The competent behaviour of the metabasites (as compared to the paragneisses) caused boudinage and sometimes rotation of the inclusions.

5. Pre-Hercynian intrusions

Granitic gneisses. — Apart from a few scattered occurrences in the Banded Gneiss Formation and the Cariñogneiss Formation, no granite intrusives were found outside the Chimparragneiss Formation. Here, virtually undeformed granites were found as well as gneissified granites with foliated or glandular textures. Hercynian metamorphism caused the growth of kyanite, garnet, second-generation biotite, and second-generation muscovite secondary after the primary minerals of the granite. No evidence of catazonal metamorphism could be found.

Purrido amphibolites. — Except for a few incompletely tectonized streaks containing relic gabbroic minerals and textures, the gabbro that intruded in the western part of Cabo Ortegal was completely transformed into a schistose, nematoblastic amphibolite composed of blue-green hornblende, plagioclase, epidote, and titanite.

The presence of a narrow zone of garnet-chlorite schist with garnets measuring several centimetres cannot be accounted for.

Metagabbro at San Julian del Trebol. — This gabbro was tectonized only along the rim; in the core, the gabbroic texture has been retained, although the gabbroic mineral association has been replaced by an amphibolite-facies association (blue-green hornblende + sodic plagioclase).

6. Carreiro zone of tectonic movement

This zone, which is a tectonic unit, embraces the blastomylonites mentioned in Ch. VI, E 4, as well as ultrabasic rocks and part of the Purrido amphibolites. The extreme tectonization in this zone — expressed in mylonitization of the paragneisses, boudinage of the ultrabasites, and small-scale folding of Purrido-type amphibolite — is related to the Hercynian orogeny. Presumably, it is a zone of overthrust along which the crystalline rocks of Cabo Ortegal overrode the neighbouring post-Precambrian but pre-Hercynian gabbroic rocks.

F. POST-HERCYNIAN GEOLOGICAL EVENTS

It is difficult to assign relative ages to the various post-Hercynian geological events, but it seems clear that the local intrusion of narrow dykes of gabbro and tonalite must be placed early in the post-Hercynian period in view of the fact that the latter are cut by hydrothermal veins filled with epidote.

The other events, i.e. formation of a mainly E-W-striking subvertical fault system, mainly vertical displacement of blocks along these faults, circulation of solutions depositing hydrothermal minerals, local greenschist facies retrogradations, and serpentinization, probably took place more or less simultaneously over a long period.

Hydrothermal veins; greenschist facies retrogradations. — Narrow fissures filled with hydrothermal minerals such as epidote, quartz, adularia, prehnite, chlorite, carbonate, and sometimes pumpellyite, were found to cut through rock-types of all formations. In their immediate neighbourhood, the circulation of solutions emanating from these fissures may have caused greenschist-facies retrograde alterations. These include the alteration of clinopyroxene into actinolitic amphibole + albite, of hornblende into actinolitic amphibole, garnet into chlorite + epidote or chlorite + pistacite, plagioclase into albite + epidote + calcite (saussuritization) or into sericite (sericitization), and biotite into chlorite + opaque matter.

In the Purrido Amphibolite Formation, these alterations, particularly saussuritization, are less limited in their localization; probably circulation of the hydrothermal solutions was facilitated here by the very highly developed schistosity.

Serpentinization of the ultrabasites. — The circulation of hydrothermal solutions provided the large amounts of H₂O necessary for wholesale serpentinization of the ultrabasic rocks at nearly constant volume. This supposition is strengthened by the absence of any hydrothermal veins (except those carrying carbonate or serpentine minerals) in the ultrabasites. Si and Mg, liberated by this equal-volume serpentinization (Thayer, 1966), were carried away and deposited elsewhere in fissures or fault zones.

Mylonitization; brecciation (M₄). — Relaxation of pressure by movement along large and small fault zones sometimes caused mylonitization in extremely narrow zones. These mylonitic zones were found in various formations, usually accompanied by greenschist facies retrograde alterations and recrystallization of quartz. In cases of less extreme deformation, breccias, cemented by carbonate or quartz, sometimes formed. The size of the brecciated zones as well as that of the fragments varies considerably.

G. CONCLUDING REMARKS

The association of group B eclogites (Coleman *et al.*, 1965) with (plagio)pyrigarnites could be expected to occur frequently in view of the experimental findings of Green & Ringwood (1966a) indicating that rocks of the clinopyroxene-almandine subfacies of the granulite facies are transitional between gabbros and eclogites. Because the clinopyroxene-almandine subfacies was only recently recognized as a separate subfacies of the granulite facies (de Waard, 1965b) and (plagio)pyrigarnites are also easily mistaken for eclogites, data concerning the eclogite-(plagio)pyrigarnite association are still scarce.

Apart from the findings from the Concepenido and Capelada Complexes at Cabo Ortegal, it appears only from more recent publications that the eclogite-(plagio)pyrigarnite association is found in several classical eclogite areas, e.g. Zöblitz, Erzgebirge (Behr *et al.*, 1965) and Nordfjord, Norway (Bryhni, 1966). With respect to the older literature, the nature of the associated rocks can only be inferred from descriptions, but it seems fairly certain that the eclogite-(plagio)pyrigarnite association also occurs in the eastern Sudetes (Kozłowski, 1961), the lower Austrian Waldviertel (Becke, 1882), the Cape Hope area, Greenland (Sahama, 1935), and possibly also in the Varberg district, Sweden (Quensel, 1952).

The investigations at Cabo Ortegal provide additional confirmation of the statement by Green & Ringwood (1966a) that eclogite can be formed within the Earth's crust. This implies that the closely associated rocks of non-gabbroic composition (Banded Gneiss Formation at Cabo Ortegal) also underwent eclogite-facies metamorphism. The petrographical investigations indicate that mineral parageneses in metasedimentary rocks metamorphosed under eclogite-facies conditions do not differ significantly from those formed in the same rocks under clinopyroxene-almandine subfacies- or kyanite-almandine-muscovite-subfacies conditions. Under catazonal metamorphic conditions, however, partial anatexis was found to have taken place in the metasedimentary rocks at Cabo Ortegal, and this process did not recur under mesozonal metamorphic conditions.

SAMENVATTING

In het onderzochte gebied zijn paragneizen aangetroffen, geassocieerd met amfibolieten, metagabbros, geamfibolitiseerde eclogieten, geamfibolitiseerde (plagio)pyrigarnieten (hoge-druk-granulietfacies gesteenten) en geserpentiniseerde ultrabasische gesteenten. Op petrologische en chemische gronden kon de wordingsgeschiedenis van deze gesteenten als volgt gereconstrueerd worden:

Precambrische afzetting van grauwackes werd op de voet gevolgd door intrusie van gabbroïde kernen en intrusieplaten en door plaatsing van ultrabasische gesteenten. Gedurende een orogenese van vermoedelijk precambrische ouderdom, zijn deze gesteenten in de hoger liggende delen onderworpen geweest aan mesozonale metamorfose, terwijl de diepere delen onderhevig waren aan katazonale metamorfose. In de mesozonaal gemetamorfoseerde gneizen zijn stauroliet-almandien subfacies associaties gevormd; gabbroïde insluitsels werden tegelijkertijd veranderd in amfiboliet. In de gneizen die katazonaal werden gemetamorfoseerd trad partiële anatexis op; in het niet opgesmolten gedeelte (restiet) vormde zich de associatie granaat + distheen (\pm biotiet). In het oostelijk deel van het gebied werden de gabbroïde intrusieplaten omgezet in gefolieerde eclogiet (\pm α -zoisiet \pm distheen \pm karintien); in het centraal en westelijk deel van het gebied werden zij omgezet in niet gefolieerde (plagio)pyrigarniet. De ultrabasische gesteenten werden veranderd in granaat peridotiet. Bewijzen voor isoclinale plooïing werden aangetroffen in de eclogiet en — minder overtuigend — in de ultrabasische gesteenten.

Hernieuwde intrusie van gabbro werd gevolgd door plaatselijk optredende katazonale retrograde metamorfose (onder hoornblende-clinopyroxeen-almandien subfacies omstandigheden) in zones waar pegmatoïde injectie of penetratieve deformatie heeft plaatsgevonden. Retrograde omzettingen konden alleen in de basische gesteenten worden aangetoond, onder andere door de vorming van een groenbruine hoornblende of door de vorming van een nieuwe foliatie. De pas geïntroduceerde gabbros werden tijdens deze metamorfe fase gedeeltelijk omgezet onder vorming van een flaser textuur.

Na de precambrische orogenese vond lokaal intrusie van gabbroïde en granitische gesteenten plaats; het tijdstip van

intrusie werd naar analogie van soortgelijke intrusies in Zuid Galicië gesteld op ongeveer 500 miljoen jaar. Deze intrusies werden tijdens de hercynische metamorfose omgezet in respectievelijk schisteuze amfiboliet en orthogneis. In de metamorfe gesteenten vond retrograde metamorfose plaats onder amfibolietfacies omstandigheden (distheen-almandien-muscoviet subfacies in het gehele onderzochte gebied) waarbij bovendien (opnieuw) plooïing plaats vond. In de paragneizen werd de paragenese biotiet + muscoviet \pm granaat \pm distheen gevormd terwijl kwarts en plagioklaas rekristalliseerden. Twee opeenvolgende plooïingsfasen veroorzaakten isoclinale plooïing, in de meeste gevallen gevolgd door open plooïing. In de eclogieten en in de (plagio)pyrigarnieten werd de associatie blauwgroene hoornblende + plagioklaas + epidoot \pm granaat retrograad uit de katazonale associaties gevormd. De eclogieten werden gebouidneerd maar inwendig niet geplooid. Amfibolitatie trad op langs de randen van de boudins, langs pegmatoïde injecties en langs smalle doorbewogen zones. Door een intensievere tectonisatie (inwendige isoclinale plooïing gevolgd door open plooïing) werden de (plagio)pyrigarnieten tijdens de hercynische orogenese zwaarder aangegrepen door de retrograde metamorfose. Voor het grootste deel werden zij, evenals de metagabbros, omgezet in gelamineerde (granaat)-amfibolieten. Texturen variërend van mylonitisch tot vrijwel ongedeforceerd, werden in deze gabbros aangetroffen. De granaatperidotieten werden hercynisch omgevormd tot amfibool- of chlorietperidotieten, waarbij zowel isoclinale als open plooïen gevormd werden. De stratigrafische opeenvolging werd gedurende de hercynische orogenese zowel in het oostelijk als in het westelijk deel van het gebied omgekeerd ("paddestoelplooi") waarbij in het westelijk gedeelte een overschuivingszone met isoclinaal geplooid blastomylonieten, gebouidneerde ultrabasiëten en microgeplooid amfibolieten werd gevormd.

Posthercynisch optredende hydrothermale activiteit veroorzaakte lokaal groenschistfacies retrogradaties in de meeste gesteentetypen en uitgebreide serpentinisatie in de ultrabasische gesteenten. Blokbewegingen in voornamelijk verticale zin, langs posthercynisch aangelegde breuken, werden plaatselijk vergezeld door brecciatie of mylonitisatie. Intrusie, op kleine schaal, van tonalitische en gabbroïde gangen, vond eveneens plaats na de hercynische orogenese.

SUMARIO

Se han encontrado en la región investigada paragneises asociadas con anfíbolitas, metagabros, eclogitas anfíbolitizadas, (plagio)pirigarnitas (rocas de la facies granulítica de alta presión) anfíbolitizadas y rocas ultrabásicas serpentinizadas. Sobre bases petrológicas y químicas se puede reconstruir la historia geológica de estas rocas como sigue:

Sedimentos precámbricos de una composición grauvacica estan directamente seguidos por capas intrusivas y cuerpos de una composición gabroide y por la introducción de rocas ultrabásicas. Durante una orogénesis de una edad probablemente precámbrica, estas rocas en las partes superiores de dicha superposición, han sido metamorfoseadas mesozonalmente, mientras que las partes inferiores lo han sido kata-

zonalmente. En los gneises metamorfoseados mesozonalmente se formaron asociaciones de la subfacies estaurolita-almandina; inclusiones gabroides se transformaron al mismo tiempo en anfíbolitas. En los gneises que se metamorfosearon katazonalmente, se encuentra una anatexis parcial; en la parte no fundida ("restita") se formó la asociación de granate y distena (\pm biotita). En la parte oriental de la región se transformaron las capas intrusivas gabroides en eclogita foliada (\pm α -zoisita, \pm distena, \pm carinthina); en la parte central y occidental de la región se cambiaron en (plagio)pirigarnita no foliada. Las rocas ultrabásicas se transformaron en peridotita de granate. Se encontraron pruebas de un plegamiento isoclinal en las rocas eclogíticas y — menos claramente — en las rocas ultrabásicas.

Una nueva intrusión de un gabro ha sido seguido localmente por una metamorfosis retrógrada katazonal (bajo condiciones de la subfacies de hornblenda-clinopiroxena-almandina) en las zonas donde ocurrieron inyecciones pegmatoides o deformaciones penetrativas. Se puede comprobar solamente alteraciones retrógradas en las rocas básicas, entre tanto por la formación de una hornblenda verde-marrón, o por la formación de una nueva foliación. Los gabros recientemente introducidos se transformaron parcialmente durante esta fase metamórfica en metagabros con una textura flaser.

Después de la orogénesis precámbrica hubo una intrusión local de rocas gabroides y graníticas. El momento de esta intrusión se estima, según la analogía de intrusiones similares en el S. de Galicia, en hace aproximadamente 500 millones de años. Estas intrusiones se transformaron durante la metamorfosis hercínica respectivamente en anfibolita esquistosa y ortogneis. En las rocas metamórficas ocurrió una metamorfosis retrógrada bajo condiciones de la facies anfibolítica (en toda la región investigada subfacies de distena-almandina-moscovita) durante la cual sobre todo hubo de nuevo un plegamiento. En los paragneises se formó la paragénesis de biotita + moscovita \pm granate \pm distena, mientras que el cuarzo y la plagioclasa se recrystalizaron. Dos fases de deformación siguientes causaron un plegamiento isoclinal, en la mayoría de los casos seguido por un plegamiento abierto. En las eclogitas y en las (plagio)pirigarnitas se formó retrogradamente la asociación de hornblenda azul-verde, plagioclasa y epidota \pm granate, de las asociaciones

katazonales. De los cuerpos de eclogita se formaron "boudins" pero estos no han sido interiormente plegados. Anfibolitización ocurrió a lo largo de las "boudins", de las intrusiones pegmatoides y de las zonas estrechas deformadas penetrativamente. Por una tectonización mas intensa (plegamiento isoclinal seguido por un plegamiento abierto) las (plagio)pirigarnitas han sido metamorfoseadas más intensamente por la metamorfosis retrógrada. La mayor parte de ellas se transformó tanto como los metagabros en anfibolitas (de granate) laminadas. Texturas que oscilan de miloníticas hasta casi indeformadas han sido encontradas en estos gabros. Las peridotitas de granate se transformaron en peridotitas de anfíbol o clorita durante el Hercínico y se plegaron tanto isoclinalmente como abiertamente. La superposición estratigráfica ha sido invertida durante la orogénesis hercínica, tanto en la parte oriental como en la occidental de la región ("pliegue en forma de hongo"), mientras en la parte occidental se formó una zona de corrimiento con blastomilonitas isoclinalmente plegadas, ultrabasitas "boudinadas" y anfibolitas microplegadas.

Una actividad hidrotermal pos-hercínica originó localmente retrogradaciones de la facies de esquistos verde en la mayoría de los tipos de rocas y una serpentinización de mayor escala en las rocas ultrabásicas. Movimientos de bloques en sentido principalmente vertical por fallas pos-hercínicas están acompañadas localmente por brecciación o milonitización. Una intrusión, en escala pequeña, de filones tonalíticos y gabroides ocurrió también después de la orogénesis hercínica.

REFERENCES

- Alderman, A. R., 1936. Eclogites in the neighbourhood of Glenelg, Inverness-shire. *Quart. jour. geol. soc. London*, 92, p. 488—530.
- Angel, F., 1957. Einige ausgewählte Probleme eklogitischer Gesteinsgruppen der österreichischen Ostalpen. *N. Jb. Min. Abh.*, 91, p. 151—192.
- Anthionoz, P. M., 1966. Géologie sommaire de la région de Morais (Tras-os-Montes, Portugal). *Leidse geol. med.*, 36, p. 299—302.
- 1967a. L'unité de Bragança (Tras-os-Montes, Portugal): métamorphisme et tectonique. *C.R. acad. sci. Paris*, 264, p. 540—543.
- 1967b. Les brèches tectoniques dans les unités de Bragança et de Morais (province de Tras-os-Montes, N-E du Portugal). *C.R. acad. sci. Paris*, 264, p. 233—236.
- Appelman, D. E., 1966. Crystal chemistry of the pyroxenes. In: short course lecture notes, *Am. geol. inst.*, 24 pp.
- Backlund, H. G., 1936. Zur genetischen Deutung der Eklogite. *Geol. Rdsch.*, 27, p. 47—61.
- Bamba, T., 1958. Comparison of the chromite deposits of Hokkaido and of the Chûgoku district, Japan. *Jubilee publ. commem. Prof. J. Suzuki Sapporo*, p. 441—450 (in Japanese with english abstract).
- Banno, S., 1967. Mineralogy of two eclogites from Fichtelgebirge, and their mineralogical characteristics in relation to other eclogite occurrences. *N. Jb. Min. Mh.*, p. 116—124.
- Bautsch, H. J., 1961. Über die p-t-x-Bedingungen der Eklogitfazies. *Ber. geol. Ges. DDR*, 6, p. 33—36.
- Bearth, P., 1965. Zur Entstehung alpinotyper Eklogite. *Schweiz. min. petr. Mitt.*, 45, p. 179—188.
- 1966. Zur mineralfaziellen Stellung der Glaukophangesteine der Westalpen. *Schweiz. min. petr. Mitt.*, 46, p. 13—23.
- Becke, F., 1882. Die Gneissformation des niederösterreichischen Waldviertels. *Tsch. min. petr. Mitt.*, N.F. 4, p. 285—408.
- Beck-Mannagetta, P., 1961. Zur Deutung der Eklogite im Koralpenkristallin (Zentralalpen). *Tsch. min. petr. Mitt.*, D.F. 7, p. 437—450.
- Behr, H. J., Fritsch, E. & Mansfeld, L., 1965. Die Granulite von Zöblitz im Erzgebirge als Beispiel für Granulitbildung in tiefreichenden Scherhorizonten. *Krystalinikum*, 3, p. 7—29.
- Berthelsen, A., 1960. Structural studies in the Pre-Cambrian of Western Greenland. *Meddel. Grønland*, 123 (1), 233 pp.
- Binns, R. A., 1965. The mineralogy of metamorphosed basic rocks from the Willyama Complex, Broken Hill district, N.S. Wales, Pt I: hornblendes. *Min. mag.*, 35, p. 306—326.
- Bloxam, T. W. & Allen, J. B., 1960. Glaucophane schist, eclogite and associated rocks from Knockormal in the Girvan-Ballantrae Complex, South Ayrshire. *Trans. Roy. soc. Edinburgh*, 64 (1), p. 1—27.
- Bobryevitch, A. P., Smirnov, G. I. & Sobolev, V. S., 1959. A xenolith of diamond-bearing eclogite. *Dokl. akad. Nauk. SSSR*, 126, p. 637—640.
- Smirnov, G. I. & Sobolev, V. S., 1960. On the mineralogy of xenoliths of grossular pyroxene kyanite rocks (grosopydite) from the kimberlites of Yakutia. *Sib. otd. Nauk. geol. geoph. SSSR*, 3, p. 18—24.

- Bonhomme, M., Mendès, F. & Vialette, Y., 1961. Ages absolus par la méthode au strontium des granites de Sintra et Castro Daire au Portugal. C.R. acad. sci. Paris, 252, p. 3305—3306.
- Bowen, N. L. & Schairer, J. F., 1935. The system MgO-FeO-SiO₂. Am. jour. sci., 29, p. 151—217.
- & Tuttle, O. F., 1949. The system MgO-FeO-SiO₂-H₂O. Bull. geol. soc. Am., 60, p. 439—460.
- Bown, M. G., 1964. Recalculation of pyroxene analyses. Am. min., 49, p. 190—194.
- Boyd, F. R. & England, J. L., 1959—1960. Minerals of the mantle. Ann. rept. dir. geophys. lab., Washington, p. 47—52.
- Brière, Y., 1920. Les écoligites françaises. Leur composition minéralogique et chimique; leur origine. Soc. franç. min. bull., 43, p. 72—222.
- Brunn, J. H., 1956. Contribution à l'étude géologique du Pinde septentrional et d'une partie de la Macédoine occidentale. Ann. géol. pays hellén., 7, p. 1—358.
- Bryhni, I., 1966. Reconnaissance studies of gneisses, ultrabasites, eclogites and anorthosites in Outer Nordfjord, western Norway. Norges geol. undersøg., 241, 68 pp.
- Burri, C., 1959. Petrochemische Berechnungsmethoden auf äquivalenter Grundlage. Basel, Birkhäuser Verlag, 334 pp.
- Capdevila, R., 1965. Sur la géologie du précambrien et du paléozoïque dans la région de Lugo et la question des plissements assyntiques et sardes en Espagne. Notas comuns. inst. geol. minero Esp., 80, 157—174.
- Matte, P. & Parge-Pondal, I., 1964. Sur la présence d'une formation porphyroïde infracambrienne en Espagne. C.R. somm. scé. soc. géol. France, 7, p. 249.
- & Vialette, Y., 1965. Premières mesures d'âge absolu affectuées par la méthode au strontium sur des granites et micaschistes de la province de Lugo (Nord-Ouest de l'Espagne). C.R. acad. sci. Paris, 260, p. 5081—5083.
- Cardoso, M. G. I. & Parga-Pondal, I., 1951. Kotschubeita de la Sierra de la Capelada. Cabo Ortegal, Galicia (España). Notas comuns. inst. geol. minero Esp., 24, p. 93—100.
- Carlé, W., 1945. Ergebnisse geologischer Untersuchungen im Grundgebirge von Galicien, NW. Spanien. Geotekt. Forsch., 6, p. 13—36.
- Chayes, F., 1965. Titania and alumina content of oceanic and circum-oceanic basalt. Min. mag., 34, p. 126—131.
- Chenevoy, M., 1955. Sur l'origine des écoligites de Sauviat (Creuse). C.R. acad. sci. Paris, 241, p. 426—428.
- Cherotzky, G., 1963. Lexique pétrographique. Notes mém. serv. geol. Maroc, 171, 116 pp.
- Chensnokow, B. V., 1964. Dreiwertiges Titan in den Eklogiten des südlichen Urals. Zentralbl. Min., II, p. 465.
- Church, W. R., 1964. Metamorphic eclogites from Co Donegal, Eire. Ind. min., I.M.A. sp. number, p. 22—23.
- Clark, J. R. & Papike, J. J., 1966a. Eclogitic pyroxenes, ordered with P2 symmetry. Science, 154 (3752); p. 1003—1004.
- & Papike, J. J., 1966b. Cation distribution in the crystal structure of omphacite, the eclogitic pyroxene. Progr. ann. meeting G.S.A., p. 40.
- Clark, R. H. & Fyfe, W. S., 1961. Ultrabasic liquids. Nature, 191, p. 158—159.
- Clarke, F. W., 1924. The data of geochemistry. US. geol. surv. bull., 770, 841 pp.
- Cloos, E., 1947. Boudinage. Trans. Am. geoph. union, 28, p. 626—632.
- Coelewij, P. A. J., 1959. Geologische, petrografische en mineralogische beschrijving van eklogietische en andere gesteenten in Cabo Ortegal (Galicië, Spanje). Unpublished report, Leiden.
- Cogné, J., 1966. Une "nappe" Cadomienne de style Pennique: la série cristallophyllienne de Champtoceaux en bordure méridionale du synclinal d'Ancenis (Bretagne-Anjou). Bull. serv. carte géol. Als. Lorr., 19, p. 107—136.
- & Eller, J. P. v., 1961. Défense et illustration des termes leptynite et granulite en pétrographie des roches métamorphiques. Bull. serv. carte géol. Als. Lorr., 14, p. 59—64.
- Cohen, E., 1879. Ueber einen Eklogit von Jagersfontein, Oranjevrijstaat. N. Jb. Min. Geol. Paläont., p. 864.
- Coleman, R. G., Lee, D. E., Beatty, L. B. & Brannock, W. W., 1965. Eclogites and eclogites: Their differences and similarities. Bull. geol. soc. Am., 76, p. 483—508.
- Collée, A. L. G., 1964. The geology of the coastal section from Cabo de San Adrian to Playa de Baldayo (Galicia). Leidse geol. med., 30, p. 121—130.
- Compton, R. R., 1960. Charnockitic rocks of Santa Lucia Range, California. Am. jour. sci., 258, p. 609—636.
- Dana, E. S., 1932. A textbook of mineralogy, 4th ed. New York, John Wiley & sons inc., 851 pp.
- Daniels, J. L., Skiba, W. J. & Sutton, J., 1965. The deformation of some banded gabbros in the northern Somali fold-belt. Quart. jour. geol. soc. London, 121, p. 111—141.
- Davidson, C. F., 1943. The Archaean rocks of the Rodil district, South Harris, Outer Hebrides. Trans. Roy. soc. Edinburgh, 61, p. 71—112.
- Deer, W. A., Howie, R. A. & Zussmann, J., 1965. Rock forming minerals. Vol. I, Ortho- and ring silicates, 333 pp. Vol. II, Chain silicates, 379 pp. London, Longmans, Green & Co. Ltd.
- Drever, H. I. & Johnston, R., 1966. A natural high-lime silicate liquid more basic than basalt. Jour. petr., 7, p. 414—420.
- Dubertret, L., 1959. Géologie des roches vertes du Nord-Ouest de la Syrie et du Hatay (Turquie). Notes. mém. Moyen-Orient, mus. natl. d'hist. nat. Paris, 6, p. 5—224.
- Düll, E., 1902. Ueber die Eklogite des Münchberger Gneissgebietes. Geogn. Jahresh. München, 15, p. 1—92.
- Eigenfeld-Mende, I., 1948. Metamorphe Umwandlungserscheinungen an Metabasiten des Südschwarzwaldes im Raume Kandel Freiburg. Mitt. Bad. geol. Landesanst. N.F. 1, p. 1—111.
- Engel, A. E. J. & Engel, C. G., 1962a. Hornblendes formed during progressive metamorphism of amphibolites, Northwest Adirondack Mountains, New York. Bull. geol. soc. Am., 73, p. 1499—1514.
- & Engel, C. G., 1962b. Progressive metamorphism of amphibolite, Northwest Adirondack Mountains, New York. Geol. soc. Am. Budd. vol., p. 37—82.
- Engels, J. P. & Vogel, D. E., 1966. Garnet reaction-rims between plagioclase and hypersthene in a meta-norite from Cabo Ortegal (NW. Spain). N. Jb. Min. Mh., p. 13—19.
- Erdmannsdörffer, O. H., 1931. Über Zoisitogiklaspegmatit und seine Beziehung zu anorthositischen Magmen. Sitzber. Heidelb. Akad. Wiss. Math. nat. Kl. 4. Abh. 9 S.

- Eskola, P., 1921. On the eclogites of Norway. *Videns. skr. I, math. naturv. kl., Kristiania*, 8, p. 1—118.
- Evans, B. W. & Leake, B. E., 1960. The composition and origin of the striped amphibolites of Connemara, Ireland. *Jour. petr.*, 1, p. 337—363.
- Fiedler, A., 1936. Über Verflössungserscheinungen von Amphiboliten mit diatektischen Lösungen im östlichen Erzgebirge. *Tsch. min. petr. Mitt.*, N.F. 47, p. 470—516.
- Floor, P., 1966. Petrology of an aegirine-riebeckite gneiss-bearing part of the Hesperian massif: the Galiñeiro and surrounding areas, Vigo, Spain. *Leidse geol. med.*, 36, p. 1—203.
- Fonteilles, M., 1965. Sur la profondeur de formation des veines à disthène géodique de la région de Baud (Morbihan) et sur la signification des veines à disthène en général. *Bull. soc. franç. min. crist.*, 88, p. 281—289.
- Forbes, R. B., 1965. The comparative chemical composition of eclogite and basalt. *Jour. geophys. res.*, 70, p. 1515—1521.
- Frietsch, R., 1957. Determination of the composition of garnets without chemical analysis. *Geol. fören. förh.*, 79, p. 43—51.
- Fritsch, W., 1966. Zum Einteilungsprinzip der Gesteine nach dem Umwandlungsgrad mit besonderer Berücksichtigung der Anchimetamorphose. *N. Jb. Min. Abh.*, 105, p. 111—132.
- Geul, J. J. C., 1964. The petrology of the region between Lage and Carballo. *Leidse geol. med.*, 30, p. 103—120.
- Gjelsvik, T., 1952. Metamorphosed dolerites in the gneiss area of Sunnmøre on the West coast of southern Norway. *Norsk geol. tidsskr.*, 30, p. 33—134.
- Green, D. H., 1964a. The petrogenesis of the high-temperature peridotite intrusion in the Lizard area, Cornwall. *Jour. petr.*, 5, p. 134—188.
- 1964b. The metamorphic aureole of the peridotite at the Lizard, Cornwall. *Jour. geol.*, 72, p. 543—563.
- & Lambert, I. B., 1965. Experimental crystallization of anhydrous granite at high pressures and temperatures. *Jour. geophys. res.*, 70, p. 5259—5268.
- & Ringwood, A. E., 1966a. An experimental investigation of the gabbro to eclogite transformation and its petrological applications. *Dept. geophys. geochem. Austr. natl. univ. Canberra, publ. nr. 444*.
- & Ringwood, A. E., 1966b. An experimental investigation of the gabbro-eclogite transformation and some geophysical implications. *Tectonophysics*, 3, p. 383—427.
- Groves, A. W., 1935. The charnockite series of Uganda, British East Africa. *Quart. jour. geol. soc. London*, 91, p. 150—207.
- Hahn-Weinheimer, P. & Luecke, W., 1963. Chemismus und Spurengehalte von eklogitischen Gesteinen und deren Granatphasen. *N. Jb. Min. Mh.*, p. 272—278.
- Hauy, R. J., 1822. *Traité de minéralogie*. Pt. 2, 617 pp. Pt. 4, 592 pp. Paris, Delance.
- Heritsch, H. & Kahler, E., 1960. Strukturuntersuchung an zwei Kluftkarinthinen. *Tsch. min. petr. Mitt.*, D.F. 7, p. 218—234.
- Hess, H. H., 1938. A primary peridotite magma. *Am. jour. sci.*, 35, p. 321—344.
- 1949. Chemical composition and optical properties of common clinopyroxenes. *Am. min.*, 34, p. 621—666.
- 1955. Serpentine, orogeny and epeirogeny. *Geol. soc. Am., sp. pap.*, 62, p. 391—408.
- Hezner, L., 1903. Ein Beitrag zur Kenntnis der Eklogite und Amphibolite. *Tsch. min. petr. Mitt.*, 22, p. 437—472 & p. 505—580.
- Hietanen, A., 1943. Über das Grundgebirge des Kalantigebietes im südwestlichen Finnland. *Bull. comm. géol. Finl.*, 130, 105 pp.
- 1967. On the facies series in various types of metamorphism. *Jour. geol.*, 75, p. 187—214.
- Hintze, C., 1897. *Handbuch der Mineralogie*. Leipzig, von Veit & Comp.
- Hoppe, G., 1966. Zirkone aus Granuliten. *Ber. deutsch. Ges. geol. Wiss. B Min. Lagerstättenf.*, 11, p. 47—81.
- Howie, R. A., 1955. The geochemistry of the Charnockite Series of Madras, India. *Trans. Roy. soc. Edinburgh*, 62, p. 725—768.
- & Subramaniam, A. P., 1957. The paragenesis of garnet in charnockite, enderbite and related granulites. *Min. mag.*, 31, p. 565—586.
- Huckenholz, H. G., 1963. A contribution to the classification of sandstones. *Geol. fören. förh.*, 85, p. 156—172.
- Jaffe, H. W., 1951. The role of Yttrium and other minor elements in the garnet group. *Am. min.*, 36, p. 133—155.
- Joukowski, E., 1901. Sur les eclogites des Aiguilles Rouges. *C.R. acad. sci. Paris*, 133, p. 1312.
- Kalsbeek, F., 1962. Petrology and structural geology of the Berlanche-Valloire area (Belledonne massif, France). Thesis, Leiden, 136 pp.
- Khitarov, N. I. & Pugin, V. A., 1962. Temperature of incipient fusion of sandstone-shale sequences as a function of pressure. *Geochemistry*, p. 342—347.
- Kieslinger, A., 1928. *Geologie und Petrographie der Koralpe VI. Pegmatite der Koralpe*. Sitz. ber. Akad. Wiss. Wien, math. nat. Kl., 137, p. 123—142.
- Knorring, O. v. & Kennedy, W. Q., 1958. The mineral paragenesis and metamorphic status of garnet-hornblende-pyroxene-scapolite gneiss from Ghana (Gold Coast). *Min. mag.*, 31, p. 846—859.
- Koritnig, S., 1940. Ein Beitrag zur Kenntnis über den "Karinthin". *Zentralbl. Min. Geol. Pal. Abt. A*, p. 31—36.
- Kozłowski, K., 1958. On the eclogite like rocks of Stary Gieraltów (East Sudeten). *Bull. acad. polon. sci. sér. sci. chim. géol. géog.*, 6, p. 723—728.
- 1961. The granulite complex of Stary Gieraltów, East Sudetes. *Arch. mineralogiczne*, 25, p. 5—122.
- Kuno, H., 1960. High alumina basalt. *Jour. petr.*, 1, p. 121—145.
- Kunitz, W., 1930. Die Isomorphieverhältnisse in der Hornblendegruppe. *N. Jb. Min. Geol. Paläont. Abh. Abt. A*, 60, p. 171—250.
- Kushiro, I., 1962. Clinopyroxene solid solutions part I. The $\text{CaAl}_2\text{SiO}_6$ component. *Jap. jour. geol. géog.*, 33, p. 213—220.
- 1964—1965. Clinopyroxene solid solutions at high pressures. *Ann. rept. dir. geophys. lab.*, Washington, p. 112—117.
- Lange, H., 1963. Zur petrographischen Gliederung amphibolitischer und eklogitischer Gesteine. *Bergakad. Deutschl.*, 15, p. 92—96.
- 1964. Die chemische Zusammensetzung von Granaten aus Metabasiten des Erzgebirges. *Geol.*, 13, p. 325—352.
- 1965. Zur Genese der Metabasite im sächsischen Erzgebirge. *Freib. Forsch. H.*, C 177, 136 pp.

- Lane, A. C., 1904. The role of possible eutectics in rock magmas. *Jour. geol.*, 12, p. 83—93.
- Lappin, M. A., 1960. On the occurrence of kyanite in the eclogites of the Selje and Åheim districts, Nordfjord. *Norsk geol. tidsskr.*, 40, p. 289—296.
- Layton, W., 1963. Amphibole paragenesis in the Birrimian Series of the Winneba district of Ghana. *Jour. geol. soc. Austr.*, 10, p. 261—271.
- Leake, B. E., 1964. The chemical distinction between ortho- and para-amphibolites. *Jour. petr.*, 5, p. 238—254.
- Lee, D. E., Coleman, R. G. & Erd, R. C., 1963. Garnet types from the Cazadero area, California. *Jour. petr.*, 4, p. 460—492.
- Lohmann, P., 1884. Neue Beiträge zur Kenntnis des Eklogits vom mikroskopisch-mineralogischen und archäologischen Standpunkte. *N. Jb. Min. Geol. Paläont.*, p. 83—117.
- Lotze, F., 1945a. Einige Probleme der Iberischen Meseta. *Geotekt. Forsch.*, 6, p. 1—12.
- 1945b. Zur Gliederung der Varisziden der Iberischen Meseta. *Geotekt. Forsch.*, 6, p. 78—92.
- Loving, J. F., 1964. The eclogite-bearing basic igneous pipe at Ruby Hill near Bingara, N.S. Wales. *Jour. proc. Roy. soc. N.S. Wales*, 97, p. 73—79.
- & White, A. J. R., 1964. The significance of primary scapolite in granulitic inclusions from deep-seated pipes. *Jour. petr.*, 5, p. 195—218.
- Macdonald, G. A. & Katsura, T., 1964. Chemical composition of Hawaiian lavas. *Jour. petr.*, 5, p. 82—133.
- Machatski, F., 1953. Spezielle Mineralogie auf geochemischer Grundlage. Wien, Springer Verlag, 378 pp.
- & Walitzki, E. M., 1962. Hornblendes aus Eklogiten und Amphiboliten der südlichen Koralpe. *Tsch. min. petr. Mitt.*, D.F. 8, p. 140—151.
- Macpherson, J., 1881. Apuntes petrográficos de Galicia. *An. soc. esp. hist. nat.*, 10, p. 49—87.
- Matte, P., 1964. Remarques préliminaires sur l'allure des plis hercyniens en Galice orientale. *C.R. acad. sci. Paris*, 259, p. 1981—1984.
- Mehnert, K. R., 1960. Das Problem des Alkalihaushalts im Orogen. *Geol. Rdsch.*, 50, p. 124—131.
- Mikkola, E. & Sahama, T. G., 1936. The region to the South-West of the "granulite series" in Lapland and its ultrabasics. *Bull. comm. géol. Finl.*, 115, p. 357—371.
- Miranda, H. de, 1964. De petrografische kartering van het zuidelijk gedeelte van de Cabo Ortegal. Unpublished report, Leiden.
- Miyashiro, A., 1958. Regional metamorphism of the Gosai-syo Takanuki district in the central Abukuma Plateau. *Jour. fac. sci. univ. Tokyo, sec. II*, 11, p. 219—272.
- 1966. Some aspects of peridotite and serpentinite in orogenic belts. *Jap. jour. geol. geog.*, 37, p. 45—61.
- Morimoto, N., Appleman, D. E. & Evans, H. T., 1960. The crystal structures of clinoenstatite and pigeonite. *Zeitschr. Krist.*, 114, p. 120—147.
- Murgoci, G., 1924. Sur les propriétés des amphiboles bleues. *N. Jb. Min. Geol. Paläont.*, 1924 II, p. 348—349.
- Myer, G. H., 1966. New data on zoisite and epidote. *Am. jour. sci.*, 264, p. 364—385.
- O'Hara, M. J., 1960. A garnet-hornblende-pyroxene rock from Glenelg, Inverness-shire. *Geol. mag.*, 97, p. 145—156.
- & Mercy, E. L. P., 1962—1963. Petrology and petrogenesis of some garnetiferous peridotites. *Trans. Roy. soc. Edinburgh*, 65, p. 251—314.
- & Yoder, H. S., 1962—1963. Partial melting of the mantle. *Ann. rept. dir. geophys. lab.*, Washington, p. 66—71.
- Parga-Pondal, I., 1956. Nota explicativa del mapa geológico de la parte N.O. de la provincia de la Coruña. *Leidse geol. med.*, 21, p. 468—484.
- 1963. Mapa petrográfico estructural de Galicia. *Inst. geol. minero Esp.*, Madrid.
- 1966a. La investigación geológica en Galicia. *Leidse geol. med.*, 36, p. 207—210.
- 1966b. Datos geológico-petrográficos de la provincia de la Coruña. In: *Estudio agrobiológico de la provincia de la Coruña*. Vigo, Art gráf. de Faro de Vigo S.A. (1967).
- Matte, P. & Capdevila, R., 1964. Introduction à la géologie de "l'ollo de sapo". Formation porphyroïde antésilurienne du Nord Ouest de l'Espagne. *Notas comuns. inst. geol. minero Esp.*, 76, p. 119—154.
- Peters, T., 1963. Mineralogie und Petrographie des Totalpserserpentins bei Davos. *Schweiz. min. petr. Mitt.*, 43, p. 529—685.
- & Niggli, E., 1964. Spinellführende Pyroxenite ("Ariégite") in den Lherzolitkörpern von Lherz und Umgebung (Ariège, Pyrenäen) und der Totalp (Graubünden, Schweiz), ein Vergleich. *Schweiz. min. petr. Mitt.*, 44, p. 513—517.
- Pettijohn, F. J., 1957. *Sedimentary rocks* 2nd ed. New York, Harper & Row, 718 pp.
- Philipsborn, H. v., 1930. Zur chemisch-analytischen Erfassung der isomorphen Variation gesteinsbildender Minerale. Die Mineralkomponenten des Pyroxengranulits von Hartmannsdorf (Sa). *Chemie d. Erde*, 5, p. 233—253.
- Phillips, R., 1963. The recalculation of amphibole analyses. *Min. mag.*, 33, p. 701—711.
- Pistorius, C. W. F. T., Kennedy, G. C. & Sourirajan, S., 1962. Some relations between the fuses anorthite, zoisite and lawsonite at high temperatures and pressures. *Am. jour. sci.*, 260, p. 44—56.
- Plas, L. v. d., 1959. Petrology of the northern Adula region, Switzerland. *Leidse geol. med.*, 24, p. 415—602.
- Platen, H. v. & Höller, H., 1966. Experimentelle Anatexis des Stainzer Plattengneises von der Koralpe, Steiermark, bei 2, 4, 7 und 10 kb H₂O-Druck. *N. Jb. Min. Abh.*, 106, p. 106—130.
- Portugal V. Ferreira, M. R., 1965. Geologia e petrologia da região de Rebordelo-Vinhais. *Rev. fac. cienc. univ. Coimbra*, 36, 287 pp.
- 1966a. As granadas e a sua paragénesese em rochas com elevado grau de metamorfismo. *Mém. e notícias*, 61, 28 pp.
- 1966b. Sobre um piroxenito con hercinite granada e corindo de Nunes (Vinhais-NE de Portugal). *Mém. e notícias*, 61, 17 pp.
- Priem, H. N. A., Boelrijk, N. A. I. M. & Verschure, R. H., 1964. Radiometrische ouderdomsbepalingen volgens de Rb-Sr methode aan "whole rock" monsters en aan mineraalconcentraten van de grofporfierische biotietgraniet in de Serra do Morão, Noord Portugal (61 Mar. 4). *Geol. mijnb.*, 43, p. 14—17.

- Boelrijk, N. A. I. M., Verschure, R. H. & Hebeda, E. H., 1965. Isotopic ages of two granites on the Iberian continental margin: the Traba granite (Spain) and the Berenga granite (Portugal). *Geol. mijnb.*, 44, p. 353—354.
- Boelrijk, N. A. I. M., Verschure, R. H., Hebeda, E. H. & Floor, P., 1966. Isotopic evidence for Upper-Cambrian or Lower-Ordovician granite emplacement in the Vigo area, north-western Spain. *Geol. mijnb.*, 45, p. 36—40.
- Quensel, P., 1952. The charnockite series of the Varberg district on the southwestern coast of Sweden. *Ark. min. geol.*, 1, p. 227—332.
- Ragan, D. M., 1963. Emplacement of the twin sisters dunite, Washington. *Am. jour. sci.*, 261, p. 549—565.
- Rajasekaran, K. C., 1961. Smaragdite from a garnetiferous pyroxenite, Mettupalaiyam Coimbatore district, Madras state, India. *Ind. min.*, 2, p. 42—47.
- Rammelsberg, C. F., 1875. *Handbuch der Mineralchemie*. Leipzig, Wilhelm Engelmann Verlag, 744 pp.
- Reed, J. J., 1964. Mylonites, cataclasites, and associated rocks along the alpine fault, South Island, New Zealand. *New Zeal. jour. geol. geophys.*, 7, p. 645—685.
- Richardson, S. W., 1965—1966. Staurolite. *Ann. rept. dir. geophys. lab.*, Washington, p. 248—252.
- Riess, E. R., 1878. Untersuchungen über die Zusammensetzung des Eklogits. *Tsch. min. petr. Mitt.*, N.F. 1, p. 165—241.
- Roever, W. P. de, 1957. Sind die alpinotypen Peridotitmassen vielleicht tektonisch verfrachtete Bruchstücke der Peridotitschale? *Geol. Rdsch.*, 46, p. 137—146.
- Romijn, E., 1959. Petrografische kartering van het westelijke gedeelte van Cabo Ortegal (Galicie, Sp.). Unpublished report, Leiden.
- Rost, F., 1959. Probleme ultrabasischer Gesteine und ihrer Lagerstätten. *Freib. Forsch. H.*, C 58, p. 28—65.
- 1961. Zur Stellung der Granat-ultrabasite des sächsischen Grundgebirges. *Freib. Forsch. H.*, C 119, p. 121—134.
- 1963. Ultrabasite der Kruste und ihr Mineralbestand. *N. Jb. Min. Mh.*, p. 263—272.
- & Grigel, W., 1964. Über accessorische Elemente in mitteleuropäischen Eklogiten und ihre Mineralien. *Geochim. cosmoch. acta*, 28, p. 1933—1951.
- Rubbens, I. B. H. M., 1963. Resultaten van kartering en petrografisch onderzoek in het "Complejo Antiguo". Galicie, Spanje. Unpublished report, Leiden.
- Sahama, T. G., 1935. Petrographie der Eklogiteinschlüsse in den Gneisen des südwestlichen Liverpoollandes, Ostgrönland. Anhang: Granulitartiger Gneiss nordöstlich von Kap Hope. *Meddel. Grönl.*, 95 (5), 41 pp.
- Saravanan, S., 1960. Eclogites of Kanjamalai, Salem district, Madras state. *Ind. min.*, 1, p. 69—84.
- Scharbert, H. G., 1954. Die eklogitischen Gesteine des südlichen Groszvenedigergebietes (Osttirol). *Jahrb. geol. Bundesanst.*, 97, p. 39—63.
- 1963. Zur Nomenklatur der Gesteine im Granulitfazies. *Tsch. min. petr. Mitt.*, D.F. 8, p. 591—598.
- 1964. Die Granulite des südlichen niederösterreichischen Moldanubikums. *N. Jb. Min. Abh.*, 101, p. 27—66.
- Scheumann, K. H., 1954. Bemerkungen zur Genese der Gesteins- und Mineralfazies der Granulite. *Geologie*, 3, p. 99—154.
- 1956. Boudinagen und Mikroboudinagen im meta-gabbriischen Plagioklas-Amphibolit von Rosswein. *Abh. Sächs. Akad. Wiss. Leipzig, math. nat. Kl.*, 45, p. 1—18.
- 1960. Das Kornerupingestein von Waldheim in seinem genetischen Zusammenhang. *Abh. Sächs. Akad. Wiss. Leipzig, math. nat. Kl.*, 47 (2), p. 5—22.
- 1961. "Granulit" eine petrographische Definition. *N. Jb. Min. Mh.*, p. 75—80.
- Schuilare, R. D., 1965. Residual cipolino: end product of calcareous rocks in regional metamorphism. *Norsk. geol. tidsskr.*, 45, p. 303—313.
- Schüller, A., 1945. Zur tektonischen Analyse der Münchberger Gneismasse. *Zeitschr. deutsch. geol. Ges.*, 97, p. 66—94.
- 1948. Petrogenetische Studien zum Granulitproblem an Gesteinen der Münchberger Masse. *Heidelb. Beitr. Min. Petr.*, 1, p. 269—340.
- Schulz, G., 1835. *Descripción geognóstica del Reino de Galicia, avec une carte pétrographique de 1834*. Madrid, Gráficas Reurnidas S.A., 1935, 176 pp.
- Segnit, E. R., 1953. Some data on synthetic aluminous and other pyroxenes. *Min. mag.*, 30, p. 218—226.
- Seitsaari, J., 1962. On metamorphism and structures in the Ahlainen area, Southwestern Finland. *Bull. commis. géol. Finl.*, 204, p. 5—31.
- Sen, S. K., 1959. Potassium content of natural plagioclases and the origin of antiperthites. *Jour. geol.*, 67, p. 479—495.
- Shidô, F., 1958. Plutonic and metamorphic rocks of the Nakuso and Iritōno districts in the central Abukuma Plateau. *Jour. fac. sci. Tokyo, sec. II*, 11, p. 131—217.
- 1959. Notes on rock-forming minerals 9. Hornblende bearing eclogite from Gongen-yama of Higasi-Akai in the Bassi district, Sikoku. *Jour. geol. soc. Jap.*, 65, p. 701—703.
- Smulikowski, K., 1960. Comments on eclogite facies in regional metamorphism. 21st Internat. geol. congr. rept., 13, p. 372—382.
- 1964a. Les relations pétrogénétiques entre les éclogites et les amphibolites dans le massif cristallophyllien du Mont Śnieżnik. *Bull. soc. géol. France, sér. 6, 7*, p. 232—239.
- 1964b. An attempt at eclogite classification. *Bull. acad. polon. sci., sér. sci. géol. géog.*, 12, p. 27—33.
- 1964c. Le problème des éclogites. *Geol. Sudetica*, 1, p. 13—77.
- 1965. Chemical differentiation of garnets and clinopyroxenes in eclogites. *Bull. acad. polon. sci., sér. sci. géol. géog.* 13, p. 11—18.
- Sobolev, V. S. & Bazarova, T. Y., 1963. Crystallization temperature of disthene in pegmatites. *Dokl. akad. nauk. USSR.*, earth sci. sec., in transl., 153, p. 174—175.
- Sørensen, H., 1953. The ultrabasic rocks at Tovqussac, West Greenland. A contribution to the peridotite problem. *Meddel. Grönl.*, 136 (4), 86 pp.
- Spry, A., 1963. The occurrence of eclogite on the Lyell Highway, Tasmania. *Min. mag.*, 33, p. 589—593.
- Subramaniam, A. P., 1956. Mineralogy and petrology of the Sittampundi complex, Salem district, Madras state. *Bull. geol. soc. Am.*, 67, p. 317—390.
- 1962. Pyroxenes and garnets from charnockites and associated granulites. In: *Petrologic studies, a volume to honour Buddington*. *Publ. geol. soc. Am.*, p. 21—36.

- Tex, E. den, 1955. Secondary alteration of chromite. *Am. min.*, 40, p. 353—355.
- 1961. Some preliminary results of petrological work in Galicia (N.W. Spain). *Leidse geol. med.*, 26, p. 75—91.
- 1965. Metamorphic lineages of orogenic plutonism. *Geol. mijnb.*, 44, p. 105—132.
- 1966. Aperçu pétrologique et structural de la Galice cristalline. *Leidse geol. med.*, 36, p. 211—223.
- & Floor, P., 1967. A blastomylonitic and polymetamorphic Graben in western Galicia (N.W. Spain), colloque sur les étages tectoniques, 70me anniversaire de C.E. Wegmann, Neuchâtel. In press.
- & Vogel, D. E., 1962. A "Granulitgebirge" at Cabo Ortegal (N.W. Spain). *Geol. Rdsch.*, 52, p. 95—112.
- Thayer, T. P., 1966. Serpentinization considered as a constant volume metasomatic process. *Am. min.*, 51, p. 685—710.
- Tilley, C. E., 1937. Paragenesis of kyanite-eclogites. *Min. mag.*, 24, p. 422—432.
- Tröger, W. E., 1956. *Optische Bestimmung der gesteinsbildenden Mineralien*, T. I, 2nd ed., Stuttgart, Schweizerbart'sche Verlagsbuchhandlung, 147 pp.
- 1959. Die granatgruppe: Beziehungen zwischen Mineralchemismus und Gesteinsart. *N. Jb. Min. Abh.*, 93, p. 1—44.
- 1962. Zur Systematik und Optik der Chloromelanit-Reihe. *Tsch. min. petr. Mitt.*, D.F. 8, p. 24—35.
- Turner, F. J. & Verhoogen, J., 1960. *Igneous and metamorphic petrology*. New York, Mac Graw Hill, 694 pp.
- Udintsev, G. B., 1965. Results of upper mantle project studies in the Indian Ocean by the research vessel "Vityaz". *Geol. surv. Canad. paper*, 66 (14), p. 148—172.
- Velde, B., 1966. Étude minéralogique d'une éclogite de Fayde-Bretagne (Loire Atlantique). *Bull. soc. franç. min. crist.*, 89, p. 358—393.
- Vogel, D. E., 1966a. Nature and chemistry of the formation of clinopyroxene-plagioclase symplectite from omphacite. *N. Jb. Min. Mh.*, 6, p. 185—189.
- 1966b. Las rocas catazonales de la región de Cabo Ortegal. *Leidse geol. med.*, 36, p. 245—256.
- 1967. Excursions in the catazonal rock complexes of the polyorogenic terrain of Cabo Ortegal, NW Spain. *Leidse geol. med.*, 40, p. 75—78.
- & Bahezre, C., 1965. The composition of partially zoned garnet and zoisite from Cabo Ortegal, N.W. Spain. *N. Jb. Min. Mh.*, p. 140—149.
- & Warnaars, F. W., 1967. Meta-olivine gabbro from Cabo Ortegal (N.W. Spain): a case of incipient eclogitization. *N. Jb. Min. Mh.*, p. 110—115.
- Vogt, J. H. L., 1923. Nickel in igneous rocks. *Econ. geol.*, 18, p. 307—315.
- Waard, D. de, 1964. Mineral assemblages and metamorphic subfacies in the granulite-facies terrane of the Little Moose Mountain syncline, South-central Adirondack Highlands. *Proc. Kon. Ned. akad. wet.*, ser. B, 67, p. 344—362.
- 1965a. The occurrence of garnet in the granulite-facies terrane of the Adirondack Highlands. *Jour. petr.*, 6, p. 165—191.
- 1965b. A proposed subdivision of the granulite facies. *Am. jour. sci.*, 263, p. 455—461.
- Wang, H. S., 1939. Petrographische Untersuchungen im Gebiet der Zone von Bellinzona. *Schweiz. min. petr. Mitt.*, 19, p. 21—199.
- Watznauer, A., 1964. Der Begriff der petrographischen Facies. *Ber. geol. Ges. DDR*, 9, p. 109—122.
- Weinschenk, E., 1915. *Die gesteinsbildenden Mineralien*. Freiburg, Herdersche Verlagsbuchhandlung, 261 pp.
- Werner, A. G., 1812. In: C. A. S. Hoffmann, *Mineralogie*, Bd. 2, Freiburg, Graz & Gerlach.
- White, A. R. J., 1964. Clinopyroxenes from eclogites and basic granulites. *Am. min.*, 49, p. 883—888.
- Winchell, A. N. & Winchell, H., 1956. *Elements of optical mineralogy*. Pt. 2, description of minerals. New York, Wiley; London, Chapman & Hall, 4th ed., 551 pp.
- Winkler, H. G. F., 1965. *Die Genese der metamorphen Gesteine*. Berlin, Springer Verlag, 218 pp.
- & Platen, H. von, 1961a. Bildung anatektischer Schmelzen aus metamorphosierten Grauwacken. *Geochim. cosmoch. acta*, 24, p. 48—69.
- & Platen, H. von, 1961b. Experimentelle anatektische Schmelzen und ihre petrogenetische Bedeutung. *Geochim. cosmoch. acta*, 24, p. 250—259.
- Wolff, T. von, 1942. Methodisches zur quantitativen Gesteins- und Mineral-Untersuchung mit Hilfe der Phasenanalyse. (Am Beispiel der mafischen Komponenten des Eklogits von Silberbach.). *Tsch. min. petr. Mitt.*, N.F. 54, p. 1—122.
- Yagi, K., 1966. The system acmite-diopside and its bearing on the stability relations of natural pyroxenes of the acmite-hedenbergite-diopside series. *Am. min.*, 51, p. 976—1000.
- Yoder, H. S., 1950. The jadeite problem. *Am. jour. sci.*, 248, p. 225—248, 312—334.
- 1952. The MgO-Al₂O₃-SiO₂-H₂O system and the related metamorphic facies. *Am. jour. sci.*, Bowen volume, p. 569—627.
- & Chinner, G. A., 1958—1959. Grossularite-almandite-pyroxene-water system. *Ann. rept. dir. geophys. lab.*, Washington, p. 109—112.
- & Sahama, T. G., 1957. Olivine X-ray determinative curve. *Am. min.*, 42, p. 475—491.
- & Tilley, C. E., 1958—1959. Eclogites. *Ann. rept. dir. geophys. lab.*, Washington, p. 89—94.
- & Tilley, C. E., 1962. Origin of basalt magmas: an experimental study of natural and synthetic rock systems. *Jour. petr.*, 3, p. 342—532.
- Zvetkov, A. I., 1945. Synthesis of alumina pyroxenes and dependence of their optics on composition. *Mém. soc. Russe min.*, ser. 2, 74, p. 215—222. *Min. abs.*, 1952, 11, p. 92.

APPENDICES

APPENDIX 1

FIGURES

Fig. i-1. Simplified geological map of northern Galicia' after Parga-Pondal (1963), unpublished data of Mr. R. Capdevila and P. Matte (both of Montpellier University) and Mr. A. Ribeiro (Lisbon University), and mainly unpublished data of the Department of Petrology and Mineralogy of Leiden University.

-  Cretaceous and Caenozoic
-  post-tectonic granite
-  gabbro
-  Ordovician and Silurian
-  Cambrian
-  Precambrian/Ollo de Sapo
-  migmatites, anatexites, two-mica granites and mega
-  metasediments and granite gneisses (undifferentiated)
-  coarse-grained augen gneisses
-  metabasites
-  ultrabasites
-  metasediments
-  fault



Fig. I-1. Relic ophitic garnet mesh enclosing omphacite (cp) and carinthine (h) crystal aggregates in a carinthine eclogite (slide V 1023).

Fig. I-2. Honeycomb pattern of garnet crystals in eclogite from Martinsreuth reflecting the original plutonic character of the metamorphosed rock (after Düll, 1902).

Fig. I-3. Fissures in clinopyroxene (cpx) — showing the same orientation as cracks in garnet (gar) — are filled with stage-1 p.p. symplectite (stippling) and in some places with opaque matter (black). The fissures continue into neighbouring clinopyroxene crystals but not into neighbouring hornblende (hb). Slide V 1273; q = quartz, ru = rutile, a = apatite.

Fig. I-4. Lobular mutual penetration of clinopyroxenes (cpx) resulting from symplectitization. As the symplectitic front (stippling) advances, the texture coarsens to that of a flame-like stage-3 p.p. symplectite. Slide V 1273; q = quartz, hb = hornblende, plag = plagioclase, gar = garnet.

Fig. I-5. Clinopyroxene crystal (cpx) showing a coarse implication structure — stage-4 p.p. symplectite — with 2 plagioclase crystals (hatching in different directions); one of the plagioclase crystals is also found included in the neighbouring clinopyroxene. Along the rims, stage-1 (stippling) and stage-2 (feathered pattern) symplectites are also present. Other constituents are rutile (ru) and quartz (q) (slide V 1043).

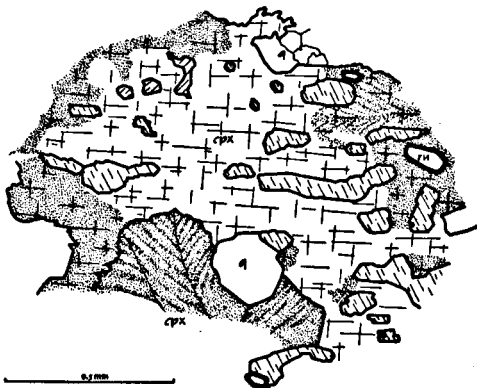
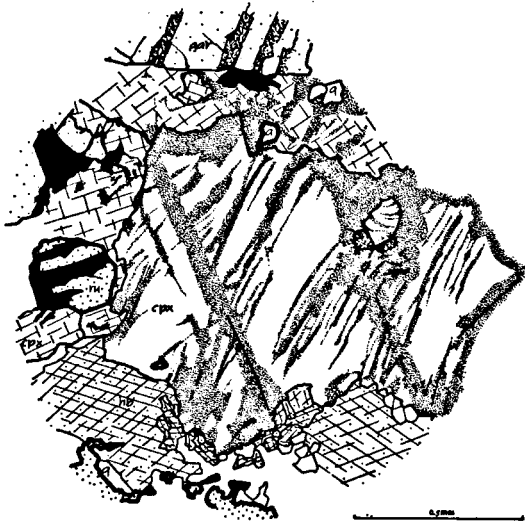
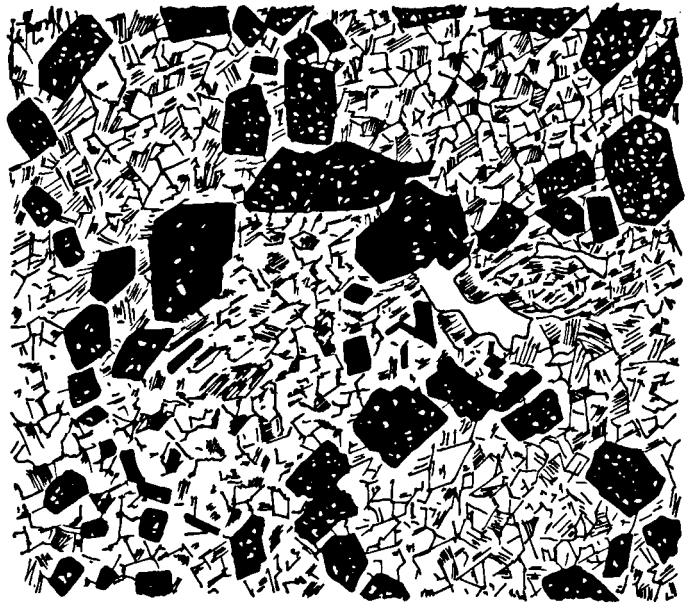
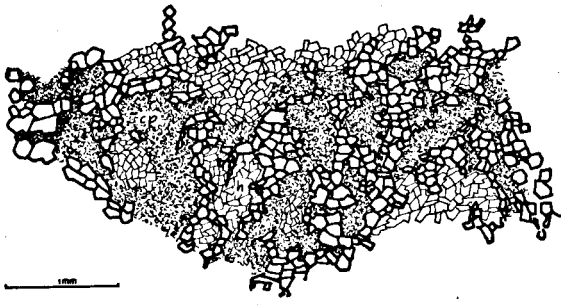


Fig. I-6. Cross-section through a penetrating p.p. symplectite lobe. The cauliflower-like stage-3 symplectite is surrounded by differently oriented stage-2 symplectite (stippling) (slide V 1121).

Fig. I-7. Quartz crystal (q) surrounded by clinopyroxene (cp). Symplectitic parts of the clinopyroxenes (stippling) are separated from quartz by narrow non-symplectitic zones. The intricate interpenetration of the omphacites is indicated by the different directions of the hatching (slide V 1346).

Fig. I-8. Part of a garnet crystal (sparse stippling) in which clouds of rutile dust (dense stippling), rutile grains (black), and sagenite surround a rutile-free part of the garnet crystal with idiomorphic outlines. Slide V 1100; hb = hornblende, cp = clinopyroxene, q = quartz, ap = apatite.

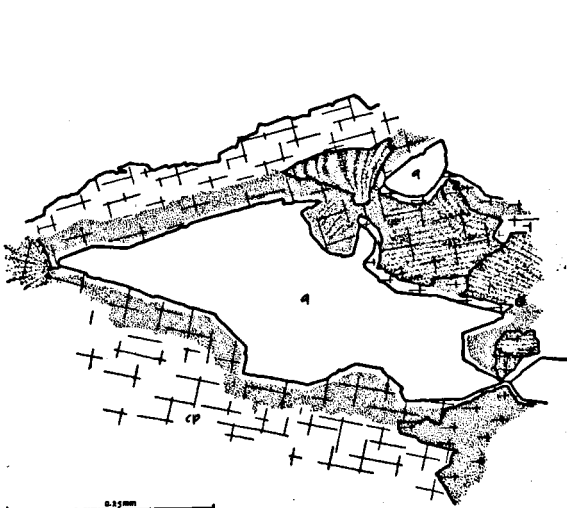
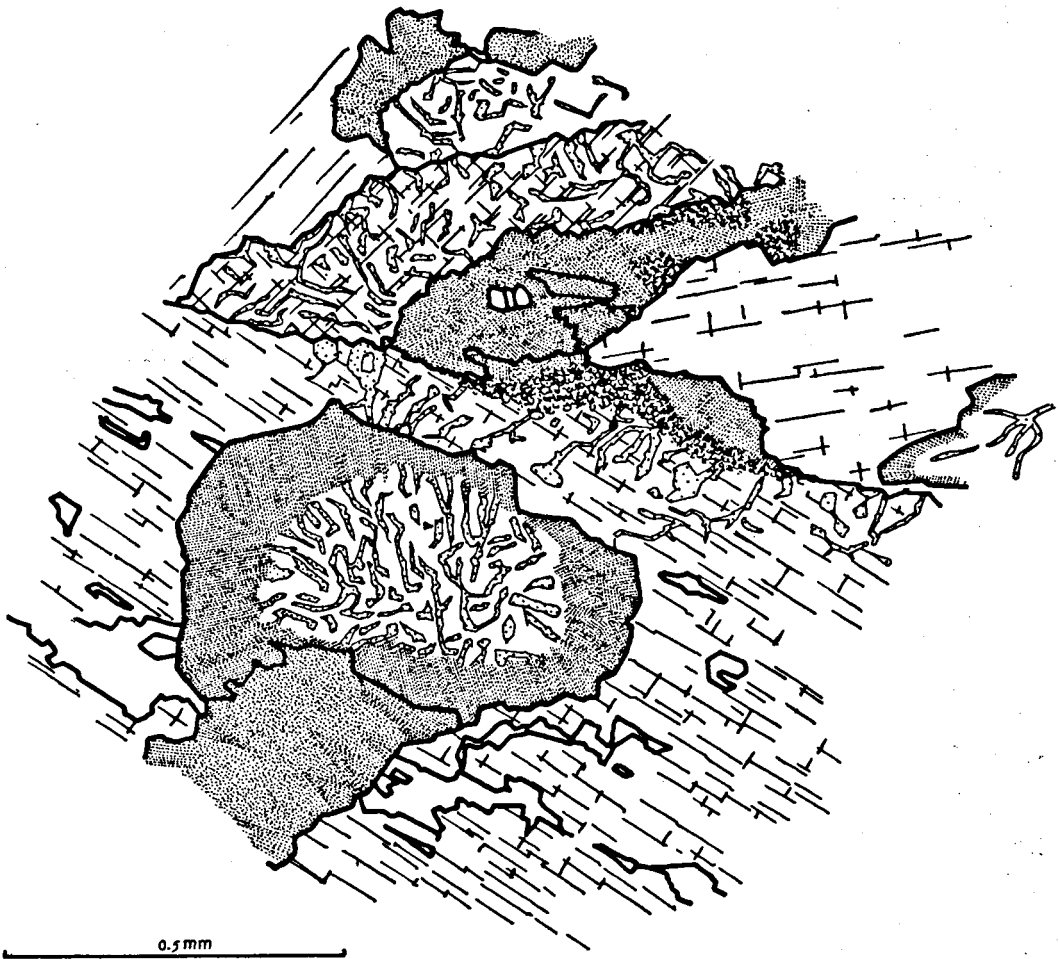


Fig. I-9. Concentrations of rutile-dust — pseudomorphous after pre-existing minerals — in an anhedral garnet crystal. Slide V 1102a; plag = plagioclase, bi = biotite, hb = hornblende.

Fig. I-10. The pattern of the rutile-dust concentrations can be seen to continue from one garnet crystal to the other. Slide V 1102a; q = quartz, bi = biotite, hb = hornblende, plag = plagioclase.

Fig. I-11. Niggli mg/c plot (after Leake, 1964) of Cabo Ortegal eclogitic rocks and contaminated eclogitic rocks, showing the characteristics of a magmatic differentiation series (indicated by arrow) in which the early- and late-stage differentiates are lacking.

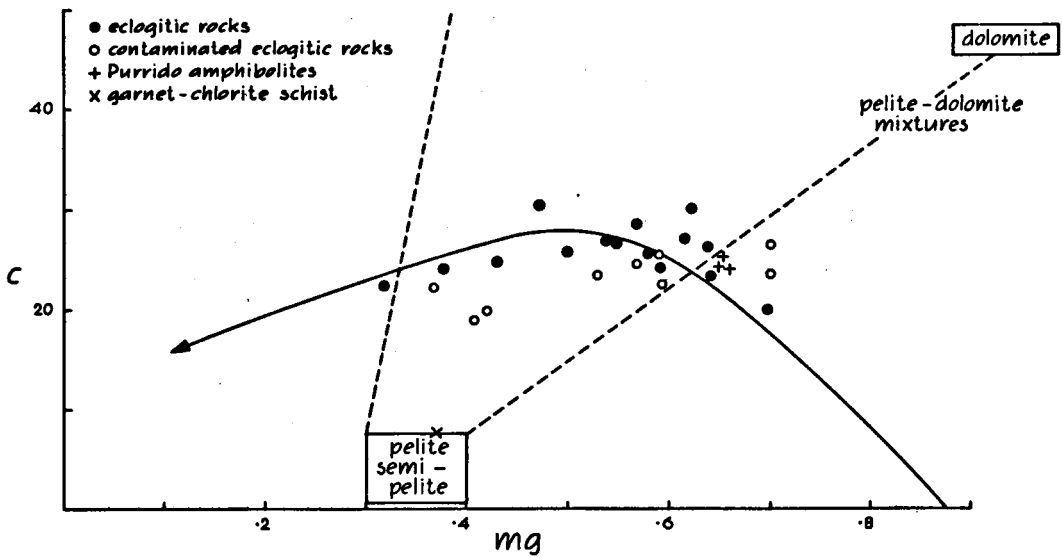
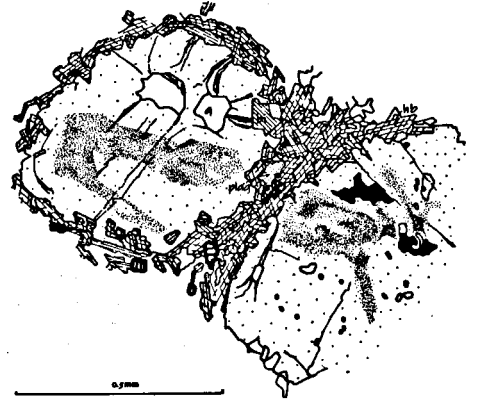
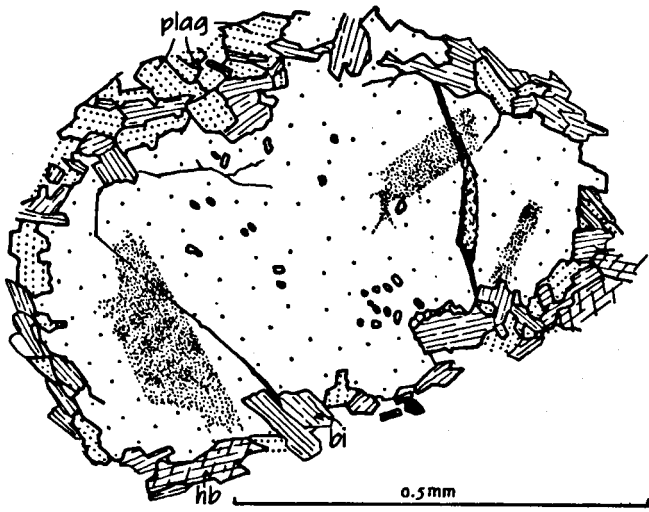
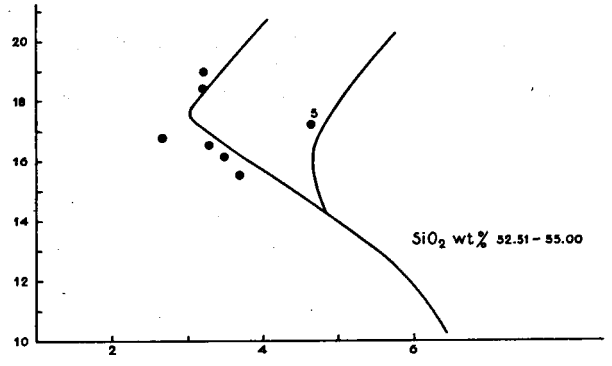
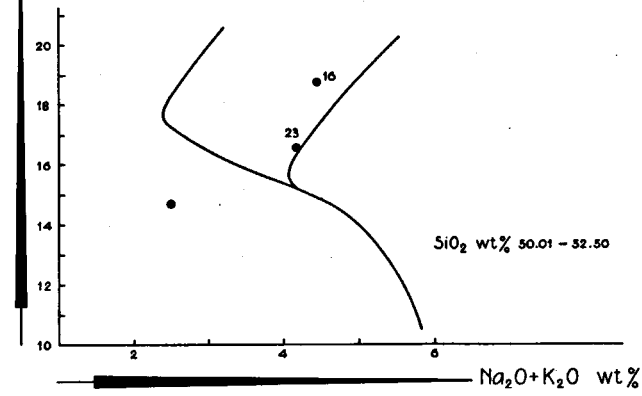
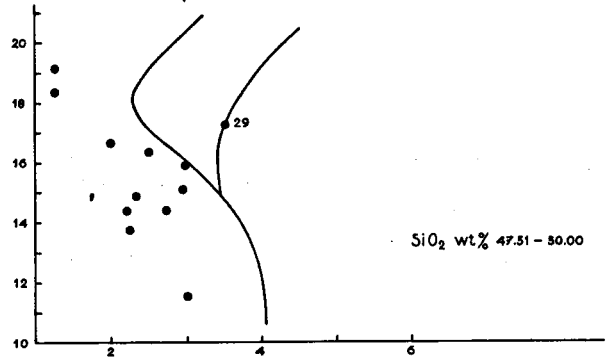
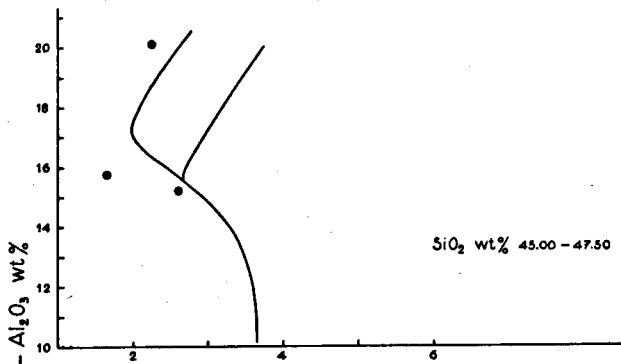


Fig. I-12. Relation of Al_2O_3 /total alkalis for given values of SiO_2 in the Cabo Ortegal eclogitic rocks. Numbers refer to Table I-1. Tholeiitic magmatic rocks plot in the lefthand field, high-alumina basalts in the central field, and alkali basalts in the righthand field.

Fig. I-13. QLM diagram for the mafic rocks from the Concepenido Complex. The differentiation trend for a pacific magmatic suite is indicated by the arrow.



- eclogitic rocks
- contaminated eclogitic rocks
- + Purrido amphibolites
- x garnet-chlorite schist

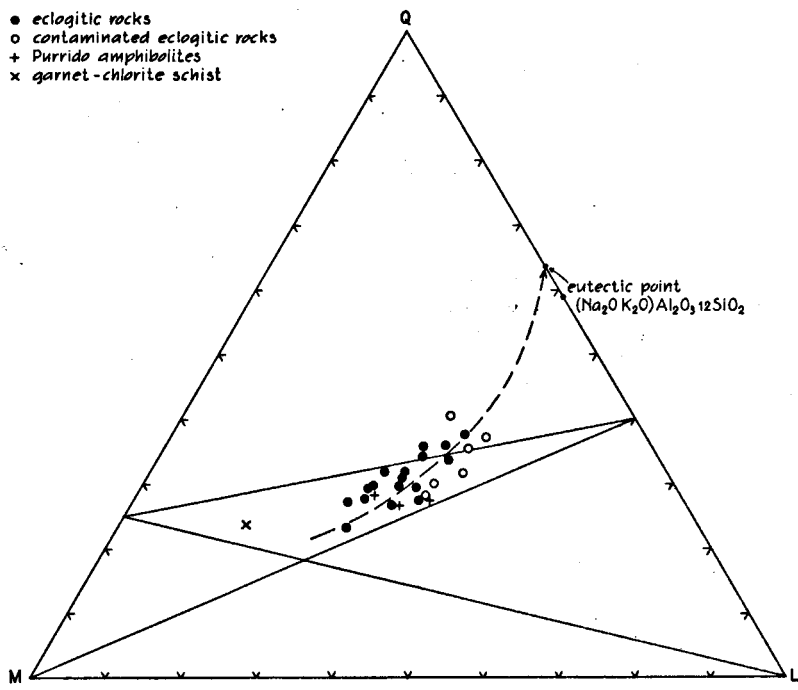


Fig. I-14. Plot of rock analysis (\times), garnet (\bullet), omphacite (\blacktriangle), and carinthine ($+$) in an ACF diagram in which the omphacite-garnet-zoisite and omphacite-garnet-kyanite fields are delineated.

- a, a', a'' clinopyroxene, garnet, and rock of eclogite (sample V 1050).
- B, b, B', b', b'' clinopyroxenes, garnets, and rock of α -zoisite eclogite (sample V 1278).
- c, c', c'', c''' clinopyroxene, garnet, whole rock, and carinthine of carinthine eclogite (sample V 1023).
- d, d', d'' clinopyroxene, garnet, and rock of eclogite (sample M 459).
- e, e', e'' clinopyroxene, garnet, and rock of kyanite eclogite from Weissenstein (Tilley, 1937).

Fig. I-15. Plots of kyanite eclogite (\circ), α -zoisite eclogite (\bullet), α -zoisite-kyanite eclogite (\oplus), and carinthine eclogite (\ominus) from Cabo Ortegal in a QLM diagram. Numbers refer to Table I-1.

Fig. I-16. QLM plot of Cabo Ortegal kyanite eclogites (\times) compared to several kyanite eclogites collected from previous publications (\bullet): Brière, 1920; Düll, 1902; Eigenfeld-Mende, 1948; Riess, 1878; Tilley, 1937, Wagner, 1914, Williams 1932.

Fig. I-17. PT graph illustrating the respective stability fields of eclogite-facies and high-pressure granulite-facies rocks for quartz tholeiitic compositions (after Green & Ringwood, 1966b). The field in which zoisite and kyanite can stably coexist is indicated by a heavier line (after Pistorius *et al.*, 1962); this line and the dashed line represent the presumed limits of P and T for the Cabo Ortegal eclogitic rocks. For comparison, the equicomposition curves of omphacite coexisting with quartz (after Kushiro, 1964—1965) and the 10 and 14° C/km geothermal gradients are also given.

Fig. I-18. Location of orthogneiss (●) and non-migmatic paragneiss (×) in the Chimparragneiss Formation. Areas in which no paragneiss was found are surrounded by a dashed line. The coincidence of non-migmatic paragneisses with a synclinal axis, constructed from three sections, is quite striking.

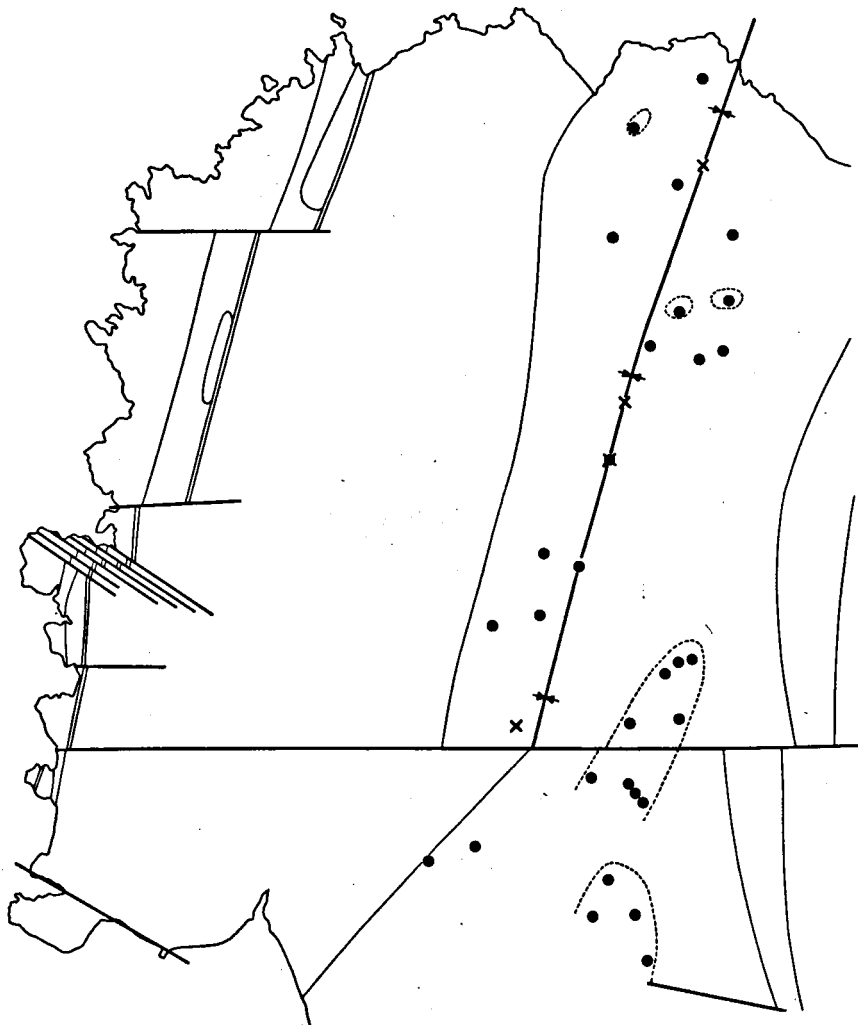
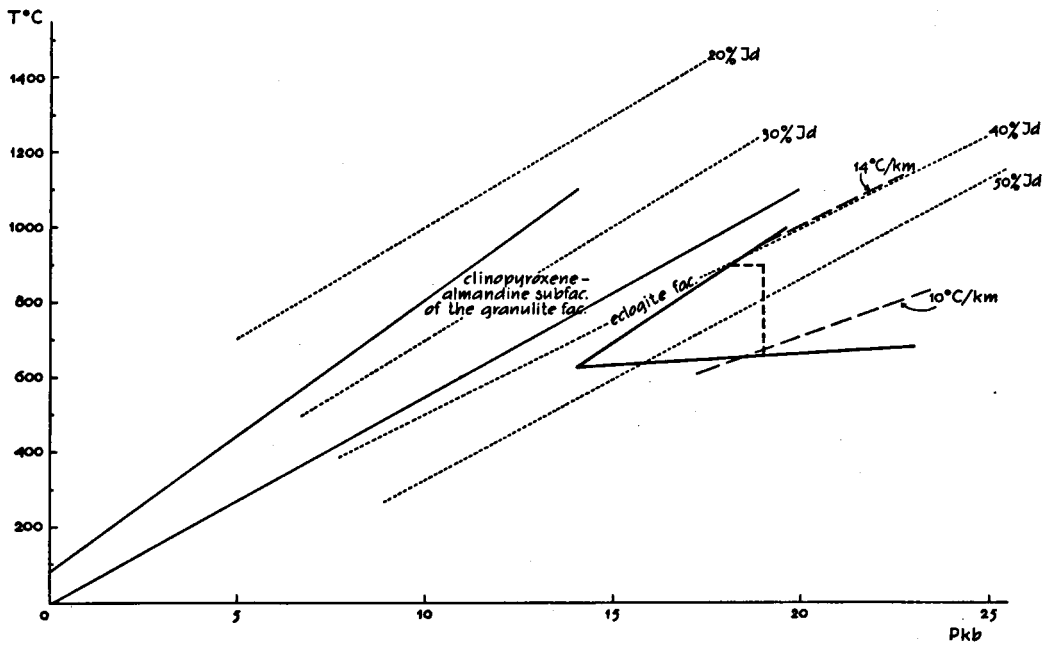


Fig. I-19. QLM plot of Cabo Ortegal paragneisses (o) as compared with graywackes (●). Numbers 1—12 refer to Table I-4. The recalculated value of analysis 12 after addition of eutectic melt is represented by 12'. The graywacke analyses (numbers 13—29) were collected from the following literature: 13, Clarke, 1924, p. 547; 14—28, Pettijohn, 1957, pp. 306—307; 29, US. Geol. surv. bull., 168, p. 245.

Fig. I-20 a—d. Projections of banded gneisses (+), Cariñogneisses (o), blastomylonite (⊖), and Chimparragneiss (●) in the following ACF and A'KF diagrams:

- Partially drawn ACF diagram for the eclogite facies.
- A'KF diagram for the kyanite-almandine-muscovite sub-facies of the almandine amphibolite facies.
- ACF diagram for the clinopyroxene-almandine sub-facies.
- A'KF diagram for the staurolite-almandine sub-facies of the almandine amphibolite facies.

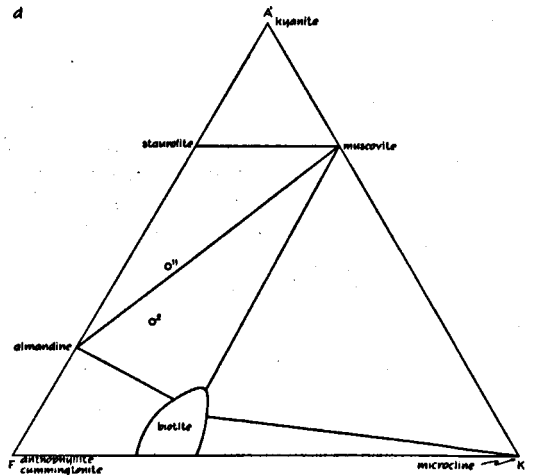
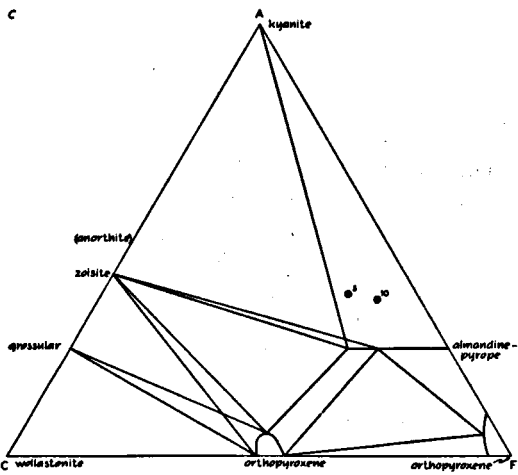
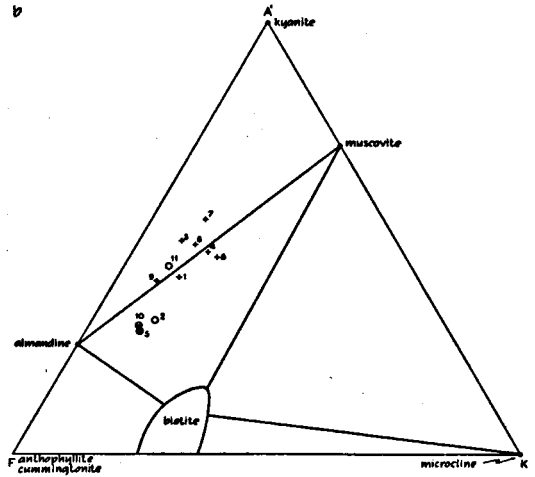
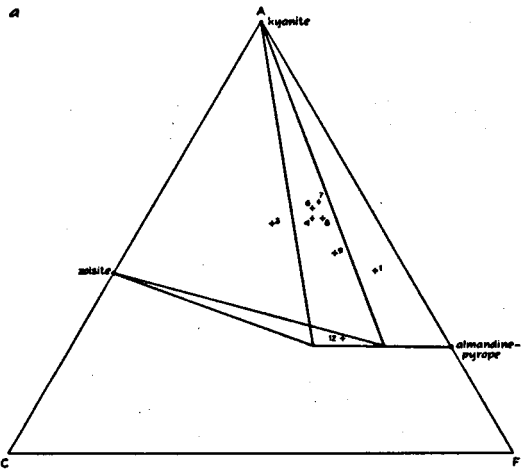
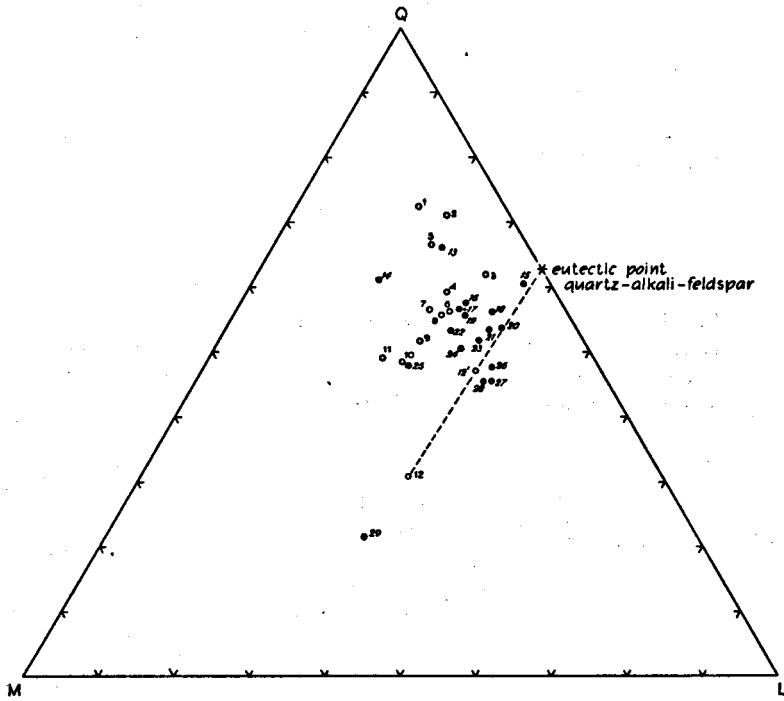
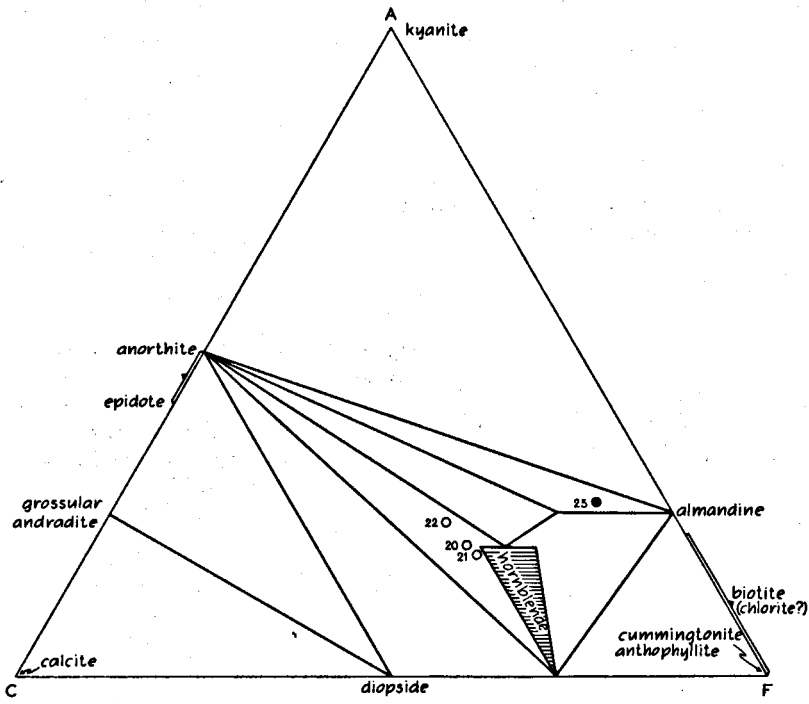


Fig. I-21. Projections of Purrido amphibolite (o) and garnet-chlorite schist (●) in an ACF diagram for the kyanite-almandine-muscovite subfacies of the almandine amphibolite facies. Numbers refer to Table I-1.

Fig. I-22. Drawing of folded amphibolite boudins in an amphibolite matrix at location V 320—V 403. The places from which the samples were taken are indicated by the number of the sample.



-  competent rock
-  plagioclase concentrations

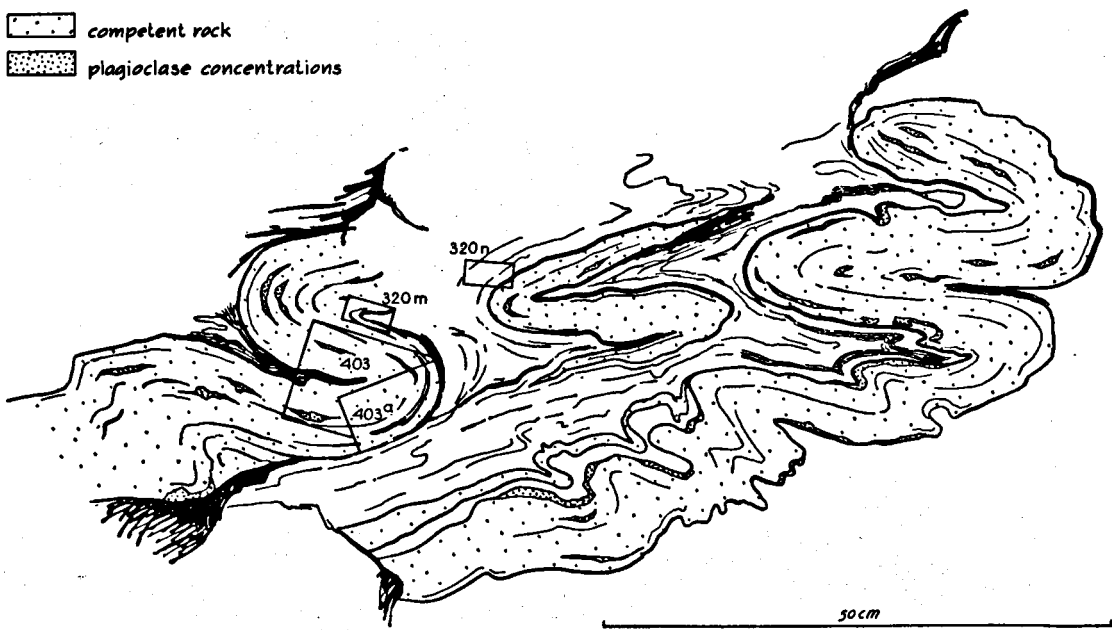


Fig. II-1. Microfolded pargasite streaks in serpentinized pargasite peridotite (stippling). Sample R 20.

Fig. II-2. Microfolded garnet pyroxenite vein (sub-horizontal) with transverse serpentine veins (subvertical) in serpentinized pargasite peridotite (stippling). Bottom left, boudin-like garnet relic (hatched; length 5 cm) from amphibolized garnet pyroxenite vein. Drawn after photograph of location V 1405, looking N.

Fig. II-3. F-corner of the ACF diagram for the granulite facies (clinopyroxene-almandine subfacies); slightly modified after O'Hara & Mercy's (1963) Al-Mg+Fe-Ca triangle. Numbers refer to Table II-1.

Fig. III-1. Schematized map of the Bacariza Formation showing location of exposures of paragneiss (●) and calc-silicate rock (○).

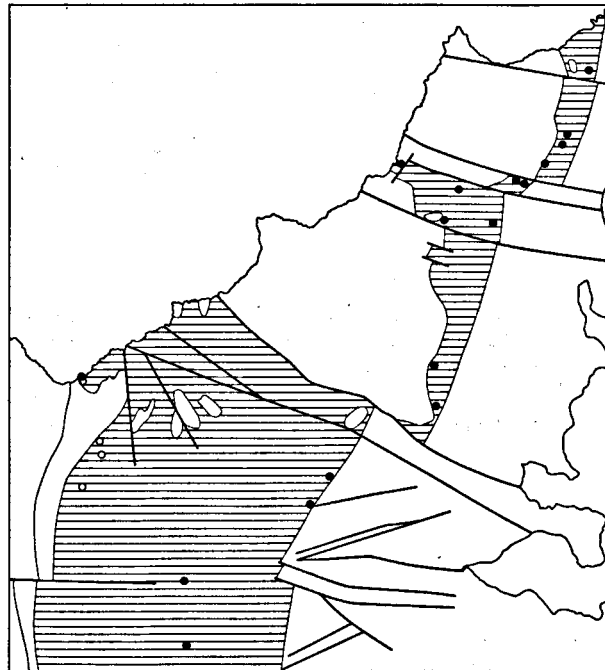
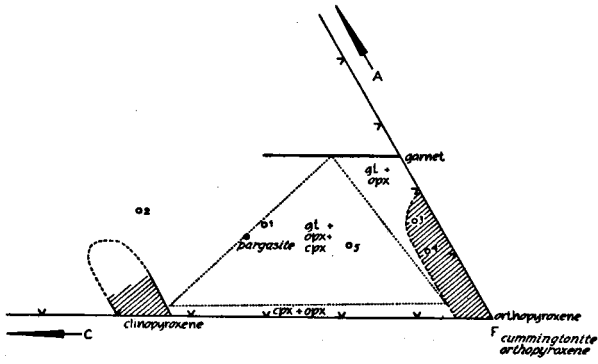
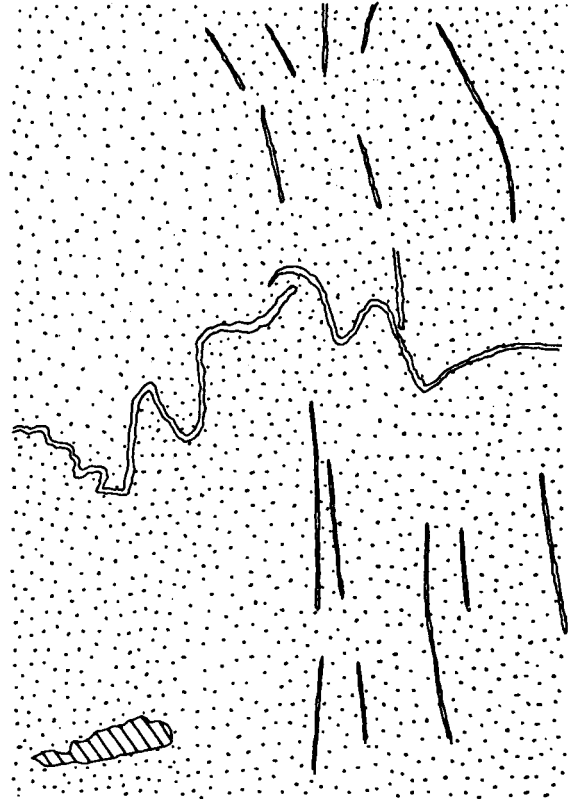
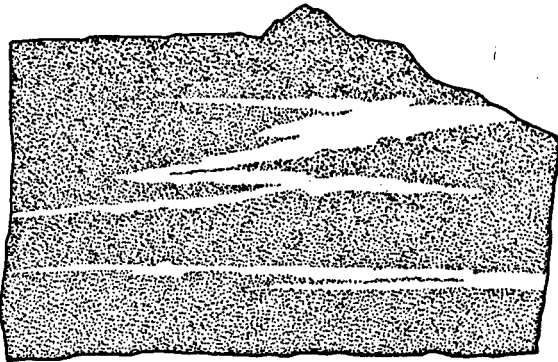


Fig. III-2. QLM plot for metabasites from the Capelada Complex, with a tentative trend-line (dashed). For comparison, the trend-line for eclogitic rocks (solid) is also given. Numbers refer to Table III-3.

Fig. III-3. c/mg Plot (after Leake, 1964) for metabasites from the Capelada Complex. Projection points of metabasites from the Concepenido Complex are given for purposes of comparison (cf. Fig. I-11). Numbers refer to Table III-3. Arrow indicates trend of Karroo dolerites as given by Leake.

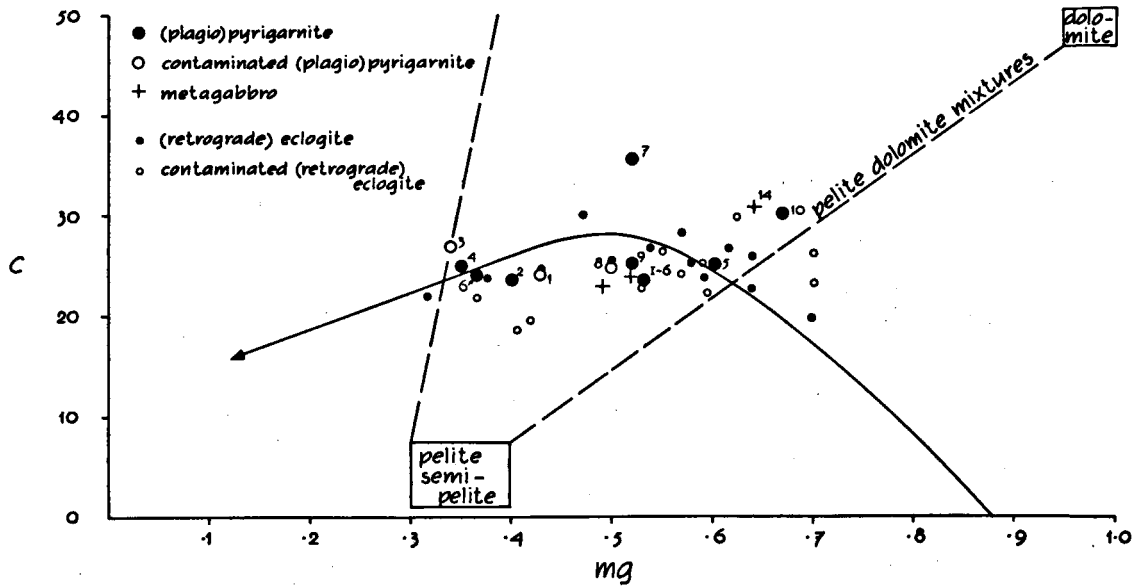
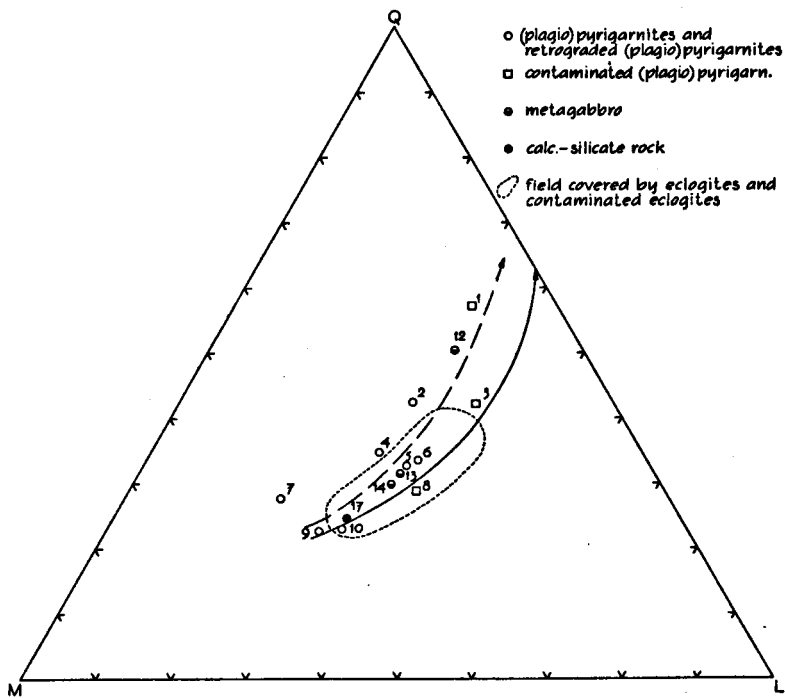


Fig. III-4. Position of QLM plots of paragneiss and leptynite with respect to the fields covered by paragneisses of the Concepenido Complex (dashed line) and graywackes selected from the literature (solid line) as given in Fig. I-19. Numbers refer to Table III-3.

Fig. III-5. ACF projection points for minerals from Capelada Complex rocks. o: garnets from (plagio)pyrigarnites (samples V 1243 -1; M 616 -2; G 1—16 -3) from leptynites (samples V 1193 -4; V 1243a -5) and from a metanorite (sample E 327b -8). ●: hornblende from sample V 1267 -7. ●: clinopyroxene from sample V 1234 -6.

Fig. III-6. Projection points of the rocks from the Capelada Complex in an ACF diagram for the clinopyroxene-almandine subfacies of the granulite facies; with added projection point and (dashed) tie-lines for the hornblende-clinopyroxene-almandine subfacies of the granulite facies. Numbers refer to Table III-3; for analysis I-6 see Table I-1.

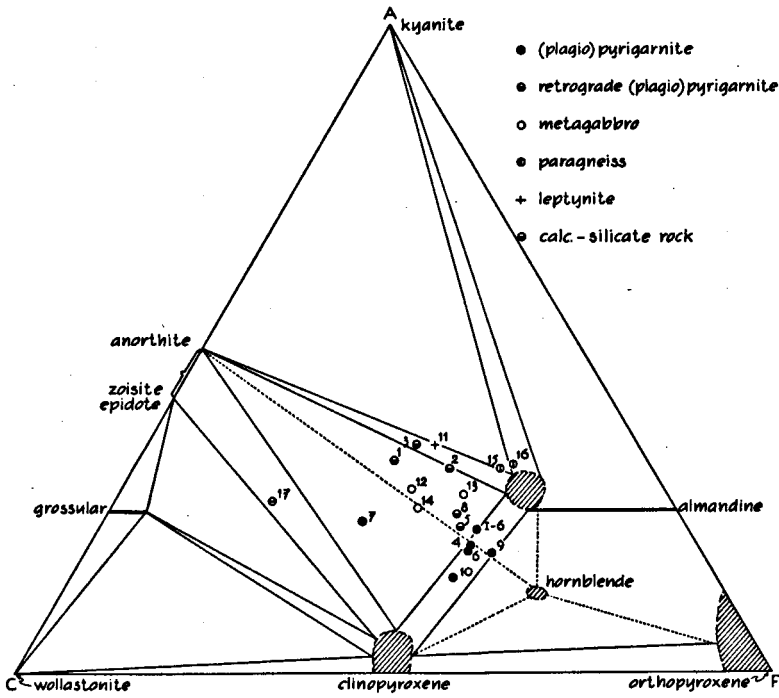
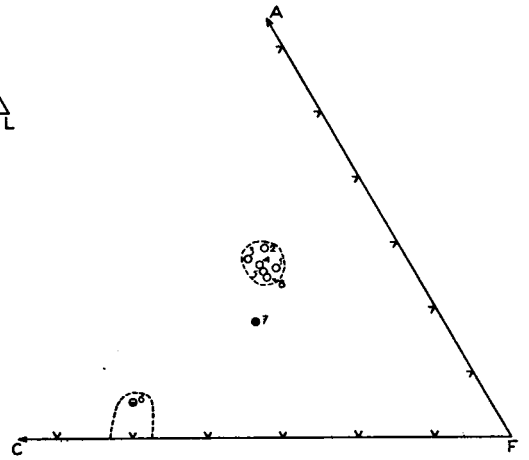
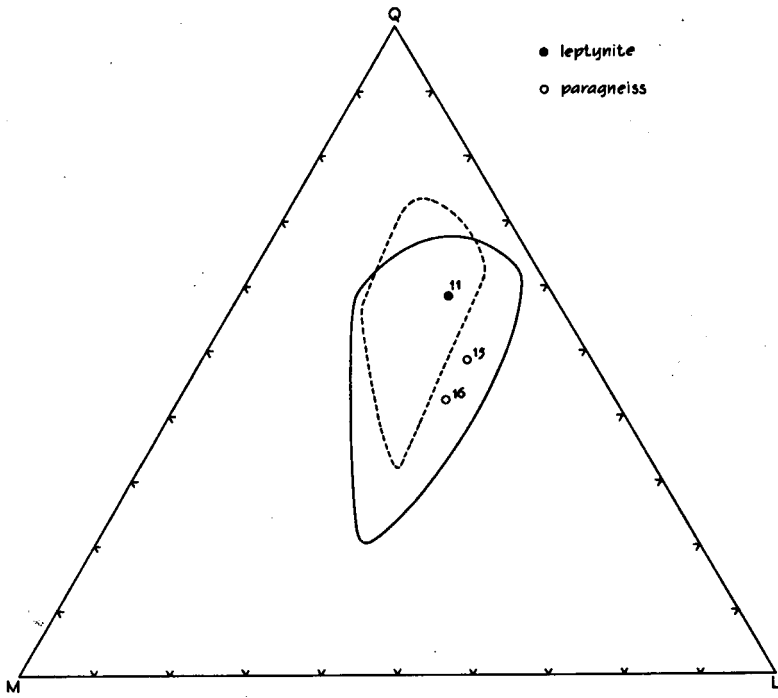
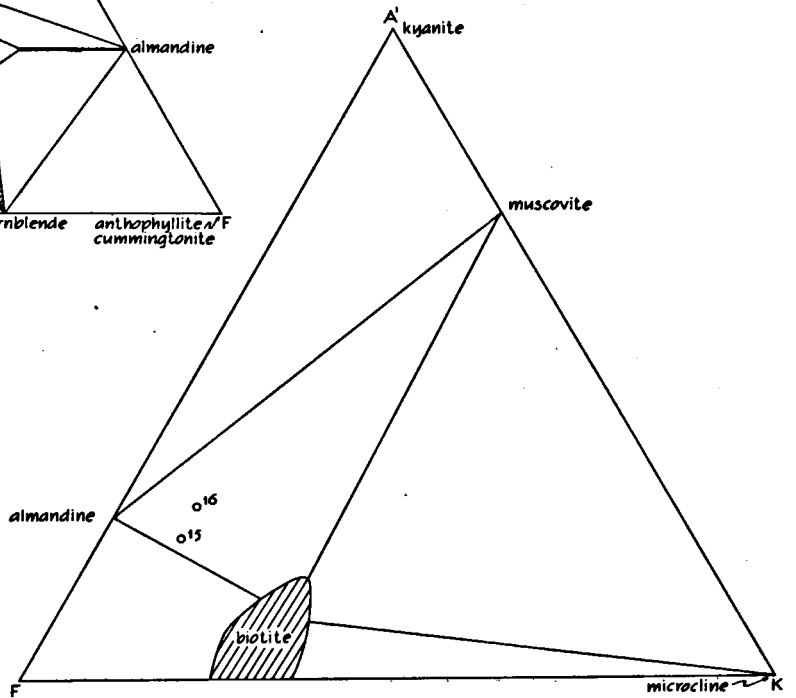
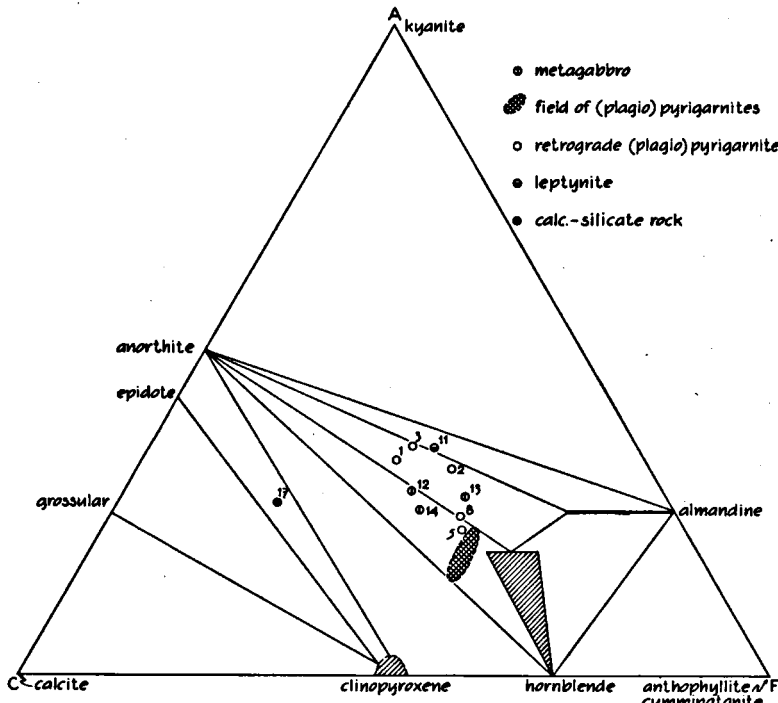


Fig. III-7. Projection points of the rocks from the Capelada Complex (paragneisses excepted) in an ACF diagram for the kyanite-almandine-muscovite subfacies of the almandine amphibolite facies. Numbers refer to Table III-3.

Fig. III-8. Projection points of paragneisses from the Capelada Complex in an A'KF diagram for the kyanite-almandine-muscovite subfacies of the almandine amphibolite facies. Numbers refer to Table III-3.

Fig. V-1. Compositions of Cabo Ortegal garnets plotted in an Al+Sp - Gr+An - Py diagram. Solid lines indicate the limits of the fields for garnets from low and intermediate pressure and high pressure lineages; dashed lines indicate limits of garnet compositions for group a, group b, and group c eclogites (Coleman *et al.*, 1966). Field indicated by solid outline shows limiting compositions for amphibolite garnets (after Tröger, 1954). Dashed and dotted outlines indicate fields covered by Cabo Ortegal pyrigarnite and eclogite garnets.



- eclogite garnet
- △ hornblende eclogite + amphibolite eclogite garnet
- banded gneiss garnet
- x pyrigarnite garnet
- leptynite garnet
- metagabbro garnet

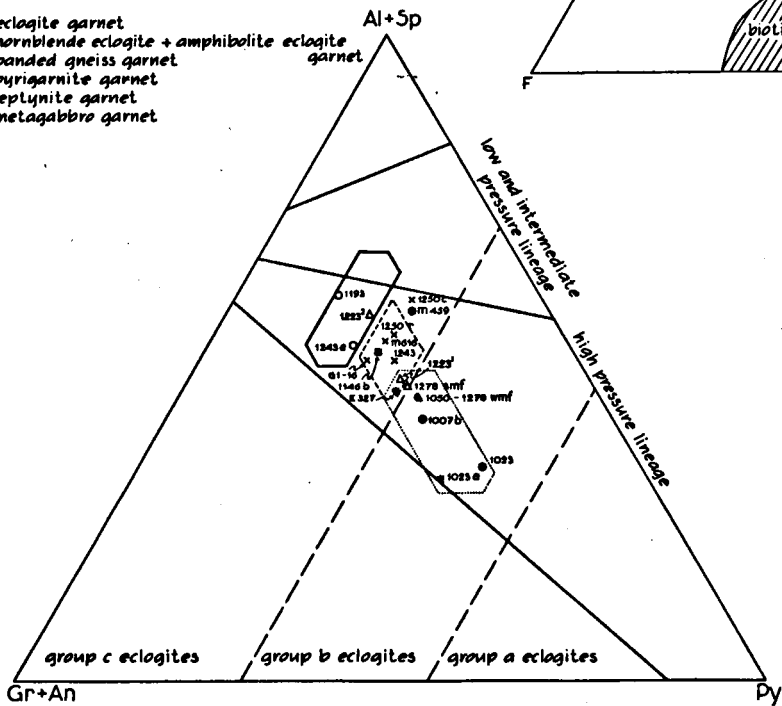


Fig. V-2. Compositions of garnets from charnockites (+), from Cabo Ortegal eclogites (×), from eclogites of other localities (■; Lee *et al.*, 1963), and from pyrigarnites of Cabo Ortegal and other localities (●), and the fields they occupy in the Al+Sp - Gr+An - Py diagram. For purposes of comparison, Tröger's (1954) limiting-compositions for garnets from eclogites, metagabbros, charnockites + granulites, and amphibolites + glaucophane schists are indicated by dotted outlines.

Fig. V-3. a_0 - n_D diagram (after Frietsch, 1957) for 12 garnets from Capelada Complex rocks. ■ plagiopyrigarnite garnet, ● leptynite garnet, □ amphibolite garnet, ○ calc-silicate rock garnet, △ garnet-biotite gneiss garnet.

Fig. V-4. a_0 - n_D diagram (after Frietsch, 1957) for 20 eclogitic and amphibolitic garnets of the Concepenido Complex. ● Eclogite garnet, × hornblende eclogite and amphibolite eclogite garnet, ▲ garnet from amphibolite retrograde after eclogite, ■ garnet from garnet-chlorite schist.

Fig. V-5. a_0 - n_D diagram (after Frietsch, 1957) for 35 garnets from the Banded Gneiss Formation. ● Garnets with constant unit-cell dimensions, × garnets with variable unit-cell dimensions, --- tie-line for garnets from one sample with strongly varying unit-cell dimensions.

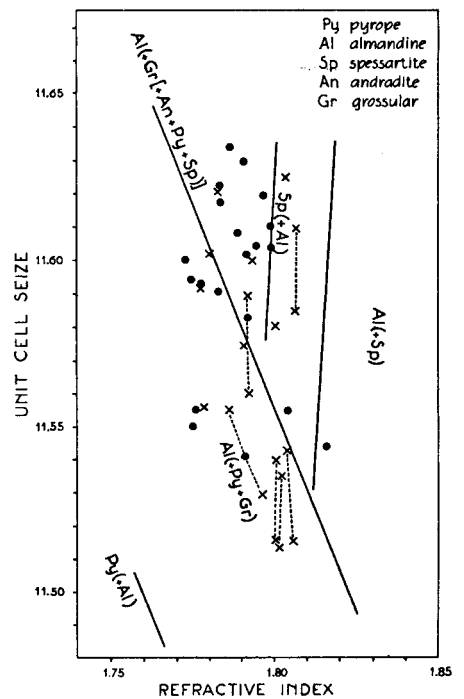
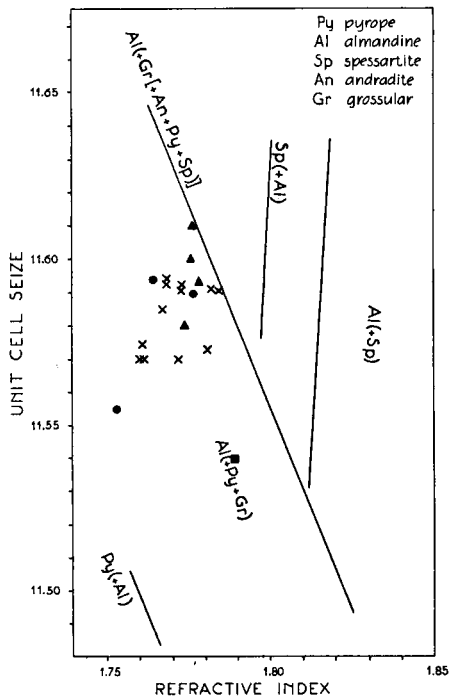
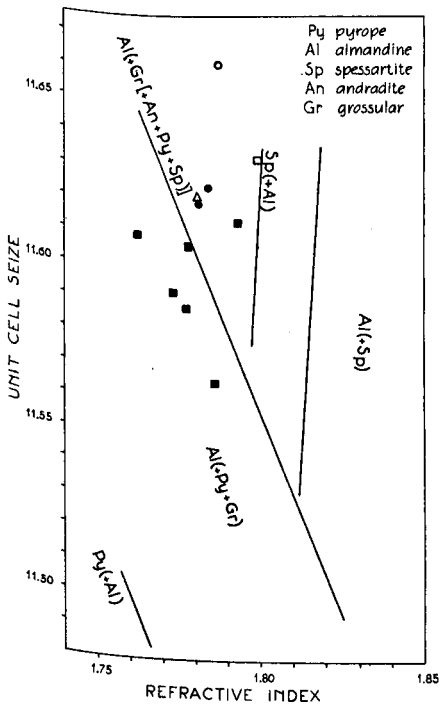
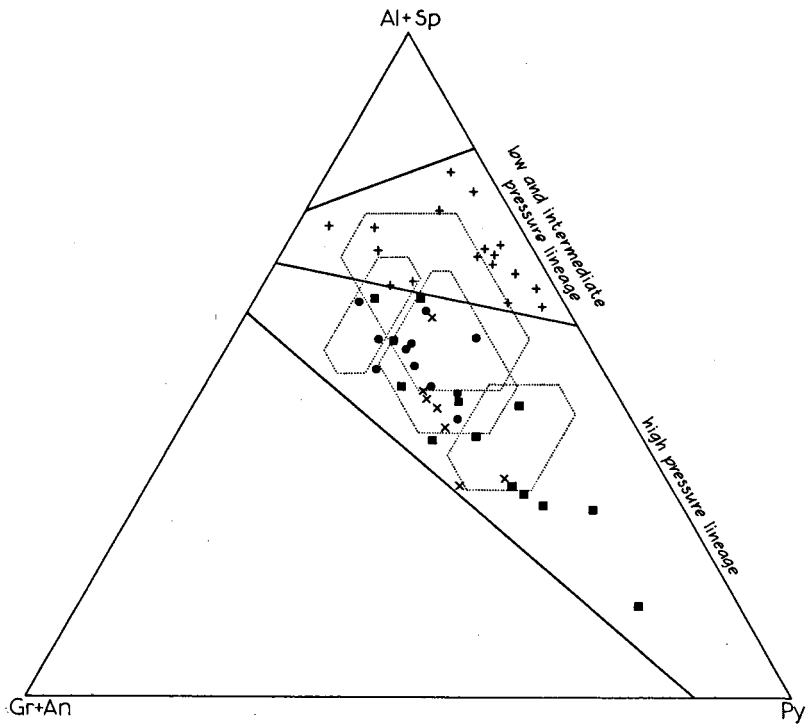
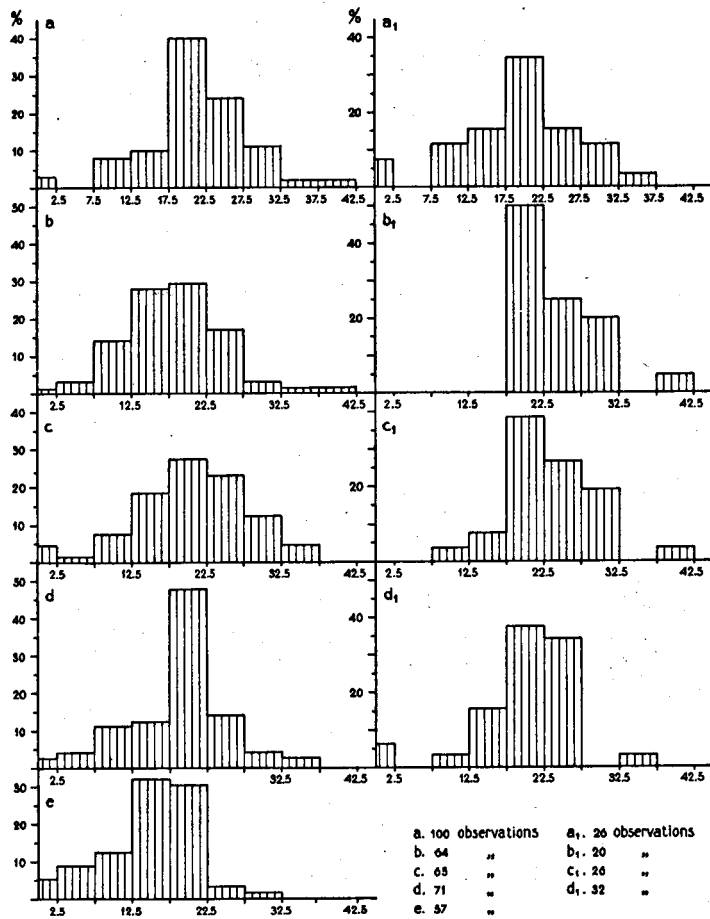
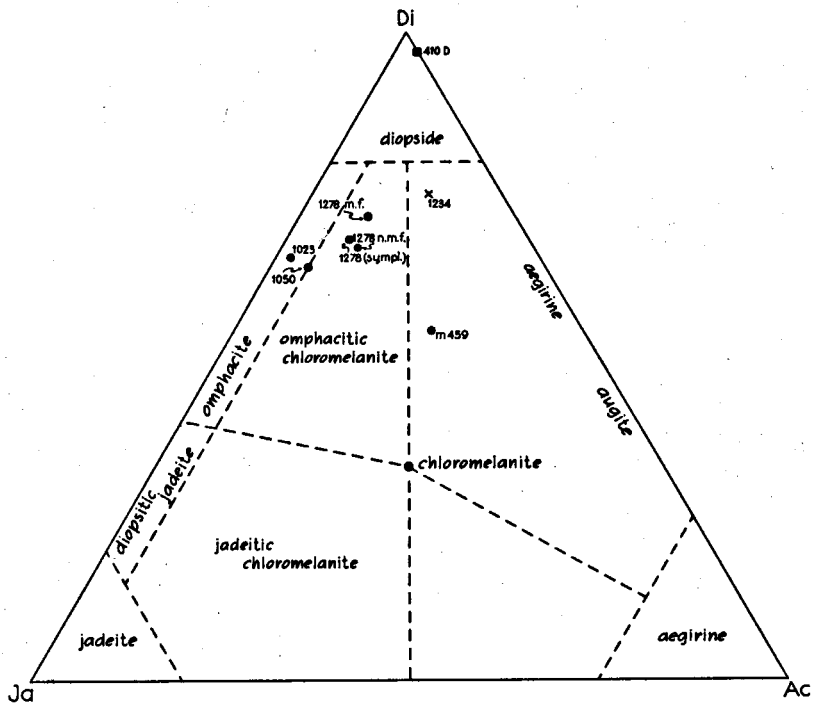


Fig. V-6. Compositions of Cabo Ortegal clinopyroxenes plotted in Tröger's (1962) diopside-jadeite-aegirine diagram. o Clinopyroxene from eclogite, × clinopyroxene from pyrigarnite, □ clinopyroxene from calc-silicate rock.

Fig. V-7. Histograms showing the frequency distribution of anorthite percentages of plagioclases from a. Capelada Complex rocks, b. Chimparragneisses, c. Cariñogneisses, d. banded gneisses, e. metabasite lenses occurring in the Banded Gneiss Formation. The plagioclases occurring in the Capelada Complex are further subdivided into: a₁. plagiopyrigarnites, b₁. retrograde (plagiopyrigarnites with relics of clinopyroxene, c₁. biotite gneisses, d₁. amphibolites without relics of clinopyroxene.



APPENDIX 2

TABLES

Wt. %	1	2	3	4	5	6	7	8	9	10	11	12	13	14	15	16	17	18	19	20	21	22	23	24	25	26	27	28	29	
	Ma 12	V102a	Ma 15	Ma 9	Ma 16	V367	V1174	D 10	V1053	V1030	V1278	V1055	Ma 6	Ma 59	V1085	V1394A	V1394B	V1016	V1054	V118	01-7	V1008	V1014B	V131a	Ma 13	V1050	V1023	V1051		
SiO ₂	52.31	57.16	52.88	49.36	53.43	54.78	53.46	54.38	49.56	48.92	48.30	47.02	47.70	49.54	49.10	51.46	52.80	48.30	49.14	47.54	48.28	48.06	50.90	48.66	40.32	46.83	48.00	44.92	48.52	
Al ₂ O ₃	14.72	15.54	16.66	15.22	17.15	16.09	18.35	16.78	19.27	13.87	16.77	15.16	14.58	11.68	16.51	18.74	18.82	18.34	14.48	15.99	14.23	17.14	16.59	15.01	15.36	20.10	16.18	15.75	17.36	
Fe ₂ O ₃	6.93	-	4.30	6.23	3.96	0.99	0.36	0.38	2.22	4.92	1.63	4.52	4.27	4.46	-	-	-	0.17	1.20	1.81	3.26	3.67	5.21	1.58	2.84	9.02	1.98	2.28	4.09	
P ₂ O ₅	9.35	9.76	7.40	9.25	6.43	8.05	6.03	5.55	7.76	11.02	10.03	6.64	8.47	12.95	9.17	5.80	7.23	7.61	8.91	6.30	6.87	3.75	7.41	8.49	16.99	7.21	9.28	7.50	9.50	
MnO	0.33	0.17	0.28	0.35	0.17	0.62	0.18	0.13	0.13	0.28	0.20	0.17	0.25	0.33	0.21	0.14	0.16	0.16	0.19	0.16	0.19	0.10	0.17	0.22	0.28	0.18	0.23	0.21	0.29	
MgO	3.71	4.86	4.70	4.08	4.84	5.93	6.63	8.34	8.00	6.71	8.01	9.49	7.03	5.96	7.60	7.82	7.44	8.41	8.03	9.47	10.45	9.19	6.67	9.60	8.82	9.03	7.78	14.08	7.53	
CaO	6.80	6.17	7.75	8.45	6.90	8.44	8.24	10.22	10.48	10.25	11.75	11.64	10.48	9.68	8.56	9.04	9.58	13.11	11.95	11.54	11.54	10.95	9.48	10.55	3.75	11.09	11.72	9.73	10.93	
MgO	2.02	2.47	2.92	2.95	3.35	2.42	2.39	2.55	1.28	2.17	2.00	2.35	1.90	3.00	2.15	3.30	3.05	1.27	2.21	2.70	1.68	3.03	3.45	2.35	0.85	2.30	2.86	1.70	3.30	
K ₂ O	0.90	1.25	0.35	0.35	1.30	1.05	0.85	0.10	0.10	0.10	0.10	0.10	0.87	0.36	0.36	1.14	0.15	-	-	-	0.05	-	0.73	-	-	-	-	-	-	
Na ₂ O	1.31	1.36	0.96	0.71	1.76	0.81	2.09	0.43	0.85	1.22	0.83	1.73	1.73	0.44	2.31	2.66	1.04	1.19	1.17	0.63	1.19	1.62	1.74	1.06	3.38	0.57	0.81	0.82	0.63	
TiO ₂	3.19	1.22	1.77	3.16	1.30	0.80	0.33	0.35	0.14	0.81	1.12	0.28	2.18	2.25	2.83	0.47	0.40	0.75	1.30	1.53	1.17	0.47	1.56	1.34	1.35	1.12	0.94	0.98	1.08	
P ₂ O ₅	0.80	0.21	0.30	1.10	0.09	0.07	0.09	0.06	0.02	0.34	0.08	0.16	0.25	0.32	0.12	0.06	0.06	0.14	0.21	0.43	0.17	0.09	0.18	0.33	0.12	0.17	0.20	0.21	0.15	
Sum	101.57	100.37	100.27	101.16	100.28	100.05	99.00	99.47	99.71	100.61	100.72	100.46	99.71	100.61	98.92	100.63	100.90	100.48	99.40	99.55	99.49	99.61	100.46	100.25	100.44	100.58	100.41	99.99	99.49	
Q	37.0	40.5	36.0	31.8	35.0	36.8	37.6	35.6	34.4	29.4	32.1	29.5	29.0	27.6	32.9	31.6	33.8	31.5	29.7	26.8	28.3	27.6	30.4	27.7	23.6	28.3	26.8	23.1	27.5	
L	41.6	35.1	36.8	33.9	40.3	35.2	38.9	34.4	35.4	29.7	30.9	34.1	31.7	28.0	34.9	41.5	38.8	33.8	30.3	33.6	28.5	36.5	38.2	31.1	16.9	38.7	34.6	30.2	37.9	
M	21.4	24.4	27.2	34.3	24.7	28.0	23.5	30.0	30.2	40.9	37.0	36.4	39.3	44.4	32.2	26.9	27.4	34.7	40.0	39.5	43.1	35.9	31.4	41.2	59.6	33.0	38.6	46.7	34.6	
al	141.9	164.1	141.9	121.6	144.2	142.7	140.6	132.1	112.8	110.0	104.7	114.8	110.3	113.6	120.5	124.9	123.8	105.0	110.8	102	103	105.3	123.6	104.7	83	99.4	104	86.6	108.5	
al	23.5	26.2	26.4	22.4	27.4	24.7	28.4	24.1	25.8	18.4	21.5	21.8	19.9	15.9	24.7	26.7	25.9	23.5	19.2	20	18	22.1	23.8	19.0	19	25.1	20.7	18.0	23.0	
fm	50.8	45.5	44.8	47.7	41.7	43.7	40.8	43.3	45.8	25.0	47.0	41.6	48.7	53.7	47.0	40.4	40.8	43.3	47.2	47	52	45.8	42.3	51.8	71	45.0	46.0	58.8	43.3	
o	19.7	19.0	22.2	22.7	19.9	23.6	23.2	26.5	25.5	24.7	27.3	30.5	25.8	23.8	22.5	23.4	26.1	30.5	28.9	27	26	25.7	24.7	24.3	8	25.2	27.2	20.1	26.2	
alk	6.0	9.3	6.6	7.2	11.0	8.0	7.6	6.1	2.9	4.9	4.2	6.0	5.6	6.6	5.8	9.5	7.2	2.6	4.7	6	4	6.4	9.2	4.9	2	4.7	6.1	3.1	7.5	
k	0.14	0.26	0.08	-	0.21	0.24	0.19	0.08	-	0.03	-	0.08	0.23	-	0.10	0.18	0.04	-	-	-	0.04	-	0.11	-	-	-	0.02	-	-	
mg	0.29	0.46	0.42	0.32	0.47	0.53	0.64	0.70	0.59	0.43	0.54	0.47	0.50	0.38	0.59	0.70	0.64	0.62	0.57	0.64	0.64	0.66	0.57	0.59	0.38	0.63	0.55	0.69	0.58	
ti	6.5	2.6	3.5	6.0	2.6	1.6	0.6	1.0	0.3	1.1	1.8	2.3	3.9	4.0	5.2	0.9	0.7	1.3	2.2	2	2	0.8	2.9	2.2	2	1.7	1.6	1.5	1.9	
p	1.0	-	0.3	1.2	0.2	0.1	0.2	-	0.2	0.1	0.1	0.3	0.3	0.3	0.1	-	-	0.1	0.1	0.4	-	0.1	0.1	0.1	0.1	0.1	0.1	0.1	0.1	
qs	+17.9	+26.9	+15.5	-5.2	+0.2	+10.7	+10.2	+7.7	+1.2	-9.6	-12.1	-9.2	-12.1	-12.8	-2.7	-13.1	-5.0	-5.4	-18.0	-22	-13	-20.3	13.2	-15.1	-25	-19.4	-20.4	-25.5	-21.5	
c/fm	0.39	0.42	0.50	0.48	0.48	0.54	0.57	0.61	0.56	0.48	0.56	0.73	0.53	0.44	0.48	0.58	0.64	0.70	0.61	0.57	0.50	0.74	0.58	0.47	0.11	0.56	0.59	0.34	0.60	
al(+alk)	-2.2	-2.1	-2.4	-7.5	-3.5	-6.4	-2.4	-8.5	-2.6	-11.2	-10.0	-14.7	-11.5	-14.5	-3.6	-6.2	-7.4	-9.6	-14.4	-13	-12	-10.0	-10.1	-10.2	+9	-4.8	-12.6	-5.2	-10.7	
Q	14.25	9.43	7.56	6.60	5.33	5.33	4.32	3.26	3.17	1.65	1.18	0.39	0.19	-	-	-	-	-	-	-	-	-	-	-	-	-	-	-	-	
Or	3.17	7.67	2.00	-	8.00	6.17	5.17	0.50	-	0.67	-	1.83	5.17	-	2.00	6.67	0.83	-	-	-	0.90	-	4.50	-	-	-	0.83	-	-	-
Ab	19.17	22.50	27.17	27.50	30.66	22.00	22.00	23.00	11.50	20.17	9.16	22.67	17.67	27.67	20.34	29.50	27.17	11.50	20.16	24.33	15.33	27.50	13.34	21.34	8.50	20.34	25.66	15.17	31.50	
An	30.34	28.33	32.17	29.00	27.24	30.50	37.84	33.84	47.50	28.67	42.32	32.17	30.00	19.00	35.84	33.00	36.67	44.83	30.34	31.70	31.07	33.33	27.84	30.50	19.67	44.20	31.16	35.17	31.67	
Coed	0.37	-	-	-	-	-	-	-	-	-	-	-	-	-	-	-	-	-	-	-	-	-	-	-	-	-	-	-	-	
Wo	-	-	-	-	-	-	-	-	-	-	-	-	-	-	-	-	-	-	-	-	-	-	-	-	-	-	-	-	-	
Di	21.20	30.00	22.53	22.40	20.87	26.06	27.33	26.40	31.07	26.20	32.74	15.80	25.67	25.77	35.28	7.27	24.72	23.48	20.60	7.98	15.65	7.79	10.63	18.29	25.72	7.89	0.40	12.29	-	
En	-	-	-	-	-	-	-	-	-	-	-	-	-	-	-	-	-	-	-	-	-	-	-	-	-	-	-	-	-	
Ol	-	-	-	-	-	-	-	-	-	-	-	-	-	-	-	-	-	-	-	-	-	-	-	-	-	-	-	-	-	
Tit	1.00	3.40	4.80	2.70	1.80	0.60	1.20	-	1.80	2.40	5.70	4.80	5.10	4.80	4.80	14.70	2.61	3.09	4.10	8.19	8.29	9.28	10.03	10.53	10.61	18.33	19.05	24.03	26.91	
Mt	7.60	-	4.60	6.70	3.80	1.10	0.40	0.40	2.40	5.30	1.70	5.00	4.70	4.80	-	-	-	-	-	-	-	-	-	-	-	-	-	-	-	
Op	1.60	0.40	0.60	2.20	0.10	0.10	0.10	-	0.70	0.10	0.10	0.10	0.60	0.60	0.10	0.10	0.10	0.30	0.40	0.80	0.30	0.10	0.40	0.10	0.20	0.30	0.30	4.20	0.30	
Ru	2.30	0.57	0.17	0.70	-	-	-	-	-	-	-	-	-	-	0.20	-	-	-	-	-	-	-	-	-	-	-	-	-	-	
z Mg	40	46	52	42	57																									

Cation numbers	Ap. Ba. JdI Di' Alm' rest					Gros. Zo. Q.			
	Ap.	Ba.	JdI	Di'	Alm'	rest	Gros.	Zo.	Q.
Si	804		82	164	234	324	54	144	126
Af	375		41		156	178	36	144	
Mf	316			82	234	-			
Ca	234	3		82		149	54	96	
Nk	41		41			-			
Ti	10	10				-			
P	2	2				-			
5 10 164 328 624							144	384	126

	wt. %	Vol. %	Mode	Gros.	Zo.	Q.
apatite	0.3	0.3	0.3			
rutile	0.6	0.5	1.1	Si	149	40 135
omphacite	27.6	29.5	34.3	Af	99	79
garnet	43.0	38.0	27.3	Ca	149	
soisite	21.5	22.4	22.6		397	119 135
quartz	7.1	9.2	6.7			
hornblende	-	-	7.0			

Table I-2 Recalculation of mineral composition from cation numbers for sample V 1016.

Di' content of omphacite in mol. %	Gross. + andr. content of garnet in mol. %	nature of accessory mineral.
80	0-31 31	soisite + kyanite kyanite
75	0-36 36	soisite + kyanite kyanite
67	19 19-40 40	soisite soisite + kyanite kyanite
50	41 over 41	soisite soisite + kyanite
38	42	

Table I-3 Dependence of the nature of the accessory mineral and the grossular + andradite content of the garnet on the Di' content of the omphacite in sample V 1016.

Wt. %	1	2	3	4	5	6	7	8	9	10	11	12	12 ^a
	V 1194 ^c	Coe 182	Ma 17	Ma 11	V 311	Ma 2	Ma 5	Ma I	V 1394 ^b	V 70 ^b	Coe 204	V 1104	
SiO ₂	79.40	78.92	74.94	69.71	75.48	66.37	66.20	65.76	61.14	61.80	58.68	46.96	64.08
Al ₂ O ₃	9.57	10.05	13.95	15.03	11.83	14.92	15.93	16.04	17.42	18.34	20.84	18.43	14.91
Fe ₂ O ₃	0.43	-	1.44	2.69	-	3.37	3.88	3.23	2.83	0.55	2.38	3.18	1.57
FeO	2.72	2.09	1.17	1.76	3.54	2.05	1.35	1.69	3.45	6.95	6.07	11.44	5.65
MnO	0.08	0.05	0.03	0.14	0.09	0.10	0.04	0.09	0.16	0.10	0.10	0.40	0.20
MgO	1.20	1.01	0.77	1.38	1.56	0.94	1.75	1.85	2.69	3.66	2.73	5.95	2.94
CaO	0.63	1.17	1.80	1.49	1.50	1.87	1.24	1.40	2.12	1.76	1.53	7.08	3.50
Na ₂ O	1.76	2.26	4.05	2.46	2.04	2.74	2.74	2.75	2.45	2.17	1.70	1.89	3.62
K ₂ O	1.14	1.10	0.73	2.18	1.35	2.40	1.70	2.04	1.70	2.55	2.45	0.90	1.73
H ₂ O ±	1.81	1.21	0.74	2.13	1.51	2.73	3.64	3.53	4.46	1.75	2.60	1.87	0.92
TiO ₂	0.66	0.55	0.27	0.74	0.58	0.90	0.68	0.76	0.94	0.90	0.86	1.59	0.78
P ₂ O ₅	0.05	0.10	0.08	0.17	0.14	0.56	0.13	0.16	0.13	0.16	0.16	0.23	0.11
	99.45	98.51	99.97	99.88	99.62	99.21 [†]	99.28	99.62 ^{**}	99.45 ^{**†}	100.69	100.10	99.92	100.01
Q	72.7	71.3	62.0	59.3	66.6	56.1	56.6	55.8	51.7	48.6	48.9	31.0	47.1
L	16.1	20.6	30.2	26.2	20.9	28.5	25.5	27.3	26.6	26.0	23.1	35.2	36.5
M	11.2	8.1	7.8	14.5	12.5	15.4	17.9	16.9	21.7	25.4	28.0	33.8	16.4
si	600.9	589.2	423.1	349.7	330.8	322.2	314.0	305.0	243.0	218.5	208.7	111.6	232.5
al	42.7	44.4	46.4	44.3	56.9	42.6	44.4	43.7	40.8	38.2	43.5	25.7	31.8
fm	34.1	24.7	18.0	28.6	23.4	27.7	31.6	30.9	36.5	41.8	39.2	50.4	38.1
e	5.0	9.4	10.8	8.1	7.1	9.6	6.3	7.0	8.8	6.6	6.0	18.1	13.5
alk	18.2	21.5	24.8	19.0	12.6	20.1	17.7	18.4	13.9	13.4	11.3	5.8	16.6
k	0.30	0.25	0.10	0.37	0.45	0.36	0.29	0.38	0.31	0.44	0.49	0.24	0.24
mg	0.40	0.45	0.36	0.36	0.43	0.24	0.40	0.21	0.44	0.46	0.37	0.42	0.42
ti	4.1	3.1	1.4	2.7	1.8	3.2	2.6	2.8	2.9	2.3	0.9	2.9	2.2
p		0.4	0.3	0.3	0.3	1.2	0.3	0.3		0.2	0.2	0.1	0.2
qs	+428.1	+451.6	+223.9	+173.7	+180.4	+141.8	+143.2	+231.4	+87.4	+64.9	+63.5	-11.6	+66.1
o/fu	0.15	0.38	0.60	0.28	0.30	0.35	0.20	0.23	0.24	0.16	0.15	0.36	0.35
A	42.5	41.1	53.3	54.3	37.6	57.3	58.1	54.4	46.5	35.8	59.3	26.7	
O	6.0	14.5	21.2	12.9	13.2	11.7	9.7	10.8	12.1	8.3	5.6	20.8	
F	51.5	44.4	25.5	32.8	49.2	31.0	32.2	34.8	41.4	55.9	34.6	52.5	
al-(o+alk)	+19.5	+13.5	+10.8	+17.2	+37.2	+12.9	+20.4	+18.3	+18.1	+18.2	+26.2	+1.8	

Table I-4 Chemical analyses of metasedimentary rocks from the Conoepido Complex. In column 12^a, the recalculated values for V 1104 + 100 % eutectic melt are also given.

Wt. %	1	2	3	4	5	6	7	8	9	10
SiO ₂	43.42	44.4	36.86	39.10	43.97	41.56	39.84	39.56	36.84	36.18
Al ₂ O ₃	12.34	11.9	15.43	8.62	10.43	0.34	1.42	2.27	2.62	0.43
Fe ₂ O ₃	3.10	5.6	4.90	6.68	1.47	4.33	5.85	5.89	8.71	8.84
FeO	5.31	-	3.72	1.50	7.14	5.08	3.16	2.80	0.98	0.78
MnO	0.22	0.31	0.02	0.03	0.20	0.13	0.12	0.12	0.04	0.03
MgO	19.80	15.4	35.30	33.00	23.44	36.00	36.08	34.77	37.80	40.80
CaO	11.84	19.2	0.97	1.85	6.84	0.10	1.93	2.47	0.43	0.17
Na ₂ O	0.47	0.61	0.58	1.51	0.30	0.08	0.20	0.28	0.40	0.30
K ₂ O	0.08	0.07	0.22	0.36	0.19	0.03	0.07	0.06	0.18	0.16
H ₂ O ⁺	2.36	1.20	2.18	6.12	0.77	11.90	10.08	10.60	11.80	13.15
H ₂ O ⁻	0.06	0.40								
TiO ₂	0.52	0.22	0.40	1.15	0.22	0.07	0.11	0.11	-	-
F ₂ O ₅	-	-	-	0.24	0.09	0.01	0.03	0.02	-	-
Cr ₂ O ₃	-	tr	nd	nd	nd	0.16	0.17	0.20	nd	nd
CO ₂	nd	nd	nd	nd	4.74	nd	nd	nd	nd	nd
	99.52	99.31	100.58	100.16	99.85	99.95	99.68	99.63	99.80	100.84

Approx. % of Serpentinisation								
Fe ⁺² + Fe ⁺³				90	50	50	80	95
Fe ⁺² + Fe ⁺³ + Mg				0.123	0.116	0.116	0.116	0.107

	A	C	F
14.5	14.5	16.2	15.0
23.1	23.1	39.4	3.1
62.4	62.4	44.4	81.9
			86.5
			75.1

Table II-1 Chemical analyses of ultrabasic rocks.

1. Spinel-garnet pyroxenite (sample R 70).
2. Pyrope-cymonite pyroxenite from the Totalserpentin (Peterson, 1963, p. 646).
3. Chlorite-amphibole orthopyroxenite (sample V 1389).
4. Chlorite cummingtonite (sample R 348).
5. Spinel bearing ultrabasic rock (sph 62 wt%, cpx 22 wt%, rest 16 wt% from Kuseulinkivaara (Mikkola & Sahama, 1936, p. 366).
6. Talc-chlorite serpentinite, secondary after chlorite-pargasite peridotite (sample R 175).
7. Partially serpentinitized pargasite peridotite (sample R 31).
8. Serpentinized peridotite with streaks of orthopyroxene-chlorite pargasite (sample R 20).
9. Serpentinized chlorite-pargasite peridotite with streaks of pargasite diallagite (sample R 137).
10. Completely serpentinitized pargasite peridotite (sample R 18).

	garnet	clinopyroxene	plagioclase	typomorphic hornblende
pyrigarnite	>10%	>10%	<5%	<5%
plagiopyrigarnite	>10%	>10%	>5%	<5%
hornblende pyrigarnite	>10%	>10%	<5%	>5%
hornblende plagiopyrigarnite	>10%	>10%	>5%	>5%

Table III-1 Proposed nomenclature for rocks of the high-pressure lineage of the granulite facies.

Nature of minor constituent (if present)	s-colour of secondary hornblende	Grade of retrograde metamorphism	nr. of sample	old Decreasing grade of retrograde metamorphism Increase of kyanite-staurolite young
no pegmatoid vein found	brown		V 367	
kyanite or none	greenish-brown	hornblende-clinopyroxene-almandine subfacies of the granulite facies	V 1185	
Y-soisite or none	brownish-green		M 217	
α-soisite or none		green	M 639	
β-soisite or none				
orthite or none	green	amphibolite facies		
orthite or none	blue-green			
epidote or none				

Table III-2 Minor constituents in pegmatoid veins and streaks; their relative ages and their relation to retrograde metamorphism.

Wt. %	1	2	3	4	5	6	7	8	9	10	11	12	13	14	15	16	17
	V 220a	G7-2a	G7-2c	V 220	V 231	V1234	M 643	V1214	V 28b	R 210	G7-2b	V 174	V 191	V174b	V1244	V1179d	M158a
SiO ₂	70.11	56.06	56.60	53.35	52.98	53.76	43.90	47.90	44.00	47.02	69.56	66.56	48.50	47.40	63.44	58.46	42.66
Al ₂ O ₃	13.53	15.68	18.85	12.96	15.82	14.78	16.31	17.45	13.60	13.39	13.08	13.69	16.45	18.19	15.44	17.27	16.11
Fe ₂ O ₃	1.74	5.68	3.99	3.13	3.74	2.27	7.63	3.49	4.97	3.05	2.38	2.48	5.84	3.58	1.57	2.40	8.43
FeO	3.10	7.40	5.11	11.06	5.36	10.22	4.23	8.01	11.00	9.41	6.17	3.15	6.97	5.40	4.21	5.49	3.54
MnO	0.08	0.25	0.20	0.31	0.25	0.21	0.13	0.15	0.33	0.15	0.20	0.13	0.22	0.12	0.16	0.11	0.13
MgO	1.96	4.72	2.58	4.32	7.56	3.96	6.94	6.43	9.46	8.25	0.97	3.41	6.74	8.61	3.16	3.93	4.14
CaO	5.26	8.08	8.74	9.02	9.58	8.53	16.85	9.96	11.57	13.19	4.66	6.36	8.92	13.36	3.68	3.76	22.40
Na ₂ O	3.23	1.41	2.95	3.00	3.28	4.00	2.80	3.00	1.30	3.20	2.47	3.43	2.30	1.42	3.17	2.70	1.05
K ₂ O	0.01	tr	tr	tr	tr	tr	0.35	0.30	0.93	0.05	tr	tr	0.01	tr	2.00	2.60	tr
H ₂ O ⁺	0.95	0.57	0.72	0.65	0.92	0.81	0.90	1.44	1.50	0.81	0.26	0.56	2.43	1.30	1.43	1.82	0.69
TiO ₂	0.43	0.48	0.64	2.18	0.90	1.77	0.54	1.53	0.78	1.89	0.57	0.29	1.03	0.51	0.94	1.18	0.92
P ₂ O ₅	0.07	0.11	0.13	0.17	0.15	0.26	0.58	0.27	0.12	0.13	0.17	tr	0.16	tr	0.27	0.18	0.61
	100.47	100.44	100.51	100.15	100.54	100.57	101.16	99.93	99.56	100.54	100.49	100.06	99.57	99.89	99.47	99.90	100.68
Q	57.0	42.5	42.2	34.6	32.7	33.8	27.4	28.9	22.6	23.2	58.4	50.9	31.8	30.2	48.4	42.8	24.4
L	31.8	30.6	39.6	30.4	34.7	35.6	20.5	37.9	28.5	30.8	27.8	32.2	34.9	34.2	35.1	35.3	30.3
M	11.3	26.9	18.2	35.1	32.5	30.6	52.1	33.0	48.9	46.0	13.8	16.7	33.5	35.6	16.6	22.1	45.3
si	296	151.2	163	139	128	141.2	86.3	111.1	89	98.4	293.9	239	116	102	237	188.9	85.1
al	34	25.0	32.1	20	22	22.9	19.8	24.0	16	16.4	32.4	29	23	23	34	33.0	19.0
fm	29	48.0	32.6	47	45	42.9	38.9	44.2	55	47.4	36.3	35	49	43	35	40.0	31.2
o	24	23.3	27.0	25	25	24.0	35.5	24.8	25	29.5	21.1	24	23	31	15	13.0	47.8
alk	13	3.7	8.3	8	8	10.2	5.8	7.1	4	6.7	10.2	12	5	3	16	14.0	2.0
k	0.02	0.00	0.00	0.00	0.00	0.00	0.08	0.06	0.32	0.02	0.00	0.00	0.03	0.00	0.29	0.39	0.00
mg	0.43	0.40	0.34	0.35	0.60	0.36	0.52	0.50	0.52	0.67	0.17	0.52	0.49	0.64	0.49	0.48	0.40
ti	1	1.0	1.4	4	2	3.5	0.8	2.6	1	3	1.8	1	2	1	3	2.9	1.3
p	0.2	0.16	0.17	-	-	0.3	0.5	0.3	0.1	-	0.25	-	-	-	0.4	0.2	0.5
qs	+144	+36.4	+29.8	+7	-4	+0.4	-36.9	-17.3	-27	-28.4	453.1	+91	-4	-10	+73	+24.9	-22.9
e/fm	0.83	0.49	0.83	0.53	0.56	0.56	0.91	0.56	0.45	0.62	0.58	0.70	0.47	0.72	0.43	0.33	1.53
T=(al-alk)	21	21.3	23.8	12	14	12.7	14	16.9	12	9.7	22.2	17	18	20	18	19	17
t=al-(o+alk)	-3	-2	-3.2	-13	-11	-11.3	-21.5	-7.9	-13	-19.8	+1.1	-7	-5	-11	+3	+6	-40.8
Q	34.1	19.5	14.3	6.6	3.0	2.97	1.55	-	-	-	37.3	26.5	4.15	-	19.95	12.0	-
Or	0.34	-	-	-	-	-	1.3	1.7	5.8	0.35	-	-	0.35	-	12.0	15.8	-
Ab	29.66	13.0	27.2	28.0	29.5	36.5	15.0	27.5	12.2	28.8	23.2	31.5	21.5	13.0	29.3	25.0	9.9
An	23.0	38.0	38.8	22.7	28.3	22.8	17.8	34.0	29.5	22.2	23.2	22.2	36.3	44.0	17.2	18.0	40.7
Ord	-	-	-	-	-	-	-	-	-	-	2.6	-	-	-	6.2	11.1	-
Wo	-	-	-	-	-	-	3.05	-	-	14.5	-	-	-	-	-	-	27.1
Di	1.4	1.4	1.75	11.8	12.2	10.2	54.5	8.2	21.0	-	-	7.0	4.0	17.4	-	-	-
Hx	8.7	21.0	11.85	22.5	20.9	20.83	-	11.3	3.1	-	10.3	9.4	24.8	19.3	12.45	14.4	-
Ol	-	-	-	-	-	-	-	9.9	21.1	26.75	-	-	-	1.6	-	-	10.3
Tit	0.9	0.9	1.5	4.8	1.8	3.6	1.5	3.3	1.8	3.9	-	0.6	2.4	0.9	-	-	1.8
Mt	1.9	6.2	4.3	3.4	3.9	2.5	4.7	3.7	5.4	3.3	2.6	2.6	6.4	3.8	1.7	2.6	9.1
Op	0.1	0.1	0.3	0.3	0.3	0.6	0.6	0.3	0.1	0.3	0.3	-	0.3	-	0.6	0.4	1.2
Ru	-	-	-	-	-	-	-	-	-	-	0.4	-	-	-	0.7	0.9	-
A	32.8	31.4	35.8	19.0	22.4	19.5	23.4	24.4	18.2	14.5	34.8	28.1	27.4	25.4	31.1	32.0	26.4
C	33.2	26.5	33.8	30.1	30.0	30.0	42.3	29.1	27.9	34.8	27.0	33.4	26.8	33.7	20.6	18.1	52.6
F	33.9	42.1	30.4	50.9	47.6	50.5	34.3	46.5	53.9	50.7	38.2	38.5	45.8	40.9	48.3	49.9	21.0
A'	-	-	-	-	-	-	-	-	-	-	-	-	-	-	21.7	26.6	-
K	-	-	-	-	-	-	-	-	-	-	-	-	-	-	10.3	10.1	-
F	-	-	-	-	-	-	-	-	-	-	-	-	-	-	68.0	63.3	-

Table III-3 Chemical analyses and derived values for rocks from the Capelada Complex.
1-10. (plagioclase)pyroxenites and amphibolites retrograde after (plagioclase)pyroxenites;
11. leptynite; 12-14. meta-gabbros; 15-16. paragneisses; 17. calc-silicate rock.

wt. %	1	2	3	4	5	6	7	8	9	10	11
SiO ₂	37.42	38.28	38.08	37.56	37.80 (37.00)	40.54 (39.45)	38.70	38.36	39.38 (38.30)	39.34 (38.45)	37.38
Al ₂ O ₃	22.14	22.29	20.72	21.99	16.82	19.98	23.00	20.20	18.16	18.72	18.78
Fe ₂ O ₃	1.04 (2.10)	2.16 (1.70)	0.13 (2.80)	2.55 (2.97)	6.00 (6.40)	3.32 (3.60)	0.00 (1.00)	3.20	4.63 (5.55)	4.99	4.48 (4.95)
FeO	26.05 (25.15)	21.51 (21.92)	25.69 (23.35)	21.09 (20.72)	22.71 (22.35)	15.25 (15.00)	20.65 (19.65)	22.45	20.30 (19.95)	19.81	25.24 (24.80)
MnO	0.98	0.73	0.77	0.71	0.70	0.36	0.55	1.03	0.48	0.51	0.67
MgO	3.56	6.80	5.05	5.81	5.80	12.28	8.40	6.11	8.10	7.74	6.21
CaO	9.70	8.73	9.80	10.22	8.49	7.81	8.69	8.73	8.89	9.04	6.99
Na ₂ O	0.15	0.22	0.10	0.12	0.23	0.40	0.05	tr	0.15	0.20	0.23
K ₂ O	tr	tr	tr	tr	tr						
TiO ₂	0.26	0.82	0.27	0.24	0.60	0.23	0.34	0.43	0.47	0.41	0.52
H ₂ O	0.00	0.00	0.00	0.00	0.07	0.47	0.24	0.00	0.22	0.07	0.10
P ₂ O ₅	0.13	0.16	0.14	0.11	0.10	0.05	0.05	0.16	0.07	0.09	0.07
	101.43	101.70	100.75	100.40	99.32	100.69	100.67	100.67	100.67	100.92	100.27

Number of oxygens to 12 oxygens; for analysis no. 5, number of oxygens-Si to 6 oxygens

	2.92	2.943	2.97	2.91	3.00	2.94	2.99	3.00	3.00	3.00	2.97
Si	0.08	0.057	0.03	0.09	-	0.06	0.01	-	-	-	0.03
Al ^{IV}	1.96	1.963	1.87	1.92	1.61	2.00	1.84	1.67	1.72	1.73	1.73
Al ^{VI}	0.04	0.037	0.13	0.08	0.39	-	0.16	0.33	0.28	0.27	0.27
Fe ⁺³	0.08	0.060	0.03	0.09	-	0.06	0.03	-	0.02	0.03	0.03
Fe ⁺²	1.64	1.407	1.52	1.34	1.52	1.25	1.46	1.28	1.29	1.64	1.64
Mn	0.07	0.046	0.05	0.05	0.05	0.04	0.07	0.03	0.03	0.04	0.04
Mg	0.41	0.780	0.59	0.67	0.70	0.95	0.71	0.95	0.90	0.73	0.73
Ca	0.80	0.706	0.81	0.85	0.73	0.63	0.72	0.74	0.75	0.56	0.56
O	-	0.001	-	-	-	-	0.01	-	0.01	-	-

Table V-1. Chemical analyses of garnets (analyses by Dr. G. de Sitter-Komans and Mrs. H.M.L. Bult-Bak) from Capelsa Complex rocks (1-5) and Concepsido Complex (6-11); recalculated values for SiO₂, FeO, and FeO are given in brackets.
 1. sample V 1278, leptynite; 2. sample V 1143, plagiopyroxenite; 3. sample V 1243a, leptynite; 4. sample 01-16, plagiopyroxenite; 5. sample M 616, plagiopyroxenite; 6. sample V 1023, carbinite eclogite; 7. sample V 1050, eclogite; 8. sample V 1146b, garnet-biotite gneiss from the Banded Onices Formation; 9. sample V 1278 (weakly magnetic fraction) w.m.f.; 10. sample V 1278 (strongly magnetic fraction) s.m.f.; 11. sample M 459, eclogite with pyroxenitic properties.

Z = 3.00
 Y = 2.00
 X = 3.00

Registration number of X-ray photograph	Sample	n_D (± 0.002)	\bar{n}_o	Composition	S.G.
CAPELADA COMPLEX					
2841	V 1181	1.763	11.609 \pm 0.003	plagiopyroxenites	
2823	V 1243	1.773	11.593 \pm 0.002	Py-26.0 I-0.1 II-1.9 Al-46.0 Sp-1.5 Gr-21.7 An-1.9	
-	V 1250 _o	1.787	11.564 \pm 0.001	Py-23.3 Al-58.7 Gr-6.5 An-11.5	
-	V 1250 _p			Py-23.7 Al-53.7 Gr-12.8 An-10.5	
2810	R 204	1.795	11.613 \pm 0.002		
3428	M 616	1.778	11.588 \pm 0.002	Py-23.3 Al-50.7 Sp-1.7 Gr-4.8 An-19.5	
2824	01-16	1.778	11.607 \pm 0.001	Py-22.3 II-3.0 Al-44.7 Sp-1.6 Gr-24.4 An-4.0 retrograde (plagio)pyroxenites	
3946	07-2b	1.790	11.621 \pm 0.001		
3947	07-2c	1.778	11.619 \pm 0.001	leptynites	
2842	V 1193	1.785	11.625 \pm 0.005	Py-13.7 II-2.7 Al-54.6 Sp-2.3 Gr-24.7 An-2.0	
2825	V 1243a	1.780	11.619 \pm 0.005	Py-19.6 II-1.0 Al-50.7 Gr-20.5 An-6.5	
3296	R 327b*	1.775	11.582 \pm 0.002	metagabbro Py-29.0 Al-42.3 Sp-1.7 Gr-7.5 An-19.5	
2627	V 174	1.773	11.857 \pm 0.002	amphibolites	
2626	V 368	1.800	11.632 \pm 0.005	calc-silicate rock	
3471	R 329	1.783	11.665 \pm 0.002	biotite gneiss	
2217	Coe 304	1.780	11.62		
CONCEPÇÃO COMPLEX					
-	V 1007b ¹	1.765	11.594 \pm 0.002	eclogites	
2890	V 1023	1.775	11.555 \pm 0.004	Py-34.3 Al-38.7 Sp-1.3 Gr-14.2 An-11.5	3.776
3040	V 1050	1.777	11.590 \pm 0.001	Py-46.3 Al-32.0 Sp-0.7 Gr-10.5 An-10.5 Py-31.7 Al-41.7 II-2.0 Sp-1.3 Gr-23.3 hornblende eclogites	3.99
3062	V 1030	1.768	11.595 \pm 0.003		
2977	V 1053	1.762	11.575 \pm 0.002		
-	V 1223 ₁	1.774	11.593 \pm 0.002	Py-28.8 Al-44.7 Sp-1.3 Gr-15.8 An-9.5	
-	V 1223 ₂	1.785	11.591 \pm 0.001	Py-19.7 Al-54.7 Sp-1.3 Gr-13.3 An-11.0	
2995	V 1223a	1.782	11.591 \pm 0.002		
3041	V 1278 _{mf}	1.768	11.594 \pm 0.002	Py-31.7 Al-42.7 Sp-1.0 Gr-8.1 An-16.5	
3042	V 1278 _{mf}	1.773	11.591 \pm 0.002	Py-30.0 I-1.0 Al-43.0 Sp-1.0 Gr-11.0 An-14.0	
2887	V 1282	1.768	11.585 \pm 0.004		
3425	M 459	1.782	11.573 \pm 0.001	Py-24.3 Al-54.7 II-1.0 Sp-1.3 Gr-5.2 An-13.5	
2373	Coe D7	1.759	11.57		
2372	Coe D10	1.761	11.57		
-	Coe D12	1.775	11.57	amphibolites	
3046	Coe 114	1.776	11.610 \pm 0.004**		
3054	Coe 141	1.775	11.599 \pm 0.001		
3055	Coe 141a	1.774	11.580 \pm 0.002**		
3058	Coe 162	1.778	11.593 \pm 0.002		
-	V 1023a**	nd	nd	metagabbro Py-41.7 Al-29.0 Sp-1.0 Gr-18.8 An-9.5 hornblende-garnet-chlorite schist	
2630	V 131a	1.790	11.541 \pm 0.003	garnet-biotite gneiss (banded gneiss)	
2874	V 1146b	1.788	11.610 \pm 0.002	Py-23.7 I-1.0 II-0.3 Al-48.7 Sp-2.3 Gr-16.0 An-8.0	
3047	Coe 127	1.787	11.556 \pm 0.001		
3084		1.797	11.530 \pm 0.001		
ULTRABASIC ROCKS					
2886	R 70	1.737	11.537 \pm 0.006	garnet pyroxenites	
2435	R 312	1.742	11.57		
2436	R 348	1.741	11.55		

Table V-2

Physical data of garnets from the Capelada Complex, the Concepción Complex, and the ultrabasic rocks (33 determinations of garnets from the Banded Gneiss Formation are not given here but are plotted in Fig. V-5).

¹ See Vogel & Beheere (1965).

² See Engels & Vogel (1966).

** Broad lines due to continuously varying unit-cell dimensions.

** See Vogel & Warnasars (1967).

		Fy	Al	Sp	Gr	An
Charnockite +						
Granulite	15 analyses	34.5±15	57±11	2.5±2	14.5±7	2.5±2
Ecolite	14 analyses	43.5±7	38±7	1±1	14±6	3.5±4
Amphibolite +						
Glaucophane schist	21 analyses	16.5±4	54±6	3.5±3	20±5	6±4
Metagabbro	8 analyses	31±10	49.5±11	2±1	12±3	5.5±5

Table V-3 Empirically determined limiting compositions for garnet (Trüger, 1959).

Wt. %	1	2	3	4	5	6	7	8
SiO ₂	51.20	53.06	53.56	53.96	54.54	53.46	- (55.10)	53.32
Al ₂ O ₃	5.63	0.99	8.36	7.84	9.88	11.41	- (8.29)	4.96
Fe ₂ O ₃	5.43	2.20 (2.24)	3.19 (3.37)	3.50	3.26	1.81	2.12 (0.85)	7.88 (9.20)
FeO	6.79	5.65 (5.60)	2.38 (2.22)	2.01	2.15	2.48	(1.27)	3.75 (2.65)
MnO	0.12	0.23	tr	tr	tr	0.06	0.05	0.03
MgO	8.90	13.28	10.25	8.87	10.17	9.18	11.58	8.08
CaO	17.60	23.81	16.68	18.86	16.08	15.26	16.25	13.51
Na ₂ O	3.42	0.42	4.00	4.70	4.70	5.18	4.99	6.43
K ₂ O	tr	tr	tr	tr	tr	tr	tr	tr
H ₂ O	0.00	0.34	0.32	0.35	0.73	0.25	0.00	0.34
TiO ₂	0.66 ¹	0.21	0.33	0.38	0.29	0.24	1.59	0.35
P ₂ O ₅	0.05	0.03	0.01	0.10	0.10	0.02	0.03	0.06
	99.80	100.22	99.08	100.57	101.90	99.35	100.00	98.71
Number of cations to 6 oxygens								
Si	1.917	1.973	1.946	1.95	1.93	1.924	1.99	1.98
Al ^{IV}	0.083	0.027	0.054	0.05	0.07	0.076	0.01	0.02
Al ^{VI}	0.167	0.018	0.304	0.28	0.34	0.408	0.34	0.20
Fe ⁺³	0.153	0.063	0.093	0.10	0.09	0.050	0.02	0.26
Fe ⁺²	0.169	0.170	0.040	0.06	0.03	0.043	0.02	0.08
Mn	0.002	0.007	-	-	-	-	-	-
Mg	0.500	0.735	0.554	0.48	0.53	0.493	0.62	0.45
Ti	0.009	0.007	0.009	0.01	0.01	0.006	-	0.01
Ca	-	-	-	0.07	-	-	-	-
Fe ⁺²	0.045	0.004	0.029	-	0.03	0.035	0.02	-
Mg	-	-	-	-	0.01	-	-	-
Ca	0.703	0.947	0.650	0.66	0.61	0.588	0.63	0.54
Na	0.250	0.031	0.281	0.33	0.32	0.361	0.35	0.46
□	0.002	0.018	0.040	0.01	0.03	0.016	-	-

Table V-4 Chemical analyses of clinopyroxenes from Cabo Ortegal rocks.
 1. sample V 1234, plagiopyroxenite; 2. sample V 410d, calc-silicose rock;
 3. sample V 1278, α -saisite-hornblende eclogite (strongly magnetic fraction, w.m.f.);
 4. sample V 1278, (weakly magnetic fraction, w.m.f.); 5. sample V 1278, p.p.
 amphibolite; 6. sample V 1050, eclogite; 7. sample V 1023, carinthine eclogite;
 8. sample M 459 eclogite with pyroxenitic properties.

¹ Half of the TiO₂-content is estimated to represent rutile contamination (inclusions)

No. of sample	name	S.O.	n_x	n_y	n_z	Δ	$2V^m$	axial dispersion	θ/s	pleochroism in thin section	percentage composition in end-member molecules
V 1234	diopside rich aegirine augite	nd	-	1.707 ⁵	-	0.018	66-68°	rxy distinct	50-53°	x green with tinge of yellow < y green with tinge of blue = z	Di-50.0 Tw'-6.5 II-0.9 Hs-12.6 IV-0.4 Cfs-4.5 Ja-9.8 Ao-15.3
V 1278	omphacite chloromelanite	nd	1.680	1.687	1.700	0.020	nd	nd	nd	slightly green, not pleochroic	Di-55.4 Tw'-3.6 II-0.9 Hs-1.1 IV-8.0 Cfs-2.9 Ja-18.8 Ao-9.3
V 1278	omphacite chloromelanite	nd	1.679	1.687	1.699	0.020	nd	nd	nd	slightly green, not pleochroic	Di-48.0 Tw'-3.0 II-1.0 Hs-6.0 IV-2.0 Wo-7.0 Ja-23.0 Ao-10.0
V 1278	symplesite	nd	nd	nd	nd	nd	nd	nd	nd	not observed	Di-52.0 Tw'-5.0 II-1.0 IV-6.0 Cfs-3.0 CEm-1.0 Ja-23.0 Ao-9.0
V 1023	omphacite	3.29	-	1.618	-	0.019	69-71°	rxy weak	42°	colourless	Di-62.0 Tw'-1.0 Cfs-2.0 Ja-33.0 Ao-2.0
V 1090	omphacite	3.22	1.676	1.682 ⁵	1.696 ⁵	0.020 ⁵	70-71°	not seen	56-57°	slightly green, not pleochroic	Di-49.3 Tw'-6.4 II-0.6 Hs-0.8 IV-1.6 Cfs 3.5 Ja-31.1 Ao-5.0
M 459	aegirine augite chloromelanite	3.32	1.688	1.697	1.710	0.022	78°	rxy strong	52°	x green with tinge of blue = y > z green with tinge of yellow	Di-45.0 I-1.0 Hs-8.0 Ja-20.0 Ao-26.0
V 4104	diopside	nd	1.677	1.691	1.703	0.028	63°	not seen	44°	colourless	Di-73.5 Tw'-1.3 II-0.7 Hs-17.3 Cfs-0.4 IV-1.8 Ao-3.2
V 1023	oeserithine	3.06	1.620	1.643	1.647	0.027	90-110°	rxy weak	18°	colourless	Di mm-1.4 Csm-2.1 St'-13.7 Glau-9.2 Tw'-13.3 Tr-50.4
V 1267	common hornblende	3.19	1.656	1.664	1.671 ⁵	0.015 ⁵	103-104°	not seen	14.5°	x light yellowish-green < y brownish-green = z bluish-green	Tr mm-2.9 St'-17.7 Hs-0.6 Tw'-29.4 Tr-49.4

Table V-5 Optical properties and chemical composition of analysed clinopyroxenes and hornblendes.

Wt. %	1	2	3	4	5	6	7	8	
SiO ₂	52.50	43.16	53.82	44.60	49.33	45.96	43.18	44.66	
Al ₂ O ₃	6.47	14.56	3.77	14.14	12.72	14.84	16.84	14.35	
Fe ₂ O ₃	5.80	4.12 (8.50)	1.23	1.76	1.72	3.73	4.55	3.40	
FeO	-	10.12 (6.20)	4.32	4.98	4.63	4.48	7.37	7.93	
MnO	0.04	0.11	-	tr	-	0.04	0.04	0.08	
MgO	20.14	11.53	19.18	15.40	17.44	14.63	10.81	12.15	
CaO	10.42	10.87	13.10	11.46	9.91	9.51	9.20	9.39	
Na ₂ O	2.48	2.20	1.12	3.20	2.25	3.25	3.61	2.27	
K ₂ O	0.12	0.35	0.80	1.17	0.63	0.43	0.93	0.91	
H ₂ O	0.65	1.56	2.27	2.01	0.50	2.58	3.44	3.11	
TiO ₂	0.54	1.07	-	1.30	-	0.62	0.93	1.75	
F ₂ O ₅	0.06	0.04	-	-	-	-	-	-	
H ₂ O	-	-	0.26	0.07	-	-	-	-	
F	-	-	-	-	0.21	-	-	-	
	99.22	99.69	99.87	100.09	99.13	100.07	100.90	100.00	
Cations relative to 23 oxygens									
Si	7.210	6.22	7.572	6.343	6.83	6.50	6.25	6.43	X = 8.00
Al ^{IV}	0.790	1.78	0.428	1.657	1.17	1.50	1.75	1.57	
Al ^{VI}	0.258	0.69	0.197	0.759	0.90	0.97	1.13	0.87	X + Y = 5.00
Fe ⁺³	0.602	0.92	0.118	0.171	0.19	0.40	0.48	0.37	
Fe ⁺²	-	0.74	0.516	0.615	0.52	0.54	0.91	0.95	X + Y = 5.00
Mn	-	0.01	-	-	-	-	-	0.01	
Mg	4.082	2.47	4.023	3.261	3.39	3.02	2.33	2.61	W = 2.00
Ti	0.058	0.12	-	0.137	-	0.07	0.10	0.19	
□	-	0.05	0.146	0.057	-	-	0.05	-	A
Mg	0.043	-	-	-	0.21	0.07	-	-	
Ca	1.526	1.68	1.978	1.742	1.47	1.44	1.43	1.45	W = 2.00
Na	0.431	0.32	0.022	0.258	0.32	0.49	0.57	0.55	
Na	0.229	0.29	0.266	0.621	0.28	0.40	0.42	0.25	A
K	0.016	0.06	0.160	0.205	0.12	0.08	0.19	-	
Mg/ ¹ / ₂ (X+Y)	0.816	0.324	0.805	0.652	0.678	0.604	0.466	0.522	
Fe ⁺² +Fe ⁺³ / ¹ / ₂ (X+Y)	0.120	0.322	0.127	0.157	0.142	0.188	0.278	0.264	

Table V-6 Chemical analyses of amphiboles. (Recalculated values between brackets).

1. Carinthine from sample V 1023, carinthine eclogite (Analyses by: Dr. C. de Sitter-Koomans, Mrs. H.M.I. Bult-Bik, Mr. F. Warnaars);
2. Hornblende from sample V 1267, garnet-hornblende rock (Analyses by: Dr. C. de Sitter-Koomans, Mrs. H.M.I. Bult-Bik);
3. Carinthine, Saualpe (M. Kunitz, 1930, p. 245);
4. Carinthine, Gertrud Saualpe (Korinzig, 1940, p.33); ' excluding 0.01 wt.% Co.
5. Carinthine, Saualpe KErnten (Rammelsberg, 1875, p. 417);
- 6-7. "Kluftkarinthin", Kupplerbrunn and Saualpe (Heritsch & Kahler, 1960, p.223);
8. Supposed carinthine, Mauthnerock (Machatski & Walitsi, 1962, p. 144).

APPENDIX 3

LOCALITIES OF SPECIMENS MENTIONED IN THE TEXT

Localities of specimens mentioned in the text (in degrees, minutes, and seconds).
 The museum registration numbers of the samples are mentioned under st. Where chemical
 analyses were made of whole rock (wr), garnet (gt), clinopyroxene (cpx), and hornblende
 (hbl) this is indicated in a separate column for the samples concerned.

Sample number	st	Longitude (W of Madrid)	Latitude	Quadrant	Chemical analyses	Sample number	st	Longitude (W of Madrid)	Latitude	Quadrant	Chemical analyses
V 28	140002	4 22 54	43 40 1	1-B4		V 1007a	140128	4 13 46	43 41 23	1-E4	
V 28b	140003	-	-	-		V 1007b	140129	-	-	-	
V 33b	140004	4 20 25	43 42 26	1-C4		V 1008	140130	4 13 26	43 42 0	1-E4	gt
V 41	140008	4 20 2	43 41 40	1-C4		V 1010	140131	4 13 23	43 42 20	1-E4	wr
V 70b	140014	4 23 5	43 40 8	1-B4	wr	V 1014	140132	4 12 49	43 43 3	1-E3	
V 70d	140015	-	-	-		V 1014b	140133	-	-	-	wr
V 70f	140016	-	-	-		V 1016	140134	4 12 39	43 43 0	1-E3	wr
V 73	140018	-	-	-		V 1019	140135	4 22 39	43 40 7	1-B4	
V 74	140019	4 23 11	43 40 8	1-B4		V 1020a	140136	4 11 12	43 43 36	1-E3	
V 118	140022	4 21 40	43 42 31	1-C3	wr	V 1023	140137	4 11 0	43 43 3	1-E3	wr,gt,cpx,hbl
V 122	140023	4 21 53	43 42 18	1-C4		V 1023a	140138	-	-	-	
V 125	140025	4 22 0	43 42 20	1-B4	wr	V 1025	140139	4 10 37	43 43 8	1-E3	
V 131a	140031	4 22 6	43 42 8	1-B4	wr	V 1030	140140	4 10 49	43 43 29	1-E3	wr
V 162	140035	4 21 22	43 42 28	1-C4		V 1031	140141	4 11 39	43 43 27	1-E3	
V 172	140037	4 21 54	43 42 30	1-C3/4		V 1037	140142	4 12 4	43 43 33	1-E3	
V 174	140038	4 22 17	43 40 40	1-B4	wr	V 1040	140143	4 12 27	43 43 29	1-E3	
V 174b	140039	-	-	-	wr	V 1042	140144	4 12 5	43 43 15	1-E3	
V 191	140041	4 21 35	43 42 3	1-C4	wr	V 1043	140145	4 12 4	43 43 15	1-E3	
V 199a	140047	4 21 52	43 41 52	1-C4		V 1050	140146	4 12 49	43 42 13	1-E4	wr,gt,cpx
V 208	140049	4 20 53	43 40 35	1-C4		V 1051	140147	4 12 57	43 42 24	1-E4	wr
V 216	140052	4 23 11	43 40 6	1-B4		V 1053	140148	4 13 8	43 42 21	1-E4	wr
V 217	140053	4 23 11	43 40 8	1-B4		V 1054	140149	4 12 37	43 42 7	1-E4	wr
V 219a	140057	4 23 10	43 40 7	1-B4		V 1055I	140150I	4 12 43	43 42 6	1-E4	wr
V 220	140058	4 22 19	43 40 3	1-B4	wr	V 1055II	140150II	-	-	-	
V 220a	140059	-	-	-	wr	V 1055a	140151	-	-	-	
V 231	140062	4 21 8	43 42 38	1-C3	wr	V 1058	140152	4 12 40	43 40 52	1-E4	
V 249	140065	4 23 10	43 40 8	1-B4		V 1067	140153	4 11 27	43 40 22	1-E4	
V 250	140066	4 23 7	43 40 7	1-B4		V 1077	140154	4 11 34	43 41 15	1-E4	
V 250a	140067	-	-	-		V 1081	140155	4 10 41	43 44 56	1-E3	
V 250b	140068	-	-	-		V 1083	140156	4 10 47	43 45 13	1-E2	
V 250c	140069	-	-	-		V 1083a	140157	-	-	-	
V 266a	140071	4 19 44	43 42 32	1-C3		V 1085	140158	4 10 22	43 45 47	1-E2	
V 283	140077	4 19 47	43 41 34	1-C4		V 1085a	140159	-	-	-	
V 289	140080	4 20 55	43 41 49	1-C4		V 1085b	140160	-	-	-	
V 300	140083	4 19 35	43 41 32	1-C4		V 1085c	140161	-	-	-	
V 302	140084	4 20 44	43 40 43	1-C4		V 1085d	140162	-	-	-	
V 307	140086	4 20 16	43 41 12	1-C4		V 1085f	140163	-	-	-	
V 307a	140087	-	-	-		V 1085g-1	140164 ₁	-	-	-	
V 311	140091	4 19 15	43 41 33	1-C4	wr	V 1085g-2	140164 ₂	-	-	-	wr
V 320a	140093	4 21 33	43 42 43	1-C3		V 1086	140165	4 10 23	43 45 46	1-E2	
V 320a	140094	-	-	-		V 1088	140166	4 11 20	43 43 45	1-E3	
V 320a	140095	-	-	-		V 1098	-	4 12 30	43 42 40	1-E3	
V 320p	140096	-	-	-		V 1100	140167	4 12 27	43 43 4	1-E3	
V 324	-	4 21 22	43 42 38	1-C3		V 1102a	140168	4 11 2	43 45 34	1-E2	wr
V 352	-	4 20 47	43 40 15	1-C4		V 1104	140169	4 10 40	43 45 59	1-E2	wr
V 358	-	4 20 12	43 42 25	1-C4		V 1111	140170	4 19 3	43 42 12	1-C4	
V 366	140105	4 19 1	43 42 11	1-C4		V 1121	140171	4 11 1	43 45 38	1-E2	
V 366a	140106	-	-	-		V 1125a	140172	4 21 27	43 42 32	1-C3	
V 366b	140107	-	-	-		V 1130a	140173	4 21 17	43 42 30	1-C3/4	
V 366c	140108	-	-	-		V 1135	140174	4 21 0	43 42 30	1-C3/4	
V 367	140109	-	-	-	wr	V 1145	140175	4 10 42	43 46 2	1-E2	
V 368	140110	4 21 15	43 41 19	1-C4		V 1146a	140176	4 10 44	43 46 4	1-E2	
V 369a	140111	4 21 22	43 42 38	1-C3		V 1146b	140177	-	-	-	gt
V 402	140115	4 23 5	43 40 8	1-B4		V 1146c	140178	-	-	-	
V 402a	140116	-	-	-		V 1155	140179	4 19 5	43 40 20	1-C4	
V 402b	140117	-	-	-		V 1155a	140180	-	-	-	
V 403	140118	4 21 33	43 42 43	1-C3		V 1157	140181	4 19 38	43 40 50	1-C4	
V 403a	140119	-	-	-		V 1164	140182	4 23 2	43 39 43	7-B1	
V 410f	140124	4 22 43	43 41 1	1-B4		V 1170a	140183	4 12 15	43 44 4	1-E3	
V 1007	140127	4 13 46	43 41 23	1-E4		V 1179a	140184	4 13 13	43 44 20	1-E3	

Sample number	st	Longitude (W of Madrid)	Latitude	Quadrant	Chemical analyses	Sample number	st	Longitude (W of Madrid)	Latitude	Quadrant	Chemical analyses	
V 1179d	140185	4 13 13	43 44 20	1-E3	wr	M 140	121095	4 20 9	43 39 56	7-C1		
V 1181	140186	4 13 37	43 44 30	1-E3		M 145	121098	4 19 12	43 40 56	1-C4		
V 1185	140187	4 12 44	43 43 37	1-E3		M 158a	121104	4 18 43	43 41 12	1-C4	wr	
V 1193	140188	4 11 14	43 45 10	1-E2	gt	M 217	121112	4 17 38	43 40 55	1-D4		
V 1193a	140189	-	-	-		M 459	121132	4 12 43	43 39 55	7-E1	wr,gt	
V 1197	140190	4 11 29	43 44 39	1-E2		M 473	121138	4 11 41	43 38 51	7-E1		
V 1199	140191	4 11 30	43 41 20	1-E4		M 474	121139	4 12 6	43 38 21	7-E1		
V 1207	140192	4 13 59	43 41 42	1-E4		M 616	121160	4 18 22	43 40 4	1-C4	gt	
V 1214	140193	4 15 29	43 41 52	1-D4	wr	M 639	121170	4 15 56	43 41 19	1-D4		
V 1220	140194	4 14 25	43 41 13	1-D4		M 643	121173	4 16 56	43 40 10	1-D4	wr	
V 1223	140195	4 14 14	43 41 12	1-D4	gt	R 1	97986	4 13 15	43 44 44	1-E3		
V 1223a	140196	-	-	-		R 9	97989	4 11 57	43 45 41	1-E2		
V 1227	140197	4 13 55	43 41 39	1-E4		R 17	97994	4 16 28	43 42 59	1-D3		
V 1234	140198	4 16 49	43 42 6	1-D4	wr,opx	R 18	97995	4 16 30	43 43 2	1-D3		
V 1238	140199	4 14 15	43 40 53	1-D4		R 18a	97996	-	-	-	wr	
V 1243	140200	4 17 35	43 40 11	1-D4	gt	R 20	98000	4 11 47	43 44 53	1-E3	wr	
V 1243a	140201	-	-	-	wr,gt	R 31	98003	4 13 11	43 45 33	1-E2	wr	
V 1244	140202	4 17 21	43 40 12	1-D4	wr	R 70	98016	4 12 1	43 44 43	1-E3	wr	
V 1250	140203	4 15 54	43 40 9	1-D4	gt	R 108	98029	4 13 42	43 42 53	1-E3		
V 1255	140204	4 15 0	43 41 18	1-D4		R 137	98036	4 13 34	43 41 53	1-E4	wr	
V 1267	140205	4 17 59	43 41 44	1-D4	hbl	R 153	98040	4 14 45	43 43 45	1-D3		
V 1271	-	4 10 57	43 45 52	1-E2		R 173	98044	4 11 41	43 45 48	1-E2		
V 1273	140206	4 11 3	43 45 45	1-E2		R 175	98046	4 12 8	43 44 31	1-E3	wr	
V 1278	140207	4 15 19	43 40 29	1-D4	wr,gt,opx	R 204	98055	4 18 26	43 41 27	1-C4		
V 1282	140208	4 14 55	43 40 53	1-D4		R 208	98056	4 16 28	43 42 59	1-D3		
V 1308	140209	4 10 46	43 43 44	1-E3		R 210	98057	4 17 58	43 42 2	1-D4	wr	
V 1309a	140210	4 10 45	43 43 45	1-E3		R 312	98067	4 18 55	43 42 14	1-C4		
V 1309b	140211	-	-	-		R 313a	98068	4 19 0	43 42 13	1-C4		
V 1312	140212	4 10 29	43 43 32	1-E3		R 329	98073	4 18 23	43 41 27	1-C4		
V 1323	140213	4 10 54	43 41 56	1-E4		R 331	98075	4 16 28	43 42 59	1-D3		
V 1340	140214	4 14 12	43 38 48	7-D1		R 332	98076	-	-	-		
V 1346	140215	4 14 33	43 39 37	7-D1		R 348	98082	4 18 34	43 42 3	1-C4	wr	
V 1351	140216	unattached fragment	7-D1			R 378	98111	4 13 10	43 44 44	1-E3		
V 1374	140217	4 12 4	43 44 4	1-E3	wr	G 1-5	-	4 21 22	43 42 38	1-C3		
V 1389	140218	4 13 30	43 44 33	1-E3	wr	G 1-6	-	-	-	-		
V 1391	140219	4 16 58	43 42 2	1-D4		G 1-7	-	4 21 42	43 42 39	1-C3	wr	
V 1394	140220	4 14 2	43 41 28	1-D4		G 1-16	-	4 11 14	43 45 10	1-E2	gt	
V 1394a	140221	4 14 0	43 41 28	1-D4	wr	G 7-2	-	unattached fragment			wr	
V 1394b	140222	4 13 58	43 41 28	1-E4	wr	G 7-2a	-	unattached fragment			wr	
V 1394c	140223	4 13 56	43 41 28	1-E4	wr	G 7-2b	-	unattached fragment			wr	
V 1394d	140224	4 13 54	43 41 28	1-E4	wr	G 7-2c	-	unattached fragment			wr	
V 1401	140225	4 10 45	43 44 26	1-E3		G 7-2e	-	unattached fragment			wr	
V 1401b	140226	4 12 40	43 44 56	1-E3		Ma 1	140242	The following samples				wr
V 1405	140227	4 13 8	43 45 5	1-E2		Ma 2	140243	are part of the geolo-				wr
V 1407	140228	4 16 50	43 42 17	1-D4		Ma 5	140244	gical section at the				wr
Coe D7	97906	4 10 58	43 45 33	1-E2		Ma 6	140245	S coast of the				wr
Coe D10	98122	4 10 58	43 45 33	1-E2	wr	Ma 9	140246	Masanteo peninsula, that				wr
Coe D12	97910	4 10 58	43 45 33	1-E2		Ma 10	140247	is situated between				
Coe E1	140229	4 10 51	43 45 49	1-E2		Ma 11	140248	4 10 38	43 42 40	1-E3	wr	
Coe E1	140230	4 11 19	43 43 34	1-E3		Ma 12	140249	-	-	-	wr	
Coe 107	140231	4 10 59	43 45 33	1-E2		Ma 13	140250	4 10 49	43 42 56	1-E3	wr	
Coe 114	140232	4 13 5	43 40 11	1-E4		Ma 15	140251	Their positions are				wr
Coe 126	140233	4 10 40	43 43 40	1-E3		Ma 16	140252	indicated in plate 2.				wr
Coe 127	140234	4 10 39	43 43 38	1-E3		Ma 17	140253	-	-	-	wr	
Coe 141	140235	4 13 12	43 41 5	1-E4		Ma 19	140254	-	-	-	wr	
Coe 141a	140236	-	-	-		B	140255	-	-	-		
Coe 162	140237	4 10 40	43 46 0	1-E2		C	140256	-	-	-		
Coe 163	140238	4 10 39	43 46 1	1-E2		D	140257	-	-	-		
Coe 182	98114	4 10 53	43 45 4	1-E2	wr	E	140258	-	-	-		
Coe 204	98112	4 10 46	43 44 25	1-E3	wr	G	140259	-	-	-		
Coe 220	97946	4 10 45	43 44 26	1-E3		H	140260	-	-	-		
Coe 251	97950	4 11 1	43 45 9	1-E2		I	140261	-	-	-		
Coe 304	140239	4 12 56	43 43 57	1-E3		J	140262	-	-	-		
E 320	140240	4 23 18	43 36 45	7-E2		L	140263	-	-	-		
E 327b	140241	4 23 54	43 39 8	7-B1	gt	61-P1	140264	-	-	-		
M 100	121081	4 20 2	43 40 46	1-C4		61-P2	140265	-	-	-		
						61-P3	140266	-	-	-		

APPENDIX 4

QUALITATIVE MINERALOGICAL COMPOSITION OF CHEMICALLY ANALYZED SAMPLES

